The Production and Function of Titan Cells in *Cryptococcus neoformans.*

A DISSERTATION
SUBMITTED TO THE FACULTY OF THE GRADUATE SCHOOL
OF THE UNIVERSITY OF MINNESOTA
BY

Laura Hana Okagaki

IN PARTIAL FULFILLMENT OF THE REQUIREMENTS
FOR THE DEGREE OF
DOCTOR OF PHILOSOPHY

Adviser: Kirsten Nielsen

May, 2012

© Laura Hana Okagaki, 2012

ACKNOWLEDGEMENTS

There are many people to thank for this body of work. First, thank you to my adviser Kirsten Nielsen for the mentorship she has provided to me over the years. Kirsten has been an exceptional advocate for her students as well as being an amazing adviser and mentor. Her excitement for our science is contagious. Kirsten has always respected my opinions and fostered a deeper understanding of the science as well as the scientific community.

This work could not have been done without the help of many people. Anna K. Strain, Judith N. Nielsen, Caroline Charlier, Nicholas J. Baltes, Fabrice Chrétien, Joseph Heitman, and Françoise Dromer contributed to the work featured in Chapter 2. Additionally, our interactions with Arturo Casadevall and Oscar Zaragoza complemented our work and it was a pleasure working with them to tell the story of titan cells.

Many thanks to Yina Wang, Elizabeth R. Ballou, Teresa R. O'Meara, Yong-Sun Bahn, J. Andrew Alspaugh, and Chaoyang Xue contributed to the work featured in Chapter 3. Collaboration with Andy and his lab members is not limited to the data presented here, and I am grateful for supportive members of the *Cryptococcus* community. Chao and Yina contributed greatly to the work shown here and have been critical for the telling of the signaling story.

Of course, members of the Nielsen Lab, past and present, deserve many thanks for their input and friendship over the years: Anna, Juliet Crabtree, Oleksandr Moskalenko, Nick, our talented undergrads, Man Shun Fu, Tammy McDonald, and Darin Weisner. I would also like to extend special thanks to Dana Davis and his lab members, especially Luci Zacchi and Julie Wolf, for their critical feedback of our work as well as making me feel like a contributing member of our field.

Thank you to my committee members: Kirsten, Dana, Bryce Binstadt, and Judy Berman. You have all dedicated your time to making me a better scientist.

Finally, I could not have completed this work without the love and support of my family and friends. My dear husband, Charlie, has been the best support system I could have had through graduate school. I'm sorry you never knew me when I was sane.

DEDICATION

This dissertation is dedicated to my father,
Takashi Okagaki.
You have been and will always be the biggest influence in my scientific career.

ABSTRACT

Cryptococcus neoformans is a common life-threatening human fungal pathogen. The size of cryptococcal cells is typically 5 to 10 μm. Cell enlargement is observed *in vivo*, producing cells up to 100 μm. These morphological changes in cell size affect pathogenicity via reducing phagocytosis by host mononuclear cells, increasing resistance to oxidative and nitrosative stress, and correlated with reduced penetration of the central nervous system. Cell enlargement is stimulated by coinfection with strains of opposite mating type, and *ste3**a**Δ* pheromone receptor mutant strains have reduced cell enlargement. Analysis of DNA content in this novel cell type revealed that these enlarged cells are polyploid, uninucleate, and produced daughter cells *in vivo*. Two G protein-coupled receptors are important for induction of the titan cell phenotype: the Ste3**a** pheromone receptor (in mating type **a** cells) and the Gpr5 protein. Both receptors control titan cell formation though elements of the cAMP/PKA pathway. This conserved signaling pathway in turn mediates its effect on titan cells through the PKA-regulated Rim101 transcription factor. Additional downstream effectors required for titan cell formation include the G1 cyclin Pcl103; the Rho104 GTPase; and two GTPase activating proteins, Gap1 and Cnc1560. These observations support growing models in which the PKA signaling pathway coordinately regulates many virulence-associated phenotypes in diverse human pathogens. In addition, altered host-pathogen interactions during the early stages of pulmonary cryptococcosis were explored. The relationship between titan cell production and phagocytosis is non-linear, where moderate increases in titan cell production result in profound decreases in phagocytosis. Production of titan cells by the wild-type strain can also confer protection to a titan deficient strain, and size alone is sufficient to protect from phagocytosis, however size does not confer protection to normal-sized cells. These data describe titan cell formation, a novel cell morphology, in *C. neoformans*. Signaling pathway analysis showed that titan cell production is coregulated with the other cryptococcal virulence factors. In addition, titan cells have reduced phagocytosis and can confer protection from phagocytosis to normal-sized cells. These data suggest that titan cell production is a novel virulence factor in *C. neoformans*.

TABLE OF CONTENTS

ABSTRACT…….……...……Page iii

LIST OF TABLES…...……..……....…..Page viii

LIST OF FIGURES...……...……..…...……..Page ix

CHAPTER ONE……..….Page 1
Introduction

I. Morphological Switching in Pathogenic fungi……...…….2
   a. Filament to Yeast Transition……..3
   b. Yeast to Hyphal Switch…….9
   c. Phenotypic Switching……..11
   d. Cell Enlargement…….…14
   e. Morphological Changes in *Cryptococcus neoformans*……..…..18
II. Signaling Pathways That Regulate Morphological switching……...26
   a. PKA Signaling…….……...27
   b. Transcription Factors……...32
III. Acquisition and Pathogenesis of *Cryptococcus neoformans*…….35
   a. Cryptococcosis…….35
   b. Cryptococcal Virulence Factors……...36
   c. Host-Pathogen Interactions……..37
IV. Summary of This Dissertation…….…..40

CHAPTER TWO…….……...……Page 42
Cryptococcal Cell Morphology Affects Host Cell Interactions and Pathogenicity

I. Introduction……..…..……43
II. Materials and Methods……...46
   a. Ethics Statement……...46
   b. Strains and Media……46
   c. Tissue Analysis……....46
   d. *ste3**a**Δ* Mutant Strains……...…..47
   e. *In Vivo* Analysis of Ste3**a**Δ Strains……..……48
   f. Interactions with the Blood Brain Barrier……48
   g. Bronchoalveloar Lavage……..51
   h. Nitosative and Oxidative Stress Assays……...……51

i. Flow Cytometry……...52
j. Cell Sorting and qPCR……..…..54
k. Statistical Analsysis…….56
III. Results…….……..*57*
a. Morphological Changes in *C. neoformans* var. *grubii* Cells *In Vivo*…….……57
b. Pheromone Signaling Affects Titan Cell Formation…….…..63
c. Pheromone Signaling Alters Dissemination to the Central Nervous System……..…64
d. Coinfection Does Not Affect Blood Brain Barrier Penetration Upon IV Injection…….68
e. Titan Cells are Resistant to Phagocytosis……..……..70
f. Titan Cells are Polyploid…….75
IV. Discussion……..……*88*

CHAPTER THREE……Page 98
Cryptococcal Titan Cell Formation is Regulated by G-Protein Signaling in Response to Multiple Stimuli

I. Copyright Permission……....*99*
II. Introduction……*107*
III. Materials and Methods……*107*
a. Ethics Statement……..……..107
b. Strains and Media……..……107
c. *In vivo* Titan Cell Assay…….108
d. Flow Cytometry…….……109
e. Yeast Two-Hybrid……...……..110
f. Coinfections…….……110
g. RNA Preparation…….……..113
h. RNA Sequencing and Transcript Analysis……113
i. Promoter Analysis……..114
j. Statistical Analysis…….……114
IV. Results……..*115*
a. G-Proteins Coupled Receptor Signaling Regulates Titan Cell Formation……..……115
b. Gpa1 Signaling Results in Titan Cell Production……..…120
c. Ste3**a** Interacts with Gpa1 but not Gpa2 or Gpa3…….……121
d. Signaling Through Ste3**a** is Sufficient for Titan Cell Formation During Coinfection……...……125
e. Rim101 and Cdc420 Regulate Titan Cell Formation……127
f. Additional Effectors of Titan Cell Induction……129
V. Discussion……*134*

CHAPTER FOUR……Page 142
Titan Cells Confer Protection from Phagocytosis in *Cryptococcus neoformans* Infections

I. Introduction……..…*143*
II. Materials and Methods……..…*146*
a. Ethics Statement…….……146
b. Strains and Media……..……146
c. *In Vivo* Titan Cell and Phagocytosis Assay……...……146
d. Coinfecctions…….147
e. *In Vivo* Bead Phagocytosis Assay…….…….147
f. Effect of Cell Age on *In Vivo* Phagocytosis……..148
g. Statistical Analysis…….……148
III. Results……..……*150*
a. Size Alone Can Confer Protection
Against Phagocytosis……..……..150
b. Association Between Phagocytosis and
Titan Cell Production is Non-Linear……..…….……...…152
c. Nascent Cells Exhibit Reduced
Titan Cell Formation and Phagocytosis…….....157
d. Titan Cell Production Protects Normal-sized Cryptococcal
Cells from Phagocytosis……159
e. Size Alone Does Not Confer Cross-Protection
From Phagocytosis……..……..…162
IV. Discussion……*163*

CHAPTER FIVE……..……Page 168
Conclusions and Final Remarks

I. Titan cells in Pulmonary Infection……...……..*169*
a. Titan Cells Are Important in the Establishment of
Pulmonary Infection…….169
b. Titan Cell Production May Promote Dormancy…….…173
c. Titan cell Influence on Penetration of the Blood Brain Barrier……...175
d. Titan Cells May Modulate the Host Immune Response……..180
II. Titan Cell Signaling and Regulation……..…*184*
a. Multiple Signals Are Required for Titan Cell Stimulation……..…184
b. Induction of Titan Cell Production Results in an
Altered Cell Cycle…….……..187
III. The Importance of Titan Cells in Global Health……...……*192*
a. Titan Cell Production is a Virulence Factor……192
b. Implications of Titan Cell Production on Human
Cryptococcosis…….193

IV. Final Remarks……*194*

REFERENCES……..……Page 195

APPENDIX……..……Page 215
Titan Cell Production is Density Dependent

I. Introduction……..……*216*
II. Materials and Methods……*217*
a. Ethics Statement……217
b. Strains and Media……..217
c. *In vivo* Titan Cell and Phagocytosis Assay……..….…….217
d. Statistical Analysis…….……218
III. Results and Discussion……..…..*218*

LIST OF TABLES

Table 2.1……...……Page 49
Primers Used in Ste3**a** Deletion

Table 3.1……..…Page 111-112
Mutant Strains Used for Titan Cell Analysis

Table 3.2……..……Page 131
Changes in gene expression in the *rim101Δ* mutant

Table 5.1……..……Page 186
In vivo conditions tested for titan cell induction

Table 5.2……..…Page 190
otc1Δ Potential Genes

LIST OF FIGURES

CHAPTER ONE
Introduction

1.1……...……Page 5
Morphological Changes in Pathogenic Fungi.

1.2……..……Page 21
Mating in *Cryptococcus neoformans.*

1.3……..……Page 24
Capsule and Cell Wall of *Cryptococcus neoformans.*

1.4……..……Page 30
PKA signaling in *Candida albicans* and *Cryptococcus neoformans.*

CHAPTER TWO
Cryptococcal Cell Morphology Affects Host Cell Interactions and Pathogenicity

2.1……..…Page 59
Titan cells in the lungs of coinfected mice.

2.2……..……Page 61
Titan cell formation in the lungs, spleen, and brain.

2.3……..……Page 62
Fluorescently labeled **a** (green) and α (red) cells in the lungs during coinfection.

2.4……..……Page 65
ste3aΔ survival assays.

2.5……..……Page 67
C. neoformans pheromone receptor mutant strains penetrate the CNS during coinfection.

2.6……..……Page 69
KN99**a** and KN99α cells interact with endothelial cells of the blood-brain barrier during coinfection.

2.7……..……Page 72
Titan cell formation and phagocytosis in the lungs of infected mice.

2.8…….……Page 74
Titan cells are resistant to oxidative and nitrosative stress.

2.9…….……Page 77
Titan cells can undergo cell division.

2.10……...……Page 80
Imaging flow cytometry.

2.11……...……Page 82
Titan cells have increased DNA content.

2.12……..……Page 84-85
C. neoformans titan cells are polyploid.

2.13……...……Page 87
In vitro titan cell production.

2.14……...……Page 91
Model of titan cell signal transduction and pathogenesis.

CHAPTER THREE
Cryptococcal Titan Cell Formation is Regulated by G-Protein Signaling in Response to Multiple Stimuli

3.1……...……Page 116
G-protein coupled receptor mutants were screened for titan cell formation.

3.2……...……Page 117
Mutant strains were screened for ploidy alterations.

3.3……...……Page 119
Titan cell signaling *in vivo* is regulated by the Gpr5 receptor.

3.4……...……Page 122
Signaling via the Gα protein Gpa1 regulates titan cell production.

3.5……...……Page 124
Ste3**a** interacts with Gpa1 in the split-ubiquitin yeast two-hybrid system.

3.6……...……Page 126
The effects of coinfection on titan cell formation.

3.7……...……Page 132
Regulators of titan cell signaling.

CHAPTER FOUR
Titan Cells Confer Protection from Phagocytosis in *Cryptococcus neoformans* Infections

4.1……...……Page 151
Large size cannot provide cross-protection from phagocytosis.

4.2……...……Page 153
The relationship between titan cell production and phagocytosis is non-linear.

4.3……...……Page 155
Titan cell production protects from phagocytosis by 24 hours post-infection.

4.4……...……Page 158
Nascent cells exhibit reduced phagocytosis.

4.5……...……Page 160
Titan cell production provides cross-protection from phagocytosis to normal size cryptococcal cells.

CHAPTER FIVE
Conclusions and Final Remarks

5.1……...……Page 171
Titan Cell Production and Pathogenesis

APPENDIX
Titan Cell Production is Density Dependent
A1…….……..Page 219
Titan cell production is density dependent.

CHAPTER ONE

Introduction

I. MORPHOLOGICAL SWITCHING IN PATHOGENIC FUNGI

In many human pathogenic fungi, environmental conditions can induce cell morphology changes that are integral to the infection cycle. There are four primary types of morphological switching that have been observed: filament to yeast dimorphism, yeast to hyphal transition, phenotypic switching, and cell enlargement (**Figure 1.1**).

Dimorphic fungi grow in the soil as long filaments and produce easily aerosolized spores (Andrianopoulos 2002; Nemecek, Wuthrich et al. 2006). Upon inhalation into the lungs of a susceptible host, the dimorphic fungi grow as round budding yeasts (**Figure 1.1A**), a change that is induced primarily by the host body temperature (Lubarsky and Plunkett 1955; Howard 1959; Nemecek, Wuthrich et al. 2006). In the human commensal *Candida albicans*, both hyphal and yeast cells are found in the host (**Figure 1.1B**). Transition from yeast to hyphae and back is induced by a number of environmental cues including pH and temperature (Odds 1985; Davis, Edwards et al. 2000). Both the yeast and the hyphal forms are required for virulence, and it has been hypothesized that the hyphae are important in tissue invasion and damage while the yeast form easily disseminates through the blood and lymph systems (Odds 1985).

More subtle changes in cell morphology, like phenotypic switching, can also have profound effects on pathogenesis. White and opaque cells in *Candida albicans* (**Figure 1.1B**) have unique properties that make each one suitable to a specific niche in the host (Alby and Bennett 2009), while *Cryptococcus neoformans* produces a large polysaccharide capsule (**Figure 1.1E**) during phenotypic switching that can modulate the immune response during infection (Heitman and American Society for Microbiology.

2011). Cell enlargement in *C. neoformans* (**Figure 1.1E**), as well as *Pneumocystis spp* (**Figure 1.1D**) and *Coccodidoides immitis* (**Figure 1.1C**), can protect from phagocytosis and provide a mechanism for the production of large quantities of daughter cells (Lubarsky and Plunkett 1955; Drutz, Huppert et al. 1981; Matsumoto and Yoshida 1984; Cushion 2004; Johannesson, Kasuga et al. 2006; Hung, Xue et al. 2007; Okagaki, Strain et al. 2010; Zaragoza, Garcia-Rodas et al. 2010). Because of their integral role in pathogenesis, the characteristics and signaling pathways in each of these morphologies may be used as targets for more effective antifungal therapies.

Filament to Yeast Transition

There are six human fungal pathogens that are considered dimorphic fungi (**Figure 1.1A**) and are distinguished by filamentous growth in the environment and a switch to yeast growth in the host (Lubarsky and Plunkett 1955; Howard 1959; Andrianopoulos 2002; Nemecek, Wuthrich et al. 2006): *Histoplasma capsulatum*, *Blastomyces dermititidis*, *Coccidioides immitis*, *Paracoccidioides brasiliensis*, *Sporothrix schenckii*, and *Penecillium marneffei* (Andrianopoulos 2002; Nemecek, Wuthrich et al. 2006). The primary signal that induces yeast phase transition is temperature (Maresca and Kobayashi 1989; Maresca, Carratu et al. 1994; Andrianopoulos 2002). At room temperature, 25°C, dimorphic fungi grow in a filamentous form, and increasing the temperature to 37°C induces yeast growth. Temperature alone appears to be sufficient to induce the yeast phase, but other environmental stimuli can also promote morphological transition.

Host specific stimuli can enhance transition to the yeast form, increasing the rate of switch beyond that of temperature alone. Addition of 5-20% CO_2 to *in vitro* cultures of *C. immitis* decreases filamentous growth when compared to ambient levels of CO_2 (Klotz, Drutz et al. 1984). In the lungs, the first defense against fungal infections is the presence of resident alveolar macrophages which are able to produce antimicrobial reactive oxygen species including hydrogen peroxide. Co-culture with macrophages as well as addition of exogenous hydrogen peroxide stimulates switching to the yeast form in *B. dermititidis* (Sugar and Picard 1991), thus components of the host immune response encourage morphological switching in the dimorphic fungi.

Transition from the filamentous to yeast phase in the dimorphic fungi induces the expression of yeast specific traits including cell wall components. In the filamentous form, the cell wall of *P. brasiliensis*, *H. capsulatum* and *B. dermititidis* contains β-(1,3)-glucan (Kanetsuna and Carbonell 1971; Klein and Tebbets 2007). Some host immune cells express the pattern recognition receptor (PRR) dectin-1 on their cell surface, which binds to β-(1,3)-glucan and induces phagocytosis and stimulation of cytokine secretion (Brown and Gordon 2001). However, when in the yeast form, *P. brasiliensis*, *H. capsulatum* and *B. dermititidis* down-regulate production of β-(1,3)-glucan and up-regulate α-(1,3)-glucan (Kanetsuna and Carbonell 1971). Production of α-1,3-glucan masks the cell surface β-(1,3)-glucan from recognition by dectin-1, preventing stimulation of the inflammatory response through dectin-1 signaling (Hogan and Klein 1994). Currently, no pattern recognition receptor for α-(1,3)-glucan has been identified and its exact role in pathogenesis has yet to be elucidated.

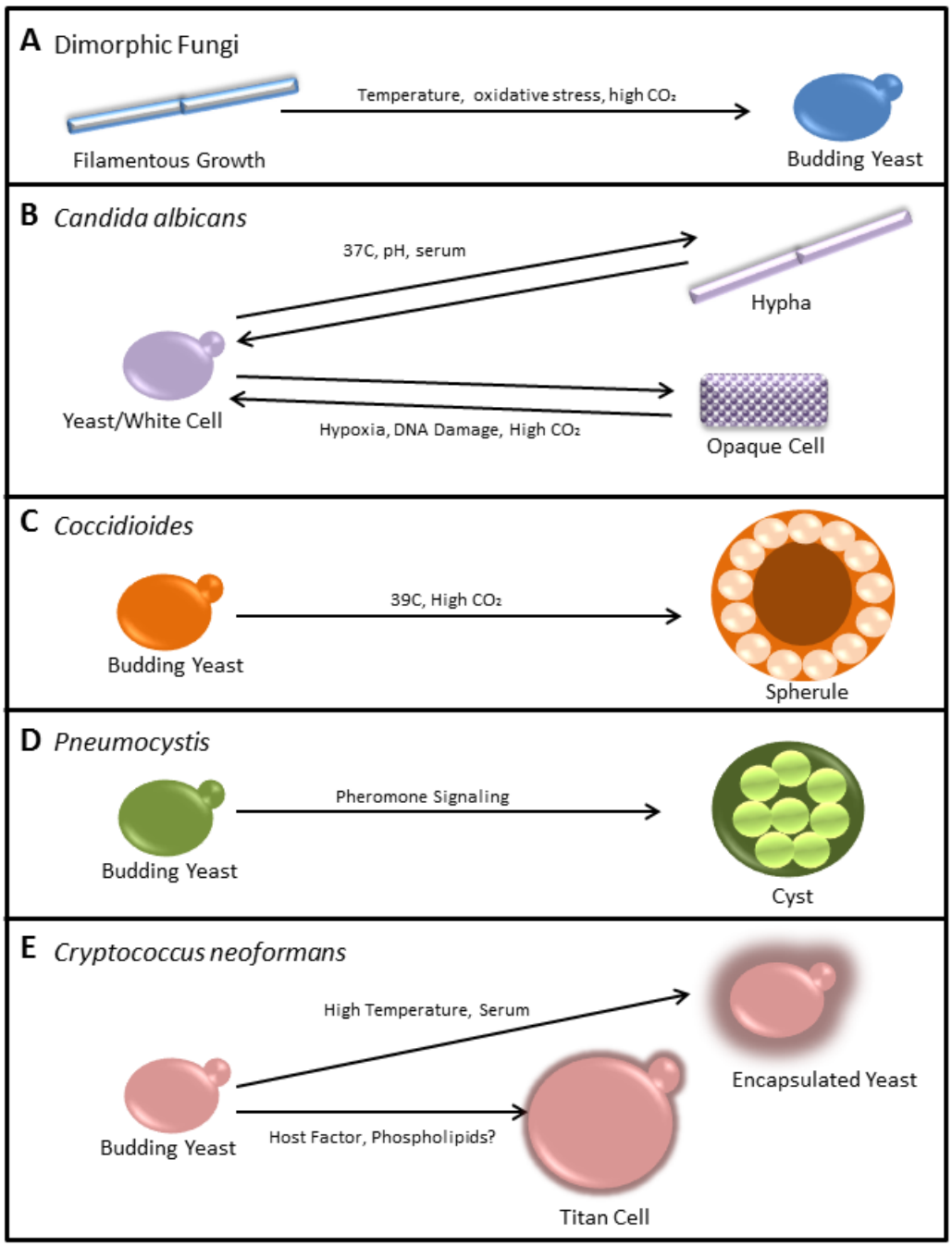

Figure 1.1 Morphological Changes in the Pathogenic Fungi.
Morphological changes occur in many of the human pathogenic fungi. These include the filament to yeast switch in the dimorphic fungi (A), the yeast to hyphal switch and the white-opaque switching in *Candida albicans* (B), cyst/spherule formation in *Pneumocystis*(C) and *Coccidioides* (D), and capsule production and titan cell formation in *Cryptococcus neoformans* (E).

Yeast cells of the dimorphic fungi secrete immune modulatory molecules that can alter host-pathogen interactions and promote fungal survival in host cells. *Histoplasma* yeast cells are susceptible to the antimicrobial activity of the surfactant proteins A and D (SP-A and SP-D) found in the respiratory tract of mammals (McCormack, Gibbons et al. 2003). To escape killing by SP-A and SP-D, *H. capsulatum* can be taken up by macrophages where it survives and proliferates (McCormack, Gibbons et al. 2003). In addition to opsonization with antibody or complement, *Histoplasma* can stimulate phagocytosis by producing a heat shock protein, Hsp60, following the filament to yeast transition, which binds to mammalian β_2 integrin, CD11/CD18, on the surface of macrophages (Gomez, Allendoerfer et al. 1995; Long, Gomez et al. 2003; Guimaraes, Frases et al. 2009). It has been suggested that binding of Hsp60 to CD11/CD18 acts as a non-stimulating route of entry into the macrophages, protecting the *H. capsulatum* yeast cells from intracellular killing mechanisms produced by activated macrophages (Woods 2002). Both *Paracoccidiodes* and *Coccidioides* also contain homologues to the *Histoplasma* HSP60 gene, but their function in infection is yet to be examined (Thomas, Wyckoff et al. 1997; Izacc, Gomez et al. 2001).

H. capsulatum, *B. dermititidis*, and *S. schenkii* yeast cells have been shown to be more resistant than filaments to killing by phagocytes (Schaffner, Davis et al. 1986), suggesting that yeast specific genes are important in the intracellular parasitism of some dimorphic fungi. One such yeast specific protein is the multi-tasking molecule called Bad1 (*Blastomyces* adhesion 1) (Rooney, Sullivan et al. 2001), which is found at the cell surface of *Blastomyces* as well as secreted into the host environment (Klein, Sondel et al.

1992; Klein and Newman 1996). Bad1 has two primary roles in *B. dermititidis* host-pathogen interactions: adhesion and immune modulation. Bad1 binds to epithelial cell surface molecules and the complement receptors found in pulmonary tissue (Newman, Chaturvedi et al. 1995), which may promote colonization of the lungs and establishment of *Blastomyces* infections. Cell surface Bad1 also binds to the complement C3 receptor on alveolar macrophages, where it acts to modulate the immune response (Newman, Chaturvedi et al. 1995). Bad1 binding to host cells results in down-regulation of the cytokine TNF-α (tumor necrosis factor α) (Finkel-Jimenez, Wuthrich et al. 2001). TNF-α is a critical molecule in stimulation of the inflammatory response, including the activation of macrophages (Murphy, Travers et al. 2008). Bad1 also stimulates production of the anti-inflammatory cytokine TGF-β when bound to macrophages (Finkel-Jimenez, Wuthrich et al. 2002). In its soluble form, Bad1 can also affect natural killer (NK) cells and stimulate altered cytokine production (Finkel-Jimenez, Wuthrich et al. 2002). Thus, Bad1 reduces the inflammatory response during infection by modulating cytokine secretion.

Histoplasma also produces a multi-tasking protein CBP (calcium binding protein), which contains several calcium binding domains (Batanghari, Deepe et al. 1998; Patel, Batanghari et al. 1998; Beck, Dekoster et al. 2009) but has been shown to be critical for the intracellular survival strategy of *Histoplasma* (Sebghati, Engle et al. 2000), suggesting other functions. CBP1 is localized in the lysosomal compartment during intracellular infection, and is necessary for preventing the acidification of the lysosome (Eissenberg and Goldman 1988; Taylor, Espinosa-Schoelly et al. 1989; Newman, Gootee

et al. 1997; Strasser, Newman et al. 1999). Structural analysis showed that CBP is similar in structure to the mammalian molecule saposin B (SapB) . The function of SapB in the host is lipid and membrane degradation in lysosomal compartments (Major, Joyce et al. 2006). Interestingly, the saposins have been shown to be important in the processing of lipids for presentation to T-cells on the MHC-like protein CD-1 (Major, Joyce et al. 2006), suggesting that CBP may disrupt antigen presentation by macrophages during the intracellular parasitism of *Histoplamsa*. Recent sequence analysis revealed that CBP has a homologue in *P. brasiliensis*, but the function of the *Paracoccidioides* CBP is unknown.

Paracoccidioides secretes an immune modulatory glycoprotein molecule, gp70 that has several roles in infection. In *in vitro* experiments, gp70 is able to block the phagocytositic activity of macrophages (de Mattos Grosso, de Almeida et al. 2003) and inhibit the production of oxidative and nitrosative stress produced by phagocytes (de Mattos Grosso, de Almeida et al. 2003). Other aspects of the immune response may also be modulated by gp70. Administration of anti-gp70 antibodies protected animals from *Paracococcidioides* infection (de Mattos Grosso, de Almeida et al. 2003). Thus the absence of gp70 results in reduced fungal cell survival and attenuated virulence of *Paracoccidioides* in the host.

The filament to yeast transition in the dimorphic fungi is accompanied by cell wall alterations and the production of immune modulatory molecules. Morphological switching to the yeast form is stimulated by host conditions and is required for virulence (Klein and Tebbets 2007). The morphological changes observed in dimorphic fungi and

the accompanying protein expression changes may be viable targets for preventing or treating fungal infections.

Yeast-Hyphal Switching

C. albicans is a commensal organism and is found on epithelial surfaces and in the gastrointestinal tract of humans (Odds 1985). Morphological changes in *C. albicans* are induced by subtle changes in the host environment (**Figure 1.1B**). While temperature is the primary stimulus to induce the transition to the yeast form in dimorphic fungi, in *C. albicans* there is a wide range of conditions that can induce cell morphology changes (Odds 1985). An increase in temperature to 37°C can induce switching to the hyphal form of *C. albicans* rather than the yeast form (Odds 1985). Other hyphal inducing conditions include the addition of serum to culture medium and increases in pH, while decreases in pH favor the yeast form (Davis, Wilson et al. 2000). These observations suggest that the different morphologies may be adaptations to different niches found in the host, such as the oral cavity or skin surface.

Yeast to hyphal switching in *C. albicans* is accompanied by a number of structural and expression changes that result in altered host-pathogen interactions. *C. albicans* undergoes a change in cell wall proteins upon switching to the hyphal form. One protein that has been well studied is Hwp1 (hyphal wall protein 1), which is up-regulated in hyphae (Sohn, Urban et al. 2003; Sohn, Senyurek et al. 2006; Kim, Wolyniak et al. 2007; Davis-Hanna, Piispanen et al. 2008). Hwp1 is an adhesion protein that is expressed on the cell wall in the hyphal growth state of *C. albicans*, and has been shown to be

important for adhesion to host tissue and biofilm formation(Staab and Sundstrom 1998; Staab, Bradway et al. 1999; Tsuchimori, Sharkey et al. 2000; Nobile, Nett et al. 2006). Also expressed at the cell surface upon hyphal formation are the agglutinin-like proteins Als3 and Als8 (Hoyer, Payne et al. 1998; Fu, Ibrahim et al. 2002; Zhao, Oh et al. 2004; Phan, Myers et al. 2007). The ALS proteins are adhesion molecules that allow *C. albicans* to bind to epithelial cells (Phan, Myers et al. 2007). In experiments examining the role of adhesion molecules in virulence, Als3 and Als8 are important for tissue invasion (Zhao, Oh et al. 2004). In its hyphal form, *C. albicans* produces SAPs (secreted aspartyl proteases) that are also needed for virulence. SAPs are able to degrade E-cadherin at adherent junctions between cells of the host epithelium (Parnanen, Meurman et al. 2010), encouraging invasion into the tissues.

The yeast to hyphal switch in *C. albicans* can also act as a defense mechanism against the host immune response during infection. *C. albicans* yeast, like those of *Histoplasma* and *Blastomyces*, are easily taken up by host macrophages. Upon phagocytosis, *C. albicans* switches its gene expression profile to up-regulate hyphal specific genes (Lorenz, Bender et al. 2004). After phagocytosis by host macrophages, cells begin to undergo a morphological transition, producing long hyphae that cannot be contained by the host cells. As the hyphae get longer, they eventually pierce the membrane of the host cell, causing cell lysis. Thus, cell morphological changes in *C. albicans* result in escape from host cells that are capable of killing yeast cells.

While studies definitively linking the yeast to hyphal transition in *C. albicans* to virulence have not been conclusive, it has been hypothesized that morphological

switching is critical for different stages of infection (Odds 1985). The increased expression of adhesion molecules during hyphal formation suggests that hyphae are more suited to colonization of the epithelial surfaces. Additionally, expression of the SAP genes in hyphae also suggests that this morphology is important in tissue invasion during active infection. The yeast form, on the other hand, is small and can easily disseminate throughout the body in the blood and lymph systems. The yeast form may be important in dissemination from the GI tract to other organs that are susceptible to *C. albicans* infection. The yeast and hyphal forms of *C. albicans* each have a specific role in infection and have provided a better understanding of different stages of *Candida* infections.

Phenotypic Switching

Phenotypic switching in the human pathogenic fungi affects host-pathogen interactions and can increase the fitness of a cell to its environment. In *C. albicans*, one well studied phenotypic switch is the white to opaque switch (**Figure 1.1B**). *C. albicans* can switch from a white cell, which has a smooth cell surface and rounded yeast appearance observed by electron microscopy, to the opaque cell morphology which has a pimpled surface and oblong cell morphology (Anderson and Soll 1987; Slutsky, Staebell et al. 1987; Soll, Langtimm et al. 1987). The white-opaque switch is bistable; once a cell switches to the opaque form, there is a positive feedback loop that can prevent reversion to the white form (Huang, Wang et al. 2006). The opaque form of *C. albicans* is the mating competent form (Slutsky, Staebell et al. 1987; Miller and Johnson 2002), suggesting that switching plays a role in increasing genetic diversity.

White opaque switching in *C. albicans* is a rare event and occurs once in every 10^4 cell divisions (Slutsky, Buffo et al. 1985; Slutsky, Staebell et al. 1987). However, a number of environmental conditions can influence switching and stabilization of morphology. Some environmental conditions favor one form over the other, while other conditions can increase switching in both directions.

The opaque form of *C. albicans* is favored by increasing levels of carbon dioxide (Huang, Srikantha et al. 2009; Liu, Li et al. 2010). The exposure of *C. albicans* to low doses of UV irradiation increases switching in both directions, opaque to white and white to opaque (Slutsky, Buffo et al. 1985; Morrow, Anderson et al. 1989). Chemical genotoxic stress agents, such as methyl methane sulfonate (MMS) or hydroxyurea (HU), can also induce switching, but primarily to the opaque form (Alby and Bennett 2009). In the host, *C. albicans* is also subject to damage by the oxidative burst produced by the immune response. Alby and Bennett showed that exposure to oxidative stress in the form of hydrogen peroxide resulted in a dose-dependent increase in the white to opaque switch (Alby and Bennett 2009). Anaerobic conditions can also result in increased switching to the opaque form in *C. albicans* (Ramirez-Zavala, Reuss et al. 2008). DNA damage, oxidative stress, and anaerobic conditions all contribute to a slower cell cycle. It has been suggested that slowing the cell cycle may result in increased switching, specifically to the opaque form (Alby and Bennett 2009).

More recently, the importance of the white-opaque switch has been studied in biofilms. Biofilm formation in the gut and on catheters and other implanted medical devices can confer resistance to antifungal activity and the host immune response

(Hawser and Douglas 1995; Nett, Guite et al. 2008). Microscopic examination of *Candida* biofilms revealed that they harbor both yeast and hyphae as well as both white and opaque cells (Daniels, Srikantha et al. 2006). Biofilm formation can result in an environment that is anaerobic, suggesting that switching to the opaque morphology may be encouraged in biofilms. Interestingly, pheromone produced by the mating competent opaque cells may induce biofilm formation in white cells by altering cell surface adhesion properties (Daniels, Srikantha et al. 2006). Therefore, switching to the opaque form during biofilm formation may strengthen the overall structure of the biofilm. In addition, these data suggest that biofilms may be an appropriate place for mating to occur.

White-opaque switching affects phagocytosis and survival in the host. *In vitro* studies showed that white cells secrete a leukocyte chemo-attractant (Geiger, Wessels et al. 2004) and are taken up by the murine macrophage cell line RAW 264.7 significantly more than opaque cells (Lohse and Johnson 2008). However, white cells are more resistant to the killing mechanisms produced by phagocytes (Kolotila and Diamond 1990). Opaque cells do not produce the leukocyte chemo-attractant, thus their reduced phagocytosis may be due to fewer interactions with host phagocytes (Lohse and Johnson 2008).

Studies using a tail-vein injection model of systemic candidiasis revealed that white cells are more virulent, however in a model of cutaneous candidiasis it was shown that opaque cells are more adapted to skin infection (Kvaal, Srikantha et al. 1997; Kvaal, Lachke et al. 1999). Thus, traits of white cells appear to make them more pathogenic in

the blood and organs of the host, while opaque cells may be more fit for survival and pathogenesis on the skin. Thus, subtle changes in environmental conditions to induce white-opaque switching in *C. albicans* result in niche specific phenotypes. These observations are an example of how cell morphology can affect the fitness of fungal cells to the environment and enhance pathogenesis.

Cell Enlargement

Cell size increases have been observed in some of the human pathogenic fungi. Cell enlargement can play several roles during the course of infection including giving rise to daughter cells and protecting the cells from the host immune response. *Coccidioides* species produce large spherules that modulate the immune response and give rise to hundreds of daughter cells (**Figure 1.1C**). *Pneumocystis* produces large cysts in the lungs that contain four to eight daughter cells (**Figure 1.1D**),

In *Coccidioides* species, cell size increases occur during the parasitic stage of infection. *Coccidioides* spores, which range in size from 2 to 4 μm, are inhaled into the lungs where they can establish a pulmonary infection (Lubarsky and Plunkett 1955; Drutz, Huppert et al. 1981; Johannesson, Kasuga et al. 2006; Hung, Xue et al. 2007). In order to produce progeny cells, the mother cell enlarges and undergoes many rounds of nuclear division, producing a mutli-nucleate spherule that is as large as 60 to 100 μm (Lubarsky and Plunkett 1955; Drutz, Huppert et al. 1981; Johannesson, Kasuga et al. 2006; Hung, Xue et al. 2007). The spherule is encased in a lipid rich outer wall and contains a large vacuole in the center, which likely provides turgor pressure or nutrient

storage (Cole, Kirkland et al. 1988; Hung, Ampel et al. 2000). As the spherule matures, cleavage planes divide the nuclei into individual cells. Once fully matured, the spherule erupts and releases the progeny cells into the host (Lubarsky and Plunkett 1955; Drutz, Huppert et al. 1981; Johannesson, Kasuga et al. 2006; Hung, Xue et al. 2007). Each spherule can produce 200 to 300 progeny cells, which are small enough to be phagocytosed. However, the production of a large numbers of cells may overwhelm the host immune response and promote the survival of many of these small cells in the lungs (Drutz and Huppert 1983).

Pneumocystis species also produce large progeny filled cysts. Approximately 90-95% of cells in the lungs during *Pneumocystis* infections are trophic cells (Aliouat-Denis, Martinez et al. 2009). Fusion of two trophic cells is the first step in the formation of cysts (Matsumoto and Yoshida 1984; Smulian, Sesterhenn et al. 2001). The fused cells then undergo several rounds of meiosis and mitosis, producing four to eight daughter cells encased in a β-(1,3)-glucan rich cyst that is approximately 4-7 μm in diameter (Cushion 2004; Aliouat-Denis, Martinez et al. 2009). Eventually, the cyst ruptures and releases the daughter cells into the pulmonary environment (Matsumoto and Yoshida 1984; Cushion 2004). While, the exact signal that induces *Pneumocystis* cyst formation is unknown, evidence suggests that pheromone signaling and mating may regulate morphological changes. Identification of the Ste2 and Ste3 pheromone receptor genes, homologous to those found in *Saccharomyces*, suggest that pheromone signaling may induce trophic cell fusion (Matsumoto and Yoshida 1984; Smulian, Sesterhenn et al. 2001). However, due to the inability to culture *Pneumocystis in vitro*, studies of pheromone signaling are limited.

Formation of *Coccidioides* spherules can be stimulated by a number of conditions in the host (Hung, Xue et al. 2007). Early studies showed that switching temperature from 30°C to 39°C in the presence of 20% CO_2 can stimulate the production of spherules *in vitro* (Breslau and Kubota 1964). Much like morphological switching in the other pathogenic fungi, spherule formation can be stimulated in the presence of serum (Lubarsky and Plunkett 1955). Interestingly, spherule formation can also be stimulated by the presence of some host derived hormones including 17β-estradiol, progesterone and testosterone (Drutz, Huppert et al. 1981), suggesting that the sex of the host may influence the infectious cycle in *Coccidioides*.

Increased fungal cell size can have a number of effects on host-pathogen interactions. First, increased cell size may protect fungal cells from phagocytosis. Alveolar macrophages can range in size from 10-20 μm in diameter, depending on species and may not be able to engulf large spherules, which can be as large as 60-100 μm in diameter(Krombach, Munzing et al. 1997). *Coccidioides* spherules also exhibit increased resistance to oxidative and nitrosative stress when compared to conidia (Galgiani 1986). Thus, cell enlargement is accompanied by other mechanisms to protect cells from the host immune assault.

When spherules are produced in *Coccidioides*, the content of the cell wall changes, resulting in the production of a lipid rich spherule outer wall (SOW), which contains a glycoprotein called SOWgp that is the primary antigen that stimulates a T-cell response to *Coccidioides* (Hung, Ampel et al. 2000; Hung, Yu et al. 2002). Interestingly, studies have shown that although SOWgp stimulates a strong inflammatory response

(Cole, Kirkland et al. 1988; Cole and Kirkland 1993; Hung, Ampel et al. 2000), it produces a Th2 response that is ineffective against coccidiomycosis (Cole, Xue et al. 2006) . In addition to modulating the immune response, SOWgp binds to the host extra cellular matrix (Hung, Yu et al. 2002), suggesting that it may play a role in colonization of the pulmonary tissue and establishment of infection.

Interestingly, the cysts produced by *Pneumocystis* contain increased β-(1,3)-glucan in the cyst walls. The increase in β-(1,3)-glucan is able to stimulate the immune system through dectin-1 (Brown and Gordon 2001; Saijo, Fujikado et al. 2007). While the increase in β-glucan may enhance recognition of *Pneumocystis* by macrophages, they can also interact with surfactant protein D in the lungs, causing aggregation of fungal cells and resistance to phagocytosis due to the size of aggregated cells (Yong, Vuk-Pavlovic et al. 2003) and can enhance pathogenesis (Vuk-Pavlovic, Mo et al. 2006). More recent evidence suggests that *Pneumocystis* cysts are the infectious particle. When animals infected with *Pneumocystis* are treated with drugs that target the cysts, they are unable to transmit the infection (Cushion, Linke et al. 2010). Interestingly, *Pneumocystis* cysts are susceptible to different antibiotics than are the trophic cells found in the lungs (Cushion, Linke et al. 2010). These data suggest that cell morphology and the alterations in protein expression upon morphogenesis may be able to confer antifungal drug resistance. It is therefore possible that morphogenesis in other pathogenic fungi may also exhibit differential antifungal drug resistance.

The production of multinucleate enlarged cysts or spherules is a mechanism by which fungi like *Coccidioides* and *Pneumocystis* can evade phagocytosis and produce

large numbers of daughter cells. Like the other morphological changes that are observed in the human pathogenic fungi, cell enlargement is stimulated by a variety of host conditions including serum, temperature, and carbon dioxide levels. Treatment options that target enlarged cells may limit fungal cell proliferation during infection and prevent severe disease.

Morphological Changes in *Cryptococcus neoformans*

Cryptococcus neoformans can be isolated from soil and has been shown to associate with various tree and bird species. *C. neoformans* undergoes several different morphological transitions: filamentous growth and spore production during mating (**Figure 1.2**), capsule production under host conditions (**Figure 1.1E, 1.3A**), and cell enlargement in the host pulmonary environment (**Figure 1.1E**).

Under mating inducing conditions, *C. neoformans* undergoes a yeast to hyphal transition, producing elongated hyphae that terminate in basidia, followed by the production of spores that form from the basidia (Heitman and American Society for Microbiology. 2011). Mating type has been identified as a virulence factor in *C. neoformans* (Nielsen, Cox et al. 2005). There are two cryptococcal mating types: **a** and α, and the vast majority of clinical isolates are mating type α.(Kwon-Chung, Edman et al. 1992; Heitman and American Society for Microbiology. 2011). Like morphological switching in the other fungal pathogens, environmental sensing can induce mating and morphological changes. Growth on V8 juice media or some media containing inositol stimulates mating (Kent, Ortiz-Bermudez et al. 2008; Heitman and American Society for

Microbiology. 2011). Inositol, which can be found in various plant materials, induces mating and suggests that the surface of plant leaves may be the natural niche for cryptococcal mating (Xue, Tada et al. 2007; Xue, Liu et al. 2010). *C. neoformans* is commonly associated with pigeons and pigeon guano, growth on media made from pigeon guano stimulates robust mating, suggesting another environmental niche (Nielsen, De Obaldia et al. 2007). Interestingly, host conditions including increased temperature and high levels of CO_2 suppress mating (Sia, Lengeler et al. 2000; Heitman and American Society for Microbiology. 2011), suggesting that mating cannot occur during *C. neoformans* infections in mammalian hosts.

Pheromones are produced by both mating types (Davidson, Moore et al. 2000). When in close proximity, pheromone binds to the pheromone receptor on the cell surface of the opposite mating type (Chung, Karos et al. 2002; Chang, Miller et al. 2003). Sensing of pheromone induces a mitogen activated protein kinase (MAPK) signaling cascade that regulates the events of mating (Chung, Karos et al. 2002; Chang, Miller et al. 2003; Davidson, Nichols et al. 2003; Hsueh, Xue et al. 2007).Upon pheromone sensing, cell fusion is induced (**Figure 1.2A**), resulting in an enlarged dikaryon (Heitman and American Society for Microbiology. 2011). The dikaryon begins to form long septated hyphae (Heitman and American Society for Microbiology. 2011). Each cell of the hyphae maintains two nuclei until later stages of mating (Heitman and American Society for Microbiology. 2011). The hyphae eventually produce round basidia at their ends, where nuclear fusion takes place (Heitman and American Society for Microbiology. 2011). After fusion, the nuclei undergo several rounds of meiosis and mitosis and

produce chains of haploid spores (**Figure 1.2A, B**) (Heitman and American Society for Microbiology. 2011). The spores are then able to be released into the environment.

In the spore morphology, *C. neoformans* is more resistance to harsh environmental conditions. Cryptococcal spores were evaluated for their resistant to a number of environmental stresses that may be encountered in nature. Exposure of spores to high temperature, oxidative stress, chemical exposure to diethyl ether, and desiccation all showed that spores are more resistant compared to yeast cells (Botts, Giles et al. 2009). The surface of cryptococcal spores has a high β-(1,3)-glucan content, suggesting that spores are easily phagocytosed upon entry into the pulmonary environment (Botts, Giles et al. 2009). Spores are able to germinate inside of macrophages and can eventually escape via non-lytic exocytosis (Giles, Dagenais et al. 2009), suggesting that the macrophage may be a protected environment for germination and may provide the nutrients necessary for germination. When spores are used as an inoculum, the differences in early host-pathogen interactions compared with yeast cells may also influence later outcomes of infection, including improved penetration of the blood brain barrier (Botts, Ersland et al. 2011).

C. neoformans also produces a polysaccharide capsule in response to the host environment (**Figure 1.1E, 1.3A**). Cryptococcal capsule can be identified by microscopy using india ink staining, appearing as a clear halo around the body of the cell (**Figure 1.3A**). The capsule is primarily made up of two major components: glucuronoxylomannan (GXM) and galactoxylomannan (GalXM) (Cherniak 1988; Cherniak, Valafar et al. 1998). Capsule production is required for virulence in

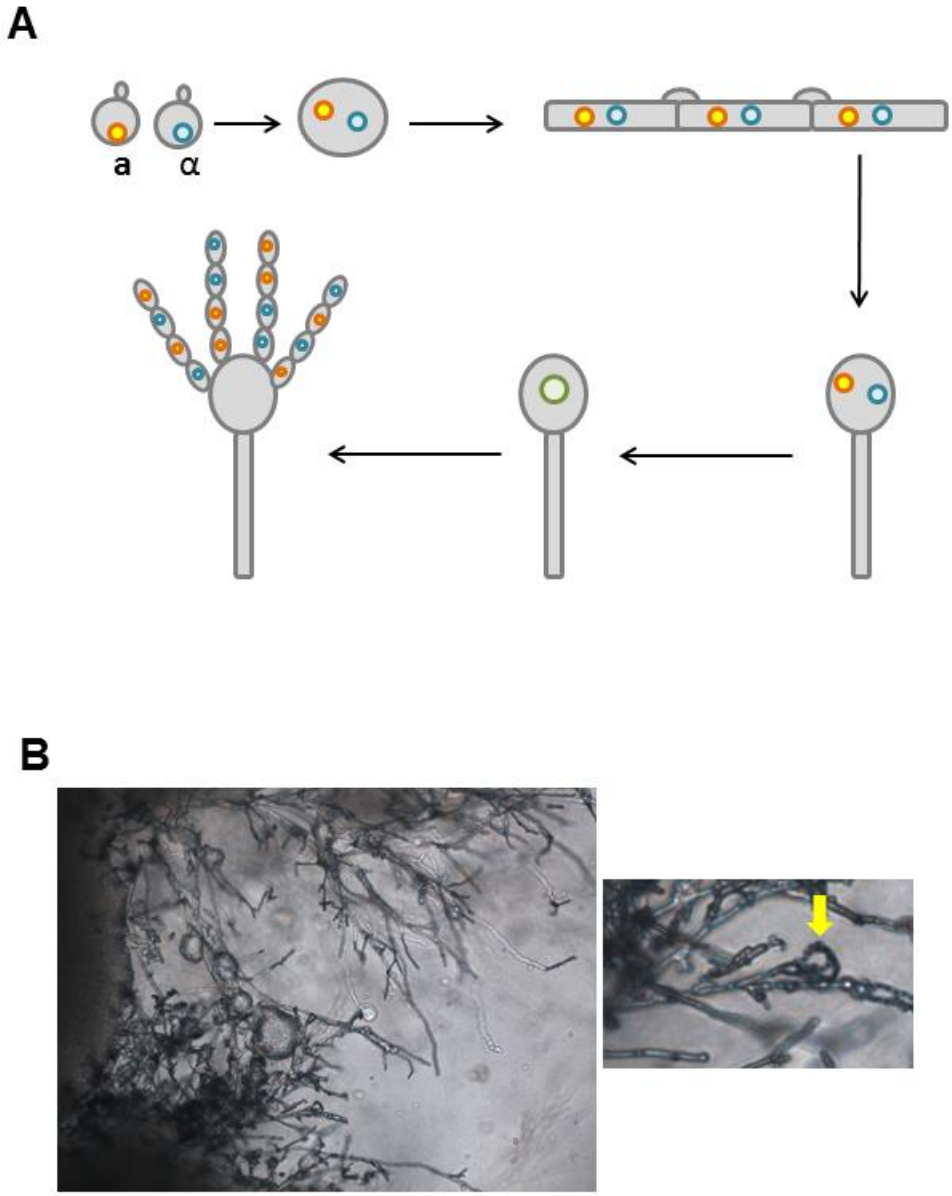

Figure 1.2 Mating in *Cryptococcus neoformans.*

A) Mating in *C. neoformans* begins when pheromone signaling induce haploid mating type **a** and mating type α cell fusion. After the dikaryon is formed, *C. neoformans* begins to form long dikaryon hyphae. The hyphae produce a basidium where the nuclei undergo fusion. The nuclei then undergo meiosis and mitosis to produce chains of haploid spores.

B) Left: Hyphal formation during mating on V8 media. Right: Basidium and spore chains indicated by the yellow arrow.

C. neoformans, and strains that are defective in capsule production are avirulent (Bulmer, Sans et al. 1967; Kozel and Cazin 1971; Fromtling, Shadomy et al. 1982; Chang and Kwon-Chung 1994; Chang, Penoyer et al. 1996; Chang, Cherniak et al. 1997; Chang and Kwon-Chung 1998; D'Souza, Alspaugh et al. 2001; Wilder, Olson et al. 2002). Capsule production is stimulated at 37°C and in the presence of serum (Jacobson and Compton 1996; Zaragoza, Fries et al. 2003). Like morphological changes in other fungi, the presence of CO_2 can also induce capsule production (Granger, Perfect et al. 1985; Zaragoza, Fries et al. 2003). Iron limitation, a condition found in the mammalian host, has been shown to increase production of capsule (Lian, Simmer et al. 2005). Interestingly, the structure of capsular components can change over the course of infection (Turner, Cherniak et al. 1992; Cherniak, Morris et al. 1995; Garcia-Hermoso, Dromer et al. 2004; McFadden, Fries et al. 2007), and may play different roles at different stages of infection.

The polysaccharide capsule is the primary antigen produced by *C. neoformans* and modulates the immune response by binding opsonins like antibodies and complement C3. During synthesis, cryptococcal capsule is added via distal elongation of the capsule, thus new capsule is on the outside while the older capsule material is closer to the cell surface (Zaragoza, Telzak et al. 2006). Once C3 is bound to the capsule and surface of the cell, new capsule material can then cover, or mask, the C3 from interaction with the C3 receptors on the surface of macrophages (Zaragoza, Taborda et al. 2003; Gates and Kozel 2006; Zaragoza, Telzak et al. 2006). Interaction of *C. neoformans* with C3 is important in activation of the immune response via the alternative complement pathway (Laxalt and Kozel 1979; Kozel, Wilson et al. 1991). Capsule has been shown to play a role in depleting C3 in the host sera during advanced infection (Macher, Bennett et al. 1978). Such

complement C3 depletion may result in reduced ability for the host to fight advancing cryptococcosis. Modulation of the immune response by capsule material also includes induction of host cell apoptosis. In both macrophages and in T-cells, *C. neoformans* capsule can induce cell death via Fas/FasL binding and caspase 8 induction (Pericolini, Cenci et al. 2006; Villena, Pinheiro et al. 2008). *C. neoformans* is able to survive inside host macrophages after phagocytosis (Levitz, Nong et al. 1999; Feldmesser, Kress et al. 2000) and may have mechanisms to survive killing that are mediated by the capsule. It has also been shown that during macrophage parasitism, *C. neoformans* capsule induces formation of polysaccharide filled vacuoles that disrupt host cell functions (Feldmesser, Kress et al. 2000; Alvarez and Casadevall 2006) and infection with acapsular strains did not induce vacuole formation (Feldmesser, Kress et al. 2000). Capsule appears to permeablize the host vesicles during intracellular parasitism and prevents the decrease in pH necessary for antimicrobial activity. Thus, capsule disrupts the ability of the host phagocytes to kill phagocytosed cryptococcal cells.

This dissertation focuses on a novel cell morphology in *C. neoformans* that can alter host-pathogen interactions. As early as the 1970s, enlarged cryptococcal cells were observed in human sputum samples and in the animal model of cryptococcosis (Cruickshank, Cavill et al. 1973). Upon exposure to the host pulmonary environment, a subset of cryptococcal cells in the lungs produce enlarged “titan” cells (Okagaki, Strain et al. 2010; Zaragoza, Garcia-Rodas et al. 2010). Approximately 20% of the cryptococcal cells grow to be as large as 50-100 μm in diameter, 5-10 fold larger than a typical cell (Okagaki, Strain et al. 2010).

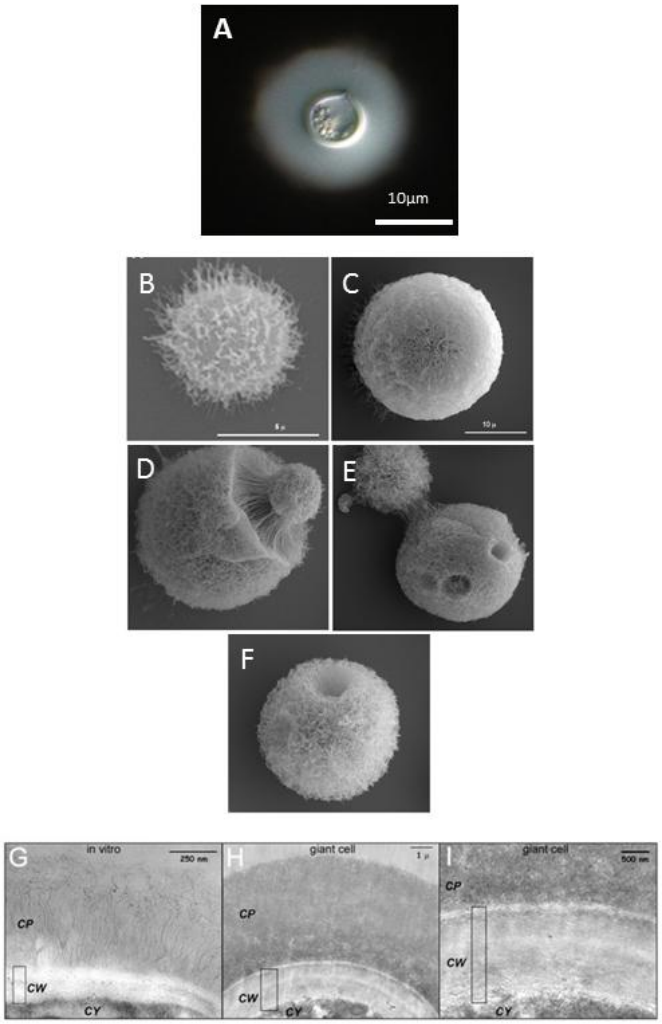

Figure 1.3 Capsule and Cell Wall in *Cryptococcus neoformans* Images B-I were previously published in (Zaragoza, Garcia-Rodas et al. 2010). Permission was generously granted by Oscar Zaragoza and Arturo Casadevall.

A) India ink staining of a normal-sized cryptococcal cell. The ink is excluded from the capsule, resulting in a clear halo of around the cell.
B) SEM of a normal-sized cell.
C) SEM of a titan cell.
D) SEM of a titan cell undergoing cell division.
E) SEM of a titan cell undergoing cell division.
F) SEM of a titan cell after cell division. Budding leaves a "tunnel" in the capsule material.
G) TEM of the cell wall of a normal-sized cryptococcal cell.
H) TEM of the cell wall of a titan cell.
I) TEM of the cell wall of a titan cell.

Titan cells have several characteristics that differentiate them from normal-sized cells. When observed by differential interference contrast (DIC) microscopy, titan cells appear to have a large vacuole that can make up 80% or more of the cell volume ((Zaragoza, Garcia-Rodas et al. 2010) and Chapter 2). Titan cells have an altered capsule structure, which appears highly cross-linked and cannot be sheared from the cryptococcal cell by chemical or physical methods (**Figure 1.3B, C, D, E**) (Zaragoza, Garcia-Rodas et al. 2010). In addition, when observed by transmission electron microscopy (TEM), the cell wall of titan cells is approximately 30-50 fold thicker than the cell wall of normal-sized cells (**Figure 1.3G, H, I**) (Zaragoza, Garcia-Rodas et al. 2010). Thus, titan cells have several barriers that may help protect the cells from various types of antimicrobial activities produced by the host immune response.

Titan cell production is primarily produced in the lungs, and titan cells are rarely observed in other host tissues even at late stages of infection (Chapter 2). Titan cells are more resistant to phagocytosis, and can confer protection from phagocytosis to non-titan cells during pulmonary infection (Chapters 2 and 4). In addition, titan cells are more resistant to the nitrosative and oxidative stresses produced by the host immune response (Chapter 2).

Unlike the cell enlargement observed in *Coccidioides* and *Pneumocystis*, titan cells contain only a single nucleus and do not contain multiple daughter cells (Chapter 2). However, titan cells do exhibit high ploidy, and are tetraploid or octoploid when analyzed by flow cytometry (Chapter 2). In addition, microscopic and video analysis revealed that

titan cells are actively dividing and produce normal-sized daughter cells by budding (Okagaki, Strain et al. 2010; Zaragoza, Garcia-Rodas et al. 2010).

C. neoformans undergoes several morphological transitions: yeast to hyphal transition during mating that results in spore formation, capsule production, and titan cell production, the major focus of this thesis. Each of the morphological changes provides a different advantage for *C. neoformans* in the host. Even though mating doesn't occur in the host, mating is a mechanism that promotes genetic diversity within the population of environmental *C. neoformans* (Heitman and American Society for Microbiology. 2011). More recently, mating has been suggested as a mechanism for genome stability, where cell-cell fusion during mating results in gene redundancy, which can protect the genome from deleterious mutations (Comai 2005; Storchova, Breneman et al. 2006). In addition, mating results in cryptococcal spores, which are more resistant to harsh environmental conditions and appear to be effective at establishing pulmonary infection. Titan cell production protects cells from phagocytosis by alveolar macrophages once they are inside the host lungs (Chapter 2 and 4). Thus, morphological changes in *C. neoformans*, including capsule production, titan cell production, and spore formation can promote survival in the host and promote overall virulence.

II. SIGNALING PATHWAYS THAT REGULATE MORPHOLOGICAL SWITCHING

Virulence in the human pathogenic fungi is regulated by many pathways that have components that are conserved between species. Environmental signals including

temperature, pH, CO_2, and soluble factors like serum have been shown to induce the production of virulence factors. A common pathway shown to regulate virulence in organisms like *C. albicans* and *C. neoformans* is the cAMP/PKA pathway. Cyclic AMP (cAMP) is a small messenger molecule that regulates the activity of some kinases including protein kinase A (PKA). Changes in the host environment induce cAMP/PKA signaling and regulate morphological changes in many of the pathogenic fungi. In addition, cAMP/PKA signaling and downstream transcription factors regulate several virulence factors in fungi, including virulence factors in *C. neoformans*.

PKA Signaling

PKA signaling has been well characterized in *Saccharomyces cerevisiae*. Stimulation by glucose, carbon and nitrogen sensing as well as other stimuli, induces PKA signaling in *S. cerevisiae*. The G-protein coupled receptor (GPCR) Gpr1 is activated by binding glucose (Tamaki 2007; Nazarko, Thevelein et al. 2008). Upon binding, Gpr1 activates adenylyl cyclase via the Gα subunit Gpa2 (Harashima, Anderson et al. 2006). Adenylyl cyclase converts ATP to cAMP, which is a secondary messenger molecule. Downstream of adenylyl cyclase, PKA is made up of several subunits including Tpk1 and Tpk2, and the regulatory subunit PKR (protein kinase regulator, also known as Bcy1) which contains several cAMP binding sites (Tamaki 2007; Rinaldi, Wu et al. 2010). Before PKA signaling is initiated, PKR is bound to PKA, inhibiting the activity of PKA. Upon activation of PKA signaling, cAMP is produced and binds to the cAMP binding sites on PKR. cAMP binding releases PKR from PKA, activating PKA for the

phosphorylation of downstream targets. (Tamaki 2007). PKA is then able to phosphorylate transcription factors that regulate the stress response (Tamaki 2007). Glucose signaling via cAMP and PKA in *S. cerevisiae* regulates cell size increases and is thought to act by altering the cell cycle (Tamaki, Yun et al. 2005).

In *C. albicans* and *C. neoformans*, the receptors that induce cAMP signaling have not been fully identified; however, current data suggests that many signals may induce cAMP production by adenlylyl cyclase. In *C. albicans*, serum, which induces hyphal growth, can stimulate PKA signaling (**Figure 1.3A**) (Cloutier, Castilla et al. 2003; Maidan, De Rop et al. 2005), possibly through the Gα protein Gpa2 and the Ras proteins (Maidan, De Rop et al. 2005) . More recently, the heat shock protein Hsp90 has been shown to regulate PKA signaling in response to temperature changes (Shapiro, Uppuluri et al. 2009).

The cAMP/PKA pathway has been implicated in regulation of capsule production in *C. neoformans* (D'Souza, Alspaugh et al. 2001; Bahn, Hicks et al. 2004; Pukkila-Worley, Gerrald et al. 2005; Xue, Bahn et al. 2006; Shen, Wang et al. 2008). Cryptococcal Gpr4 has been shown to regulate the PKA pathway in response to methionine sensing, and Gpr1 regulates the expression of many cryptococcal virulence factors via the PKA pathway including capsule and melanin (**Figure 1.3B**) (Alspaugh, Perfect et al. 1997; Xue, Bahn et al. 2006). PKA signal transduction in *C. neoformans* uses the Gα protein Gpa1 (Alspaugh, Perfect et al. 1997). Downstream of Gpa1, the cryptococcal adenylyl cyclase, Cac1, produces cAMP. Disruption of Cac1 results in acapsular and avirulent strains of *C. neoformans* (Alspaugh, Perfect et al. 1997; D'Souza,

Alspaugh et al. 2001; Alspaugh, Pukkila-Worley et al. 2002; Pukkila-Worley, Gerrald et al. 2005). Studies have also revealed that CO_2 sensing in *C. neoformans* is also mediated by Cac1 (Klengel, Liang et al. 2005). The exact environmental stimulus that induces titan cell production in *C. neoformans* has not been identified, however, a host factor, possibly phospholipids, may induce titan cell production (Okagaki, Strain et al. 2010). Signaling via the cAMP/PKA pathway in *C. neoformans* has been shown to regulate titan cell production in addition to the production of capsule and melanin (Chapter 3).

Regulation of the filament to yeast transition is regulated in a number of the dimorphic fungi by the amount of endogenous cAMP, but components of the PKA pathway are not well characterized. *P. marneffei* has three Gα subunits that are upstream of the PKA pathway, and there is evidence that the PKA pathway is critical for inhibiting asexual development and promoting conidia germination upon entry into the host environment (Zuber, Hynes et al. 2002; Zuber, Hynes et al. 2003). Deletion of the Gα protein GasA, which results in the inability for *P. marneffei* to produce conidia, can be reversed by the addition of exogenous cAMP (Zuber, Hynes et al. 2002). In *P. brasiliensis*, increased levels of cAMP result in reduced switching to the yeast form (Chen, Janganan et al. 2007), while in *S. schenckii* cAMP has been shown to stabilize the yeast form in filamentous growth favoring conditions (Rodriguez-Del Valle, Debs-Elias et al. 1984). However, in *H. capsulatum*, it appears that the opposite is true, that increased levels of cAMP during incubation of yeast at 37°C can stimulate switching to the filamentous form. During this yeast to filament transition in *H. capsulatum*,

Figure 1.4

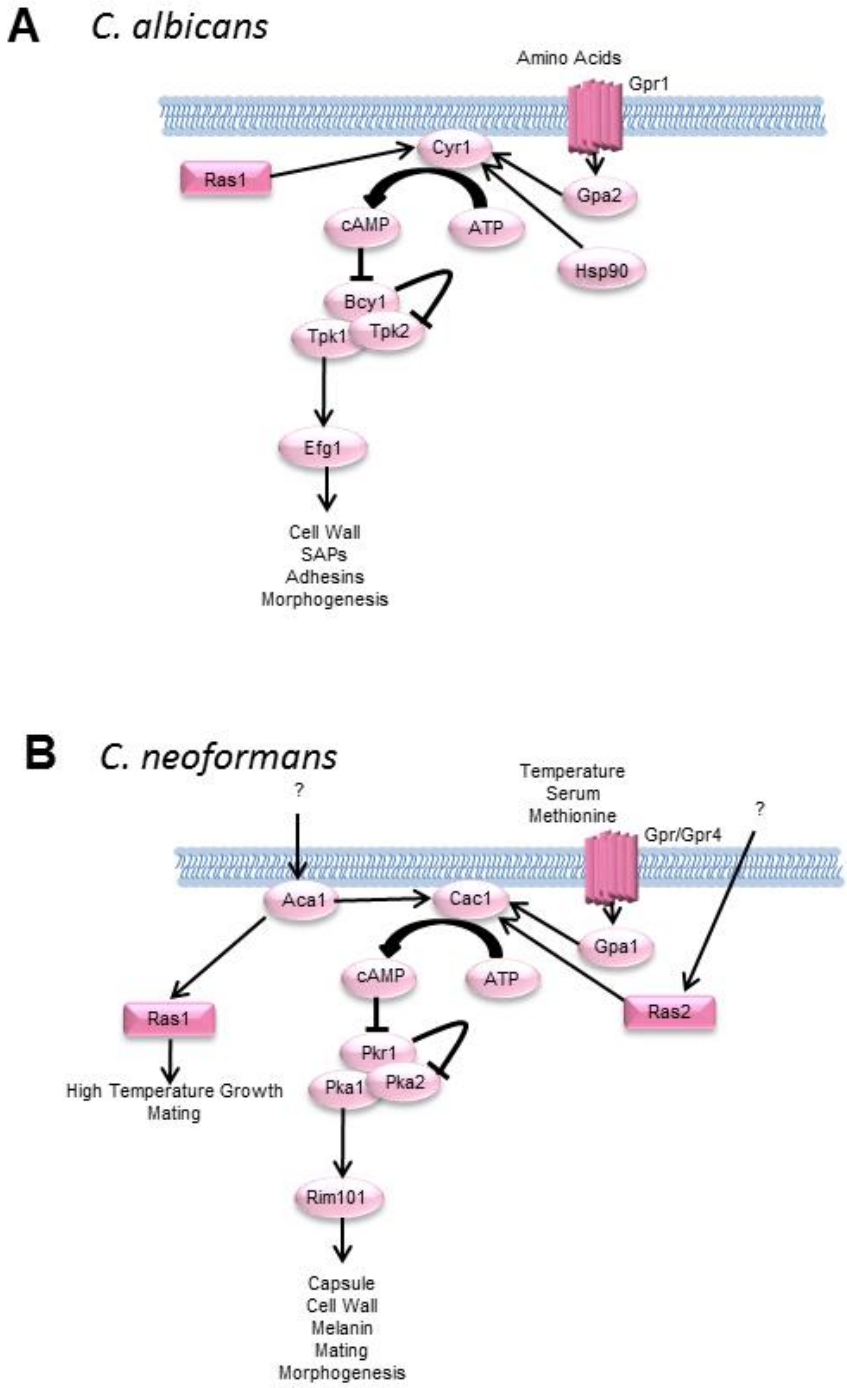
A C. albicans
Amino Acids
Gpr1
Cyr1
Ras1
Gpa2
cAMP
ATP
Hsp90
Bcy1
Tpk1
Tpk2
Efg1
Cell Wall
SAPs
Adhesins
Morphogenesis
B C. neoformans
?
Temperature
Serum
Methionine
?
Gpr/Gpr4
Aca1
Cac1
Gpa1
cAMP
ATP
Ras1
Ras2
Pkr1
Pka1
Pka2
High Temperature Growth
Mating
Rim101
Capsule
Cell Wall
Melanin
Mating
Morphogenesis

Figure 1.4 cAMP/PKA Signaling in the Pathogenic Fungi.
PKA signaling via the second messenger molecule cAMP is conserved in the pathogenic fungi and regulates morphological changes and virulence.

A) In *C. albicans*, multiple environmental signals including serum induce cAMP signaling. ATP is converted to cAMP upon activation of adenylyl cyclase (Cry1). cAMP then binds to the PKA regulatory protein Bcy1. Upon cAMP binding, Bcy1 is released from the PKA subunits Tpk1 and Tpk2, activating the kinase activity of the subunits. The PKA subunits then activate the transcription factor Efg1, which regulates expression of hyphal proteins including cell wall components and secreted aspartyl proteases.
B) In *C. neoformans*, methionine and other environmental stimuli activate PKA signaling through the Gα protein Gpa1. Cac1 is activated by Gpa1 and converts ATP to cAMP. Like cAMP signaling in *C. albicans*, Pkr1 is released from the PKA subunits when bound to cAMP. Downstream of PKA is the transcription factor Rim101, which regulates morphogenesis, cell wall, capsule, and nutrient acquisition genes.

extracellular cAMP levels were observed to increase 15-50 fold more than what is observed in the yeast form (Medoff, Jacobson et al. 1981).

The PKA pathway and cAMP signaling are conserved in the human pathogenic fungi as major regulators of virulence. In many of the fungi, PKA signaling or the addition of exogenous cAMP induces morphological changes and other virulence factors. It is unlikely that the PKA pathway can be targeted for drug therapeutics because similar proteins are ubiquitous in mammalian hosts. However, studying the components of PKA signaling may be a tool to identify novel virulence factors in the pathogenic fungi.

Transcription Factors

Downstream of PKA are the transcription factors Egf1 in *C. albicans* and Rim101 in *C. neoformans*. Efg1 activity up-regulates the transcription of several hyphal specific gene groups that are important in virulence, including hyphal wall proteins and secreted aspartyl proteases (Bockmuhl and Ernst 2001; Leng, Lee et al. 2001; Sohn, Urban et al. 2003). Rim101 activation in *C. neoformans* alters a large subset of genes that are important for the synthesis and attachment of capsule to the cell wall and iron acquisition (O'Meara, Norton et al. 2010). More recently, Rim101 has been shown to be a major transcription factor that regulates titan cell production (Chapter 3).

Rim101 signaling in *C. albicans* regulates pH response ((Davis, Edwards et al. 2000) and reviewed in (Davis 2009)). Unlike the *C. neoformans* Rim101, *C. albicans* Rim101 is not downstream of the Pka pathway (Davis, Edwards et al. 2000; Davis 2009). Instead, upon exposure to alkaline environments, the surface receptors, Dfg16 and

Rim21, become activated (Barwell, Boysen et al. 2005). It has been hypothesized that signaling through these receptors induces the ubiquitination of Rim8, which ultimately leads to Rim20 and Rim13 recruitment to the inactive Rim101, resulting in Rim13 cleavage of Rim101 to its active form (Li, Martin et al. 2004; Gomez-Raja and Davis 2012),however, this has yet to be shown in *C. albicans.s* Rim101 is then able to activate transcription of a number of hyphal specific genes including adhesion molecules, proteases, and proteins involved in nutrient acquisition (Bensen, Martin et al. 2004). The pathway has not been fully characterized in *C. neoformans*, but several components of the Rim101 pathway have been identified, including Rim20.

In some of the dimorphic fungi, the regulators of morphological switching have been identified. In *Histoplasma* and *Blastomyces* the master regulator of morphological switching is DRK1 (dimorphism regulator kinase 1). DRK1 is required for the transition to yeast phase, disruption of DRK1 locks *Histoplasma* and *Blastomyces* in the filamentous form (Nemecek, Wuthrich et al. 2006). DRK1 may also regulate a number of yeast-phase virulence factors such as calcium binding proteins and α-(1,3)- glucan in addition to affecting cellular morphology (Nemecek, Wuthrich et al. 2006).

Histoplasma has a group of morphology transition transcription factor genes in addition to DKR1 called the RYP genes (required for yeast phase). Culturing *Histoplasma* at 37°C up-regulates the production of RYP gene transcripts (Nguyen and Sil 2008; Webster and Sil 2008). Microarray experiments showed that the RYPs are responsible for regulation of about 98% of yeast-phase genes (Nguyen and Sil 2008). Evidence suggests that RYP genes can regulate the expression of other members of the

same family; some can bind to their own promoter regions, creating a positive feedback loop (Nguyen and Sil 2008). In *P. marneffei* and *S. schenckii*, several transcription factors have been identified that affect development and growth, however no major regulators of the filament to yeast transition have been identified.

In *C. albicans* phenotypic switching, there is one master regulator called Wor1 (white-opaque regulator 1) that is a homologue of the *Histoplasma* transcription factor RYP. (Zordan, Galgoczy et al. 2006). Expression of *WOR1* is increased to significantly higher concentrations in opaque cells compared with white cells (Huang, Wang et al. 2006; Zordan, Galgoczy et al. 2006). Wor1 is able to bind to its own promoter region, stimulating additional expression of the Wor1 protein (Huang, Wang et al. 2006; Zordan, Galgoczy et al. 2006). Thus *WOR1* expression is under a positive feedback loop, allowing for the stabilization of the opaque morphology. It has been suggested that cells that experience a slower cell cycle, such as those exposed to genotoxic stress may accumulate higher levels of Wor1, thus inducing switching to the opaque form (Alby and Bennett 2009).

Virulence factors, including cell morphology, in the human pathogenic fungi are regulated by conserved signaling pathways and transcriptional regulators. It may be possible to target the fungal specific transcription factors required for virulence as novel drug targets. Understanding transcription factors required for fungal virulence may also lead to the identification of novel virulence factors.

III. ACQUISITION AND PATHOGENESIS OF *CRYPTOCOCCUS NEOFORMANS*

Cryptococcus neoformans undergoes several different morphological changes in response to its environment. The yeast to hyphal switch and subsequent spore formation during mating is a mechanism to create genetic diversity through meiosis and mitosis, as well as the production of hearty spores that can survive harsh environmental conditions (Heitman and American Society for Microbiology. 2011). Once inhaled into the lungs, *C. neoformans* produces polysaccharide capsule, which modulates the immune response (Heitman and American Society for Microbiology. 2011). In addition, the host pulmonary environment stimulates the production of cryptococcal titan cells (Chapter 2). *C. neoformans* has become a major disease causing microbe, thus, long term studies of *C. neoformans* titan cell production are focused on understanding how titan cells affect virulence and the outcome of cryptococcal disease.

Cryptococcosis

C. neoformans is an opportunistic fungal pathogen (Heitman and American Society for Microbiology. 2011). Like many of the other pathogenic fungi, cryptococcosis is acquired from the environment when spores or desiccated yeast cells are aerosolized and inhaled by the host (Heitman and American Society for Microbiology. 2011). *C. neoformans* is able to establish a pulmonary infection in the alveoli of the lungs (Heitman and American Society for Microbiology. 2011). During early pulmonary infection, *C. neoformans* produces titan cells in response to the host environment (Chapter 2). At later stages of infection, *C. neoformans* escapes the lungs and

circulates throughout the body in the blood or lymph systems (Heitman and American Society for Microbiology. 2011). At late stages of infection, *C. neoformans* penetrates the blood brain barrier where it can proliferate and cause meningitis (Heitman and American Society for Microbiology. 2011).

Cryptococcosis is typically diagnosed in HIV+ patients when their CD4+ T-cell count drops below 100 cells/dL, and in many patients cryptococcosis is an AIDS defining illness (Heitman and American Society for Microbiology. 2011). Recent epidemiological studies estimated that approximately one million people are diagnosed with cryptococcosis per year, and of those about 600,000 are expected to succumb to the infection (Park, Wannemuehler et al. 2009). Patients primarily present with headache, which is indicative of the meningitis stage of infection (Heitman and American Society for Microbiology. 2011). Upon diagnosis, patients are treated with a combination of antifungal drugs that includes amphotericin B and fluconazole (Heitman and American Society for Microbiology. 2011). The development of antifungal drug resistance in some pathogenic fungi, including *C. neoformans* and *C. albicans*, has been attributed to altered ploidy. Titan cells contain four to eight copies of the cryptococcal genome, while *in vitro* grown *C. neoformans* is haploid. Thus, titan cells may contribute to antifungal drug resistance in *C. neoformans*.

Cryptococcal Virulence Factors

There are several cryptococcal virulence factors that promote survival in the pulmonary environment: capsule, melanin, urease, and growth at high temperatures. Capsule plays a critical role in the modulation of the immune system. Protection from the oxidative and nitrosative stress is also conferred by the dark pigment melanin. Synthesis of melanin is regulated by the laccase gene group and can be induced on media containing L-dopa (Heitman and American Society for

Microbiology. 2011). Urease has been shown to be critical for the pathogenesis of *C. neoformans* and is important in the penetration of the blood brain barrier (Olszewski, Noverr et al. 2004). *C. neoformans* is a facultive intracellular parasite and can survive inside of the phagolysosomes of host phagocytes (Heitman and American Society for Microbiology. 2011). Production of both melanin and urease are able to protect the cryptococcal cells from the antimicrobial activity of the phagolysosome and promote survival and proliferation (Heitman and American Society for Microbiology. 2011). More recently, cell morphology had been implicated as a novel virulence factor (Chapter 2, 3, 4), affecting host-pathogen interactions and the penetration of the blood brain barrier.

Host-Pathogen Interactions

C. neoformans first interacts with the resident alveolar macrophages after inhalation. Phagocytosis and subsequent survival inside of macrophages appears to be required for disease progression and efficient dissemination from the lungs (Charlier, Nielsen et al. 2009). Chemical depletion of phagocytes resulted in reduced penetration of blood-brain barrier (Luberto, Martinez-Marino et al. 2003; Del Poeta 2004). Injection of mice with pre-phagocytosed cryptococcal cells increased the efficiency of the development of CNS infection (Charlier, Nielsen et al. 2009). Acapsular strains of *C. neoformans* are quickly recognized by mannose and glucan receptors (Heitman and American Society for Microbiology. 2011). The cryptococcal capsule masks the recognizable cell wall components including β-(1,3)-glucan preventing binding to the PRR dectin-1 (Kozel and Gotschlich 1982; Levitz 1991). Capsule polysaccharide is easily shed into the host environment and at later stages of infection can be detected in

the peripheral blood (Heitman and American Society for Microbiology. 2011). Free capsule material can sequester opsonins in the host, but can also interact with macrophages, preventing them from interacting with fungal cells. C3 bound capsule is recognized by the complement receptor 3 (CR3) which then induces phagocytosis of the cryptococcal cell. In addition to complement binding, *C. neoformans* specific antibodies are present in the sera of the vast majority of the population (Currie and Casadevall 1994). The antibodies are primarily against capsule polysaccharides (Heitman and American Society for Microbiology. 2011). *C. neoformans* opsonized with antibodies are recognized by the Fc receptor on macrophages and are phagocytosed by endocytosis (Heitman and American Society for Microbiology. 2011). The capsule of titan cells is highly cross-linked (**Figure 1.3C, D, E**), and alters interactions between *C. neoformans* and components of the host immune response, including complement and antibody binding (Zaragoza, Garcia-Rodas et al. 2010). Therefore, it is important to understand the overall effects of titan cell production on the host immune response.

There are several possible fates for phagocytosed cryptococcal cells. Studies have shown that activation of a Th1 response is required to induce killing by macrophages (Clemons, Brummer et al. 1994; Joly, Saint-Julien et al. 1994; Kawakami, Kohno et al. 1994; Kawakami, Qifeng et al. 1996; Kawakami, Tohyama et al. 1996; Kawakami, Tohyama et al. 1996; Kawakami, Qureshi et al. 1997; Qureshi, Zhang et al. 1999; Clemons, Lutz et al. 2001). *C. neoformans* has mechanisms by which it can survive intracellularly (Kawakami, Zhang et al. 1997). It has been proposed that the capsule can alter the phagolysosomal membrane and promote membrane permeablization

(Feldmesser, Mednick et al. 2002; Tucker and Casadevall 2002). The disruption of the phagolysosomal membrane results in the eventual killing of the host cells, releasing *C. neoformans* into the environment (Tucker and Casadevall 2002). More recently, it has been shown that *C. neoformans* can induce a non-lytic mechanism for exocytosis, called vomocytosis (Alvarez and Casadevall 2006; Ma, Croudace et al. 2006; Alvarez and Casadevall 2007). Here, cryptococcal cells are taken up by phagocytes and can induce release into the host environment or transfer from cell to cell without destruction of the host cells (Alvarez and Casadevall 2006; Ma, Croudace et al. 2006; Alvarez and Casadevall 2007). Lysed cell materials can induce an inflammatory response, thus, preventing host cell lysis may prevent inflammation.

Increased titan cell production is correlated with decreased penetration of the blood brain barrier in animal models of cryptococcosis (Chapter 2). Besides the host-pathogen interactions in the lungs, interactions at the blood brain barrier influence the outcome of disease. There are two primary hypotheses as to how *C. neoformans* can cross the blood brain barrier: direct transcytosis and the Trojan horse model. To cross the blood brain barrier by direct transcytosis, cryptococcal cells may interact with the vascular endothelial cells in the brain and induce uptake (Chen, Stins et al. 2003). The endothelial cells may then carry the cryptococcal cells across the blood brain barrier and release the yeast cell into the brain. The Trojan horse model suggests that host phagocytes may engulf cryptococcal cells and carry the intracellular yeast cells into the brain (Charlier, Nielsen et al. 2009). Thus, understanding mechanisms that may alter phagocytosis and

penetration of the blood brain barrier at early stages of infection, including titan cell production, could lead to novel drug targets or improved treatment plans.

IV. SUMMARY OF THIS DISSERTATION

The goal of the studies presented in this dissertation was to further examine the enlarged cell morphology observed in *Cryptococcus neoformans* infections, that we have termed the "titan" cell morphology. First, we explored the basic cell biology of titan cells to understand when and how titan cells are formed (Chapter 2). We found that titan cells are primarily produced in the lungs and are rarely found in other tissues during infection. Titan cells are uninucleate, actively replicating, and are tetraploid or octoploid. In addition, titan cells are more resistant to phagocytosis and oxidative/nitrosative stresses. Second, we identified the signaling pathways that regulate the production of titan cells in response to environmental stimuli (Chapter 3). We found that cryptococcal titan cell production is regulated by the GPCRs Gpr5 and Ste3**a**. Our studies show that pheromone signaling in mating type **a** cells is rewired compared to the signaling pathway in mating type α cells; in addition to regulating morphological changes during mating, pheromone signaling in mating type **a** cells regulates titan cell production. We identified Rim101 as a key transcription factor that regulates titan cell formation downstream of the PKA pathway. Finally, we sought to understand the role of titan cells in the pathogenesis of *Cryptococcus neoformans* (Chapter 4). Titan cells are able to confer protection from phagocytosis to normal-sized cells, thus protecting the entire population from the host

immune response. These observations suggest that titan cell formation is a novel virulence factor and is important in the establishment of pulmonary cryptococcosis.

CHAPTER TWO

Cryptococcal Cell Morphology Affects Host Cell Interactions and Pathogenicity

Okagaki LH, Strain AK, Nielsen JN, Charlier C, Baltes NJ, Chrétien F, Heitman J, Dromer F, and Nielsen K.(2010) Cryptococcal Cell Morphology Affects Host Cell Interactions and Pathogenicity. PLoS Pathog 6(6): e1000953.

I. INTRODUCTION

Unicellular organisms exhibit morphological changes under a wide variety of environmental conditions. In many pathogenic fungi, the ability to switch cell morphology is integral to the infection cycle. Dimorphic fungi, such as *Blastomyces dermatitidis* and *Histoplasma capsulatum*, grow in the environment in a hyphal form. When a susceptible host inhales spores, these fungi grow as yeasts. This change in morphology is induced by the high mammalian body temperature (San-Blas, Travassos et al. 2000; Klein and Tebbets 2007; Morrow and Fraser 2009). Other pathogenic fungi, such as *Candida albicans* and *Coccidioides immitis*, change to specific cell morphologies based on environmental cues or stage of infection (Lorenz, Bender et al. 2004; Mavor, Thewes et al. 2005; Hung, Xue et al. 2007). Morphological changes in the pathogenic fungus *C. albicans* affect tissue tropism and dissemination. Hyphal cells are important in the invasion of host tissues, while yeast cells can easily disseminate through the blood and lymph systems to spread the infection (Jayatilake, Samaranayake et al. 2005; Mavor, Thewes et al. 2005). Additionally, phagocytosis of yeast cells induces differentiation into hyphal cells (Lorenz, Bender et al. 2004).

Cryptococcus neoformans is an opportunistic fungal pathogen that is most commonly associated with disease in immunocompromised patient populations, such as HIV/AIDS patients, transplant recipients, patients with lymphoid disorders, chronic treatment with corticosteroids, or patients undergoing certain types of chemotherapies (Currie and Casadevall 1994; Mitchell and Perfect 1995; Perfect and Casadevall 2002). *C. neoformans* infections present clinically as skin lesions, pneumonia, or meningitis

(Casadevall and Perfect 1998). Over 30% of the HIV/AIDS population in Sub-Saharan Africa present with cryptococcal meningitis and cryptococcosis is currently the fifth leading cause of fatalities in this region (Park, Wannemuehler et al. 2009).

Infection with *C. neoformans* begins when desiccated yeast cells or spores are inhaled and lodge in the alveoli of the lungs. Cryptococcosis occurs when yeast cells disseminate to the bloodstream and ultimately penetrate the blood-brain barrier (BBB) (Hull, Davidson et al. 2002; Perfect and Casadevall 2002). While the exact mechanism for trafficking from the lungs to the central nervous system (CNS) remains unknown, interactions with host phagocytes and the endothelial cells of the BBB have been shown to be important in this process (Levitz, Nong et al. 1999; Feldmesser, Tucker et al. 2001; Chen, Stins et al. 2003; Luberto, Martinez-Marino et al. 2003; Chang, Stins et al. 2004; Del Poeta 2004; Santangelo, Zoellner et al. 2004; Shea, Kechichian et al. 2006; Charlier, Nielsen et al. 2009).

Morphogenesis in *C. neoformans* has primarily been observed as a result of pheromone signaling and mating (McClelland, Chang et al. 2004; Nielsen and Heitman 2007). There are two varieties of *C. neoformans*: *neoformans* and *grubii*. Historically, mating has been studied *in vitro* in var. *neoformans* even though the vast majority of human cryptococcosis cases are caused by var. *grubii*.

C. neoformans has two mating types: **a** and α. Mating is initiated when pheromone (**a** or α) secreted by one mating type binds to the pheromone receptor, Ste3α or Ste3**a** respectively, of the other mating type to trigger a mitogen-activated protein kinase (MAPK) signaling cascade (Davidson, Nichols et al. 2003; McClelland, Chang et al. 2004). Pheromone signaling results in morphological changes in var. *neoformans*,

including germ tube formation by mating type α cells and enlargement of mating type **a** cells (McClelland, Chang et al. 2004; Nielsen and Heitman 2007). Pheromone-induced MAPK signaling ultimately results in fusion of **a** and α cells followed by dikaryotic filamentation. Dikaryotic hyphae eventually give rise to basidia where nuclear fusion occurs and meiosis produces haploid spores (Kwon-Chung 1976; McClelland, Chang et al. 2004). In var. *grubii*, no *in vitro* morphogenesis in wild-type strains has been observed during early pheromone signaling, although hyphal formation and basidium production mimic that seen in var. *neoformans* (Nielsen, Cox et al. 2003).

In this study, we show that cell enlargement is observed *in vivo* in var. *grubii*, and that this cell enlargement can be regulated by pheromone signaling. Additionally, we show that these morphological changes in cell size affect pathogenicity by altering phagocytosis and dissemination to the central nervous system (CNS). Finally, we characterized DNA content of this novel cell type to reveal that these enlarged cells are polyploid.

II. MATERIALS AND METHODS

Ethics Statement. All animals were handled in strict accordance with good animal practice as defined by the relevant national and/or local animal welfare bodies, and all animal work was approved by the appropriate committee. Experiments at the University of Minnesota were reviewed and approved by the university Institutional Animal Care and Use Committee (IACUC) under protocol number 0712A22250. Experiments at the University of North Carolina – Chapel Hill were reviewed and approved by the university IACUC under protocol number 09-166.0. Studies at the Institut Pasteur we reviewed and approved under protocol number CHSCT#03-344.

Strains and Media. The congenic *C. neoformans* var. *grubii* strains KN99**a** and KN99α were used in this study (Nielsen, Cox et al. 2003). Strains were stored as glycerol stocks at -80°C and grown at 30°C in yeast extract-peptone-dextrose (YPD) agar or broth medium (BD, Hercules, CA).

Tissue Analysis. *C. neoformans* cells were cultured overnight in YPD broth. The resulting yeast cells were pelleted and resuspended in sterile phosphate-buffered saline (PBS) at a concentration of $1x10^6$ cells/ml based on hemocytometer count. Groups of 6- to 8-week-old female A/J mice (Charles Rivers, NCI, Frederick, MD; Jackson Labs, Bar Harbor, MA) were anesthetized by intraperitoneal pentobarbital injection. Three mice per treatment per time point were infected intranasally with $5x10^4$ KN99**a**, KN99α, or an approximate 1:1 mixture of KN99**a**:KN99α cells in 50 μl PBS. The concentration of cells in the inoculum was confirmed by plating serial dilutions and enumerating colony

forming units (CFU). At 1, 2, 3, 7, 14, or 21 days post-infection mice were sacrificed by CO_2 inhalation. The heart, lungs, brain, kidneys, liver, and spleen were harvested, fixed in 10% buffered formalin, paraffin-embedded, sectioned, and stained with PAS (periodic acid Schiff) or H&E (hematoxylin and eosin). Tissue sections were examined for cell size and morphology by microscopy. To examine fluorescently labeled cells in tissue sections, the yeast cells were incubated with AlexaFluor 350 (blue), AlexaFluor 488 (green), or AlexaFluor 594 (red) succinyl esters for 10-20 minutes at 25°C using the appropriate Protein Labelling Kit (Invitrogen, Carlsbad, CA). Labeled cells were washed >3 times in sterile PBS to remove unbound dye. The cells were resuspended in PBS at a concentration of $1x10^8$ based on hemocytometer count. Three mice per treatment (**a**, α, or coinfection) were infected intranasally with $5x10^6$ fungal cells. The concentration of yeast cells in the inoculum was confirmed by plating serial dilutions and enumerating CFU and the proportion of **a** cells in the coinfection inoculum was determined by mating assay (Nielsen, Cox et al. 2003). Infected mice were sacrificed at 1, 2, or 3 days post-infection by CO_2 inhalation. Lungs were extracted and fixed as described above and unstained sections were examined for cell size, morphology, and fluorescence. Data presented are representative of three independent experiments with two or three mice per treatment per experiment.

ste3aΔ* Mutant Strains.** Two independent ste3**a**Δ mutant strains were generated by gene disruption as previously described (Fraser, Subaran et al. 2003).The nourseothricin transgene (NAT) was used to replace the *STE3**a gene coding region. PCR was used to generate the 5' (KN0035 and KN0036) and 3' (KN0037 and KN0040) flanking regions

containing linkers to a NAT^r cassette and overlap PCR generated the NAT insertion allele (**Table 2.1**). The mutant allele was introduced by biolistic transformation into KN99**a** to generate *ste3**a**Δ#1* and into the spontaneous ura- strain JF99**a** (Hsueh, Fraser et al. 2008) to generate *ste3**a**Δ#2*. Transformed colonies resistant to nourseothricin (100 μg/ml) were identified by PCR amplification and sequencing of PCR products spanning a region upstream of the 5' flanking region into the NAT cassette (KN0079 and KN0031) and from the NAT cassette to downstream of the 3' flanking region (KN0032 and KN0109). Gene deletion was further confirmed by mating the mutant strains with KN99α on V8, pH 5 media for >14 days at 25°C in the dark. The mutant strains were sterile. The *ste3**a**Δ#2* was passaged on SD-ura media to isolate a URA+ revertant for use in virulence tests.

***In vivo* Analysis of *ste3aΔ* Strains.** Groups of 5-10 mice were infected with 5x10^4 cells in an approximate 1:1 ratio of *ste3**a**Δ#1*:KN99α, *ste3**a**Δ#2*:KN99α, or KN99**a**:KN99αNAT. The actual proportion of **a** cells in the infecting inoculum was determined by growth on selective media. At 21 days post-infection, animals were sacrificed. The lungs, spleen, and brain from each animal were homogenized in 2-4ml PBS and serial dilutions were plated on YPD for CFU enumeration. >500 colonies per organ were isolated and assayed for antibiotic resistance on YPD containing 100μg/ml nourseothricin to determine mating type.

Interactions with the Blood-Brain Barrier (BBB). KN99**a** and KN99α cells were fluorescently labeled as described above. Three mice per treatment were inoculated

Table 2.1

Primer Designation	Sequence
STE3a Knockout construct	
KN0035	GCCCTAGCAATGTCGATACCC
KN0036	AGCTCACATCCTCGCAGC GCACGTCCGGAGTACACG
KN0032	GCTGCGAGGATGTGAGCT
KN0031	GGTTTATCTGTATTAACACGG
KN0037	CCGTGTTAATACAGATAAACCCTGTATGGCGCTCCTTGGAAG
KN0040	CACAGCAAAGGCACATTCGCAAG
Outside PCR Checks	
KN0079	GGAGTTGACGCACGTTTATGGCAA
KN0109	CACTGGTGGAGCATTCATGTCG
qPCR with primers for CHS1	
KN104	GTCCCAGGAGGACTCCTTTC
KN105	TGTCGTTCAGGTCGAGTGAG

by tail vein injection with KN99**a**, KN99α, or an approximate 1:1 ratio of KN99**a**:KN99α at a final concentration of $5x10^6$ cells. At 1 day post-infection animals were sacrificed, perfused with 20 ml PBS then 20 ml 4% paraformaldehyde (PFA). Brains were harvested, placed in 4% PFA then 40% w/v sucrose solution in PBS, frozen in isopentane and liquid nitrogen, stored at -80°C, and 50 μm sections were generated. For immunohybridizations, slides were washed in PBS for 15 minutes followed by incubation with 100 μl trypsin-EDTA (Invitrogen) at 37°C for 10 minutes. Slides were then washed in PBS containing 20% fetal calf serum (Invitrogen) for 10 minutes, blocked with PBS containing 20% FCS, 0.1% bovine serum albumin (BSA) and 0.1% triton X-100 (Sigma, St. Louis, MO) for 20 minutes, then washed with PBS containing 0.1% triton X-100. Anti-collagen IV antibody (Santa Cruz Biotechnology, Santa Cruz, CA) was diluted to a 1/50 concentration in PBS with 0.1% BSA and 0.1% Triton X-100. Antibody-treated slides were incubated overnight at 4°C followed by washing in PBS. Cy3 labeled goat anti-rabbit antibody was diluted to a 1/200 concentration and added to the slides. After 5 hours of incubation at 37°C, slides were washed three times in PBS for 15 minutes. Hoechst medium was diluted to a 1/500 concentration and added to the slides for 30 seconds. Slides were washed for 5 minutes in PBS and mounted in Vectashield mounting medium. Capsule antigen staining was as described in Charlier et al., 2005 using the CRND-8 and E1 antibodies. Slides were imaged by fluorescence microscopy (Zeiss Axioplan) or by 2-photon confocal microscopy (Zeiss LSM 510 equipped with a Coherent Mira 900 tunable laser) with sections compiled as a projection or as a 3D rendering.

Bronchoalveolar Lavage (BAL). Four mice per treatment were infected as described above with $5x10^6$ AlexaFluor 488 labeled KN99**a**, KN99α, and *ste3**a**Δ*#1, or an approximate 1:1 ratio of one stained and one unstained strain. Infected mice were sacrificed at 3 days post-infection by CO_2 inhalation. Lungs were lavaged with 1.5 mL sterile PBS three times using a 20 gauge needle placed in the trachea. For flow cytometry, cells in the lavage fluid were pelleted at 16,000*g*, resuspended in 3.7% formaldehyde, and incubated at room temperature for 30 minutes. Cells were then washed once with PBS, resuspended in PBS containing 300 ng/ml 4',6-diamidino-2-phenylindole (DAPI) (Invitrogen), incubated at room temperature for 10 minutes, washed with PBS, and resuspended in PBS. >500 cells per animal were analyzed for size and fluorescence by microscopy (AxioImager, Carl Zeiss, Inc). Confocal microscopy (LSM710, Carl Zeiss, Inc) and z-stack imaging (AxioImager with Apotome, Carl Zeiss, Inc) were used to examine interactions with host mononuclear cells. Images were analyzed using Axiovision and Zen software (Carl Zeiss, Inc). Crescent shaped and other fluorescently-labeled cryptococcal cell fragments (i.e. not round cells) were observed within host mononuclear cells. These cell fragments were not included in the analysis.

Nitrosative and oxidative stress assays. Twelve mice were intranasally infected with $2x10^7$ cells in 50 μL PBS of an approximately 1:1 ratio of KN99**a** and KN99α cells. At 3 days post-infection, mice were sacrificed by CO_2 inhalation and BALs were performed. Cells were sorted by FACS using an iCyt Reflection cell sorter (iCyt, Champaign, IL). Cells were sorted based on size using forward scatter (FSC) into small cell and titan cell populations. Purity of samples was checked by flow cytometry and microscopy. Samples

were resuspended in Roswell Park Memorial Institute (RPMI) medium 1640 (Invitrogen) supplemented with 10% fetal bovine serum (FBS) (ATCC, Manassas, VA), 4.5 g glucose/L (BD), 1 mM sodium pyruvate (Invitrogen), 0.01 M HEPES (MP Biomedicals, Solon, OH), 5% penicillin/streptomycin (Invitrogen) and 0.05 mM β-mercaptoethanol (Chemicon) to a concentration of $2x10^4$ cells per 100 μL. Samples were then treated with 10 mM $NaNO_3$ (Sigma-Aldrich, St Louis, MO), 3 mM H_2O_2 (Walgreens Co., Deerfield, IL), or 1 mM tert-butyl hydroperoxide (TBHP) (Sigma-Aldrich). At 0, 6, 16 or 24 hours post treatment, 10 μL aliquots of each sample were plated onto YPD agar for CFU enumeration.

Flow Cytometry. Fixed BAL samples from 4 mice per treatment were generated as described above and analyzed using an ImageStream imaging flow cytometer and INSPIRE software (Amnis Corporation, Seattle Washington). Briefly, images for 5000 cells per sample were collected and analyzed for single cells (R1), doublets (R0), or aggregates of cells (**Figure 2.10A**). Only single cells (R1) were used in our analyses because cell aggregates would misrepresent cell sizes. Single cells were further analyzed for AlexaFluor 488 fluorescence and DAPI staining (**Figure 2.10B**). Due to the high nuclear content of mammalian cells, these cells had extremely high DAPI staining (R2 and R3). Non-phagocytosed yeast cells (R5) we identified based on their low DAPI staining. Visual confirmation of cell size in the flow cytometry images was used to identify small and titan cell populations (R6 and R7), that each gate contained only the target cells, and that no contamination between the populations was observed (**Figure 2.10C**). Data analysis and gating was performed using IDEAS software (Amnis

Corporation). Cryptococcal cells grown *in vitro* in YPD or DMEM to log or stationary phase were used as controls to identify haploid cells (1C) and actively dividing cells (1C + 2C).

To examine titan cell ploidy, fixed BAL samples from 4 mice per treatment were generated as described above. *In vitro* control samples were grown in YPD or Dulbecco's modified eagle medium (DMEM, 37°C, supplemented with 10% fetal bovine serum (FBS) (ATCC), 4.5g glucose/L (BD), 1M sodium pyruvate (Invitrogen), 0.01M HEPES (MP Biomedicals, Solon, OH), 5% penicillin/streptomycin (Invitrogen) and 0.05mM β-mercaptoethanol (Chemicon)) for 6 hours (log phase) or 5 days (stationary phase). Spent DMEM or RPMI was collected from MH-S macrophages after 3-5 days culture at 37°C and 5% CO_2. Spent endothelial cell (EC) media (complete EGM medium, Clonetics, San Diego, CA, USA) was collected from human umbilical vein endothelial cells (HUVEC) after 3-5 day culture at 37°C and 5% CO_2. *In vitro* titan cells were grown in filter sterilized spent media at 30°C or 37°C for 7 days. *In vitro* and *in vivo* samples were fixed in 3.7% formaldehyde and stained with 300ng/ml DAPI in PBS. Autofluorescence of non-DAPI stained fixed titan cells was measured and used to set the baseline for ploidy measurements. Cells were examined for cell size by forward scatter (FCS) and nuclear content by DAPI using an LSRII flow cytometer with FACSDiva software (BD) using gating defined by imaging flow cytometry. FCS cell sizes in each gate were verified by microscopy (Zeiss Axioplan). Data presented are representative of three independent experiments with four mice per treatment. 50,000 cells per treatment were analyzed to determine titan cell formation *in vitro*. *In vitro* titan cell formation was variable from experiment to experiment but trends between treatments remained constant. Data

presented are representative of five independent experiments. Because the absolute number of cells in each population and in each mouse differed, the DAPI fluorescence for each population was normalized to the number of cells in that population in order to clearly visualize peaks on a histogram representation of the data (**Figure 2.10, Figure 2.11**). Cells were examined for cell size by forward scatter (FCS) and nuclear content by DAPI using an LSRII flow cytometer with FACSDiva software (BD) using the gating defined by imaging flow cytometry. FCS cell sizes in each gate were verified by microscopy to identify the ≤ 10 μm, >10 μm but ≤ 20 μm, and >20 μm cell populations (Zeiss AxioImager). Data presented are representative of three independent experiments with four mice per treatment. 50,000 cells per treatment were analyzed to determine titan cell formation *in vitro*. *In vitro* titan cell formation was variable from experiment to experiment but trends between treatments remained constant. Data presented are representative of five independent experiments.

Cell sorting and qPCR: Ten to fourteen mice were infected with $5x10^6$ AlexaFluor 488-stained cells at an approximate 1:1 ratio of KN99**a**:KN99α as described above. Infected mice were sacrificed at 3 days post-infection and BALs were performed. BALs were pelleted and resuspended in 0.05% SDS in sterile water for 1 minute to promote host cell lysis. Cells were then fixed in 1 ml PBS containing 1% formaldehyde and incubated for 30 minutes at room temperature with mixing. Samples were incubated in 125 mM glycine for 5 minutes, centrifuged at 1500*g* for 10 minutes, and the pellets were resuspended in ice cold TBS (20 mM Tris, pH 7.6, 150 mM NaCl) containing 125 mM glycine. Cells were washed once in TBS, resuspended in 1 ml PBS and the cell concentration was

determined by hemocytometer count. Cell numbers were adjusted to 10^6 cells/ml, and 1% BSA was added to the fixed cell suspension. Cells were sorted using a FACSAria fluorescence activated cell sorter (FACS) using FACSDiva software (BD). Small and titan cell populations were isolated by FACS using gating as described above. DNA was isolated from 10^6 cells from small, titan, and 37°C DMEM (control) cell populations. A portion of the control cell population was DAPI stained and the number of haploid and diploid cells in the population was determined by flow cytometry (**Figure 2.10**). Small cells were classified as ≤10 µm and titan cells were >10 µm. After sorting, the two cell populations were pelleted and resuspended in lysis buffer (50 mM HEPES, 140 mM NaCl, 1% Triton X-100, 0.1% Sodium deoxycholate, 1mM EDTA). The cell suspensions were transferred to tubes containing 0.3 mm glass beads and vortexed for six 5 minute cycles at 4°C. The bottoms of the tubes were then pierced with a hot 21-gauge needle. The tubes were placed into 15 ml conical tubes and centrifuged at 1500*g* for 5 minutes at 4°C. The pellets and supernatants were combined and transferred to new tubes. These mixtures were centrifuged for 10 minutes at 10,000*g* at 4°C and the supernatants transferred to clean tubes. After a further 5 minute centrifugation, the DNA crosslinks were reversed by adding 200 µl TE (10 mM Tris, pH 7.5, 1 mM EDTA) containing 1% SDS to the clarified supernatants and incubating for 6 hours at 65°C. Samples were then incubated 2 hours at 37°C with 250 µl TE containing 0.4 mg/ml proteinase K. After adding 55 µl 4 M LiCl, the DNA was extracted with 0.5 ml phenol and the DNA was precipitated with 100% ethanol. The DNA pellets were washed with 70% ethanol, dried, and resuspended in TE containing 1.5 µl RNase (Ambion AM22886). Samples were stored at -20°C until analyzed by qPCR with primers KN104 and KN105 for chitin

synthase (*CHS1*) (**Table 1**). Gene copy number in the control sample was calculated based on the known number of 1C and 2C cells present in that sample (1.4C) based on flow cytometry. The small and titan cell gene copy numbers were normalized to the control sample.

Statistical Analysis. All analyses were performed using Analyse-It (Analyse-it Ltd., Leeds, England). Wilcoxon rank sum analysis was used to analyze differences in coinfection data and *P*-values <0.001 were considered significant. The Mann-Whitney U test was performed to analyze differences between survival curves and *P*-values <0.001 were considered significant. One-way ANOVA was used to analyze differences in titan cell production or phagocytosis and *P*-values <0.05 were considered significant for titan cell production experiments. *P*-values <0.1 were considered significant for phagocytosis experiments.

III. RESULTS

Morphological changes in *C. neoformans* var. *grubii* cells *in vivo*

Pheromone signaling in *C. neoformans* is known to cause morphological changes including formation of conjugation tubes, dikaryotic filaments, and production of basidia and spores (Kwon-Chung 1976; McClelland, Chang et al. 2004; Hull, Boily et al. 2005; Nielsen and Heitman 2007). Mating type **a** cell enlargement has also been observed in confrontation assays [23]. Cell enlargement has been observed in both human and mouse specimens (Cruickshank, Cavill et al. 1973; Love, Boyd et al. 1985; D'Souza, Alspaugh et al. 2001; Feldmesser, Kress et al. 2001). Thus, we systematically analyzed cellular morphology in various tissues of mice intranasally infected with var. *grubii* mating type **a** or α strains or mice coinfected with both mating types to determine the effect of pheromone signaling and mating type on *in vivo* cell morphology. Histopathologic tissue sections from the lungs, heart, spleen, liver, kidneys, and brain at 1, 2, 3, 7, 14, and 21 days post-infection were examined for changes in cryptococcal cell morphology. Dramatic changes in cryptococcal cell size were observed in the lungs, although a few cells with increased cell size were also observed in the spleen and brain at late time points. (**Figure 2.1A, Figure 2.2**). Most fungal cells in the lungs remained small (5-10 μm in diameter) resembling yeast cells grown in rich medium *in vitro*. However, a proportion of the cryptococcal cells in the lungs were much larger. For ease of reference, we designated this group of enlarged cryptococcal cells as “titan” cells. These titan cells were >10 μm in diameter, with some cell sizes approaching 50 to 100 μm in diameter (**Figure 2.1A**). Titan cell diameter measurements were based on actual cell body size and

excluded capsule changes which were highly variable. Titan cells were observed as early as 1 day post-infection in the lungs, accounted for approximately 20% of the cryptococcal cells in the lungs by 3 days post-infection, and remained relatively constant throughout the rest of the infection (**Figure 2.1B, 2.1C; Figure 2.2**). Titan cells were occasionally observed in the spleen and brain but at low levels (**Figure 2.2)**. In contrast, coinfection with both mating types resulted in an increase in titan cell production to almost 50% of the cells present in the lungs (**Figure 2.1B, 2.1C**).

Because pheromone signaling induces mating type **a** cell enlargement during *in vitro* mating of var. *neoformans*, we hypothesized that the increase in titan cell formation during coinfection was specific to mating type **a** cells. To test this hypothesis, we differentially stained **a** cells with AlexaFluor 488 (green) and α cells with AlexaFluor 594 (red) prior to intranasal inoculation of mice. Mice were sacrificed at 1-3 days post-infection, and unstained histopathological sections were examined for cryptococcal cell fluorescence (**Figure 2.3**). At 1 day post-infection, no difference in the proportion of **a** or α titan cells in individual or coinfections was observed (data not shown). However, at 2-3 days post-infection, the proportion of mating type **a** titan cells in coinfections increased while the α titan cell proportion remained equivalent to the individual infections (**Figure 2.1C**). Almost half of the stained mating type **a** cells in coinfected lungs had converted to titan cells.

To further quantify titan cell formation during coinfection, cells were differentially stained green with AlexaFluor 488 prior to intranasal instillation with the following treatments: **a** only (green), α only (green), **a**(green)/α, or **a**/α(green). At 3 days post-infection, bronchoalveolar lavage (BAL) was performed. The resulting mix of

Figure 2.1

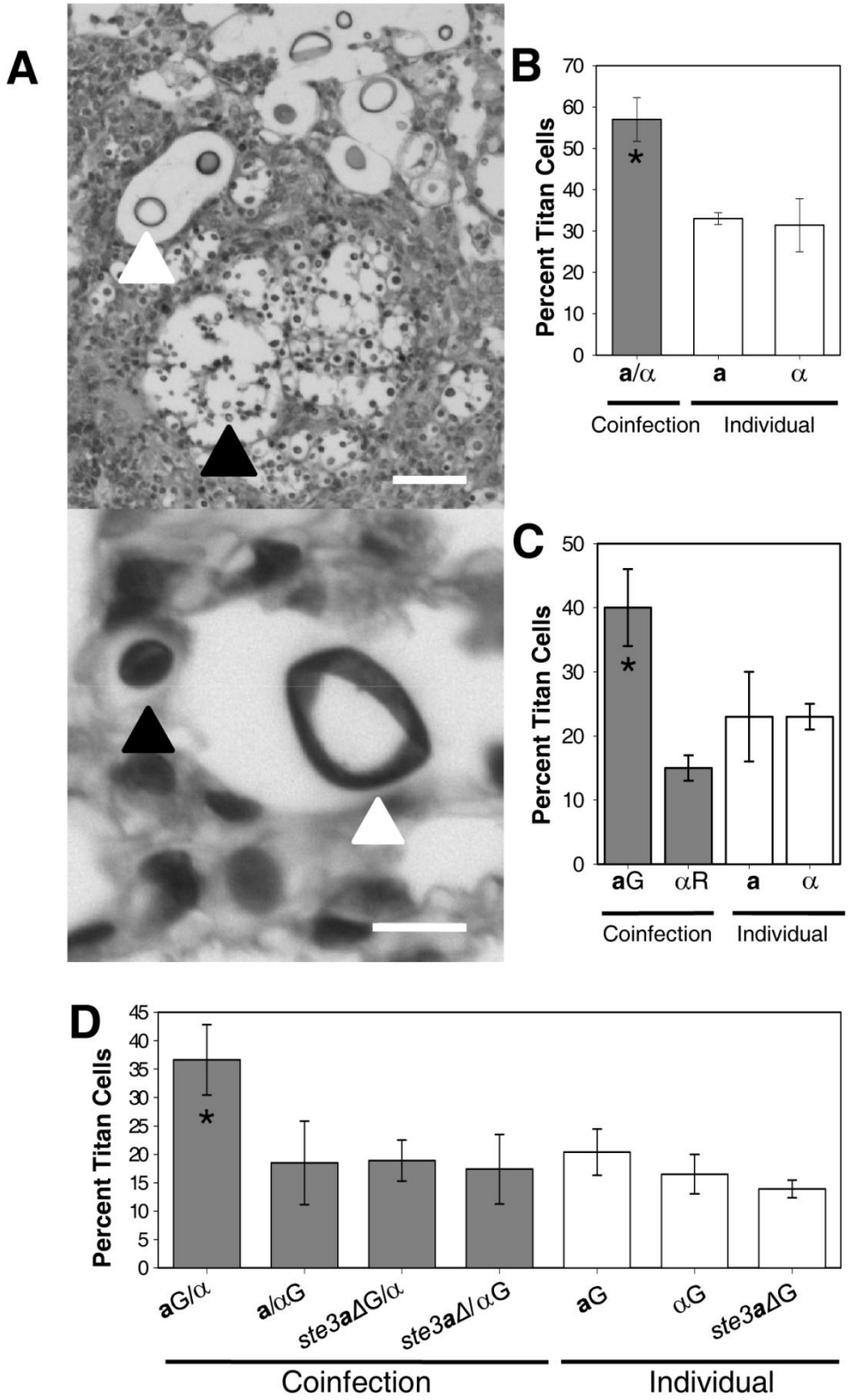
A
B
Percent Titan Cells
70
60
50
40
30
20
10
0
*
a/α
a
α
Coinfection
Individual
C
Percent Titan Cells
50
40
30
20
10
0
*
aG
αR
a
α
Coinfection
Individual
D
Percent Titan Cells
45
40
35
30
25
20
15
10
5
0
*
aG/α
a/αG
ste3aΔG/α
ste3aΔ/αG
aG
αG
ste3aΔG
Coinfection
Individual

Figure 2.1. Titan cells in the lungs of coinfected mice. A) Mice were coinfected with an approximate 1:1 ratio of **a**:α intranasally at a final concentration of $5x10^4$ cells. Lung sections were stained with periodic acid Schiff (PAS) 14 days (top) or 3 days (bottom) post-infection. White arrow denotes *C. neoformans* cells >10 µm in diameter. Black arrow denotes cells ≤ 10 µm in diameter. Top: bar = 100 µm, bottom: bar = 10 µm. **B)** The number of small cells (≤ 10 µm) and titan cells (>10 µm) were quantified in single and coinfections at 7 days post-infection. >500 cells were counted per treatment per mouse. Error bars indicate SD from 3 mice per treatment. Asterisk indicates $p<0.01$ in pair-wise comparisons to all other samples. **C)** Mice were infected by inhalation with $5x10^4$ of either **a** cells labeled with AlexaFluor 488 (green, **a**G), α cells labeled with AlexaFluor 594 (red, αR), or coinfected with an approximate 1:1 ratio of each mating type. At 2-3 days post-infection, animals were sacrificed and unstained tissue sections were examined for fluorescence and cell size. >80 cells were analyzed per mouse per treatment. Data are representative of three independent experiments with three mice per treatment. Error bars indicate SD. Asterisk indicates $p<0.01$ in pair-wise comparisons to all other samples. **D)** Mice were infected with $5x10^7$ cells by inhalation of either **a**, α, or *ste3**a**Δ* cells labeled with AlexaFluor 488 or coinfected with one labeled and one unlabeled strain. Cells obtained by bronchoalveolar lavage (BAL) were fixed and examined by microscopy for green fluorescence and cell size. >500 cells were examined per animal. Error bars indicate SD from four mice per treatment. Asterisk indicates $p<0.01$ in pair-wise comparisons to all other samples; p-values >0.2 were observed for other pair-wise comparisons.

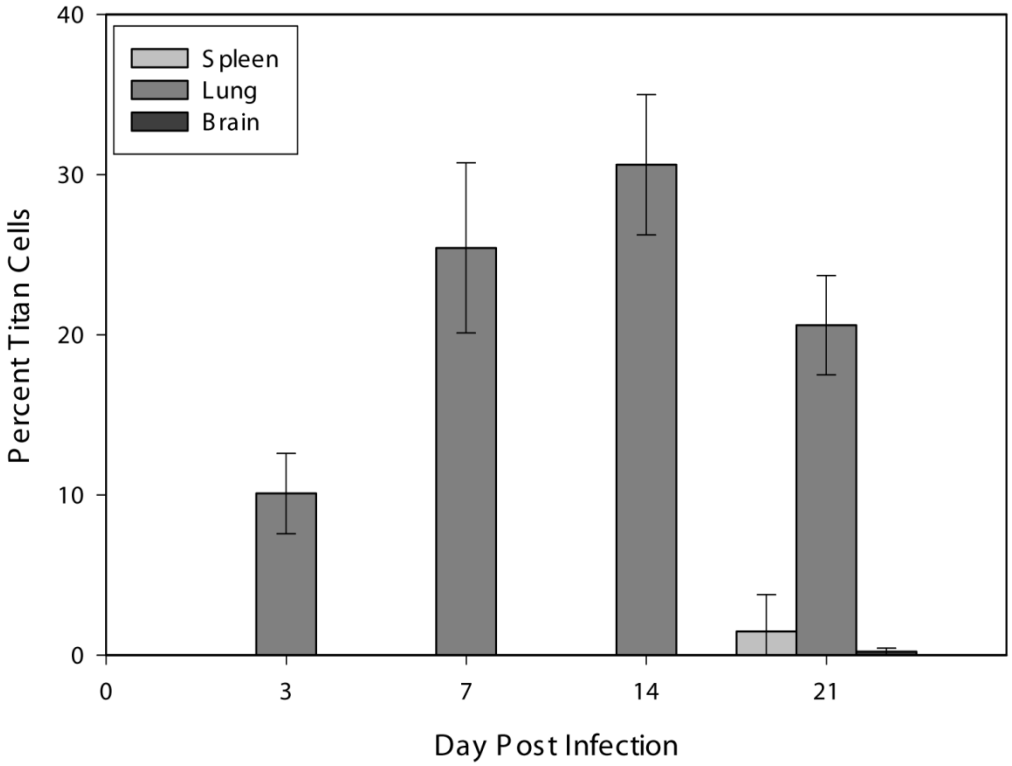

Figure 2.2. Titan cell formation in the lungs, spleen, and brain. Mice were intranasally infected with $5x10^4$ **a** or α cryptococcal cells. Lungs, brain, and spleen were collected at 1, 3, 7, 14 or 21 days post-infection. Samples were fixed in 10% formalin and stained with hematoxylin and eosin (H&E). The percentage of titan cells (>10 μm in diameter) was determined by microscopic examination of >500 cells per sample per mouse. Sufficient cell numbers were unavailable in tissue sections from 1 day post-infection lungs and 1, 3, 7, and 14 days post-infection spleen and brain for quantification. Error bars indicate SD from six mice per time point.

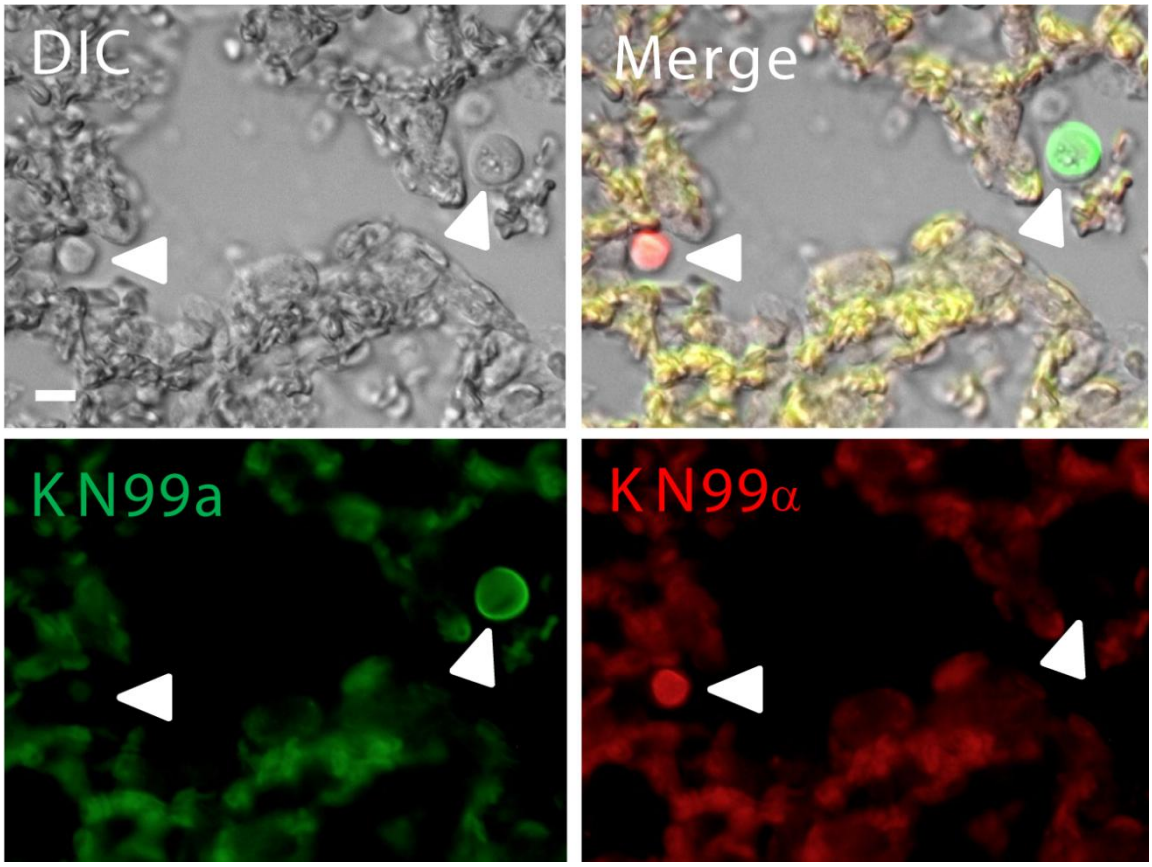

Figure 2.3. Fluorescently labeled a (green) and α (red) cells in the lungs during coinfection. *C. neoformans* **a** and α strains were combined with AlexaFluor 488 (green) or AlexaFluor 594 (red), respectively, and incubated for 20 minutes. Cells were washed with PBS to remove excess dye. Mice were inoculated with an approximate 1:1 ratio of **a:**α cells at a final concentration of $5x10^7$ cells. At 2 days post-infection animals were sacrificed, lungs extracted, fixed in 10% buffered formalin, paraffin-embedded, and 5µm sections generated. Host tissues are autofluorescent at both wavelengths resulting in a yellow color upon overlay. White arrows denote fluorescent *C. neoformans* cells. Bar = 20µm

cryptococcal and mouse cells was immediately fixed and the proportion of green titan cells was determined by microscopic examination (**Figure 2.1D, Figure 2.5A-C**). Similar to the tissue sections, approximately 20% titan cells were observed in the individual infections with no difference in titan cell formation between the two mating types ($p=0.2$, **Figure 2.1D**). In the coinfections, mating type α titan cell formation remained at the basal level ($p>0.64$, **Figure 2.1D**) while mating type **a** titan cell formation increased ($p<0.01$, **Figure 2.1D**). In the BAL samples, titan cell formation was increased to 37% of the fluorescently labeled **a** cells. Additionally, the proportion of titan cells in the tissue sections and the BAL samples was similar, suggesting that BAL samples obtained at 3 days post-infection provide an accurate representation of the cryptococcal cells present in the lungs.

Pheromone signaling affects titan cell formation

Cryptococcal cells can signal to cells of the opposite mating type using pheromones. Pheromone from one cell type binds to a G-protein coupled receptor, Ste3, on the opposite cell type to trigger a MAPK signaling cascade that can alter cell morphology (Davidson, Nichols et al. 2003; McClelland, Chang et al. 2004). We examined whether the increase in titan cell formation during coinfection was due to pheromone signaling by mutating the *STE3**a*** pheromone receptor gene.

The *STE3**a*** coding sequence was replaced with a nourseothricin (NAT) resistance gene by homologous recombination. The resulting *ste3**a**Δ* mutant lacks the receptor to recognize α pheromone, thus the pheromone signaling pathway is not activated and *ste3**a**Δ* mutant cells fail to mate with α strains. Two independent congenic mutants were

generated: *ste3**a**Δ*#1 and *ste3**a**Δ*#2. Both *ste3**a**Δ::NAT* mutant strains were sterile in mating assays with an α strain (data not shown). Murine survival assays verified that the *ste3**a**Δ* mutants had equivalent virulence to the parental strain KN99**a** and no differences in mean survival time were observed between wild-type and *ste3**a**Δ* coinfections (**Figure 2.4**).

To assess the role of pheromone sensing in titan cell formation, BAL samples were obtained from mice infected with fluorescently labeled *ste3**a**Δ*#1 only (green), *ste3**a**Δ*#1(green)/KN99α, or *ste3**a**Δ*#1/KN99α(green) (**Figure 2.1D**). Average titan cell formation was 14% in the *ste3**a**Δ*#1 infection, which was lower than the average for wild-type **a** cells (p=0.03), but similar to wild type α cells (p=0.22). In contrast, no increase in titan cell formation was observed in coinfections with the *ste3**a**Δ*#1 mutant (p>0.6, **Figure 2.1D**). Thus, the increase in titan cell formation by mating type **a** cells during coinfection requires the Ste3**a** receptor. However, the presence or absence of the Ste3**a** pheromone receptor has little effect on the basal level of titan cell formation observed in individual infections.

Pheromone signaling alters dissemination to the central nervous system

To examine the role of titan cell formation in pathogenicity, individual and coinfections with the wild-type and *ste3**a**Δ* mutant strains were compared. The *Cryptococcus* infectious cycle can be divided into three stages: an initial pulmonary infection (lungs), dissemination (spleen), and penetration of the CNS (brain). Previous studies with *C. neoformans* var. *grubii* congenic strains showed no differences in virulence between the **a** and α mating types (Nielsen, Cox et al. 2005). However,

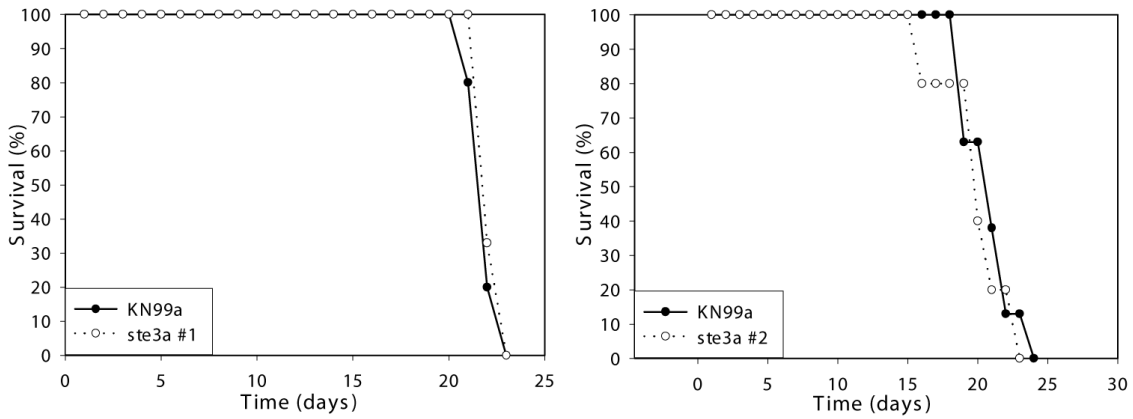

Figure 2.4. *ste3aΔ* survival assays. Mice were inoculated with $5x10^4$ cells of either wild-type **a**, *ste3aΔ#1* (left) or *ste3**a**Δ#2* (right) cells and progression to morbidity was monitored.

coinfection with both mating types simultaneously resulted in reduced **a** cell penetration of the CNS (Nielsen, Cox et al. 2005). Interestingly, while **a** cell CNS penetration was reduced compared with α cells, both cell types had equivalent accumulation at the first two stages of infection.

During coinfection, only mating type **a** cells displayed an increase in titan cell formation and a subsequent reduction in CNS penetration. Thus we hypothesized that pheromone signaling and the resulting increase in titan cell formation reduces **a** cell CNS penetration. To determine whether pheromone signaling affected dissemination to the brain during coinfection, we compared wild-type and *ste3**a**Δ* mutant strains for CNS penetration when coinfected with α (**Figure 2.5**). In both wild-type and *ste3**a**Δ* coinfections, the number of **a** and α cells recovered from the spleen and lungs was equivalent to the proportion of the two cell types in the initial inocula ($p>0.1$). These data show, even at late time points, alterations in titan cell production in response to pheromone signaling do not affect persistence of the cells in the lungs. However, a significant decrease was seen in the proportion of wild-type **a** cells recovered from the brain ($p=0.001$, **Figure 2.5A**). In contrast, coinfections with the *ste3**a**Δ* mutants restored **a** cell accumulation in the CNS to levels equivalent to the initial inocula ($p>0.4$, **Figure 2.5B, C**). Both independent *ste3**a**Δ* mutants showed similar results. Together, these data suggest that pheromone signaling during **a**/α coinfection affects the pathogenicity of **a** cells by increasing titan cell formation which inhibits the ability of **a** cells to establish a CNS infection.

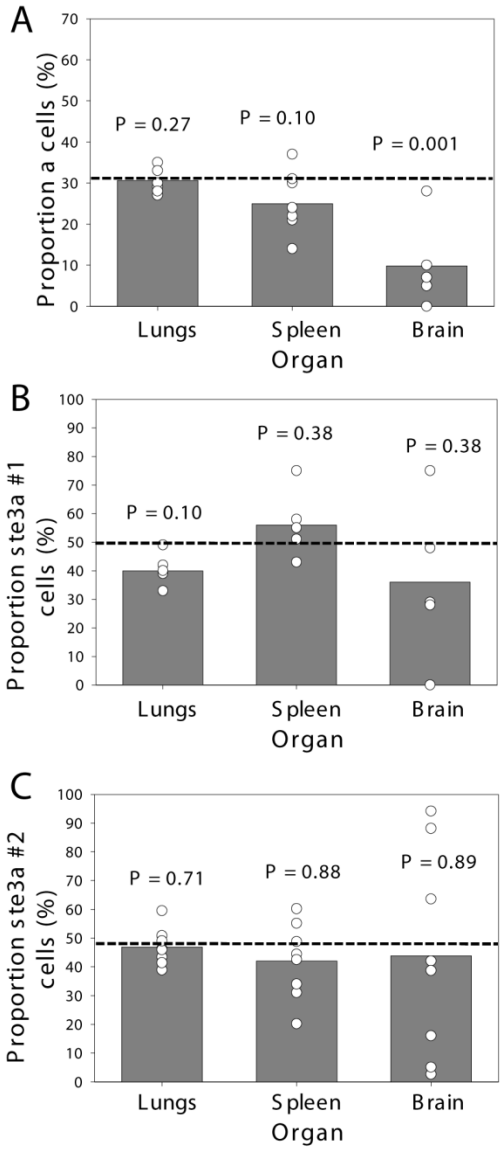

Figure 2.5. *C. neoformans* pheromone receptor mutant strains penetrate the CNS during coinfection. Mice were coinfected intranasally with an approximate 1:1 ratio of **A) a:**αNAT, **B)** *ste3**a**Δ*#1:α, or **C)** *ste3**a**Δ*#2:α at a final concentration of $5x10^4$ cells. The actual proportion of **a** cells in the infecting inoculum was determined by growth on selective medium and is plotted as a horizontal dashed line. At 21 days post-infection animals were sacrificed, the lungs, brain, and spleen were homogenized and serial dilutions plated. >500 colonies per organ per mouse were isolated and assayed for drug resistance to determine mating type. The proportion of **a** cells is plotted with open circles denoting values from individual animals and bar height representing the geometric mean. To determine *P*-values, Wilcoxon rank sum analysis was performed on the measured number of **a** and α cells compared with the expected number, assuming that both strains remained at the initial inoculum proportions.

Coinfection does not affect blood brain barrier penetration upon IV injection

An *in vivo* murine tail vein injection model was employed to determine whether coinfection disrupts CNS penetration by reducing **a** cell interactions with the endothelial cells of the BBB (Chretien, Lortholary et al. 2002; Charlier, Chretien et al. 2005). In this model, cells bypass the lungs and are injected directly

into the bloodstream via the mouse tail vein. The cells then lodge in the small capillaries of the brain and cross the endothelial cell layer of the BBB. To test whether interaction with the BBB was directly affected by mating type or coinfection, **a** and α cells were fluorescently labeled and examined for their interactions with the BBB. Both cell types were able to traffic to the small capillaries of the brain (**Figure 2.6A**) and quantification revealed equal proportions of the two mating types in the capillaries (data not shown). During coinfection, the two mating types were observed in close proximity approximately 25% of the time, consistent with random interactions between cells in a mixed population. The finding that cells of opposite mating type are found in close association would enable pheromone signaling to occur between them in the capillaries of the brain (**Figure 2.6B**). Both mating types could induce phagocytosis by the endothelial cells of the BBB (**Figure 2.6C**). Capsule structural changes are important for interactions with the endothelial cells of the BBB (Charlier, Chretien et al. 2005). These structural changes can be characterized by alterations in anti-capsular antibody binding. The binding patterns to the cryptococcal capsule for two monoclonal antibodies, E1 and CRND-8, recognizing distinct epitopes on the capsular polysaccharide were studied over time and found to be similar for both mating types. Cells observed in the capillaries shortly after inoculation and up to 6 hours post-infection exhibited only E1 antibody

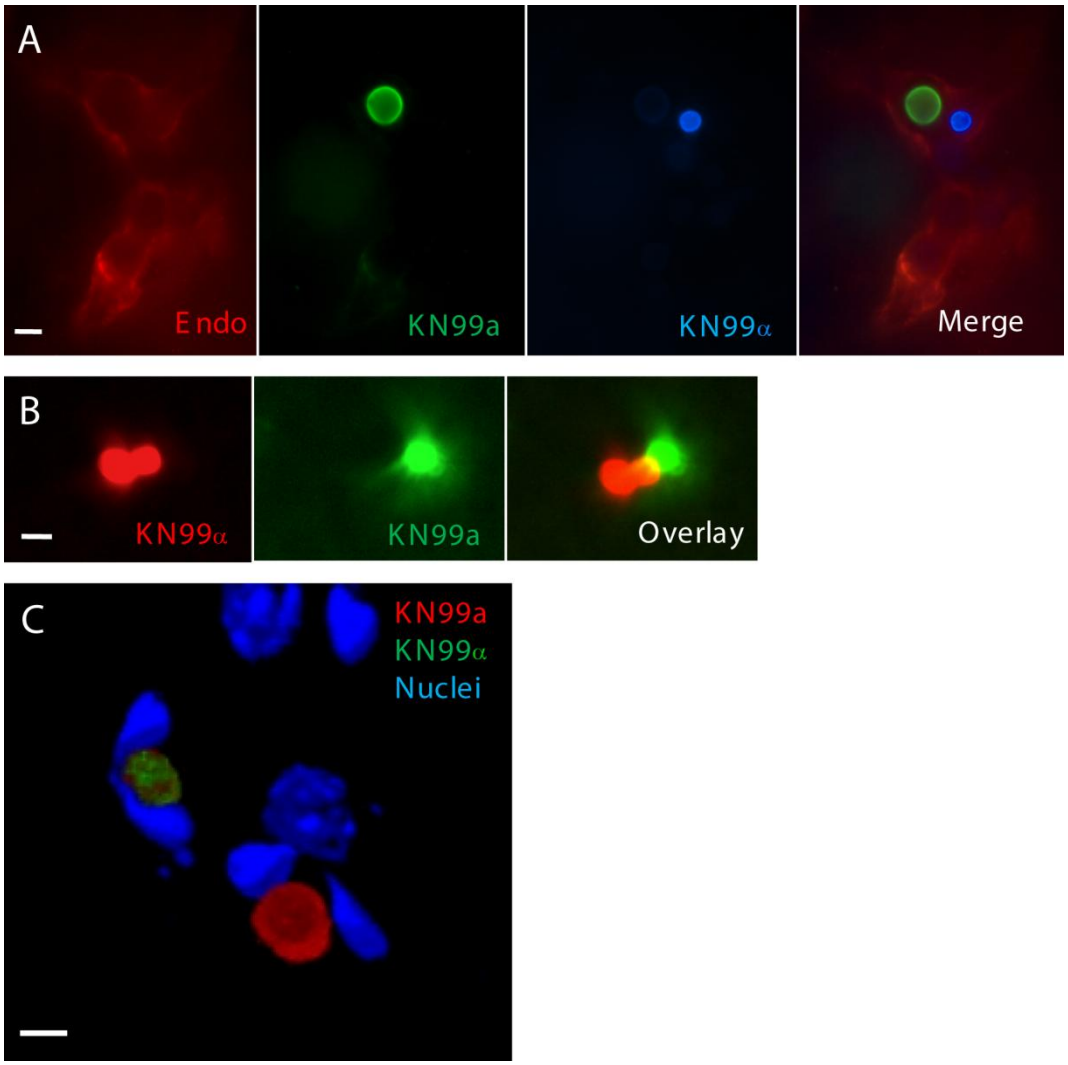

Figure 2.6. KN99a and KN99α cells interact with endothelial cells of the blood-brain barrier during coinfection. a or α were combined with AlexaFluor 350 (blue), AlexaFluor 488 (green) or AlexaFluor 594 (red) and incubated for 20 minutes. Mice were inoculated by tail vein injection with an approximate 1:1 ratio of **a**:α at a final concentration of $2x10^7$ cells. At 1 day post-infection, animals were sacrificed and 50 µm frozen brain sections were obtained. **A)** Sections from mice infected with **a** (green) and α (blue) were immunostained with anti-collagen IV primary antibody (endothelial cell membrane) with a TRITC (red) labeled secondary antibody. Bar = 20 µm **B)** Sections from mice infected with **a** (green) and α (red) were imaged by confocal microscopy and sections were compiled as a projection. Bar size = 20 µm **C)** Frozen sections from mice infected with **a** (red) and α (green) were treated with Hoechst (host cell nuclei), imaged by confocal microscopy, and sections were compiled as a 3D rendering. The U-shaped nuclei are indicative of endothelial cells containing cryptococcal cells. Bar = 10 µm.

binding. In contrast, cells observed in the brain parenchyma were mostly labeled with CRND-8, as described previously for KN99α (Charlier, Chretien et al. 2005). No difference in the capsular antigen staining or the kinetics of capsular changes upon crossing of the BBB were observed between the **a** and α cells during interactions with the endothelial cells of the BBB – either alone or during coinfection (data not shown). These data suggest that the inability of **a** cells to penetrate the CNS during coinfection is not due to innate differences between the two cell types or their interactions with the BBB itself, but instead may be due to an inability of the **a** cells to traffic appropriately from the lungs to the brain.

Titan cells are resistant to phagocytosis

One of the first lines of defense by the host immune system is phagocytosis and the resultant killing of pathogens by mononuclear macrophages and monocytes in the lungs. These host cells identify pathogens, phagocytose them, and either kill the pathogen outright via oxidative and/or nitrosative bursts or present antigens to T-cells for further activation of the host immune response (Janeway, Murphy et al. 2008). Recent studies suggest phagocytosis by monocytes or macrophages is important for subsequent CNS penetration (Del Poeta 2004; Santangelo, Zoellner et al. 2004; Shea, Kechichian et al. 2006; Charlier, Nielsen et al. 2009). Thus, we examined titan cell interactions with lung host immune cells.

Fixed BAL samples were analyzed microscopically for yeast cell interactions with host phagocytic cells. Titan cells were never observed inside host phagocytes, presumably due to their large size. Engulfed small cryptococci were observed inside

phagocytic host cells (**Figure 2.7A, B**). No difference in phagocytosis was observed between mating types (p=0.82, **Figure 2.7D**). The percentage of intracellular α cells during coinfection was similar to that observed in single mating type infections (p>0.89, **Figure 2.7D**). In contrast, a decrease in the percentage of phagocytosed **a** cells was seen during coinfection (p<0.09, **Figure 2.7D**). Phagocytosis was restored in the *ste3**a**Δ#1* mutant (p>0.53 **Figure 2.7D**). Interestingly, titan cells were often surrounded by one or more host immune cells (**Figure 2.7C**). Yet complete phagocytosis of titan cells was not observed upon characterization of these cellular interactions by confocal microscopy (data not shown). Taken together, these data indicate titan cell formation was negatively correlated with phagocytosis by host immune cells.

Both macrophages and neutrophils employ oxidative and nitrosative bursts as a means of killing pathogens (Janeway et al., 2008). Titan cell resistance to these stresses was characterized by comparing the growth of purified titan and small cells isolated by cell sorting of BAL samples. Both cell types showed equivalent growth in the absence of oxidative or nitrosative stress (**Figure 2.8A**). Treatment with sodium nitrate ($NaNO_3$) slowed the growth of the small cell population compared to the titan cell population (**Figure 2.8B**). Treatment with tert-butyl hydroperoxide (TBHP) resulted in killing of small cells, represented by a decrease in cell counts relative to the initial time point (**Figure 2.8C**). In contrast, titan cells exhibited continued growth in the presence of these oxidative stresses (**Figure 2.8C**). Similar results were observed with stabilized hydrogen peroxide treatment. Thus, titan cells are more resistant than normal cells to both oxidative and nitrosative stresses similar to those employed by cells of the host immune system.

Figure 2.7

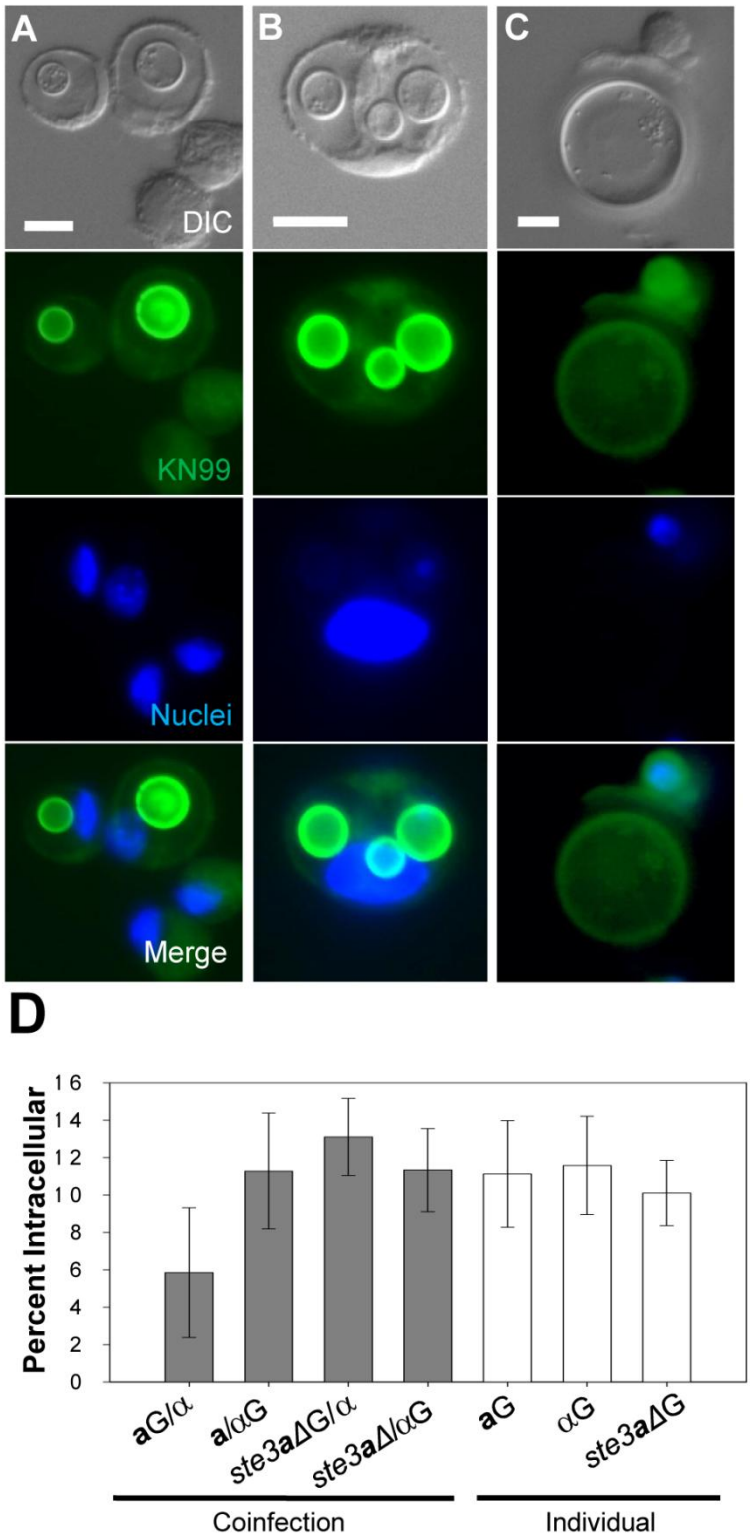
A
B
C
DIC
KN99
Nuclei
Merge
D
Percent Intracellular
16
14
12
10
8
6
4
2
0
aG/α
a/αG
ste3aΔG/α
ste3aΔ/αG
aG
αG
ste3aΔG
Coinfection
Individual

Figure 2.7. Titan cell formation and phagocytosis in the lungs of infected mice. Mice were intranasally infected with either **a**, α, or *ste3**a**Δ* cells labeled with AlexaFluor 488 (green) or coinfected with one labeled and one unlabeled strain (four mice per treatment). Cells obtained by BAL were fixed, stained with DAPI, and examined by microscopy for green fluorescence (cell type) and cell size. >500 cells were examined per animal. Bar = 10 μm **A)** *C. neoformans* **a** cells (green) ≤ 10 μm in diameter were visible inside host phagocytes. Host cells were identified by large blue DAPI stained nuclei. **B)** Several small α (≤ 10 μm) cells (green) can be seen inside a single host cell. **C)** Mating type **a** titan cells (>10 μm) are seen in contact with host phagocytes but are too large to be phagocytosed. **D)** Cells obtained by bronchoalveolar lavage (BAL) were fixed and examined by microscopy for green fluorescence and percent phagocytosis. >500 cells were examined per animal. Error bars indicate SD from four mice per treatment. Asterisk indicates $p<0.09$ in pair-wise comparisons to all other samples; p-values >0.4 were observed for other pair-wise comparisons.

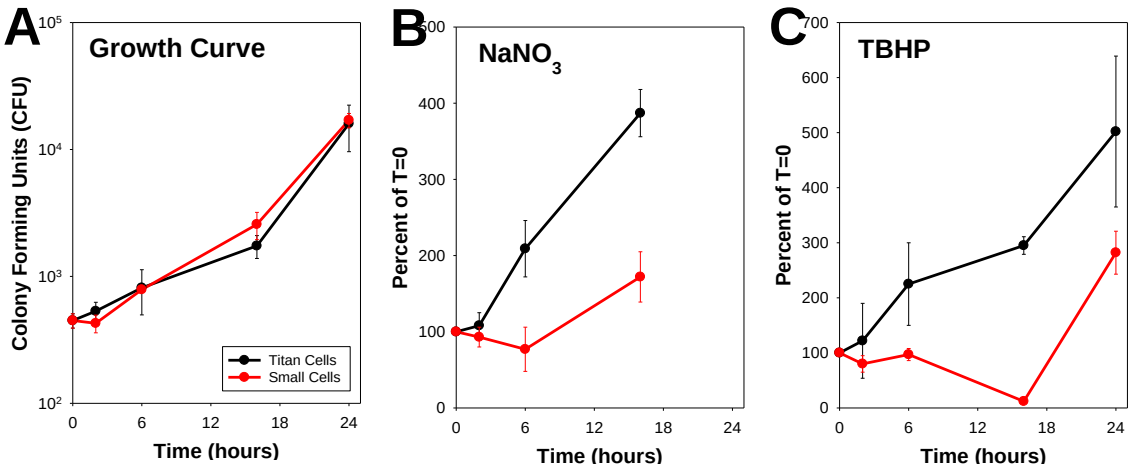

Figure 2.8. Titan cells are resistant to oxidative and nitrosative stress. Mice were coinfected intranasally with $4x10^7$ cryptococcal cells. At 3 days post-infection, BALs were performed and cells were sorted by FACS based on size. $2x10^4$ titan cells or small cells were resuspended in 100 µL RMPI. Cryptococcal cells received **A)** no treatment, **B)** 10 mM $NaNO_3$, **C)** 1 mM TBHP. At 0, 6, 16, or 24 hours, aliquots of each treatment were plated on YPD agar and colony forming units (CFU) were determined. Error bars indicate SD from three replicates.

Titan cells are polyploid

In yeasts, cell enlargement is often associated with either cell cycle arrest or increased DNA content (Sloat, Adams et al. 1981; Harold 1990; Bloom and Cross 2007). Pheromone sensing in the model yeasts *Schizosaccharomyces pombe* and *Saccharomyces cerevisiae* is known to trigger a cell cycle arrest. We examined titan cells for their progression through the cell cycle by characterizing their ability to bud and produce daughter cells. In addition, we determined the DNA content of titan cells.

Titan cells produced *in vivo* were obtained from BAL of mice with single or coinfections. The cells were immediately fixed and stained with DAPI. Microscopic examination of titan cells revealed a single nucleus (**Figure 2.9A**). Analysis of titan cell nuclear structure by confocal microscopy and z-stack sectioning showed the nucleus had an elongated tubular shape instead of the classic round shape observed in smaller cells (data not shown). Because of its elongated shape, only a portion of the nucleus was observed in each focal plane. Several stages of the cell cycle were identified. In early bud formation (**Figure 2.9B**), titan cells had a nucleus in the mother cell while the daughter cell lacked a nucleus. The mother cell nucleus was observed at the bud site and entering the daughter cell (**Figure 2.9C**). After nuclear division the mother and daughter each contained single nuclei (**Figure 2.9D**). Finally, after cytokinesis was complete, individual nuclei were visible in the mother and associated daughter cell (**Figure 2.9E**). Budding of the titan cells was readily observed from *in vivo* samples suggesting complete cell cycle arrest would not explain the increased titan cell size.

Increases in cell size in plants, or gigantism, is often correlated with increased ploidy (Otto 2007). Because titan cells contain only one nucleus, we quantified their

DNA content by flow cytometry and quantitative PCR. Fluorescently labeled cells from individual or coinfections were isolated by BAL and immediately fixed and stained with DAPI. The fixed cell suspensions were then analyzed using an imaging flow cytometer to define cell populations (**Figure 2.10**). Two distinct populations of fluorescent cryptococcal cells were identified: cryptococcal cells alone and cryptococcal cells inside host cells. Because phagocytosed cryptococcal cell size cannot be accurately measured with flow cytometry, only single non-phagocytosed yeast cells were examined further. The single non-phagocytosed yeast cells were then divided into three populations based on cell diameter: ≤ 10μm, >10μm but ≤ 20μm, and >20μm. The ≤ 10μm cell population was designated as small cells of typical size for *Cryptococcus*. The group of cells >20μm were designated as the titan cell population. The intermediate cell population, >10μm but ≤ 20μm, contained a mixture of small and titan cells, thus could not be accurately characterized by flow cytometry.

Flow cytometry and cell sorting of 50,000 cells were used to obtain an accurate representation of the DNA content for each population (**Figure 2.11**). DNA content determinations were based on DAPI fluorescence in haploid cells grown *in vitro* in Dulbecco's modified eagle medium (DMEM) at 37°C and 5% CO_2 (non- titan-inducing conditions) (**Figure 2.12**). The small cell population isolated from coinfected mice showed a prominent peak consistent with a majority of the cells in the population containing two copies (2C) of DNA. These data would suggest that most of the small cell population *in vivo* were in G2 of the cell cycle (**Figure 2.11A**). In contrast, the titan cell population showed two peaks consistent with 4C or 8C DNA content (**Figure 2.11A**). No differences in titan cell DNA content were observed between the two mating types or in

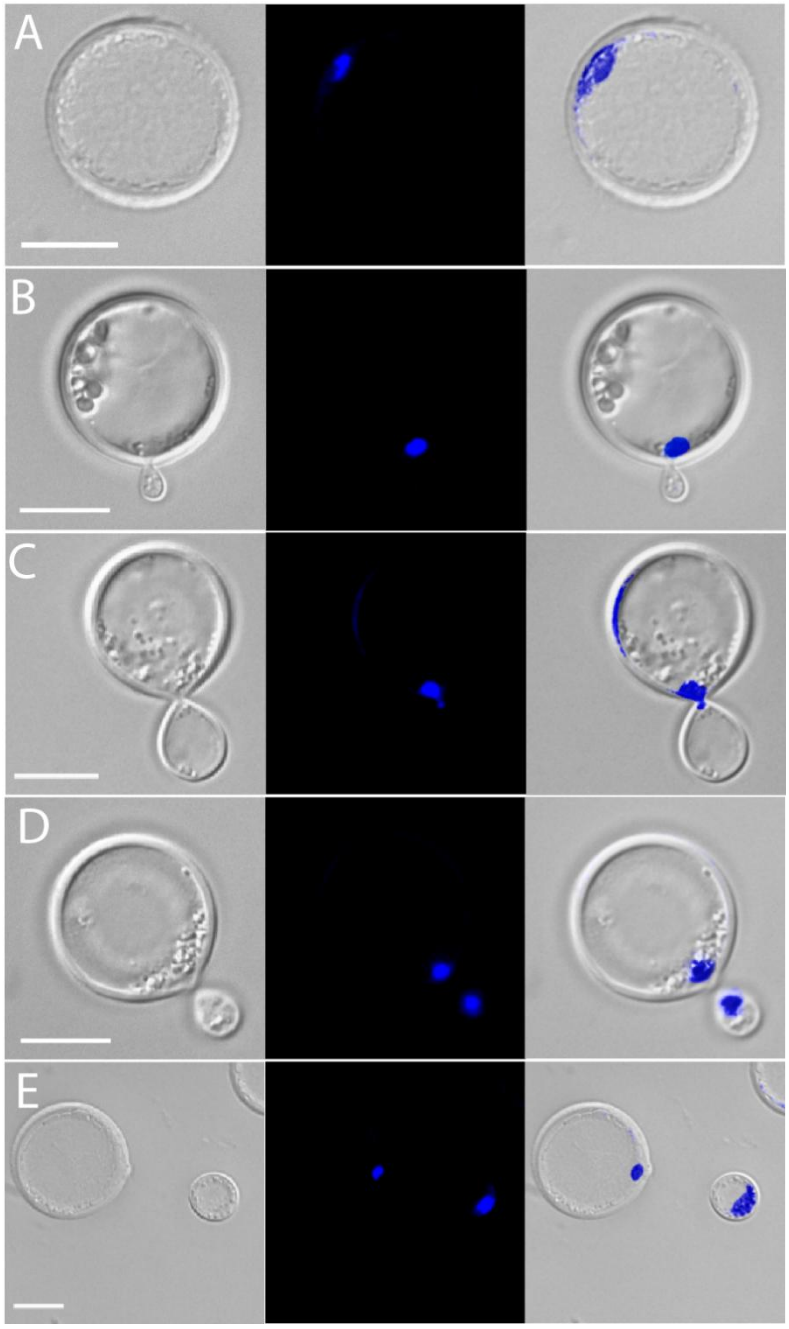

Figure 2.9. Titan cells can undergo cell division. Mice were infected with $5x10^6$ cells by inhalation of an approximate 1:1 ratio of **a:**α cells. At 3 days post-infection, mice were sacrificed, BALs performed, and the resulting cells were fixed and DAPI stained for nuclear content. **A)** Titan cell containing a single nucleus. **B)** Titan cell early bud formation. **C)** Nuclear transfer from a mother (titan cell) to a daughter cell. **D)** Titan cell late bud formation. **E)** Cytokinesis of a daughter cell from a titan cell. Bar = 10 µm.

individual versus coinfections, indicating that titan cell DNA content was not altered by coinfection (**Figure 2.12**). Analysis of the *in vivo* samples suggested that both the small cells and titan cells could be undergoing active cell growth and replication, making characterization of titan cell ploidy difficult in these *in vivo* samples. To determine the ploidy of titan cells, we identified *in vitro* conditions that stimulated titan cell production. Titan cell formation was only observed in cryptococcal samples grown in spent media previously used to culture mammalian cells (**Figure 2.13**). Differences in titan cell formation were observed based on the media used, the temperature of incubation, and mammalian cell type. Optimal *in vitro* titan cell production was observed when cryptococcal cells were grown in spent DMEM derived from MH-S alveolar macrophages at 30°C. When grown to stationary phase for 5 days in this medium approximately 4% of the total population was titan cells. On average, titan cells generated *in vitro* were smaller than those observed *in vivo*, ranging from 15 μm to 30 μm in diameter. Due to the smaller size of the *in vitro* titan cells, the intermediate cell population (>10μm but ≤ 20μm) was included in the flow cytometric DNA content analysis (**Figure 2.11B**). In contrast to the *in vivo* samples, the DNA content of the *in vitro* small cell population at 5 days was consistent with 1C cells, suggesting that the cells were in stationary phase (**Figure 2.11B**). Cells grown to stationary phase in a standard growth medium were also 1C (data not shown). The intermediate cell population had a single peak consistent with 4C cells and the larger titan cell population (>20 μm) had a single peak consistent with 8C cells (**Figure 2.11B**). Thus, titan cells in stationary phase appeared to be either tetraploid or octoploid based on cell size.

Quantitative PCR was used to determine the average copy number per cell of the chitin synthase 1 (*CHS1*) gene as an additional molecular characterization of DNA content in the *in vivo* small and titan cell populations. Quantitative PCR was performed on the isolated DNA from three cell populations (small, titan, control). This quantitative PCR analysis confirmed that the titan cells had increased *CHS1* DNA content compared with the small cells ($p<0.001$, **Figure 2.11C**). Consistent with the flow cytometry results, the small cells had an average *CHS1* gene copy number of 2 in the *in vivo* samples, suggesting that the majority of the population had a 2C DNA content. The titan cell population had an average *CHS1* gene copy number of 5, consistent with a 3:1 ratio of 4C to 8C cells. Taken together, the *CHS1* gene copy number and flow cytometry data suggest that titan cells are tetraploid and octoploid.

Figure 2.10

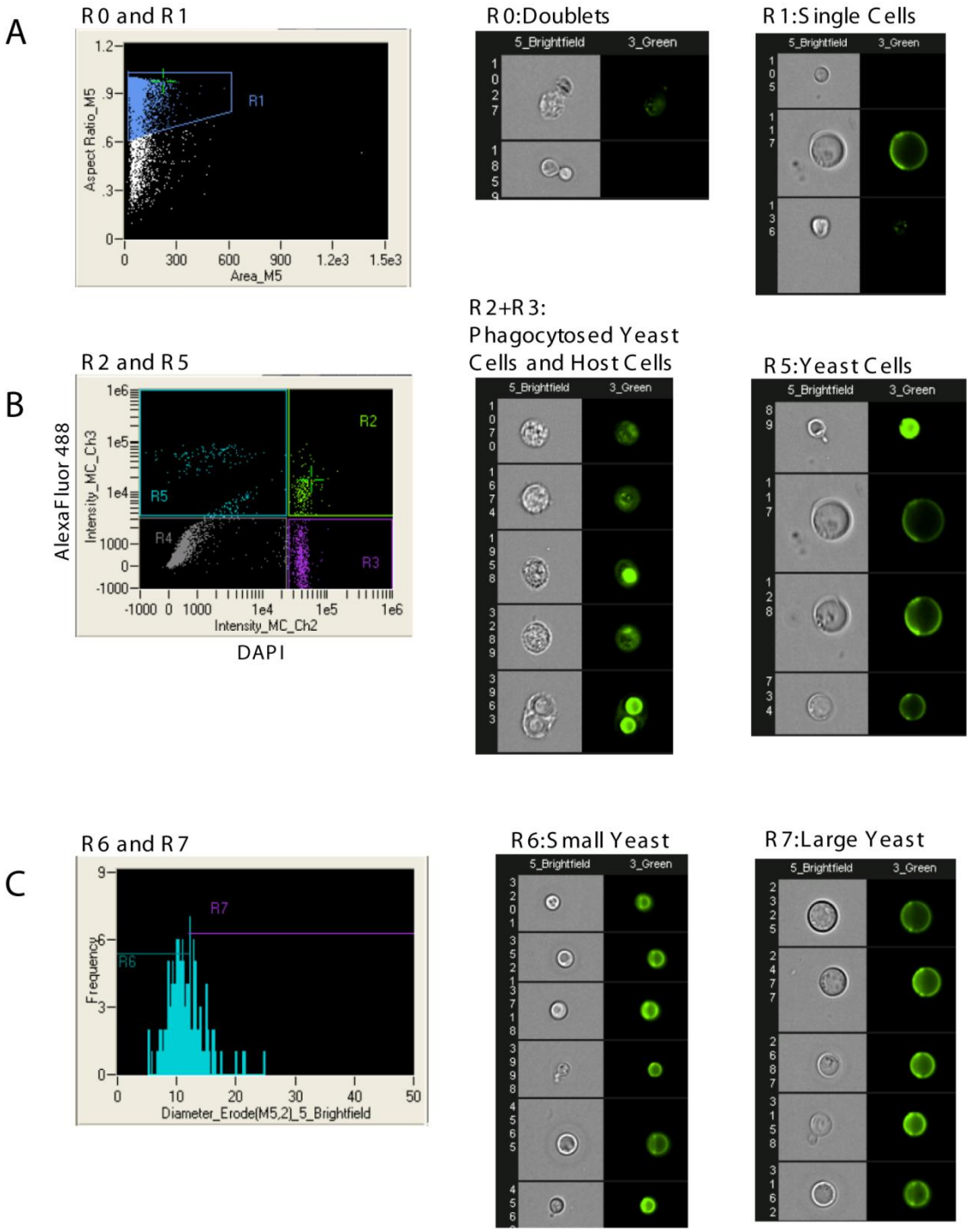
A
R 0 and R 1
Aspect Ratio_M5
Area_M5
R1
R 0:Doublets
R 1:Single Cells
5_Brightfield
3_Green
B
R 2 and R 5
AlexaFluor 488
DAPI
Intensity_MC_Ch3
Intensity_MC_Ch2
R2
R3
R4
R5
R 2+R 3:
Phagocytosed Yeast
Cells and Host Cells
R 5:Yeast Cells
C
R 6 and R 7
Frequency
Diameter_Erode(M5,2)_5_Brightfield
R6
R7
R 6:Small Yeast
R 7:Large Yeast

Figure 2.10. Imaging Flow Cytometry. *C. neoformans* a and α strains were combined with AlexaFluor 488 (green) and incubated at 25°C for 20 minutes. Cells were washed with sterile PBS to remove excess dye. Mice were inoculated with an approximate 1:1 ratio of **a**:α cells. At 3 days post-infection animals were sacrificed and BALs were performed. The resulting cells were fixed, DAPI stained and analyzed using an ImageStream flow cytometer using IDEAS software (Amnis Corporation). **A)** Cells were first examined for single cells (R1). Aggregates and doublets were excluded from further analysis. **B)** The R1 population was analyzed for DAPI intensity (X-axis) and AlexaFluor 488 intensity (Y-axis). $DAPI^{hi}$ host cells and phagocytosed cryptococcal cells (R2 and R3) as well as unstained yeast cells (R4) were excluded from further analysis. **C)** Diameter was used to divide the remaining population, R5, into cells <10 μm (R6) and >10 μm (R7). Samples from four mice per treatment were analyzed and gates determined by consensus among the samples.

Figure 2.11

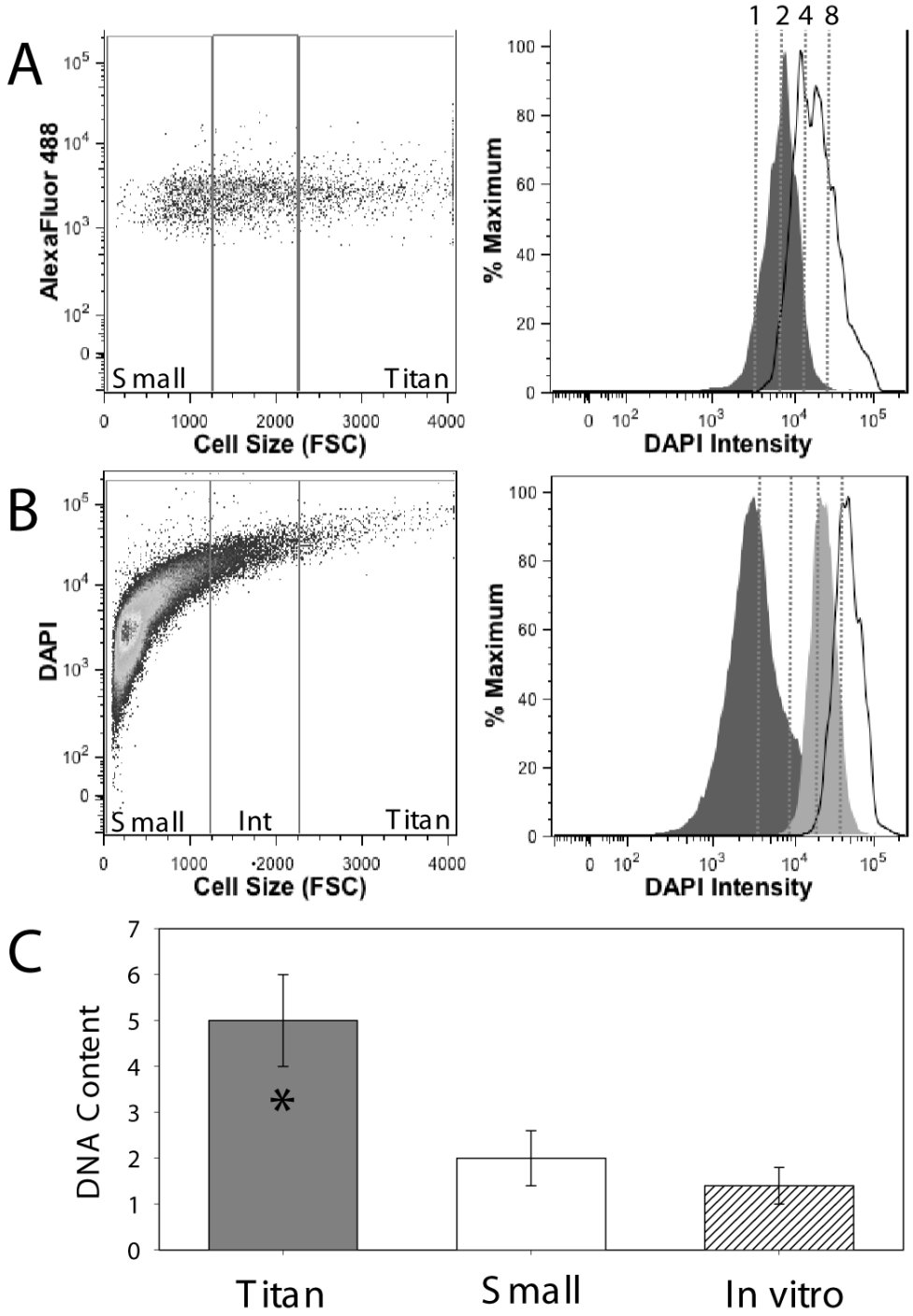
A
AlexaFluor 488
Small
Titan
Cell Size (FSC)
1 2 4 8
% Maximum
DAPI Intensity
B
DAPI
Small
Int
Titan
Cell Size (FSC)
% Maximum
DAPI Intensity
C
DNA Content
*
Titan
Small
In vitro

Figure 2.11. Titan cells have increased DNA content. Mice were intranasally infected with $5x10^6$ cells with an approximate 1:1 ratio of **a:**α cells labeled with AlexaFluor 488 (green). At 3 days post-infection, mice were sacrificed, BALs performed, and the resulting cells were fixed. **A)** Cells were stained with DAPI to measure nuclear content by flow cytometry. Left panel indicates small (≤ 10 μm) and titan (>20 μm) cell population gates. Right panel indicates DNA content based on DAPI fluorescence for small (dark gray) and titan (white) populations normalized to cell number (% maximum). Dashed lines indicate predicted 1C, 2C, 4C, and 8C DNA content based on DAPI intensity of the 1C and 2C control cells stained and analyzed in the same experiment. **B)** Cells were grown *in vitro* in spent DMEM liquid medium for 7 days at 30°C. Cells were fixed and stained with DAPI. Left panel indicates small (≤ 10 μm), intermediate (>10 μm, ≤ 20 μm), and titan (>20 μm) cell population gates. Right panel indicates DNA content based on DAPI fluorescence for small (dark gray), intermediate (light gray), and titan (white) populations normalized to cell number. Dashed lines indicate predicted 1C, 2C, 4C, and 8C DNA content based on DAPI intensity of the 1C and 2C control cells strained and analyzed in the same experiment. **C)** Fixed BAL samples were sorted into small and titan cell populations by fluorescence activated cell sorting. DNA was purified from the sorted populations, normalized to cell number, and chitin synthase 1 (*CHS1*) gene copy number was determined by comparison to a log phase control sample with a known ratio of 1C:2C cells with a total gene copy number equivalent to 1.4.

Figure 2.12

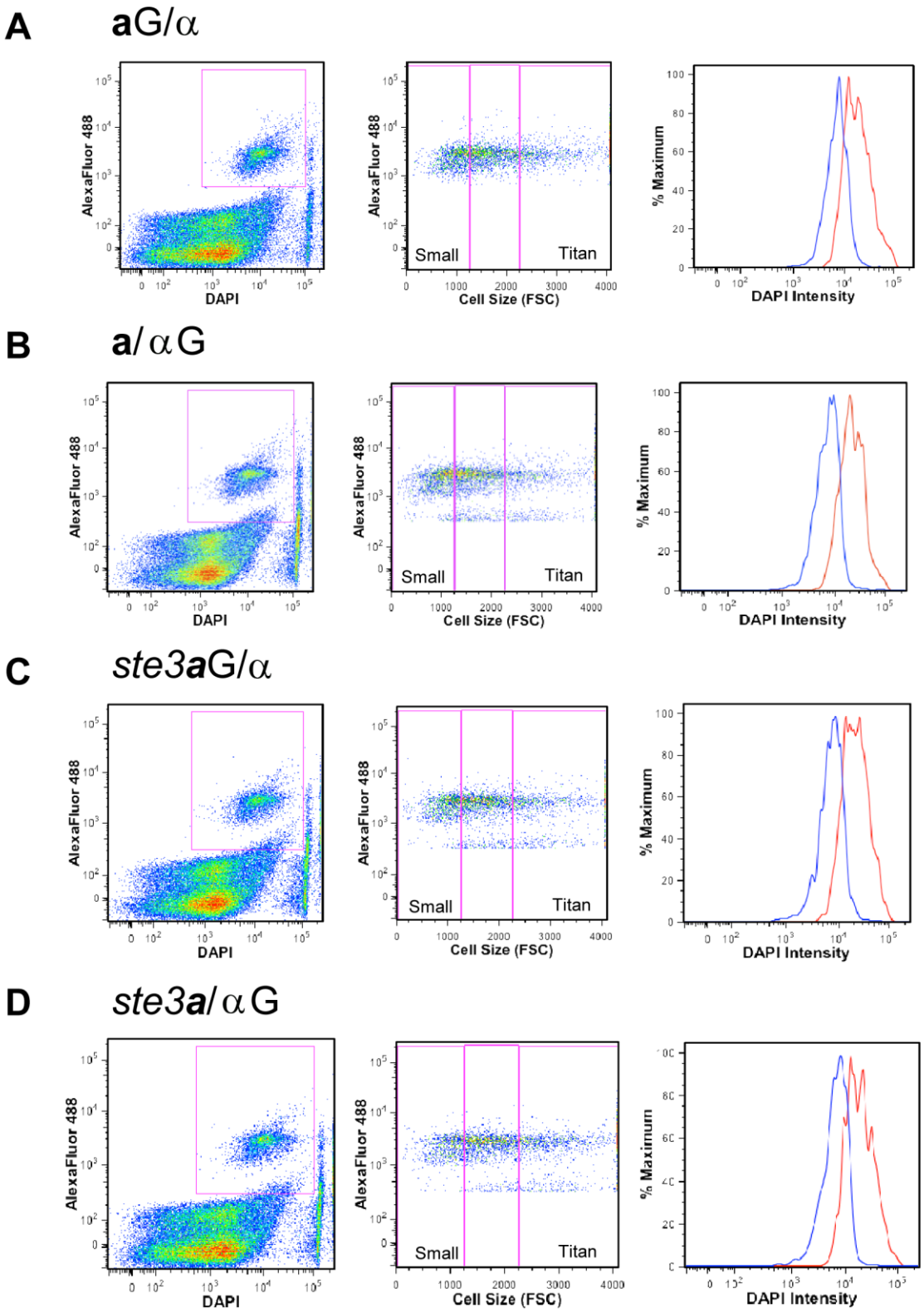
A
aG/α
B
a/αG
C
ste3aG/α
D
ste3a/αG
AlexaFluor 488
DAPI
Cell Size (FSC)
% Maximum
DAPI Intensity
Small
Titan

Figure 2.12 Continued

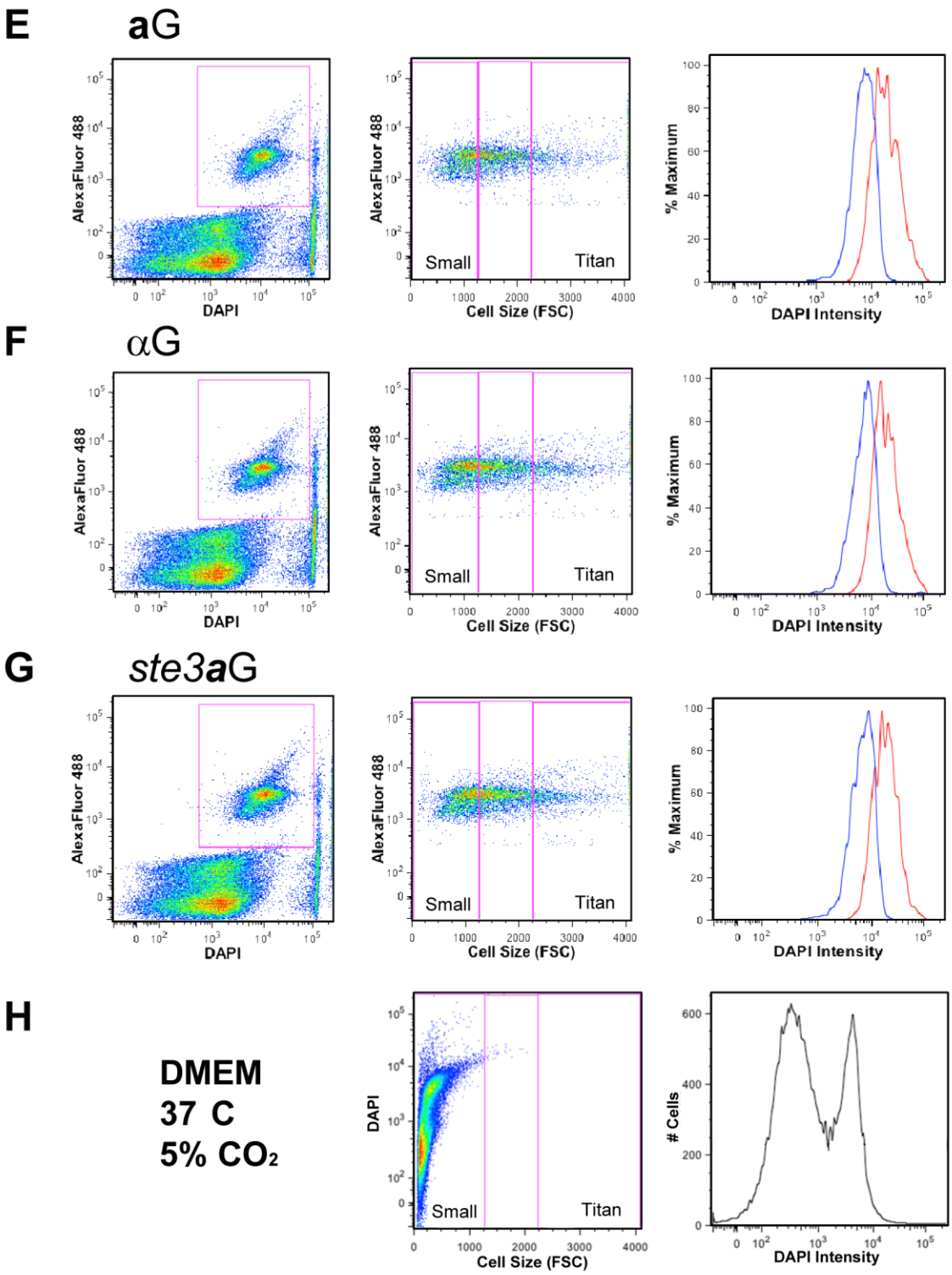

Figure 2.12. *C. neoformans* titan cells are polyploid. a and α strains were combined with AlexaFluor 488 (green) and incubated at 25°C for 20 minutes. Cells were washed with sterile PBS to remove excess dye. Mice were inoculated with an approximate 1:1 ratio of **a**:α cells. At 3 days post-infection animals were sacrificed and BALs were performed. The resulting cells were fixed, DAPI stained and analyzed using and LSRII flow cytometer using FACSDiva software (BD). Fluorescently labeled yeast cells were first identified as 488^{hi} and $DAPI^{low}$ (left). Forward scatter (FSC) was used to identify small (≤ 10 μm) and titan (>20 μm) cells. Small (blue line) and titan (red line) cell populations were analyzed for DNA content (DAPI) and normalized for cell number (right). **A-D** coinfections **E-G** individual infections **H)** *C. neoformans* cells were grown for 5 days at 37°C and 5% CO_2 in DMEM, fixed and DAPI stained. Both 1C and 2C peaks can be seen in this cell population. Absolute levels of DAPI intensity in these control cells varied from experiment to experiment thus were included as internal controls for every experiment.

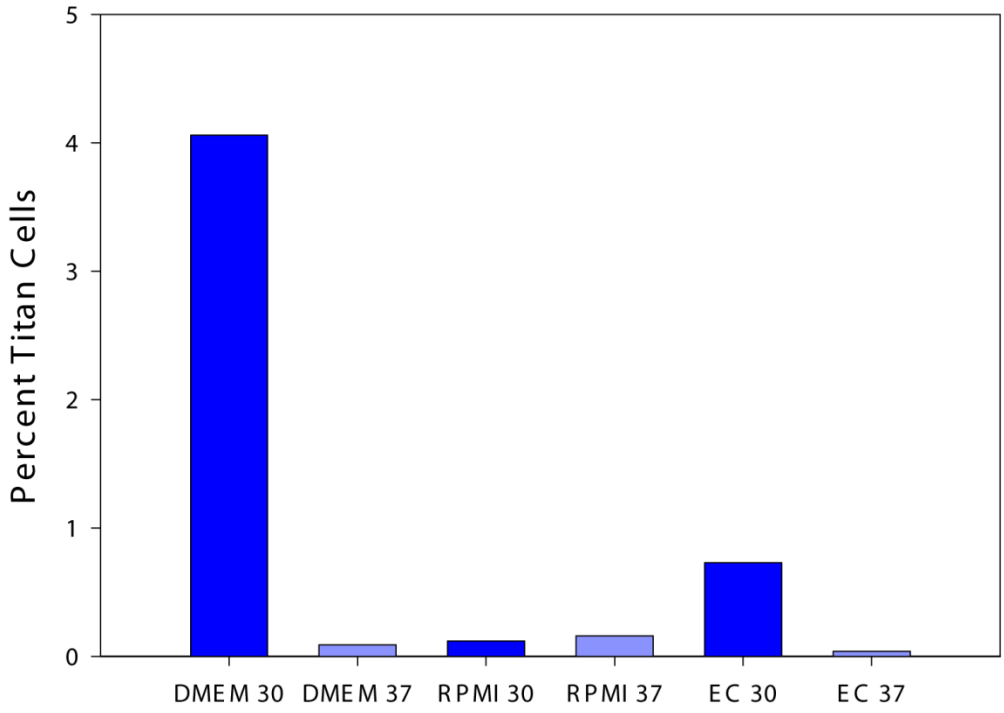

Figure 2.13. *In vitro* titan cell production. Cryptococcal cells were grown in spent DMEM (MH-S alveolar macrophages), RPMI (MH-S alveolar macrophages), or endothelial cell media (human umbilical vein endothelial cells, HUVEC) at 30°C or 37°C. Samples were fixed in 3.7% formaldehyde and 50,000 cells per sample were analyzed for cell size (forward scatter). Data presented are representative of five independent experiments

IV. DISCUSSION

We characterized a novel cell morphology produced by *C. neoformans*, referred to as "titan" cells. These enlarged cells have been observed in the lungs of mice following intranasal instillation (Feldmesser, Kress et al. 2001) and can be up to 100 µm in diameter. Titan cells are commonly seen in human clinical isolates (Cruickshank, Cavill et al. 1973; Love, Boyd et al. 1985). As early as the 1970s, cells greater than 50µm in diameter were observed in sputum samples of an infected patient (Cruickshank, Cavill et al. 1973). Our studies demonstrate that titan cells are resistant to oxidative/nitrosative stresses and phagocytosis by host macrophages. We propose that alterations in phagocytosis are beneficial to cell survival in the lungs early in the infectious process but impede dissemination to the major site of disease in the brain.

One fifth of the cells in mouse lungs were titan cells following an initial pulmonary infection. The level of titan cell production varied depending on inoculum size. Inoculation with $5x10^4$ cryptococcal cells resulted in almost 30% titan cell formation. In contrast, inoculation with $5x10^6$ cryptococcal cells resulted in approximately 15% titan cell formation. Differences in titan cell formation in response to cryptococcal cell density/burden in the lungs were also observed by Zaragoza and colleagues (Zaragoza, Garcia-Rodas et al. 2010).

Titan cell formation was stimulated by coinfection with strains of opposite mating type. Analysis of titan cell formation in the two mating types revealed that only **a** cells increased titan cell production upon coinfection. Concomitant with this increased titan cell formation we observed a decrease in **a** cell accumulation in the brain. Interestingly, **a** cell hematogenous dissemination to other organs, such as the spleen, was unaffected by

increased titan cell formation. Our molecular studies implicate the pheromone response MAPK signal transduction pathway as a regulator of titan cell production. The increase in titan cell formation and reduction in CNS penetration during coinfection was dependent upon the Ste3**a** pheromone receptor. Mutant strains lacking Ste3**a**, and therefore unable to sense the presence of pheromone, did not enhance titan cell formation during coinfection and exhibited BBB penetration equivalent to α strains. The clinical relevance of *in vivo* pheromone signaling and its effect on the infectious process cannot be determined without first understanding the prevalence of coinfections in humans. Irrespective of the biological significance of pheromone signaling, alteration of titan cell formation using the pheromone signaling pathway is a powerful tool to dissect the effect of titan cell formation on disease progression.

The *ste3**a*** mutant strain exhibited only a slight decrease in the basal level of titan cell formation in the absence of α cells, suggesting that pheromone sensing is not the only pathway leading to titan cell production. The observation that pheromone signaling only modifies the level of titan cells suggests that identification of other signaling pathway(s) involved in titan cell formation will be key to understanding other biologically relevant signals that trigger titan cell formation.

The observation that titan cells can be generated *in vitro* by culture in spent medium suggests that cryptococcal cells may sense the presence or absence of a compound in this medium. Titan cell production was predominantly stimulated by spent media from a macrophage cell line. In contrast, little titan cell production was observed in spent media from an endothelial cell line, suggesting the compound could be cell-type specific. An increase in cell size has also been observed in mice deficient in T cells and

NK cells (Shea, Kechichian et al. 2006). Differences in titan cell formation were also observed in different media and at different temperatures. Thus, we cannot rule out the possibility that the signal is an absence or unavailability of specific nutrients. Taken together, these data suggest there could be four or more signals leading to titan cell formation: host, temperature, nutrients, and pheromone.

At least three possibilities could account for pathway interactions affecting titan cell formation (**Figure 2.14A**). First, the pheromone signaling pathway may positively affect an environmental sensing pathway to increase the signal leading to titan cell production (**Figure 2.14A top**). Second, pheromone signaling may inhibit a negative regulator of titan cell formation (**Figure 2.14A middle**). Finally, the pheromone signaling pathway may be independent of the environmental sensing pathway leading to titan cell formation (**Figure 2.14A bottom**). Mutant analysis has revealed that signaling pathways such as PKA, cAMP, and RAS can affect cell size *in vitro* (D'Souza, Alspaugh et al. 2001; Waugh, Nichols et al. 2002; Zaragoza, Garcia-Rodas et al. 2010) and may be involved in the environmental sensing or pheromone signaling pathways leading to titan cell formation.

Titan cells have higher DNA content compared with smaller cells. Titan cell production may be a result of a cell cycle pause or increased DNA replication due to other mechanisms. In *S. cerevisiae* the cell cycle mutant, *cdc24*, can be induced to produce yeast cells up to six times greater in volume than normal cells due to continued growth in the absence of cell division (Sloat, Adams et al. 1981). However, because titan cells are able to continue producing daughter cells, it is unlikely they are generated by a complete cell cycle arrest, as in the *cdc24* mutant. An increase in DNA content from

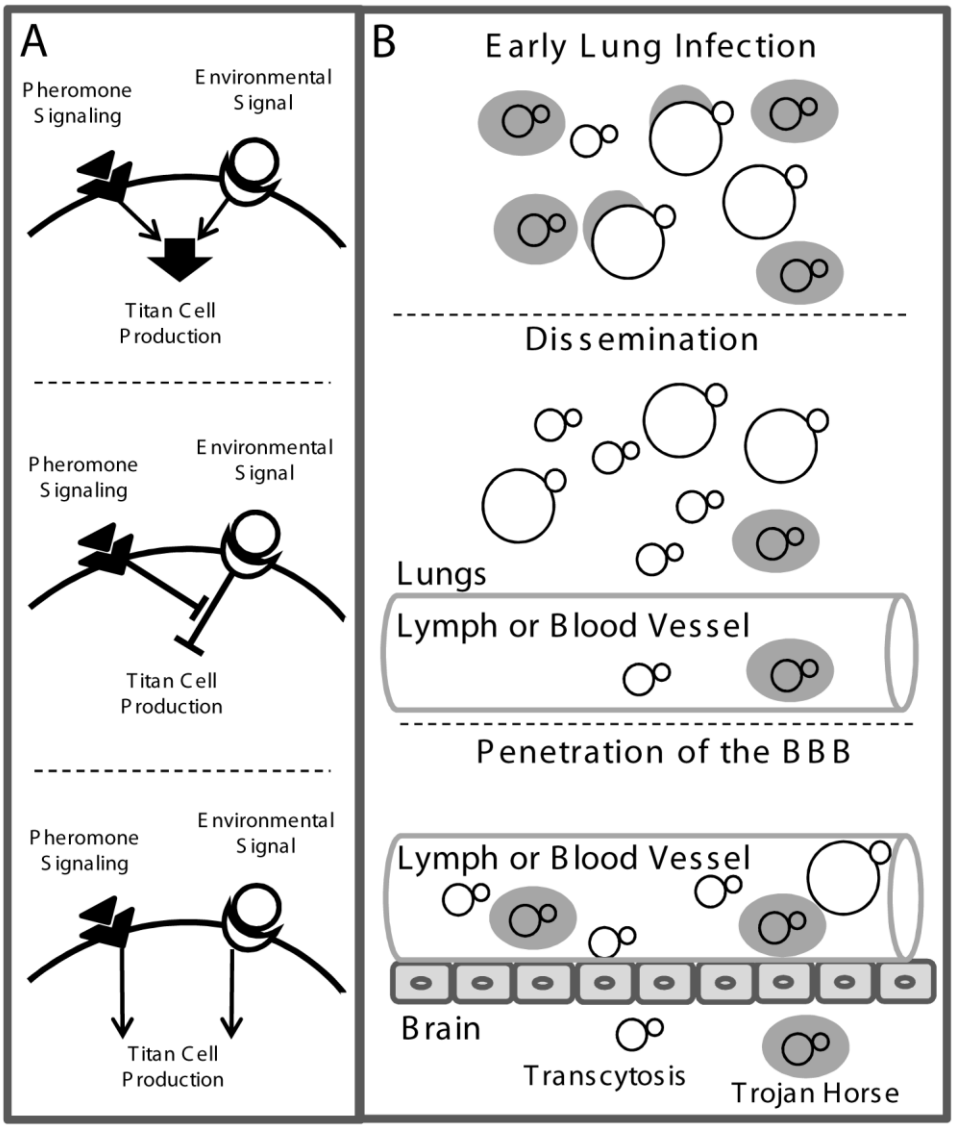

Figure 2.14. Model of titan cell signal transduction and pathogenesis. A) Putative pathways involved in titan cell production. *Top:* Pheromone signaling may enhance an environmental sensing signal leading to titan cell production. *Middle:* Pheromone signaling may inhibit a negative regulator of titan cell formation. *Bottom:* Pheromone signaling may act independently of the environmental sensing and/or other pathways leading to titan cells formation. **B)** The effect of titan cell formation on pathogenesis. *Top:* Upon initial infection, titan cell production protects a subset of cells from phagocytosis and killing, to establish the infection. *Middle: C. neoformans* cells disseminate from the lungs either as free cells or inside host phagocytes. *Bottom:* Phagocytosis is required for efficient penetration of the blood-brain barrier. Cryptococcal cells may enter the brain by transcytosis, or as a "Trojan horse" inside of host phagocytes. Over-production of titan cells reduces blood-brain barrier penetration as a result of decreased phagocytosis.

haploid to tetraploid has been implicated in increased cell size and morphology changes in *S. cerevisiae* (Galitski, Saldanha et al. 1999). This may be due to an increase in transcripts that regulate passage from G1 to S phase in the tetraploids (Galitski, Saldanha et al. 1999). *C. neoformans* titan cells do not appear to have the mitosis defects and lowered viability seen in *S. cerevisiae* tetraploid cells (Andalis, Storchova et al. 2004; Storchova, Breneman et al. 2006). These data suggest *C. neoformans* may have a distinct cell cycle regulation that allows titan cell replication. An increase in DNA content may be necessary to generate and sustain titan cells. Zaragoza and colleagues (Zaragoza, Garcia-Rodas et al. 2010) have shown that titan cells have altered capsule formation and cell wall composition. These processes, along with the need to sustain a large cell, may require increased transcriptional and translational capacity by the cell. Additional copies of DNA may facilitate this process.

An alternative hypothesis is that the increase in cell size protects against the host immune system and that the increase in DNA content promotes rapid generation of daughter cells. This phenomenon is observed in other human pathogenic fungi. *Pneumocystis* and *Coccidioides* species also exhibit increases in cell size and nuclear content in the lungs of infected hosts. In *Pneumocystis*, many cells are in a trophic haploid state and reproduce by binary fission, yet a subset of cells is thought to undergo a sexual cycle to produce enlarged cysts (Cushion 2004; Beck and Cushion 2009). It is hypothesized that the *Pneumocystis* sexual cycle involves fusion of two haploid trophic cells to produce a diploid cell. Although the exact signal for fusion is unknown, molecular analysis has revealed a MAPK pathway similar to the *C. neoformans* pheromone signaling pathway, including a homolog of the Ste3 pheromone receptor

(Smulian, Sesterhenn et al. 2001; Thomas, Park et al. 2001). The resulting diploid cell undergoes meiosis followed by mitosis, forming a cyst containing eight nuclei (Cushion 2004; Beck and Cushion 2009). As the *Pneumocystis* cyst matures, the nuclei develop into new trophic cells and are released into the surrounding environment (Cushion 2004; Thomas and Limper 2004; Beck and Cushion 2009). In contrast to cryptococcal titan cells, *Pneumocystis* cyst formation produces β-glucan resulting in increased recognition and phagocytosis by host immune cells (Beck and Cushion 2009).

Coccidioides immitis also undergoes dramatic morphological changes *in vivo* (Huppert, Sun et al. 1982; Hung, Xue et al. 2007). Infection begins with inhalation of spores, or arthroconidia, from the environment that are roughly 2 to 4μm in diameter. The arthroconidia produce round cells in which nuclear division gives rise to multinucleated cells called spherules (Huppert, Sun et al. 1982; Johannesson, Kasuga et al. 2006; Hung, Xue et al. 2007; Li, Schmelz et al. 2007). The developing spherules range in size from 60 to100 μm or larger. Host immune cells, such as macrophages and neutrophils, are unable to phagocytose the *Coccidioides* spherules due to their large size, protecting the cell from destruction while it generates endospores (Hung, Xue et al. 2007). Eventually the spherule ruptures, releasing the endospores, and the cycle starts again. In *C. neoformans*, titan cells are also protected from phagocytosis. Titan cells do not rupture but instead produce daughter cells both *in vitro* and *in vivo* by budding. Unlike *Pneumocystis* and *Coccidioides* where enlarged cells contain multiple nuclei, the cryptococcal titan cells appear to have a single nucleus. Interestingly, titan daughter cells are small, suggesting they may be haploid. These findings imply ploidy changes occur both during formation of titan cells and their daughter cell progeny. Ploidy changes can occur via sexual,

parasexual, and endoreplicative processes. Further studies are necessary to determine the method by which ploidy changes occur in *C. neoformans*.

Titan cell production was observed within 1 day post-infection, yet the proportion of titan cells present in the lungs plateau by 7 days post-infection and remain constant throughout the rest of the infection. The observation that titan cell production is only stimulated at early stages of infection implies titan cells may promote pathogenesis early in the infectious process but are dispensable later. *Cryptococcus* is acquired from the environment by inhalation of spores or desiccated yeast cells. Previous studies examining changes in transcription and subsequent up-regulation of virulence factors in response to changes in temperature or phagocytosis by macrophages show that the initial population of inhaled cells is unlikely to be prepared for survival and replication in the host (Mitchell and Perfect 1995; Steenbergen and Casadevall 2003; Kraus, Boily et al. 2004; Fan, Kraus et al. 2005; Idnurm, Bahn et al. 2005). Thus, the vast majority of cells in the initial inoculum are likely to be engulfed and destroyed by host mononuclear phagocytes. Titan cell production protects a subset of cells from phagocytosis, possibly due to increased size. While not tested directly in this study, the observed *in vitro* survival in the presence of oxidative/nitrosative stresses may also promote titan cell resistance to killing mechanisms utilized by host immune cells. Thus, the titan cells are able to survive the initial host immune response.

Pheromone-mediated titan cell production did not increase the prevalence of **a** cells in the lungs over time. These data show that titan cell formation does not enhance persistence in the lungs. In support of this conclusion, titan cell formation is not readily observed in the rat persistence model of cryptococcosis (Goldman, Lee et al. 1994;

Goldman, Cho et al. 1996; Goldman, Lee et al. 2000; He, Casadevall et al. 2003; Shao, Mednick et al. 2005; Shao, Rivera et al. 2005; Goldman, Davis et al. 2006). Yet, the *C. neoformans* var. *neoformans* strain most commonly used in the rat model readily generates titan cells in mice (Shao, Mednick et al. 2005; Zaragoza, Garcia-Rodas et al. 2010). Because titan cells are readily observed in human tissue, where dormancy is thought to be important in the infectious process (Dromer, Aucouturier et al. 1988; Casadevall and Perfect 1998; Garcia-Hermoso, Janbon et al. 1999), we cannot rule out the possibility that titan cells play a role in dormancy and/or reactivation in human infections.

Dysregulation of titan cell production in the coinfection model did not affect hematogenous dissemination from the lungs to the spleen; yet increased titan cell formation was correlated with a significant decrease in dissemination to the CNS. Survival in macrophages has been shown to be important for trafficking to the CNS (Luberto, Martinez-Marino et al. 2003; Del Poeta 2004). Additionally, recent studies have demonstrated that phagocytosed cryptococcal cells are more efficient at disseminating to the CNS than non-phagocytosed cells (Santangelo, Zoellner et al. 2004; Charlier, Nielsen et al. 2009). Thus, interactions with host phagocytes promote cryptococcal BBB penetration and subsequent neurological disease. Increased titan cell formation in the lungs during coinfection reduced phagocytosis which subsequently inhibited dissemination to the CNS. It is still unclear whether coinfections are a common occurrence in *Cryptococcus* pathogenesis, yet the effect of coinfection on titan cell production has allowed us to study this important morphological transition. Our data support a model in which titan cells are advantageous at early stages of the infection

(**Figure 2.14B**). The ability of titan cells to evade phagocytosis allows *C. neoformans* to establish the initial lung infection and overcome the initial immune response generated by resident macrophages (**Figure 2.14B top**). Because severe cryptococcal infections are often seen in patients with T cell deficiencies, it is likely that the clearance of the initial infection is T cell mediated. (**Figure 2.14B middle**). Our model predicts that phagocytosis of the daughter cells allows dissemination to the CNS, resulting in neurological disease (**Figure 2.14B bottom**).

Examples of cell morphology changes and cell surface alterations that are important in the infectious process can be found throughout the microbial world. In the protozoan pathogen *Toxoplasma gondii*, cysts are formed in response to elements of the host immune response, including IFNγ, pH changes, and nitrosative stress. These cysts are able to escape immune recognition and establish an asymptomatic chronic infection (Dubey 2004; Blader and Saeij 2009). Uropathogenic *Escherichia coli* strains are known to undergo filamentation in response to TLR4 signaling by host immune cells (Justice, Hunstad et al. 2008). During development of these bacterial colonies, a subset of the cells filament. The filaments are then able to evade phagocytosis by host neutrophils that are recruited to the area in response to infection (Justice, Hunstad et al. 2008). Reovirus undergoes dramatic morphological changes in the host. The reovirus virion can be degraded by proteases revealing a stable intermediate subvirion particle (ISVP). Although both viral morphologies are infectious, the virion is more restricted in host range, while the ISVP can infect a wider variety of cell types (Nibert, Furlong et al. 1991; Golden, Linke et al. 2002; Chandran and Nibert 2003).

Similar to morphological changes in other microbes, titan cell formation alters the host-pathogen interaction in the lungs during early cryptococcal infection. By studying these host-pathogen interactions and the molecular triggers involved in *C. neoformans* titan cell production, we may gain general insight into how morphological changes can affect pathogenicity of microbes. Our studies highlight the complex morphological variations microbes deploy to avoid recognition and killing by the host immune system.

CHAPTER THREE

Cryptococcal Titan Cell Formation is Regulated by G-Protein Signaling in Response to Multiple Stimuli

Okagaki LH, Wang Y, Ballou ER, O'Meara TR, Bahn YS, Alspaugh JA, Xue C, Nielsen K. (2011) Cryptococcal Titan Cell Formation is Regulated by G-Protein Signaling in Response to Multiple Stimuli. *Eukaryotic Cell* 2011, 10(10):1306.

I. COPYWRITE PERMISSION

AMERICAN SOCIETY FOR MICROBIOLOGY LICENSE TERMS AND CONDITIONS

Mar 20, 2012

This is a License Agreement between Laura H Okagaki ("You") and American Society for Microbiology ("American Society for Microbiology") provided by Copyright Clearance Center ("CCC"). The license consists of your order details, the terms and conditions provided by American Society for Microbiology, and the payment terms and conditions.

All payments must be made in full to CCC. For payment instructions, please see information listed at the bottom of this form.

License Number	2873121334058
License date	Mar 20, 2012
Licensed content publisher	American Society for Microbiology
Licensed content publication	Eukaryotic Cell
Licensed content title	Cryptococcal Titan Cell Formation Is Regulated by G-Protein Signaling in Response to Multiple Stimuli
Licensed content author	Laura H. Okagaki, Yina Wang, Elizabeth R. Ballou, Teresa R. O'Meara, Yong-Sun Bahn, J. Andrew Alspaugh, Chaoyang Xue, Kirsten Nielsen
Licensed content date	Oct 1, 2011
Volume	10
Issue	10
Start page	1306
End page	1316
Type of Use	Dissertation/Thesis
Format	Print and electronic
Portion	Full article
Order reference number	
Title of your thesis / dissertation	The Production and Function of Titan Cells in Cryptococcus neoformans
Expected completion date	May 2012
Estimated size(pages)	200
Billing Type	Invoice
Billing address	6312 Olympia Street Golden Valley, MN 55427 United States
Customer reference info	
Total	0.00 USD
Terms and Conditions	

Publisher Terms and Conditions

The publisher for this copyrighted material is the American Society for Microbiology (ASM). By clicking "accept" in connection with completing this licensing transaction, you agree that the following terms and conditions apply to this transaction (along with the Billing and Payment terms and conditions established by Copyright Clearance Center, Inc. ("CCC"), at the time that you opened your Rightslink account and that are available at any time at http://myaccount.copyright.com).
1. ASM hereby grants to you a non-exclusive license to use this material. Licenses are for one-time use only with a maximum distribution equal to the number that you identified in the licensing process; any form of republication must be completed within 1 year from the date hereof (although copies prepared before then may be distributed thereafter). The copyright of all material specified remains with ASM, and permission for reproduction is limited to the formats and products indicated in your license. The text may not be altered in any way without the express permission of the copyright owners.

2. The licenses may be exercised anywhere in the world.

3. You must include the copyright and permission notice in connection with any reproduction of the licensed material, i.e. Journal name, year, volume, page numbers, DOI and reproduced/amended with permission from American Society for Microbiology.

4. The following conditions apply to photocopies:
a. The copies must be of high quality and match the standard of the original article.
b. The copies must be a true reproduction word for word.
c. No proprietary/trade names may be substituted.
d. No additional text, tables or figures may be added to the original text.
e. The integrity of the article should be preserved, i.e., no advertisements will be printed on the article.
f. The above permission does NOT include rights for any online or other electronic reproduction.

5. The following conditions apply to translations:
a. The translation must be of high quality and match the standard of the original article.
b. The translation must be a true reproduction word for word.
c. All drug names must be generic; no proprietary/trade names may be substituted.
d. No additional text, tables or figures may be added to the translated text.
e. The integrity of the article should be preserved, i.e., no advertisements will be printed on the article.
f. The translated version of ASM material must also carry a disclaimer in English and in the language of the translation. The two versions (English and other language) of the disclaimer MUST appear on the inside front cover or at the beginning of the translated material as follows:

The American Society for Microbiology takes no responsibility for the accuracy of the translation from the published English original and is not liable for any errors which may occur. No responsibility is assumed, and responsibility is hereby disclaimed, by the American Society for Microbiology for any injury and/or damage to persons or property as a matter of product liability, negligence or otherwise, or from any use or operation of methods, products, instructions or ideas presented in the Journal. Independent verification of diagnosis and drug dosages should be made. Discussions, views, and recommendations as to medical procedures, choice of drugs and drug dosages are the responsibility of the authors.

g. This license does NOT apply to translations made of manuscripts published ahead of print as "[ASM Journal] Accepts" papers. Translation permission is granted only for the final published version of the ASM article. Furthermore, articles translated in their entirety must honor the ASM embargo period, and thus may not appear in print or online until 6 months after the official publication date in the original ASM journal.

6. While you may exercise the rights licensed immediately upon issuance of the license at the end of the licensing process for the transaction, provided that you have disclosed complete and accurate details of your proposed use, no license is finally effective unless and until full payment is received from you (either by ASM or by CCC) as provided in CCC's Billing and Payment terms and conditions. If full payment is

not received on a timely basis, then any license preliminarily granted shall be deemed automatically revoked and shall be void as if never granted. In addition, permission granted is contingent upon author permission, which you MUST obtain, and appropriate credit (see item number 3 for details). If you fail to comply with any material provision of this license, ASM shall be entitled to revoke this license immediately and retain fees paid for the grant of the license. Further, in the event that you breach any of these terms and conditions or any of CCC's Billing and Payment terms and conditions, the license is automatically revoked and shall be void as if never granted. Use of materials as described in a revoked license, as well as any use of the materials beyond the scope of an unrevoked license, may constitute copyright infringement and ASM reserves the right to take any and all action to protect its copyright in the materials.

7. ASM reserves all rights not specifically granted in the combination of (i) the license details provided by you and accepted in the course of this licensing transaction, (ii) these terms and conditions and (iii) CCC's Billing and Payment terms and conditions.

8. ASM makes no representations or warranties with respect to the licensed material and adopts on its own behalf the limitations and disclaimers established by CCC on its behalf in its Billing and Payment terms and conditions for this licensing transaction.

9. You hereby indemnify and agree to hold harmless ASM and CCC, and their respective officers, directors, employees and agents, from and against any and all claims arising out of your use of the licensed material other than as specifically authorized pursuant to this license.

10. This license is personal to you, but may be assigned or transferred by you to a business associate (or to your employer) if you give prompt written notice of the assignment or transfer to the publisher. No such assignment or transfer shall relieve you of the obligation to pay the designated license fee on a timely basis (although payment by the identified assignee can fulfill your obligation).

11. This license may not be amended except in a writing signed by both parties (or, in the case of ASM, by CCC on ASM 's behalf).

12. Objection to Contrary terms: ASM hereby objects to any terms contained in any purchase order, acknowledgment, check endorsement or other writing prepared by you, which terms are inconsistent with these terms and conditions or CCC's Billing and Payment terms and conditions. These terms and conditions, together with CCC's Billing and Payment terms and conditions (which are incorporated herein), comprise the entire agreement between you and ASM (and CCC) concerning this licensing transaction. In the event of any conflict between your obligations established by these terms and conditions and those established by CCC's Billing and Payment terms and conditions, these terms and conditions shall control.

13. The following terms and conditions apply to Commercial Photocopy and Commercial Reprint requests and should be considered by requestors to be additional terms. All other ASM terms and conditions indicating how the content may and may not be used also apply.

Limitations of Use:

The Materials you have requested permission to reuse in a commercial reprint or commercial photocopy are only for the use that you have indicated in your request, and they MAY NOT be used for either resale to others or republication to the public. Further, you may not decompile, reverse engineer, disassemble, rent, lease, loan, sell, sublicense, or create derivative works from the Materials without ASM's prior written permission.

14. Revocation: This license transaction shall be governed by and construed in accordance with the laws of Washington, DC. You hereby agree to submit to the jurisdiction of the federal and state courts located in Washington, DC for purposes of resolving any disputes that may arise in connection with this licensing transaction. ASM or Copyright Clearance Center may, within 30 days of issuance of this License, deny the

permissions described in this License at their sole discretion, for any reason or no reason, with a full refund payable to you. Notice of such denial will be made using the contact information provided by you. Failure to receive such notice will not alter or invalidate the denial. In no event will ASM or Copyright Clearance Center be responsible or liable for any costs, expenses or damage incurred by you as a result of a denial of your permission request, other than a refund of the amount(s) paid by you to ASM and/or Copyright Clearance Center for denied permissions.

II. INTRODUCTION

Cryptococcus neoformans is an opportunistic fungal pathogen most commonly observed in immunocompromised patient populations. *C. neoformans* spores or desiccated yeast cells are inhaled into the lungs where they are small enough to lodge in the alveoli. In healthy patients, the cryptococcal pulmonary infection is cleared or contained in granulomas; however, in immunocompromised patients, *C. neoformans* is able to disseminate from the lungs to cause a systemic infection (Heitman and American Society for Microbiology. 2011). At late stages of infection, *C. neoformans* penetrates the blood brain barrier (BBB) and causes infections of the central nervous system. Due to an increase in the number of HIV+ individuals, *C. neoformans* has become the 3rd leading cause of death in HIV-infected adults in sub-Saharan Africa (Park, Wannemuehler et al. 2009). Each year, *C. neoformans* is responsible for approximately one million infections world-wide, resulting in over 600,000 deaths (Park, Wannemuehler et al. 2009).

C. neoformans has several well studied virulence factors, including polysaccharide capsule, melanin production, and mating type (Casadevall and Perfect 1998; Heitman and American Society for Microbiology. 2011). The cryptococcal polysaccharide capsule has been shown to modulate the host immune response (Casadevall and Perfect 1998; Heitman and American Society for Microbiology. 2011). Capsule material can bind both antibody and complement, preventing phagocytosis by host macrophages. Production of melanin protects cryptococcal cells from oxidative stress produced by the host immune system in response to infection and phagocytosis (Casadevall and Perfect 1998; Heitman and American Society for Microbiology. 2011).

C. neoformans mating type has also been shown to be a factor in pathogenesis. *Cryptococcus* has two mating types: **a** and α. Of these, mating type α cells account for the majority of clinical isolates (Casadevall and Perfect 1998; Heitman and American Society for Microbiology. 2011). In experiments where both mating types were used to co-infect mice, mating type **a** cells were unable to efficiently penetrate the blood brain barrier (Nielsen, Cox et al. 2003; Nielsen, Cox et al. 2005). Previously, we demonstrated that dramatic alterations in the rate of titan cell formation between mating types accounted for the difference in BBB penetration during co-infections (Okagaki, Strain et al. 2010).

Many *Cryptococcus* virulence factors are regulated by the cAMP/PKA pathway (Alspaugh, Perfect et al. 1997; D'Souza, Alspaugh et al. 2001; Alspaugh, Pukkila-Worley et al. 2002; Pukkila-Worley, Gerrald et al. 2005). The Gα protein Gpa1 activates the cAMP pathway, and strains with mutations in the *GPA1* gene display alterations in surface capsule, melanin production, and virulence (Alspaugh, Perfect et al. 1997; D'Souza, Alspaugh et al. 2001). Disruption of other positive regulators of the cAMP/PKA pathway, including Pka1 and Cac1, also results in an avirulent phenotype (Alspaugh, Perfect et al. 1997; D'Souza, Alspaugh et al. 2001; Alspaugh, Pukkila-Worley et al. 2002; Cramer, Gerrald et al. 2006). The Rim101 transcription factor is downstream of Pka1 in *C. neoformans* (O'Meara, Norton et al. 2010). Signaling through both the cAMP/PKA pathway and the pH/Rim pathways activates Rim101 under host conditions (O'Meara, Norton et al. 2010). In the pathogenic fungus *Candida albicans*, Rim101 regulates the yeast to hyphal switch in response to iron starvation and increased pH, which are relevant conditions for infection (Davis, Edwards et al. 2000; Davis, Wilson et al. 2000). The role

for Rim101 in morphological changes in *C. neoformans* under host conditions was previously uncharacterized.

C. neoformans can produce enlarged "titan" cells in response to the host lung environment. Titan cells can reach 50-100 µm in diameter, a 5-10 fold increase in size compared with cells grown *in vitro* (Okagaki, Strain et al. 2010; Zaragoza, Garcia-Rodas et al. 2010). During pulmonary infection, titan cells account for approximately 20% of the cryptococcal cell population. Characterization of titan cells revealed that they are inefficiently engulfed by host immune cells (Okagaki, Strain et al. 2010). In addition, titan cells are more resistant to the oxidative and nitrosative antimicrobial mechanisms produced by the host immune response (Okagaki, Strain et al. 2010). Titan cells also exhibit alterations in the cell wall and capsule. The cell wall is thickened compared with normal cells, and the capsule is highly cross-linked and cannot be sheared from the cell by chemical or physical means (Zaragoza, Garcia-Rodas et al. 2010). Analysis of nuclear content showed that titan cells have increased ploidy and can be tetraploid or octoploid (Okagaki, Strain et al. 2010).

Titan cell production is regulated by elements of the pheromone signaling pathway in mating type **a** cells. In coinfections with both mating types, mating type **a** cells double their production of titan cells to approximately 40% while mating type α cells remain at the basal titan cell production level of 20% (Okagaki, Strain et al. 2010). Additionally, increased titan cell formation was correlated with decreased penetration of the BBB by mating type **a** cells during coinfection, suggesting that pheromone signaling leading to titan cell formation affects virulence (Okagaki, Strain et al. 2010). *C. neoformans* pheromone peptides are sensed by the G- protein coupled receptors Ste3**a**

and Ste3α (Davidson, Moore et al. 2000; Karos, Chang et al. 2000; Shen, Davidson et al. 2002). Ste3α interacts with the Gα proteins Gpa2 and Gpa3 to signal via a MAPK signal transduction pathway to regulate mating (Davidson, Moore et al. 2000; Davidson, Nichols et al. 2003; Hsueh, Xue et al. 2007). Disruption of pheromone sensing in mating type **a** cells during coinfection by deletion of the pheromone receptor Ste3**a** reduced titan cell formation in mating type **a** cells to the basal level of 20% (Okagaki, Strain et al. 2010). Thus, increased production of titan cells during mixed infection is dependent on intact Ste3**a** signaling.

Previous work identified and characterized titan cell formation during early pulmonary infection (Okagaki, Strain et al. 2010; Zaragoza, Garcia-Rodas et al. 2010). However, the mechanism by which pheromone signaling affected titan cell production in mating type **a** cells but not mating type α cells remained unclear. Additionally, the signaling pathway necessary for production of the basal level of titan cells during a typical infection had not been identified. Here, we sought to identify receptors that sense the host environment to regulate titan cell production. We also identified Gα proteins downstream of these receptors important for titan cell formation. Additionally, we sought to identify downstream effectors of the signaling pathway and potential transcription factors responsible for titan cell induction. We determined that the conserved cAMP/PKA pathway signaling pathway controls the dramatic titan cell morphological change through activation of the Rim101 transcription factor.

III. MATERIALS AND METHODS

Ethics Statement. All animals were handled in strict accordance with good animal practice as defined by the relevant national and/or local animal welfare bodies, and all animal work was approved by the Institutional Animal Care and Use Committee (IACUC) under protocol numbers 0712A22250 and 1010A91133.

Strains and Media. *C. neoformans* var. *grubii* strains used in this study are described in **Table 3.1.** Strains were stored as glycerol stocks at -80°C and grown at 30°C in yeast extract-peptone-dextrose (YPD) agar or broth medium (BD, Hercules, CA).

Double mutant strains were isolated from the progeny of matings between YSB25 and YSB105 for *gpa2Δgpa3Δ* double mutant strains LHO7 and LHO8. Single *gpa3Δ* strains LHO5 and LHO6 were isolated from the progeny of matings between YPH308 (Hsueh, Xue et al. 2007) and KN99**a**. Briefly, matings were performed on V8 agar and basidiospores were micromanupulated as previously described (Hsueh, Idnurm et al. 2006). Strains were isolated using YPD agar containing 200µg/mL nourseothriacin (NAT) and/or 200µg/mL neomycin (NEO). Mutant strains were then screened by PCR using the primers listed in **Table 3.1** to verify gene deletions and marker insertion into the appropriate loci. *gpr8Δ* and *gpr9Δ* mutants were generated in the H99 strain background by overlap PCR as previously described (Davidson, Blankenship et al. 2002). The 5' and 3' regions of the *GPR8* gene were amplified from H99 genomic DNA with primers JH13288/JH13289, and JH13290/JH13291, respectively. The flanking regions of the GPR9 gene were amplified by JH13295/JH13296, and JH13297/JH13298, respectively. The dominant selectable markers (NEO^{r}) were amplified with the M13

primers (M13F and M13R) from plasmid pJAF1 (Fraser, Subaran et al. 2003). The target gene replacement cassettes of *GPR8* and *GPR9* were generated by overlap PCR with primers JH13288/JH13291, and JH13295/JH13298, respectively. Purified overlap PCR products were precipitated onto 10 µl gold microcarrier beads (0.6 µm; Bio-Rad), and strain H99 was biolistically transformed as described previously (Davidson, Cruz et al. 2000). Stable transformants were selected on YPD medium containing G418 (200 mg/L). To screen for mutants of *GPR8* and *GPR9*, diagnostic PCRs were performed by analyzing the 5' junction of the disrupted mutant alleles with primers JH13287/JH8994 (GPR8), and JH13294/JH8994 (GPR9) (**Table 3.1**). Positive transformants identified by PCR screening were further confirmed by Southern blot analysis.

Gene complementation in the double mutant strains was performed by isolating progeny from matings between CDX18 and KN99α or CDX19 and KN99**a**. Briefly, matings were performed on V8 agar and basidiospores were micromanupulated as previously described (Hsueh, Idnurm et al. 2006). Strains were isolated using YPD agar containing 200µg/mL nourseothriacin (NAT) or neomycin (NEO). Single mutant strains were then screened by PCR using the primers listed in **Table 3.1** to verify gene deletions and marker insertions into the appropriate loci.

***In vivo* titan cell assay.** *C. neoformans* cells were cultured overnight in YPD broth. The resulting yeast cells were pelleted and resuspended in sterile phosphate-buffered saline (PBS) at a concentration of $1x10^8$ cells/ml based on hemocytometer count. Groups of 6- to 8-week-old female A/J mice (Jackson Labs, Bar Harbor, MA) were anesthetized by intraperitoneal pentobarbital injection. One mouse (preliminary experiments) or three to

five mice per treatment were infected intranasally with $5x10^6$ cells in 50 µl phospho-buffered saline (PBS, Lonza, Rockland, ME). At 3 days post-infection mice were sacrificed by CO_2 inhalation. Lungs were lavaged with 1.5 mL sterile PBS three times using a 20 gauge needle placed in the trachea. Cells in the lavage fluid were pelleted at 16,000*g*, resuspended in 3.7% formaldehyde, and incubated at room temperature for 30 minutes. Cells were then washed once with PBS and >300 cells per animal were analyzed for size by microscopy (AxioImager, Carl Zeiss, Inc). Cell body size was measured and cells were classified as small cells (<10 µm in diameter), or titan cells (>10 µm in diameter).

Flow Cytometry. KN99α was grown overnight in YPD medium to log phase. Cells were centrifuged at 16,000g for 1 minute and the supernatant discarded. Cells were washed 3 times in sterile PBS and resuspended in 3.7% formaldehyde in PBS and incubated for 30 minutes at room temperature. BAL samples were washed once in 0.05% SDS to lyse mammalian cells, then washed two times in sterile water. Cells in the lavage fluid were pelleted at 16,000*g*, resuspended in 3.7% formaldehyde, and incubated at room temperature for 30 minutes. All samples were then washed once with PBS, resuspended in PBS containing 300 ng/ml 4',6-diamidino-2-phenylindole (DAPI) (Invitrogen). Samples were incubated at room temperature for 15 minutes, washed with PBS, and resuspended in PBS. Cells were examined for cell size by forward scatter (FCS) and nuclear content by DAPI using an LSRII flow cytometer with FACSDiva software (BD). Cell populations were analyzed using FlowJo software (Tree Star, Inc, Ashland, OR) (**Figure 3.2**).

Yeast Two-hybrid. The spit-ubiquitin system has been designed to specifically detect the potential interactions between membrane proteins (Osman 2004). This system was utilized to investigate the interaction between several G-protein coupled receptor proteins (Ste3**a**, Ste3α, Gpr5, and Gpr4) and Gα proteins (Gpa1, Gpa2, and Gpa3). Vectors and yeast strains were included in the DUALmembrane Kit 2 (Dualsystem Biotech, Zürich, Switzerland). Full length cDNAs of *STE3**a***, *STE3α*, *GPR5*, and *GPR4* were cloned into pCCW (Cub was fused to the C-terminus of each protein), respectively. *GPA1*, *GPA2*, and *GPA3* full-length cDNAs were cloned into the pDL2XN vector (the mutated N-terminal half of ubiquitin NubG protein was fused to the G protein C-termini). *GPA1* dominant active allele ($GPA1^{Q284L}$) and dominant negative allele ($GPA1^{G283A}$) were also cloned into pDL2XL. All cDNA sequences were confirmed by DNA sequencing. Cub and NubG fusion constructs were cotransformed into host yeast strain NMY32. Interaction was determined by the growth of yeast transformants on medium lacking histidine or adenine and also by measuring beta-galactosidase activity.

Coinfections. Four mice per treatment were infected as described above with $5x10^6$ AlexaFluor 488 labeled KN99**a**, KN99α, *gpr4Δgpr5Δ* mating type **a**, *gpr4Δgpr5Δ* mating type α, or an approximate 1:1 ratio of one stained and one unstained strain. Infected mice were sacrificed at 3 days post-infection by CO_2 inhalation. Lungs were lavaged with 1.5 mL sterile PBS three times using a 20 gauge needle placed in the trachea. Cells in the lavage fluid were pelleted at 16,000*g*, resuspended in 3.7% formaldehyde, and incubated at room temperature for 30 minutes. Cells were then washed once with PBS and resuspended in PBS. >300 cells per animal were analyzed for size and fluorescence by

Table 3.1 Strains used in this study.

Strain	Genotype	Reference
KN99a	MAT**a**	(Nielsen, Cox et al. 2003)
KN99α	MATα	(Nielsen, Cox et al. 2003)
YSB83	MATα *gpa1Δ*::NAT	(Xue, Bahn et al. 2006)
CDX153	MATα *gpa1Δ*::NATura5 + GDP1-GPA1(Q^{284L})URA5	(Xue, Bahn et al. 2006)
YSB85	MAT**a** *gpa1Δ*::NEO	(Xue, Bahn et al. 2006)
CDX40	MAT**a** *gpa1Δ*::NATura5 + GDP1-GPA1(Q^{284L})URA5	(Xue, Bahn et al. 2006)
CDX42	MAT**a** *gpa1Δ*::NEOura5 + GDP1-GPA1wtURA5	(Xue, Bahn et al. 2006)
YSB25	MATα *gpa2Δ*::NEO	(Hsueh, Xue et al. 2007)
LHO6	MATα *gpa3Δ*::NEO	This Study
LHO8	MATα *gpa2Δ*::NAT *gpa3Δ*::NEO	This Study
YSB110	MAT**a** *gpa2Δ*::NAT	(Hsueh, Xue et al. 2007)
LHO5	MAT**a** *gpa3Δ*::NEO	This Study
LHO7	MAT**a** *gpa2Δ*::NAT *gpa3Δ*::NEO	This Study
YPH308	MATα *gpa2Δ*::NAT *gpa3Δ*::NEO	(Hsueh, Xue et al. 2007)
YPH106	MAT**a** *gpa2Δ*::NAT *gpa3Δ*::NEO	(Hsueh, Xue et al. 2007)
CDX1	MATα *gpr1Δ*::NAT	(Xue, Bahn et al. 2006)
CDX3	MATα *gpr2Δ*::NEO	(Xue, Bahn et al. 2006)
CDX5	MATα *gpr3Δ*::NEO	(Xue, Bahn et al. 2006)
CDX6	MATα *gpr4Δ*::NEO	(Xue, Bahn et al. 2006)
CDX11	MATα *gpr5Δ*::NAT	(Xue, Bahn et al. 2006)
CDX18	MATα *gpr4Δ*::NEO *gpr5Δ*::NAT	(Xue, Bahn et al. 2006)
LHO17	MATα *gpr4Δ*::NEO + GPR5	This Study
CDX9	MAT**a** *gpr4Δ*::NAT	(Xue, Bahn et al. 2006)
CDX10	MAT**a** *gpr5Δ*::NAT	(Xue, Bahn et al. 2006)
CDX19	MAT**a** *gpr4Δ*::NEO *gpr5Δ*::NAT	(Xue, Bahn et al. 2006)
LHO18	MAT**a** *gpr4Δ*::NEO + GPR5	This Study
CDX14	MATα *gpr8Δ*::NAT	This Study
CDX16	MATα *gpr9Δ*::NAT	This Study
CDC7	MATα *pkr1Δ*::URA5	(D'Souza, Alspaugh et al. 2001)
JKH7	MATα *pka1Δ*::URA5	(Hicks, Bahn et al. 2005)
RPC3	MATα *cac1Δ*::URA5	(Alspaugh, Pukkila-Worley et al. 2002)
TOC2	MATα *rim101Δ*::NAT	(O'Meara, Norton et al. 2010)
TOC4	MATα *rim101Δ*::NAT + RIM101::NEO	(O'Meara, Norton et al. 2010)
CBN32	MATα *cdc24Δ*::NAT	(Nichols, Perfect et al. 2007)
ERB010	MATα *cdc42Δ*::NAT	(Ballou, Nichols et al. 2009)
ERB007	MATα *cdc420Δ*::NEO	(Ballou, Nichols et al. 2009)
ERB012	MATα *cdc420Δ*::NAT + CDC420::NEO	(Ballou, Nichols et al. 2009)
KLC109	MAT**a** *nrg1Δ*::NEO	(Cramer, Gerrald et al. 2006)
KLC113	MATα *nrg1Δ*::NEO	(Cramer, Gerrald et al. 2006)
NB007	MAT**a** *ste3Δ*::NAT	(Okagaki, Strain et al. 2010)
XL1598	MATα *mat2Δ*::NEO	(Lin, Jackson et al. 2010)
XL1601	MATα *znf2Δ*::NEO	(Lin, Jackson et al. 2010)
YSB345	MATα *ste7Δ*::NEO	(Lin, Jackson et al. 2010)
CHY776	MATα *sxi1αΔ*::NAT	(Hull, Davidson et al. 2002)
YSB317	MATα *ste50Δ*::NAT-STM#296	(Jung, Kim et al.)

Table 3.1 - continued

Strain	Genotype	Reference
D782	*zap102Δ* (CNAG_03366)	(Liu, Chun et al. 2008)
D1480	*sks1Δ* (CNAG_06568)	(Liu, Chun et al. 2008)
D1477	*cnf0270Δ* (CNAG_06554)	(Liu, Chun et al. 2008)
D989	*cnh0970Δ* (CNAG_04455)	(Liu, Chun et al. 2008)
D439	*expressed sequence AA960436Δ* (CNAG_01624)	(Liu, Chun et al. 2008)
D1059	*ypl260WΔ* (CNAG_05236)	(Liu, Chun et al. 2008)
D1131	*yor378W07-AΔ* (CNAG_03713)	(Liu, Chun et al. 2008)
D1139	*tpo105Δ* (CNAG_04546)	(Liu, Chun et al. 2008)
D1258	*rim10102Δ* (CNAG_05431)	(Liu, Chun et al. 2008)
D1023	*fms102Δ* (CNAG_05027)	(Liu, Chun et al. 2008)
D949	*cnh3700Δ* (CNAG_04248)	(Liu, Chun et al. 2008)
D986	*yak103Δ* (CNAG_04433)	(Liu, Chun et al. 2008)
D1462	*cnb1770-AΔ* (CNAG_06457)	(Liu, Chun et al. 2008)
D521	*mlh1Δ* (CNAG_02073)	(Liu, Chun et al. 2008)
D88	*zap103Δ* (CNAG_04352)	(Liu, Chun et al. 2008)
D488	*ksp1Δ* (CNAG_01905)	(Liu, Chun et al. 2008)
D545	*hap3Δ* (CNAG_02215)	(Liu, Chun et al. 2008)
D425	*bem2Δ* (CNAG_01533)	(Liu, Chun et al. 2008)
D689	*cnc1560Δ* (CNAG_02953)	(Liu, Chun et al. 2008)
D1381	*ykl071WΔ* (CNAG_06074)	(Liu, Chun et al. 2008)
D1068	*crn102Δ* (CNAG_05301)	(Liu, Chun et al. 2008)
D359	*lsb1Δ* (CNAG_01183)	(Liu, Chun et al. 2008)
D156	*rck2-AΔ* (CNAG_00130)	(Liu, Chun et al. 2008)
D1179	*liv16Δ* (CNAG_07193)	(Liu, Chun et al. 2008)
D722	*upb6Δ* (CNAG_03109)	(Liu, Chun et al. 2008)
D671	*rsp3102Δ* (CNAG_02827)	(Liu, Chun et al. 2008)
D1490	*rho104-AΔ* (CNAG_06606)	(Liu, Chun et al. 2008)
D785	*pcl103Δ* (CNAG_03385)	(Liu, Chun et al. 2008)
D61	*bni4Δ* (CNAG_02071)	(Liu, Chun et al. 2008)
D173	*ubp1Δ* (CNAG_00187)	(Liu, Chun et al. 2008)
D1340	*gap1Δ/rdg1Δ* (CNAG_05838)	(Liu, Chun et al. 2008)
D1255	*ypl230W03-CΔ* (CNAG_05420)	(Liu, Chun et al. 2008)

microscopy (AxioImager, Carl Zeiss, Inc).

RNA preparation. RNA was prepared as previously described (O'Meara, Norton et al. 2010). Briefly, strains were incubated to mid-log phase, washed twice, then incubated in Dulbecco's Modified Eagle's medium (DMEM) at 37°C with 5% CO_2 for three hours. The cells were then washed twice before centrifugation, freezing on dry ice, and lyophilization. Total RNA extraction was performed using the Qiagen RNeasy Plant Minikit (Qiagen, Valencia, CA).

RNA sequencing and transcript analysis. Clonal library preparation, mRNA enrichment through poly(A) capture, and Illumina sequencing on a GAII Illumina Genome Analyzer was performed from total RNA at the Duke Sequencing Core Facility (Duke University). Briefly, total RNA was purified using Sera-Mag oligo(dT) magnetic beads according to the manufacturer's protocol (Illumina, San Diego, CA). The mRNA was fragmented and used as a template for first-strand cDNA synthesis. Second-strand synthesis was then performed, and the resulting double-stranded cDNA was end repaired, adenylated, and ligated into PE adaptors, according to the manufacturer's protocols (Illumina). Afterwards, the cDNA templates were purified, enriched and used for sequencing on the Illumina GAII Genome Analyzer. The wild-type (strain H99) sample was sequenced with 72 bp paired-end reads, and the *rim101Δ* sample was sequenced with 36 bp single-end reads.

All reads were then mapped to the *C. neoformans* reference genome provided by the Broad Institute ["*Cryptococcus neoformans var. grubii* H99 Sequencing Project",

Broad Institute of Harvard and MIT (http://www.broadinstitute.org/)] using TopHat v1.3.0 (Langmead, Trapnell et al. 2009; Trapnell, Pachter et al. 2009). The aligned reads were then analyzed for FPKM (Fragments Per Kilobase of transcript per Million mapped reads) using Cufflinks v.1.0.3. Statistically significant differences between strains were determined by CuffDiff (Trapnell, Williams et al. 2010).

Promoter analysis. The DNA sequence 1000 base pairs upstream of the start codon, as defined by the Broad Institute *Cryptococcus neoformans var. grubii* H99 Sequencing Project, was examined for the presence of the predicted Rim101 binding site (GCCAAG) on either strand (O'Meara, Norton et al. 2010).

Statistical Analysis. All analyses were performed using Analyse-It (Analyse-it Ltd., Leeds, England). One-way ANOVA was used to analyze differences in titan cell production and *P*-values <0.02 were considered significant.

IV. RESULTS

G-protein coupled receptor signaling regulates titan cell formation

Previously, we showed that signaling through Ste3**a** in mating type **a** cells stimulates titan cell production during coinfection with cells of the opposite mating type (Okagaki, Strain et al. 2010). While Ste3**a** signaling increases titan cell production from the basal level, disruption of Ste3**a** does not completely abolish titan cell production. Thus, another receptor likely senses environmental cues that stimulate titan cell production. Because G-protein coupled receptors play an integral role in environmental sensing, and Ste3**a**, a G-protein coupled receptor, is known to regulate titan cell production, we hypothesized that there is at least one additional G-protein coupled receptor responsible for titan cell regulation.

Therefore, we screened a library of G-protein coupled receptor mutants for alterations in titan cell production using an intranasal model of cryptococcal infection (**3.1**). Fungal cells were collected by bronchoalveolar lavage (BAL) at 3 days post-infection, immediately fixed and examined by microscopy for cell size and by flow cytometry for cell ploidy (**3.2**). Of the G-protein coupled receptor mutant strains, only *gpr5Δ* mutants showed a decrease in titan cell formation. Pulmonary infections with the wild-type strains result in 20.4% titan cells in the mating type **a**, and 16.1% titan cells in the MATα mating type. In contrast, infections with *gpr5Δ* mutants resulted in a 2-fold reduction in titan cell formation in both mating types to 8.8% titan cells in mating type **a** and 7.3% in mating type α (p=0.004 and p=0.013, respectively, **Figure 3.3A**). Interestingly, titan cells produced by the *gpr5Δ* mutant strains rarely exceeded 12 µm

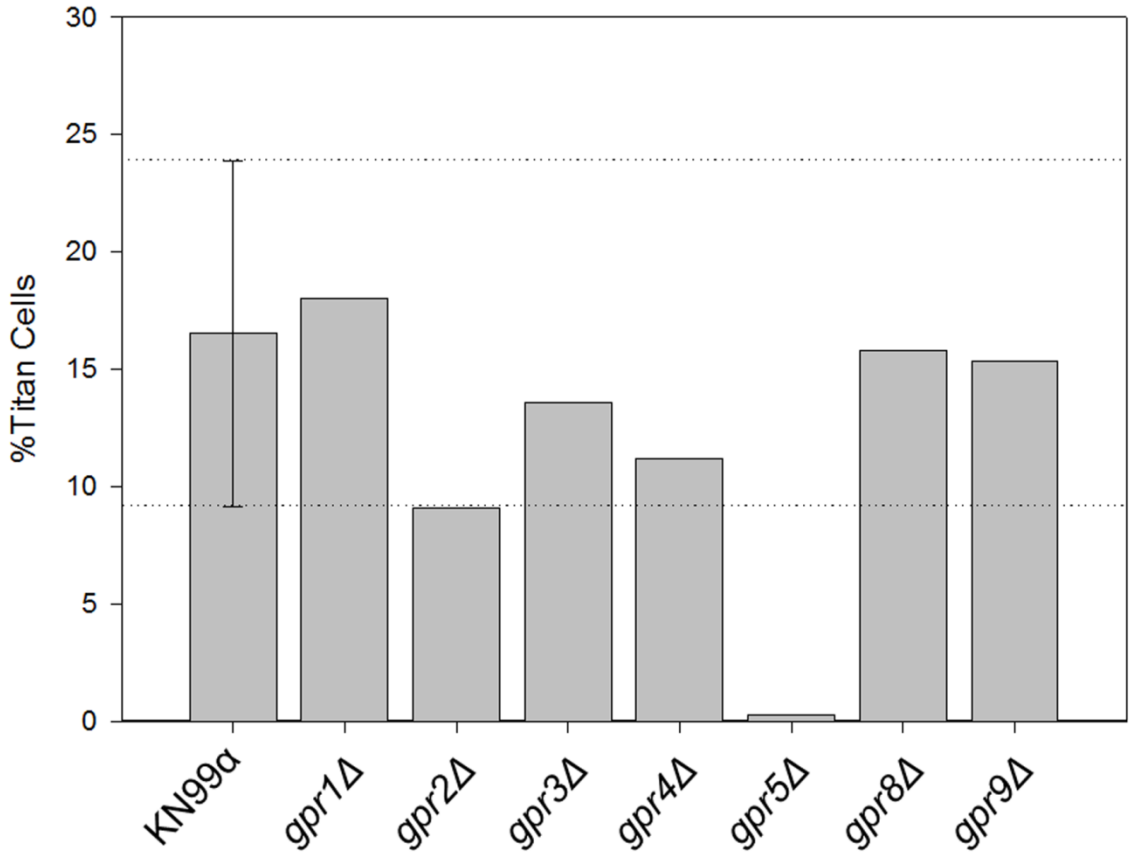

Figure 3.1. G-protein coupled receptor mutants were screened for titan cell formation. Mice were intranasally infected with $5x10^6$ cells of wild type (KN99α), *gpr1Δ*, *gpr2Δ*, *gpr3Δ*, *gpr4Δ*, *gpr5Δ*, *gpr8Δ*, or *gpr9Δ*. At 3 days post-infection, bronchoalveolar lavages (BALs) were performed. The number of small cells (<10µm cell body diameter) and titan cells (>10µm cell body diameter) were quantified by microcopy. >300 cells were counted per treatment per mouse.

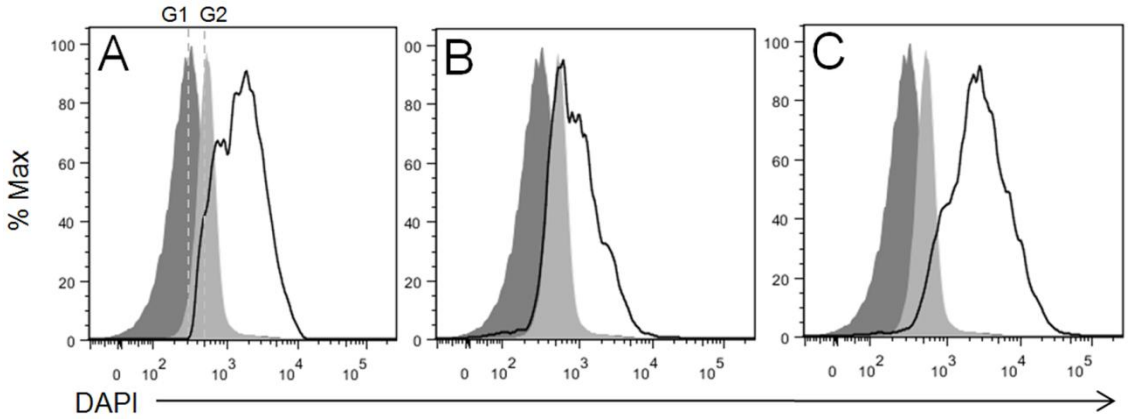

Figure 3.2. Mutant strains were screened for ploidy alterations. G1 (dark grey) and G2 (light grey) peaks were identified by flow cytometry in an *in vitro* grown culture of KN99α. Ploidy was analyzed based on DAPI fluorescence for **A)** *In vivo* populations of wild-type titan cells (black linke) **B)** *in vivo* total cell populations of the *gpr4Δgpr5Δ* double mutant (Black line) that does not produce titan cells and **C)** *in vivo* titan cell populations of the *rho104Δ* mutant strain that overproduces titan cells.

in diameter (**Figure 3.3B**). The *gpr5Δ* mutants had no defects in capsule, melanin, urease or high temperature growth *in vitro* (data not shown).

Previous studies showed that Gpr4 and Gpr5 share a high degree of sequence homology (Xue, Bahn et al. 2006). To further assess the relative contributions of these two GPCRs in titan cell production, we directly compared titan cell production in *gpr5Δ*, *gpr4Δ*, and *gpr4Δgpr5Δ* mutants of both mating types. Deletion of *GPR4* alone had no effect on titan cell formation. The *gpr4Δgpr5Δ* double mutants showed significant decreases in titan cell production, with an average of 5.3% titan cells in mating type **a** and 4.4% in mating type α ($p=0.001$ and $p=0.011$, respectively, when compared to the appropriate wild type mating type, **Figure 3.3A**). However, there was no statistically significant difference between the double mutant and the *gpr5Δ* single mutant ($p=0.435$). Complementation of Gpr5 in either the *gpr5Δ* or *gpr4Δgpr5Δ* mutant restored titan cell production to wild-type levels (data not shown). In addition, neither the presence nor absence of various amino acids stimulated titan cell formation *in vitro* (data not shown). Similarly, no difference in cell enlargement between wild type and the *gpr5Δ* mutant in response to phosphotidylcholine treatment was observed (data not shown). These data suggest that signaling through the GPCR Gpr5, and not the related Gpr4 protein, controls titan cell production in both mating type **a** and mating type α cells. None of the titan cell defects in these GPCR mutants were affected by mating type, demonstrating that the regulation of basal titan cell production by Gpr5 is separate from induction of titan cells by the mating pathway.

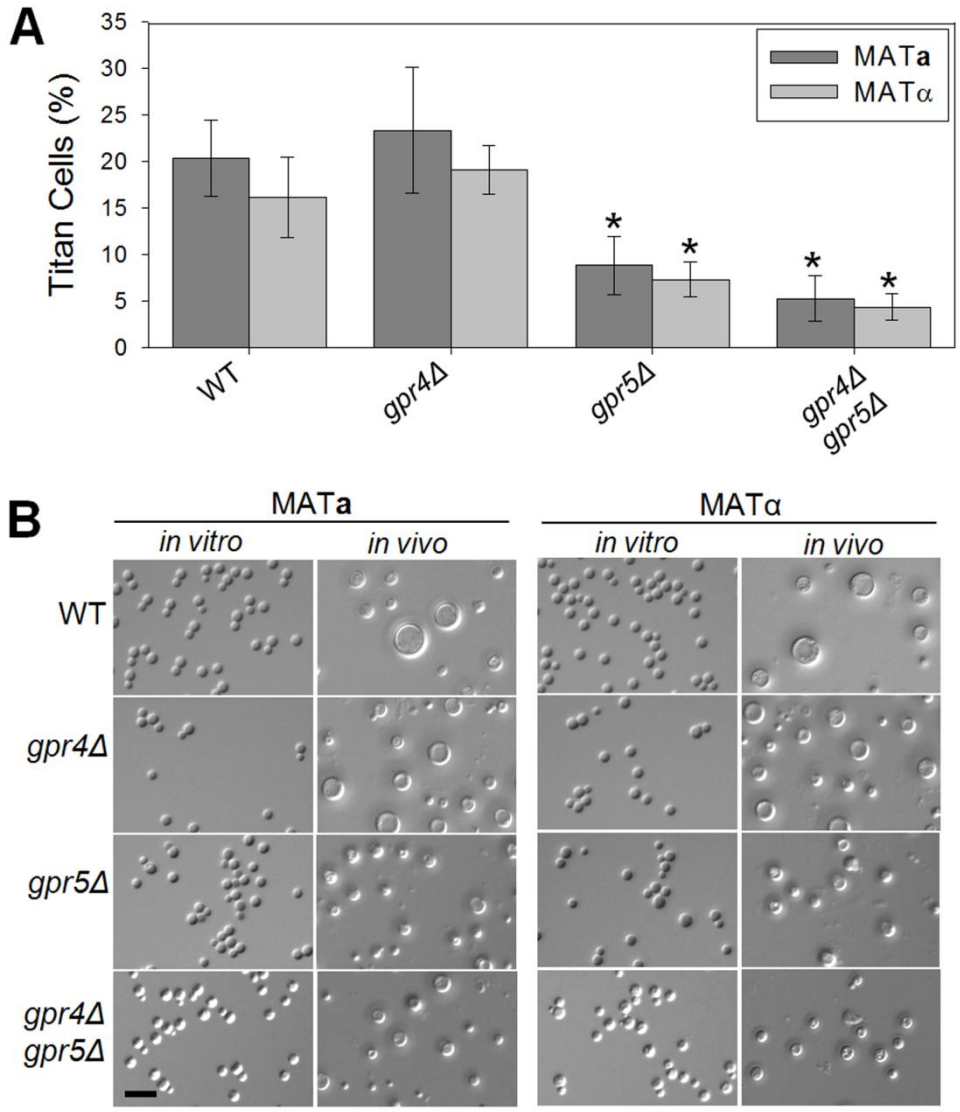

Figure 3.3. Titan cell signaling *in vivo* is regulated by the Gpr5 receptor. Mice were infected intranasally with $5x10^6$ cells of wild-type KN99**a** or KN99α, *gpr4Δ* mating type **a**, *gpr4Δ* mating type α, *gpr5Δ* mating type **a**, *gpr5Δ* mating type α, *gpr4Δgpr5Δ* mating type **a**, or *gpr4Δgpr5Δ* mating type α. At 3 days post-infection, bronchoalveolar lavages (BALs) were performed. **A)** The number of small cells (<10µm cell body diameter) and titan cells (>10µm cell body diameter) were quantified by microcopy. >300 cells were counted per treatment per mouse. Error bars indicate standard deviation (SD) from 3-5 mice per treatment. Statistical analysis was performed between mutant strains and the wild type strain of the same mating type. Asterisk indicates $p<0.02$. **B)** *In vitro* cells were grown overnight in rich medium (YPD), fixed in 3.7% formaldehyde and examined by microscopy. *In vivo* BAL samples isolated at 3 days post-infection were fixed in 3.7% formaldehyde and examined by microscopy. Bar = 20µm.

Gpa1 signaling results in titan cell production

C. neoformans has three known Gα proteins that can interact with G-protein coupled receptors. Gpa2 and Gpa3 regulate signaling through Ste3α in mating type α cells by acting in opposition to each other (Hsueh, Xue et al. 2007). Mutation of either Gpa2 or Gpa3 alone does not cause a defect in virulence in a mating type α background, but the double mutant was slightly attenuated (Li, Shen et al. 2007). Based on the Ste3α data and the role of Ste3**a** in titan cell induction, we hypothesized that Gpa2 and Gpa3 would interact with Ste3**a** to regulate titan cell production. We anticipated that deletion of Gpa2 and/or Gpa3 in mating type **a** cells would alter the rate of titan cell formation.

Therefore, we determined the degree of titan cell production in *gpa2Δ* and *gpa3Δ* mutants in each mating type. In both mating types, the *gpa2Δ* mutant strains exhibited no significant alteration in titan cell production (**Figure 3.4**) when compared to the appropriate wild-type strains (p=0.812 and p=0.752). Similarly, the *gpa3Δ* mutant strains in both mating types showed normal titan cell production (p=0.379 and 0.087). The *gpa2Δgpa3Δ* double mutant strains also showed no significant alteration in titan cell production (p=0.708 and p=0.075), demonstrating that neither Gpa2 nor Gpa3 play a role in the regulation of titan cell production.

Since the two Gα proteins predicted to interact with Ste3**a** did not affect titan cell production, we then hypothesized that the Gα protein Gpa1 might regulate titan cell formation. Gpa1 plays an integral role in the regulation of many virulence factors, including capsule and melanin (Alspaugh, Perfect et al. 1997; Alspaugh, Pukkila-Worley et al. 2002). Because Gpa1 controls production of these virulence factors, *gpa1Δ* strains are avirulent (Alspaugh, Perfect et al. 1997; Alspaugh, Pukkila-Worley et al. 2002). As

early as 24 hours post-infection, the vast majority of *gpa1Δ* cells are phagocytosed and killed (data not shown), preventing us from quantifying *in vivo* titan cell production of the deletion mutants. Instead we used a constitutively active *GPA1* mutant allele ($GPA1^{Q284L}$) to elucidate the role of Gpa1 in titan cell formation (Xue, Bahn et al. 2006). Infections with mating type **a** cells expressing the dominant active $GPA1^{Q284L}$ allele resulted in a significant increase in titan cell production to approximately 40%, representing a 2-fold increase in titan cells when compared to mating type **a** wild-type strains (p=0.012, **Figure 3.4**). Interestingly, the mating type α strain expressing the $GPA1^{Q284L}$ mutant allele showed no difference in titan cell production when compared to the mating type α wild-type strain (p=0.172). These results are consistent with a model in which the Gpa1 protein interacts with the Gpr5 and Ste3**a** receptors to induce titan cell formation.

Ste3a interacts with Gpa1 but not Gpa2 or Gpa3

Our data suggest that in mating type **a** cells, Ste3**a** may interact with Gpa1, rather than Gpa2 or Gpa3, to regulate titan cell production. Therefore, we assessed the interactions between Ste3**a** and the Gα proteins using a split-ubiquitin yeast two-hybrid system. In this system, membrane protein interactions release an artificial transcription factor that is made up of three proteins: protein A, LexA and VP16 (Xue, Bahn et al. 2006). Upon release, the transcription factor translocates to the nucleus and activates reporter genes.

Three versions of Gpa1 were screened for possible interactions with Ste3**a** and Ste3α: wild-type Gpa1; $Gpa1^{G283A}$, which contains a dominant negative mutation; and

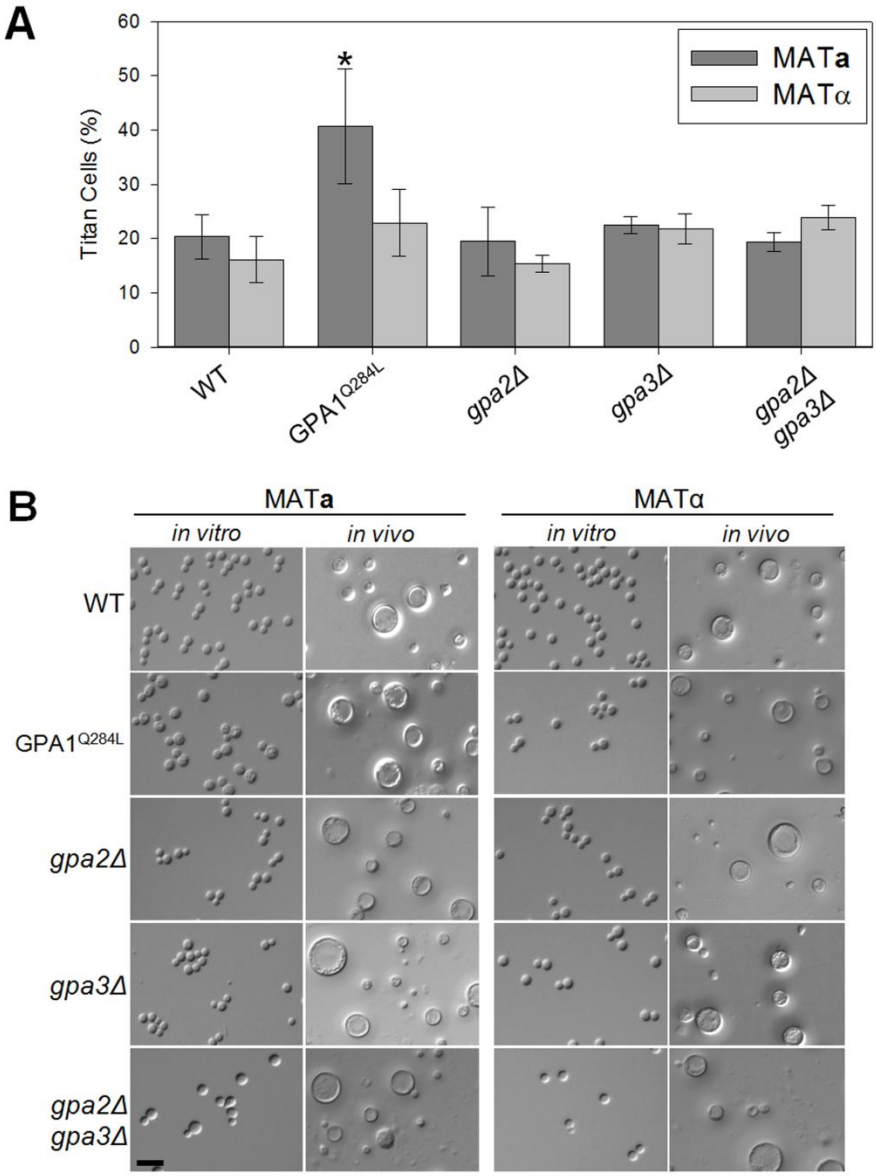

Figure 3.4. Signaling via the Gα protein Gpa1 regulates titan cell production. Mice were infected intranasally with $5x10^6$ cells of wild-type KN99**a** or KN99α, $GPA1^{Q284L}$ mating type **a**, $GPA1^{Q284L}$ mating type α, *gpa2Δ* mating type **a**, *gpa2Δ* mating type α, *gpa3Δ* mating type **a**, *gpa3Δ* mating type α, *gpa2Δgpa3Δ* mating type **a**, or *gpa2Δgpa3Δ* mating type α. At 3 days post-infection, BAL samples were collected. **A)** The number of small cells (<10µm cell body diameter) and titan cells (>10µm cell body diameter) were quantified by microcopy. >300 cells were counted per treatment per mouse. Error bars indicate SD from 3-5 mice per treatment. Statistical analysis was performed between mutant strains and the wild type strain of the same mating type. Asterisk indicates $p<0.02$. **B)** *In vitro* cells were grown overnight in rich medium (YPD), fixed in 3.7% formaldehyde and examined by microscopy. *In vivo* BAL samples isolated at 3 days post-infection were fixed in 3.7% formaldehyde and examined by microscopy. Bar = 20µm.

Gpa1^{Q284L}, which renders the protein constitutively active. In addition, we examined interactions with Gpa2 and Gpa3 (Xue, Bahn et al. 2006). Our results show that Ste3**a** interacts with both the Gpa1 and Gpa1 dominant negative alleles, but no detectable interaction was observed with the Gpa1 constitutively active allele, Gpa2 or Gpa3 (**Figure 3.5**). G-protein coupled receptors normally serve as guanine nucleotide exchange factors (GEF) and bind to the inactive form of Gα proteins to activate the G protein. Therefore, the stronger interaction between Ste3**a** and Gpa1^{G283A} compared to the wild-type Gpa1 construct indicated that the weak interaction in this assay with the wild-type Gpa1 protein was likely valid.

As a control, we also measured the interactions between Ste3α and the Gα proteins. We confirmed robust interactions between Ste3α and Gpa2 and Gpa3, but not Gpa1. These data are consistent with previously published results demonstrating that Ste3α interacts with Gpa2 and Gpa3 to control the mating pathway (Hsueh, Xue et al. 2007; Hsueh, Xue et al. 2009). Unlike the case for Ste3α, we were unable to detect any interactions between Ste3**a** with either Gpa2 or Gpa3.

Previous studies found that the G-protein coupled receptor Gpr4 is important for activating Gpa1 in response to methionine (Xue, Bahn et al. 2006). These same studies showed that Gpr5 shares sequence similarity with Gpr4, but does not respond to methionine. Thus, the function of Gpr5 remained unknown (Xue, Bahn et al. 2006). In the split-ubiquitin assays, we did not detect any interactions between Gpr5 and any of the Gα proteins (**Figure 3.5**). In contrast, Gpr5 and Gpr4 demonstrated a robust interaction in this system, indicating that these predicted G-protein coupled receptors can form heterodimer or oligomer structures.

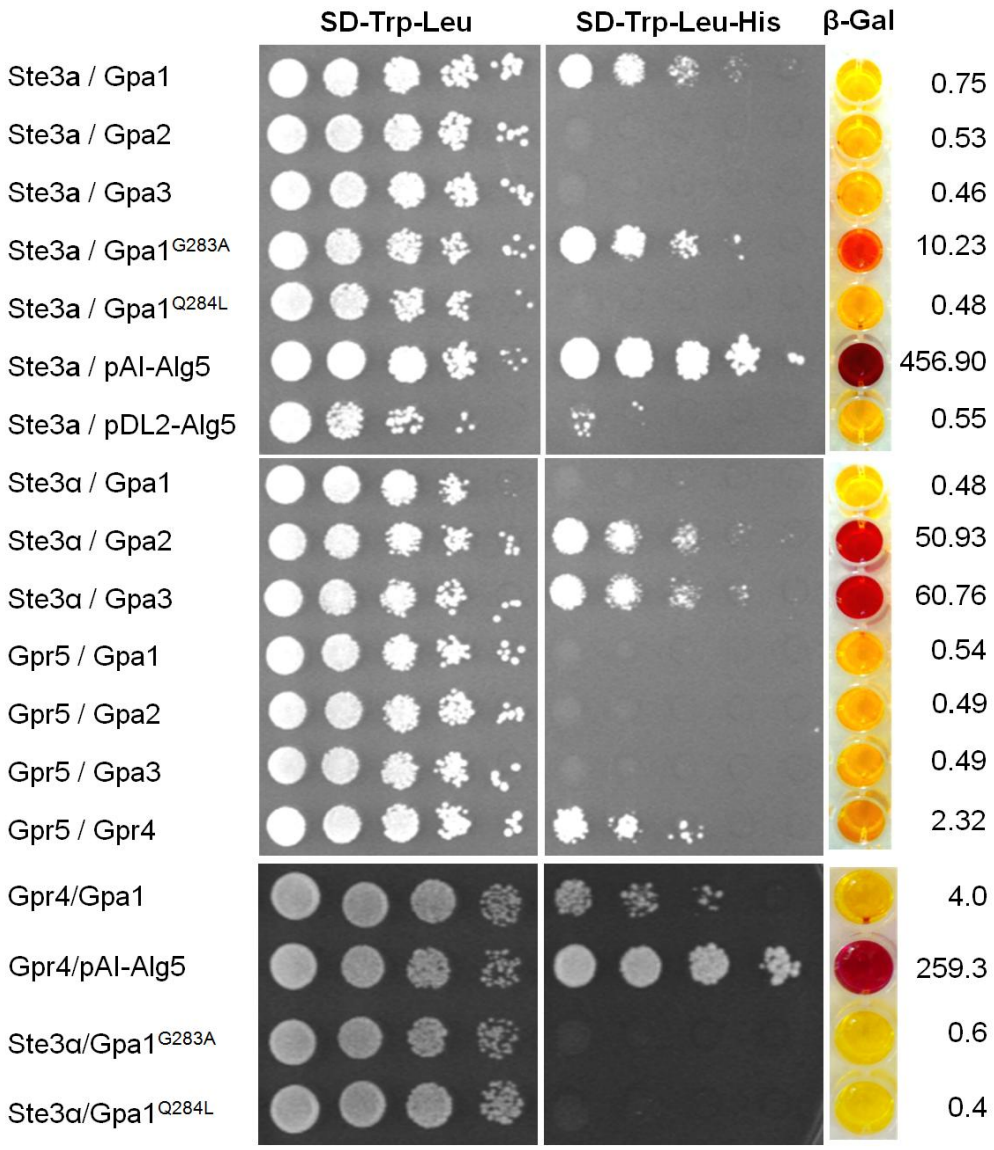

Figure 3.5. Ste3a interacts with Gpa1 in the split-ubiquitin yeast two-hybrid system. The C-terminal half of ubiquitin (Cub) was fused to the C-terminus of the full-length cDNAs of Ste3**a** (Ste3**a**::Cub), Ste3α (Ste3α::Cub) and Gpr5 (Gpr5::Cub). The N-terminal half of ubiquitin (NubG) was fused to the C-terminus of full-length cDNAs of Gpa1 (Gpa1::NubG), Gpa2 (Gpa2::NubG), Gpa3 (Gpa3::NubG), Gpa1^{G283A} (Gpa1^{G283A}::NubG), and Gpa1^{Q284L} (Gpa1^{Q284L}::NubG). Ste3**a**::Cub interaction with the control vector pAI-Alg5 served as a positive control to ensure the correct topology of the Ste3**a**:Cub fusion protein, Ste3**a**::Cub interaction with the empty vector pDL2-Alg5 served as a negative control. Yeast transformants contained both a Cub fusion and a NubG fusion construct and were grown on selective medium lacking histidine or adenine after serial dilution. β-galactosidase activity assays were performed to further verify interactions. Interactions between Ste3**a** and the Gα proteins (top), interactions between Ste3α and the Gα proteins (middle) and controls (bottom) are shown on selective media.

Signaling through Ste3a is sufficient for titan cell formation during coinfection

Previously, we showed that coinfection with both mating types results in increased titan cell formation in mating type **a** cells and that this increase is dependent on Ste3**a** (Okagaki, Strain et al. 2010). We also demonstrate here that titan cell production in both mating types is regulated by signaling through the Gpr5 receptor. Therefore, we wanted to determine whether titan cell signaling through Ste3**a** is dependent on simultaneous signaling via Gpr5 or whether Ste3**a** signaling is sufficient to produce titan cells in the presence of mating type α cells.

To assess whether Ste3**a** titan cell signaling is dependent on Gpr5 signaling, BAL samples were obtained 3 days post-infection from mice infected with fluorescently labeled *gpr4Δgpr5Δ*MAT**a** only (green), *gpr4Δgpr5Δ*MATα only (green), KN99**a**/*gpr4Δgpr5Δ*MATα(green) coinfections, *gpr4Δgpr5Δ*MAT**a**(green)/KN99α coinfections, KN99α only (green), KN99**a** only (green), KN99**a**(green)/KN99α coinfections, or KN99**a**/KN99α(green) coinfections (**Figure 3.6**). BAL samples were immediately fixed, and the proportion of green titan cells was compared to the total population of fluorescently marked cells by microscopy. Consistent with previous findings, infections with either individual wild type strain, KN99**a** or KN99α, produced approximately 20% titan cells. Coinfection with both mating types yielded an increase in titan cell production in mating type **a** cells to approximately 40%, while mating type α cells were unaffected and remained at the basal level of 20%. Infection with a *gpr4Δgpr5Δ* double mutant strain of either mating type alone resulted in a dramatic reduction in titan cell formation (**Figure 3.3**, **Figure 3.6**). The mating type α *gpr4Δgpr5Δ* mutant was unaffected by coinfection, and titan cell production remained low at 1.54%.

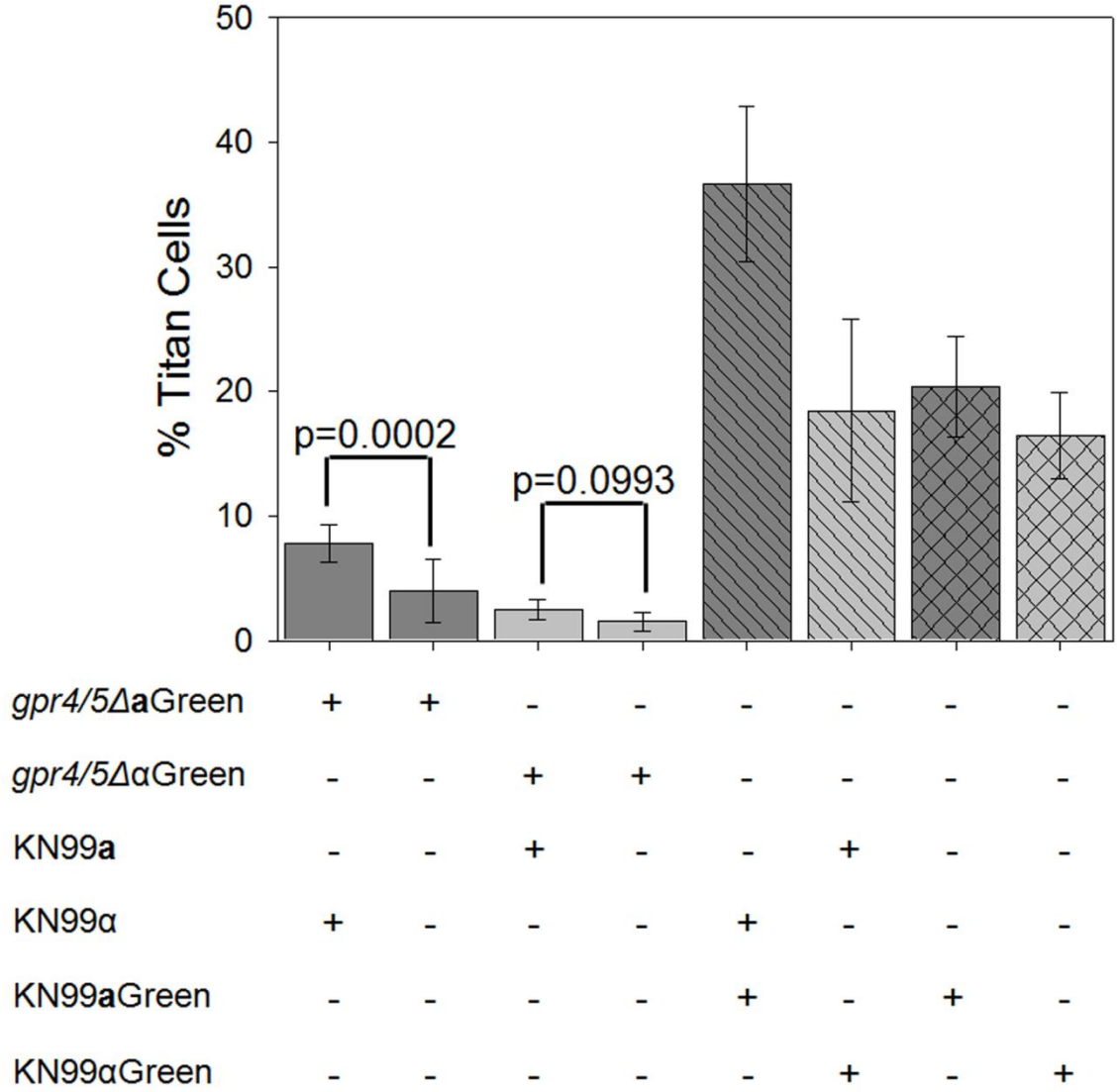

Figure 3.6. The effects of coinfection on titan cell formation. Mice were intranasally infected with $5x10^6$ wild type (KN99**a** or KN99α) or *gpr4Δgpr5Δ* mutant cells labeled with AlexaFluor 488 or coinfected with one labeled and one unlabeled strain. Cells obtained by BAL were fixed and examined by microscopy for green fluorescence (cell type) and cell size. >300 cells were examined per animal and the number of small cells (<10μm) and titan cells (>10μm) were quantified. Error bars indicate SD from 3-4 mice per treatment.

Surprisingly, coinfection of the mating type **a** *gpr4Δgpr5Δ* double mutant with wild-type mating type α (*gpr4Δgpr5Δ*MAT**a**(green)/KN99α) resulted in a significant increase in titan cell production to an average of 7.79% titan cells ($p<0.001$) demonstrating that the mating type **a** strain was still able to undergo induction of titan cell production. Thus, the Ste3**a** signal is sufficient for titan cell induction, independent of the signals for basal titan cell production. However, signaling though both Ste3**a** and Gpr5 is required for optimal titan cell production during coinfection.

Rim101 and Cdc420 regulate titan cell formation

We have shown that pheromone sensing via Ste3**a** is able to induce titan cell production in mating type **a** cells. Our data also shows that Ste3**a** does not interact with the Gα proteins, Gpa2 and Gpa3, which are known to regulate the MAPK mating pathway in *C. neoformans*. To determine what role, if any, the MAPK mating pathway has in titan cell production we characterized titan cell formation in strains with gene deletion mutations in the MAPK mating pathway members Ste20, Ste50, Ste7, Ste12. Additionally, we examined the downstream transcription factors Sxi1α, Znf2, or Mat2 (Jung, Kim et al. ; Karos, Chang et al. 2000; Hull, Davidson et al. 2002; Lin, Jackson et al. 2010). All mutant strains showed wild-type levels of titan cell production (data not shown). These data show that the MAPK mating pathway does not regulate titan cell production.

Instead, Ste3**a** was shown to interact with Gpa1, a member of the cAMP/PKA pathway, to regulate titan cells. Thus, we examined transcription factors that were downstream of PKA to determine their role in titan cell production. Rim101 is a

transcription factor regulated by the PKA pathway in *C. neoformans*, and deletion of Rim101 affects capsule attachment (O'Meara, Norton et al. 2010). Additionally, this transcription factor is responsible for the major morphological switch from yeast to hyphae during systemic infection by *C. albicans* (Davis, Edwards et al. 2000). Based on these observations, we tested a *rim101Δ* mutant strain for its ability to produce titan cells to determine whether Rim101 is involved in titan cell formation.

Unlike the *gpa1Δ* mutant and other activating mutants in the PKA pathway (*pka1Δ*, *cac1Δ*), the *rim101Δ* strain does not have a virulence defect. Therefore, *rim101Δ* cells can be recovered from infected lungs and analyzed for titan cell production (**Figure 3.7A**). The *rim101Δ* mutant strain exhibited a dramatic reduction in titan cell formation, with a rate of 0.46% compared with approximately 17% in wild type (**Figure 3.7A,** $p<0.001$). Complementation of Rim101 restored titan cell production to wild-type levels ($p=0.579$). These results suggest that Rim101 is a major regulator of titan cell production.

Morphological changes have also been shown to be controlled by the stress response protein Cdc42 in other fungi (Rincon, Coll et al. 2007). Unlike other pathogenic fungi, *Cryptococcus* has two paralogues for Cdc42: Cdc42 and Cdc420. In *C. neoformans*, Cdc42 confers thermotolerance and regulates morphogenesis during mating. Both paralogues can also regulate morphological changes in response to increased temperature. Based on their roles in regulating morphology in response to host body temperature, we tested the effects of Cdc42 and Cdc420 deletions on titan cell production (**Figure 3.7B**). The *cdc42Δ* mutant exhibited an average of 24.3% titan cell production, similar to wild type ($p=0.101$). In contrast, the *cdc420Δ* mutant had a reduction in titan cell production to 7.81%, which is significantly lower than wild type levels ($p=0.017$).

Complementation of Cdc420 restored titan cell production to wild type levels (p=0.131). Thus, Cdc420 but not Cdc42 stimulates titan cell formation.

Additional effectors of titan cell induction

To identify additional members of the titan cell signaling pathway, we analyzed strains from a large collection of *C. neoformans* mutant strains that exhibited alterations in pathogenesis (Liu, Chun et al. 2008). BAL samples were collected at 3 days post-infection, fixed and examined by microscopy. This preliminary screen identified several strains with altered titan cell formation compared with the wild type strain background (CMO18) used to create this mutant collection (**Figure 3.7C**). From the strains with altered titan cell formation, we chose 4 strains with mutations in genes with known functions for further analysis (**Figure 3.7D**). One strain exhibited reduced titan cell production compared to the wild type and contained a mutation in the coding sequences for the GTPase activating protein (GAP) Gap1. Infection with the *gap1Δ* mutant resulted in only 5.79% titan cell formation, which was significantly lower than the wild type levels of 16.9% (p<0.0001). Three mutations demonstrated an increase in titan cell formation: a GAP gene, Cnc1560 (p=0.002), a rho-family GTPase, Rho104 (p<0.001), and a cell cycle regulation gene, Pcl103 (p=0.003). Each protein encoded by these genes is predicted to control aspects of morphogenesis in other organisms.

To determine if the expression levels of genes involved in titan cell formation are regulated by Rim101, we analyzed the promoter regions for predicted Rim101 binding sites and examined their expression through RNAseq experiments (**Table 3.2**). *CNC1560* and *RHO104* both contain predicted Rim101 binding sites in their promoters, and both

exhibited Rim101-dependent alterations in expression. Additionally, the *CDC420* gene contains a Rim101 binding site in its promoter while *CDC42* does not. No alteration in expression of CDC420 was observed in the *rim101Δ* mutant, although titan cell production in the wild-type strain was also not observed under the RNAseq conditions, suggesting that Rim101 binding may not be the only signal leading to alterations in *CDC420* expression. Taken together, this data suggest that titan cell formation is regulated by Rim101 and acts through multiple effectors controlling aspects of cell morphogenesis.

Table 3.2. Changes in gene expression in the *rim101Δ* mutant.

Gene	Function	Rim101 binding site	Fold change in expression
CNC1560	GTPase activating protein	Yes	+4.7
PCL103	G1 cyclin E	No	-17.7
GAP1	GTPase activating protein	Yes	0.0
RHO104	Rho-GTP	Yes	-3.5
CDC420	Stress response protein	Yes	+1.3
CDC42	Stress response protein	No	+1.4
GPA1	Gα protein	Yes	+2.4
CAC1	Adenylyl cyclase	Yes	+1.5
PKA1	Protein kinase A	Yes	0.0
PKR1	PKA regulatory subunit	No	-1.6

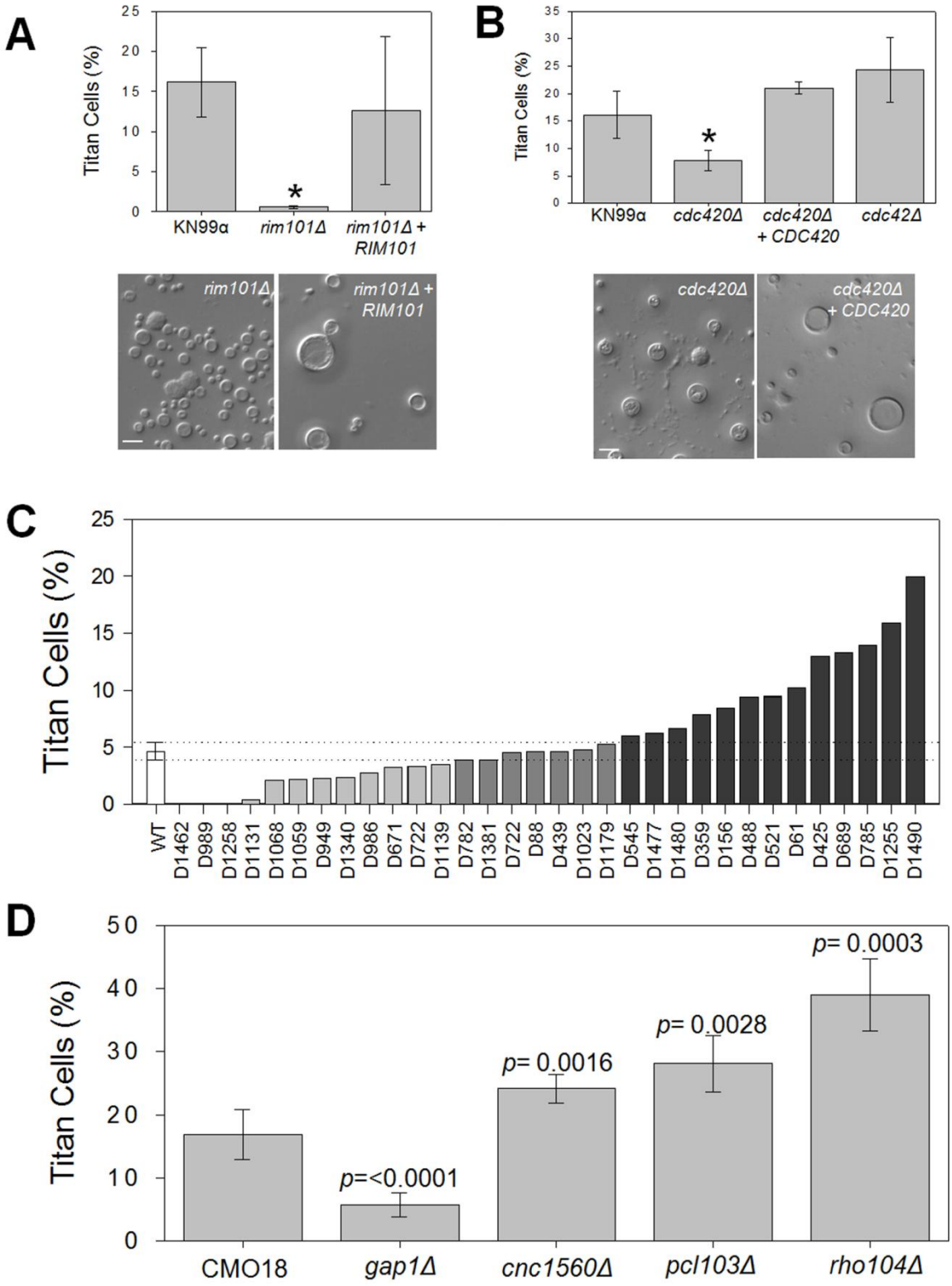
A
Titan Cells (%)
KN99α
rim101Δ
rim101Δ + RIM101
B
Titan Cells (%)
KN99α
cdc420Δ
cdc420Δ + CDC420
cdc42Δ
C
Titan Cells (%)
WT
D1462
D989
D1258
D1131
D1068
D1059
D949
D1340
D986
D671
D722
D1139
D782
D1381
D722
D88
D439
D1023
D1179
D545
D1477
D1480
D359
D156
D488
D521
D61
D425
D689
D785
D1255
D1490
D
Titan Cells (%)
p= 0.0003
p= 0.0028
p= 0.0016
p=<0.0001
CMO18
gap1Δ
cnc1560Δ
pcl103Δ
rho104Δ

Figure 3.7. Regulators of titan cell signaling. Mice were intranasally infected with $5x10^6$ cryptococcal cells. At 3 days post-infection, BAL samples were collected and fixed. The number of small cells (<10µm cell body diameter) and titan cells (>10µm cell body diameter) were quantified by microcopy. >300 cells were counted per treatment per mouse. **A)** *rim101Δ* and *rim101Δ*+RIM101 mutants were assessed for titan cell formation. Error bars indicate SD from 3-5 mice per treatment. Asterisk indicates $p<0.02$ compared with wild type. **B)** *cdc420Δ*, *cdc420Δ+CDC420*, and *cdc42Δ* mutants were assessed for titan cell formation. Error bars indicate SD from 3-5 mice per treatment. Asterisk indicates $p<0.02$ compared with wild type. **C)** 32 mutant strains were assayed for titan cell formation. Standard deviation (dotted line) for the wild type (white bar) was used to identify mutant strains that exhibit altered titan cell formation. **D)** Four of the mutant strains in panel C were further analyzed for titan cell formation. All are statistically significant compared to the wild type, $p<0.02$. Error bars indicate SD from 3-5 mice per treatment.

V. DISCUSSION

Titan cells play an important role in the initial pulmonary phase of *C. neoformans* infections. The morphological transition from yeast cell to titan cell can be induced by several conditions. We showed previously that titan cell formation in both mating types results from signals in the host lung environment (Okagaki, Strain et al. 2010). Titan cell production can also be stimulated *in vitro* by spent media from macrophage cell lines (Okagaki, Strain et al. 2010). Recent studies have shown that treatment of cryptococcal cells grown *in vitro* with phosphotidylcholine can stimulate cell enlargement, suggesting that phospholipids may be at least one component of the host-derived signal (Chrisman, Albuquerque et al. 2011). We also demonstrated that cryptococcal titan cell formation is enhanced in mating type **a** cells by activation of the Ste3**a** pheromone receptor in response to the opposite mating type. Here we further explore the mating type-dependent and mating type-independent signals inducing titan cells.

We have shown that the Gpr5 receptor regulates titan cell production in response to the host lung environment. Deletion of the Gpr5 receptor significantly decreased titan cell formation during infection. The *gpr5Δ* mutant exhibits no defects in other known virulence factors suggesting that signaling through this receptor specifically targets titan cell production. Interestingly, Gpr5 has high sequence homology to the methionine-sensing Gpr4 receptor (Xue, Bahn et al. 2006). Deletion of *GPR4* had no effect on titan cell formation and alterations in amino acid prevalence did not stimulate titan cell formation *in vitro*. Similarly, we observed no difference in cell enlargement between wild-type and the *gpr5Δ* mutant in response to phosphotidylcholine treatment *in vitro*.

Thus, the ligand for Gpr5 has not yet been defined. The observation that pheromone signaling, phospholipids, and another signal recognized by Gpr5 can independently stimulate titan cell formation suggests that additional, as yet uncharacterized, receptors and signals are involved in titan cell formation under various conditions.

Our prior observations revealed that infection with both *C. neoformans* mating types resulted in enhanced titan cell formation, suggesting that the pheromone response pathway might play a role in this process (Okagaki, Strain et al. 2010). However, our recent data do not support a simple model of pheromone pathway activation leading to increased titan cells. For example, only mating type **a** cells undergo enhanced titan cell formation in response to mating partner. Also, mutations in downstream components of the pheromone response pathway do not affect titan cell induction in the setting of a lung infection. Moreover, our data suggest that the pheromone receptors may interact with distinct downstream effectors in the different mating types. The Ste3**a** pheromone receptor did not interact in the yeast two-hybrid system with Gpa2 or Gpa3, the Gα proteins that mediate pheromone response in mating type α cells. Instead, Ste3**a** demonstrates *in vitro* interactions with the Gα protein, Gpa1. The interaction between Ste3**a** and Gpa1 was transient and less stable than interactions between Ste3α and Gpa2 or Gpa3. These data suggest that Ste3**a** only weakly interacts with Gα proteins in our yeast two-hybrid assays. Thus, we cannot eliminate the possibility that Ste3**a** is able to interact with Gpa2 and/or Gpa3 under native conditions or that additional cofactors not present in the yeast two-hybrid assay are required to stabilize interactions between Ste3**a** and Gpa2 or Gpa3.Yet the interactions between Ste3**a** and Gpa1 suggest a very different signaling paradigm between the two mating types. Also, dominant, activating mutations

in Gpa1 result in striking increases in titan cell formation in mating type **a** cells only. Together, these data likely explain the mating type **a**-specific enhancement of titan cell formation in mixed infections.

It is also clear that mating type α and mating type **a** cells have very different morphological responses in other settings. For example, in confrontation assays between serotype D strains, mating type α cells primarily undergo filamentous changes in response to a mating type **a** partner; conversely, mating type **a** cells primarily undergo cell enlargement when confronted with the α mating partner (Shen, Davidson et al. 2002). Therefore, the morphological response in mating is quite distinct between *C. neoformans* mating types. Here we observed a similar divergence in morphological response to mating partner in titan cell formation. Mating type **a** cells undergo accelerated titan cell formation *in vivo* in the presence of mating type α cells; mating type α cells do not. Therefore, it is plausible that mating type-specific signaling rewiring has occurred to allow such a different cellular response between mating type α and mating type **a** cells in a number of settings.

These data raise many questions regarding current signaling models in *C. neoformans*. For instance, if the primary role of Gpa1 is simply to activate cAMP/PKA signaling, why does this protein not activate titan cell formation in both mating types? How have conserved pheromone receptors adapted to interact with distinct Gα proteins to mediate very different downstream processes – pheromone recognition for both Ste3**a** and Ste3α, and titan cell induction only for Ste3**a**? It is clear that these signaling proteins often act in multi-protein complexes. Therefore, it is possible that downstream effectors of titan cell formation are only activated by Ste3**a** and Gpa1 in a complex, and not merely

by accentuation of local cAMP/PKA activity. Additionally, mating type **a** and α cells may have different levels of basal Gpa1 activity. If mating type α cells are already utilizing maximal Gpa1 activity *in vivo*, addition of a constitutively active form of Gpa1 will not affect the level of downstream signaling.

Our yeast two-hybrid data also showed no interactions between Gpr5 and any of the three cryptococcal Gα proteins. Similar to Ste3**a**, the interactions between Gpr5 and the Gα proteins may be transient and not detectable using our yeast two-hybrid system. Alternatively, interactions between Gpr5 and the Gα protein may require a multi-protein complex to stabilize the interaction. We were able to detect interactions between Gpr4 and Gpr5 in our system showing that Gpr5 is capable of forming multi-protein complexes.

Gpa1 is a major regulator of the PKA pathway (Alspaugh, Perfect et al. 1997; D'Souza, Alspaugh et al. 2001; Alspaugh, Pukkila-Worley et al. 2002; Pukkila-Worley, Gerrald et al. 2005). The PKA pathway regulates many virulence factors in *C. neoformans* including capsule and melanin (D'Souza, Alspaugh et al. 2001; Alspaugh, Pukkila-Worley et al. 2002; Pukkila-Worley, Gerrald et al. 2005). The role of cAMP signaling in titan cell formation is strongly supported by the enhanced morphological changes induced by dominant active Gpa1. The involvement of this pathway is further supported by the striking role of the PKA-responsive transcription factor Rim101. Analysis of other cAMP pathway components is currently limited by the poor viability of these strains *in vivo*, the site of optimal titan cell induction. Emerging *in vitro* systems for titan cell formation will hopefully allow us to address the role of the cAMP pathway more extensively in this process.

Downstream of the PKA pathway is the transcription factor Rim101, which is well known to regulate morphology changes and virulence in other fungal species (Davis, Edwards et al. 2000; Davis, Wilson et al. 2000; Baek, Martin et al. 2006; Yuan, Mitchell et al. 2010). For example, in *C. albicans*, Rim101 regulates the yeast to hyphal switch in response to pH changes and is critical to pathogenesis (Davis, Edwards et al. 2000; Davis, Wilson et al. 2000). Our data shows that Rim101 is the major regulator of titan cell production downstream of the PKA pathway. Deletion of the RIM101 gene abolishes titan cell production. The *rim101Δ* mutant had a more severe defect in titan cell production compared to the *gpr5Δ* mutant, suggesting that Gpr5 is likely only one of many signals acting through Rim101. Rim101 activity in several fungi including *Ustilago maydis*, *C. albicans*, and *C. neoformans* is primarily regulated by changes in pH (Davis, Edwards et al. 2000; Davis, Wilson et al. 2000; Arechiga-Carvajal and Ruiz-Herrera 2005; Barwell, Boysen et al. 2005; O'Meara, Norton et al. 2010). At alkaline pH Rim101 directs gene expression of cell wall proteins, proteases, and iron acquisition proteins in addition to mediating morphological changes in response to pH (Davis, Edwards et al. 2000; Davis, Wilson et al. 2000; Arechiga-Carvajal and Ruiz-Herrera 2005; Baek, Martin et al. 2006; O'Meara, Norton et al. 2010). No effect of pH alone on titan cell formation *in vitro* has been observed (Okagaki and Nielsen, unpublished data), but it remains unclear if pH regulation of Rim101 *in vivo* plays a role in titan cell production. There are several pathways known to regulate Rim101 activity. In *C. albicans*, Rim101 can be activated by a number of upstream pathways, including pH sensing by membrane proteins such as Dgf16p (Barwell, Boysen et al. 2005) as well as the ESCRT pathway (Baek, Martin et al. 2006; Wolf and Davis 2010; Wolf, Johnson et al. 2010). In *C. neoformans*, Rim101 has

been shown to be regulated in a PKA dependent manner (O'Meara, Norton et al. 2010). In addition to changes in *RIM101* gene expression, Rim101 activity is regulated post-translationally (Futai, Maeda et al. 1999; Davis, Edwards et al. 2000; Davis, Wilson et al. 2000; Li, Martin et al. 2004). Thus, it seems likely that multiple, as yet uncharacterized, signals will modulate the activity of Rim101 *in vivo* to promote titan cell production.

Rim101 has numerous downstream direct and indirect targets, and it will be important to determine which targets are the most important effectors for the formation of titan cells. We have begun an initial evaluation of potential effectors of titan cell formation using existing mutant collections. Our first selection of mutants was biased toward those with predicted roles in morphogenesis and genome duplication, given the known titan cell phenotypic changes from wild-type. This allowed us to test a focused group of strains in the complicated *in vivo* induction system. Using this method, we have identified genes whose products both enhance and suppress titan cell formation *in vivo*, including the cell cycle regulators Cdc420, Pcl103, and the GTPase activating proteins Rho104, Cnc1560, and Gap1, suggesting possible mechanisms for the cell enlargement and ploidy increases associated with titan cells. Many of these genes, as well as additional cyclins, DNA synthases, and other cell cycle regulatory genes that have not been examined yet for their effect on titan cell production, are either directly or indirectly regulated by Rim101 (O'Meara, Norton et al. 2010) . Although some of the gene promoters have putative Rim101 binding sites, this level of analysis is not sufficient to truly define direct targets of this transcription factor. Moreover, it is clear from the *rim101* comparative transcriptional profiling experiments, and from the effects of these putative effector proteins on titan cell formation *in vivo*, that merely implicating Rim101

control of these proteins is overly simplistic. For example, the cell cycle regulator Pcl103 exhibited a 17.7 fold decrease in gene expression in the *rim101Δ* mutant compared to wild-type, suggesting that it might co-regulate titan cell transitions with Rim101. However, in contrast to Rim101, deletion of Pcl103 dramatically increased titan cell formation.

In *S. cerevisiae*, Pcl1 is a critical G1 cyclin that is known to interact with cell polarization proteins and cell cycle regulators including Cdc42 (Moffat and Andrews 2004; Zou, Friesen et al. 2009). Additionally, protein localization studies have shown that Pcl1 is important for the proper localization of the budneck protein Bni4 (Moffat and Andrews 2004; Zou, Friesen et al. 2009), a critical step in the cell cycle. In *C. neoformans*, the Pcl1 homolog Pcl103 may play a similar role to direct cell polarization during budding. Down regulation of Pcl103 may limit budding. Reduced budding may lengthen the G1 phase or alter the cell cycle resulting in endoreplication and increased ploidy. Endoreplication, an altered cell cycle that lacks the M phase, in *S. cerevisiae* results in genome duplication without cell division and generates enlarged cells with increased ploidy (Kondorosi, Roudier et al. 2000) similar to that observed in *C. neoformans* titan cells.

C. neoformans contains multiple paralogues of several proteins that are critical for cell cycle regulation and stress response (Waugh, Nichols et al. 2002; Ballou, Nichols et al. 2009). Cdc420 is a paralogue of Cdc42, which regulates the cell cycle by directing cell polarity (Rincon, Coll et al. 2007; Ballou, Nichols et al. 2009). The duplicated *CDC42* genes are unique to *Cryptococcus.* However, prior to our defining its role in titan cell formation, Cdc420 did not have a clear, unique role in *C. neoformans* physiology

(Ballou, Nichols et al. 2009). In addition to Cdc42/420, *C. neoformans* also has paralogues of Ras and Rac, which are members of stress response pathways involved in morphological transitions. The duplicated *RAC* genes are also unique to *C. neoformans*, suggesting they might be needed for an altered developmental stage of the cell cycle in response to stress, such as titan cell formation.

Taken together, our studies develop the foundation for a signal transduction pathway leading to titan cell production. Titan cell production can be regulated by the Ste3**a** and Gpr5 receptors, yet other receptors that might sense pH, iron limitation, and phospholipids also likely play a role in transducing signals that either stimulate or repress titan cell formation. The differences in titan cell production between mating type **a** and α cells during coinfection is likely due to rewiring of the mating pathway between the two cell types and/or utilization of the Ste3**a** receptor for purposes other than mating. Titan cell signaling is co-regulated with other cryptococcal virulence factors via the PKA pathway suggesting titan cell formation is a novel virulence factor. Understanding of the basic signal transduction pathway leading to titan cell formation will facilitate further exploration of the downstream changes in gene expression that modulate titan cell formation and allow further exploration of the role this virulence factor plays in pathogenesis of *C. neoformans*.

CHAPTER FOUR

Titan Cells Confer Protection from Phagocytosis in *Cryptococcus neoformans* Infections

Okagaki LH and Nielsen K. (2012) Titan cells confer protection from phagocytosis in *Cryptococcus neoformans* infections. *Eukaryotic Cell*. **In Press**.

I. INTRODUCTION

Cryptococcus neoformans is a human fungal pathogen that primarily infects immunocompromised patient populations (Heitman and American Society for Microbiology. 2011). The recent rise in the number of HIV+ patients, patients receiving chemotherapy treatment, and organ transplant recipients has resulted in an increase in the incidence of cryptococcal infections (Heitman and American Society for Microbiology. 2011). Cryptococcal infections are now the third leading cause of death in sub-Saharan Africa and are responsible for more deaths than *Mycobacterium tuberculosis* (Park, Wannemuehler et al. 2009). Cryptococcosis can manifest as skin lesions, pulmonary infection, and meningitis - the deadliest stage of the disease (Heitman and American Society for Microbiology. 2011). In a typical infection, cryptococcal spores or desiccated yeast cells are inhaled into the lungs. These small particles lodge in the alveoli where they can establish a pulmonary infection. At later stages of infection, cryptococcal cells can escape from the lungs and disseminate throughout the body, eventually penetrating the blood-brain barrier to cause meningitis. In sub-Saharan Africa, approximately 60% of HIV+ patients succumb to cryptococcal infections (Park, Wannemuehler et al. 2009; Heitman and American Society for Microbiology. 2011).

Upon exposure to the host pulmonary environment a subset of cryptococcal cells found in the lungs undergo a morphological change producing enlarged “titan” cells. Approximately 20% of cells in the lungs become titan cells, while the remaining cells are equivalent in size to cryptococcal cells grown *in vitro* (Okagaki, Strain et al. 2010). Cryptococcal cells grown *in vitro* are typically 5-10 µm in diameter but titan cells can be

as large as 50-100 μm in diameter (Okagaki, Strain et al. 2010; Zaragoza, Garcia-Rodas et al. 2010). Titan cell production in *Cryptococcus* has been observed as early as 24 hours post-infection and is primarily observed in the lungs, suggesting a role for titan cells in the early pulmonary infection (Okagaki, Strain et al. 2010). Titan cell production in response to the host pulmonary environment is regulated via the PKA pathway (Zaragoza, Garcia-Rodas et al. 2010; Okagaki, Wang et al. 2011), which regulates the production of other cryptococcal virulence factors including the thick antiphagocytic polysaccharide capsule and the dark pigment melanin that protects cryptococcal cells from nitrosative and oxidative stress (D'Souza, Alspaugh et al. 2001).

Titan cells exhibit several characteristics that suggest they have altered host-pathogen interactions. Under host temperature and nutrient conditions, *C. neoformans* produces a thick polysaccharide capsule (Heitman and American Society for Microbiology. 2011). The capsule is able to bind both antibody and complement C3, reducing phagocytosis by host macrophages (Heitman and American Society for Microbiology. 2011). In *Cryptococcus*, the capsule of a normal size cell recovered from the lungs appears fibrous under electron microscopy and is shed easily into the host environment (Zaragoza, Garcia-Rodas et al. 2010). However, the capsule of titan cells is highly cross-linked and is unable to be sheared from the cells by chemical or physical means (Zaragoza, Garcia-Rodas et al. 2010). Titan cells also exhibit a thickened cell wall that appears to be 20-30 fold thicker than the cell wall of normal size cells (Zaragoza, Garcia-Rodas et al. 2010). In addition, titan cells are more resistant to the antimicrobial oxidative and nitrosative stresses produced by the host immune response (Okagaki, Strain et al. 2010; Zaragoza, Garcia-Rodas et al. 2010).

Previous studies showed that increased titan cell production also results in lowered phagocytosis (Okagaki, Strain et al. 2010; Zaragoza, Garcia-Rodas et al. 2010), however the nature of the reduction in phagocytosis remained unknown. Here, the role of titan cell production in protection from phagocytosis was further examined. We show that titan cells can confer protection to normal size cells during early stages of pulmonary infection. While the large size of titan cells can provide protection from phagocytosis, size alone is not sufficient to provide cross-protection to smaller cells. These data show that the role for titan cell production during early pulmonary cryptococcosis extends beyond simple protection of the titan cell due to its large size and suggest titan cell production alters global interactions between *C. neoformans* and the host.

II. MATERIALS AND METHODS

Ethics Statement. All animals were handled in strict accordance with good animal practice as defined by the relevant national and/or local animal welfare bodies. All animal work was approved by the University of Minnesota Institutional Animal Care and Use Committee (IACUC) under protocol numbers 0712A22250 and 1010A91133.

Strains and Media. The *C. neoformans* var. *grubii* strains KN99α (wild-type)(Nielsen, Cox et al. 2003), MutX 31-1 (*otc1Δ*) (Okagaki and Nielsen, unpublished), YPH308 (*otc1Δ gpa2Δ gpa3Δ*) (Hsueh, Xue et al. 2007), CDX18 (*gpr4Δgpr5Δ*) (Xue, Bahn et al. 2006; Okagaki, Wang et al. 2011), and CDX11 (*gpr5Δ*) (Okagaki, Wang et al. 2011) were used in this study. Strains were stored as glycerol stocks at -80°C and grown at 30°C in yeast extract-peptone-dextrose (YPD) agar or broth medium (BD, Hercules, CA).

***In vivo* titan cell and phagocytosis assay.** *C. neoformans* cells were cultured overnight in YPD broth. The resulting yeast cells were pelleted and resuspended in sterile phosphate-buffered saline (PBS) at a concentration of $1x10^8$ cells/ml based on hemocytometer count. Groups of 6- to 8-week-old female C57BL/6 mice (Jackson Labs, Bar Harbor, ME) were anesthetized by intraperitoneal pentobarbital injection. Three to five mice per treatment were infected intranasally with $5x10^6$ cells in 50 μl phospho-buffered saline (PBS, Lonza, Rockland, ME). At 3 days post-infection mice were sacrificed by CO_2 inhalation. Mice were sacrificed by CO_2 inhalation at 24, 48, or 72

hours post-infection. Lungs were lavaged with 1.5 mL sterile PBS three times using an 18.5 gauge needle placed in the trachea. Cells in the lavage fluid were pelleted at 16,000*g*, resuspended in 3.7% formaldehyde, and incubated at room temperature for 30 minutes. Cells were then washed once with PBS and >500 cells per animal were analyzed for size and phagocytosis by microscopy (AxioImager, Carl Zeiss, Inc). Cell body size was measured and cells were classified as small cells (<10 µm in diameter), or titan cells (>10 µm in diameter).

Coinfections. KN99α and *gpr5Δ* were fluorescently labeled with AlexaFluor 488 (AF488) or AlexaFluor 594 (AF594) (Invitrogen, Grand Island, NY) as described previously (Okagaki, Strain et al. 2010). Three to five mice per treatment were infected as described above with $5x10^6$ AF488-labeled KN99α, AF594-labeled *gpr5Δ* mating type α, or an approximate 1:1 ratio of fluorescently-labeled KN99α and *gpr5Δ*. Infected mice were sacrificed at 3 days post-infection by CO_2 inhalation. Samples were collected by lavage and fixed as described above. Greater than 500 cells per animal were analyzed for size, phagocytosis and fluorescence by microscopy (AxioImager, Carl Zeiss, Inc).

***In vivo* bead phagocytosis assay.** Inert polystyrene beads (Phosphorex Inc., Fall River, MA) were opsonized based on the protocol by Cannon et al (Cannon and Swanson 1992). Briefly, 10 µm or 30 µm beads were washed with sterile PBS then incubated with 10 mg/mL bovine serum albumin (Sigma-Aldrich, St Louis, MO) in PBS at 4C for 2 hours. Following incubation, the beads were washed with PBS, resuspended in 0.5 mg/mL of rabbit polyclonal anti-BSA IgG (AbCam, Cambridge, MA) in PBS for 30 min at 37C,

followed by incubation at 4C for 10 min. Beads were then washed with PBS and stained with AlexaFluor 350 (30 μm) or AlexaFluor 594 (10 μm) as described above. Three to five 6-8 week old C57BL/6 mice (Jackson Labs, Bar Harbor, ME) were intranasally infected as described above with $3.5x10^6$ beads in 50 μL PBS. At three days post inoculation, lungs were lavaged with 1.5 mL PBS three times as described above. Beads and cells in the lavage fluid were pelleted at 16,000*g*, resuspended in 3.7% formaldehyde, and incubated at room temperature for 30 minutes. Samples were then washed once with PBS and resuspended in PBS. Greater than 100 beads per animal were analyzed for size, phagocytosis and fluorescence by microscopy (AxioImager, Carl Zeiss, Inc).

Effect of cell age on *in vivo* phagocytosis. Three to five mice per treatment were infected as described above with $5x10^6$ AF488-labeled KN99α, AF-488 labeled *otc1Δ* , AF594- labeled *gpr5Δ*, or AF594-labeled *gpr4Δgpr5Δ* mating type α. Infected mice were sacrificed at 3 days post-infection by CO_2 inhalation. Lungs were lavaged with 1.5 mL sterile PBS three times using an 18.5 gauge needle placed in the trachea. Cells in the lavage fluid were pelleted at 16,000*g*, resuspended in 3.7% formaldehyde, and incubated at room temperature for 30 minutes. Cells were then washed once with PBS and resuspended in PBS. Greater than 2000 cells per animal were analyzed for size, phagocytosis and fluorescence by microscopy (AxioImager, Carl Zeiss, Inc).

Statistical Analysis. All analyses were performed using Analyse-It (Analyse-it Ltd., Leeds, England). One-way ANOVA was used to analyze differences in titan cell production and phagocytosis. *P*-values <0.05 were considered significant. For

coinfections, Wilcoxon Rank Sum was used to analyze differences in the hypothesized percent phagocytosis, based on half of the phagocytosis observed in individual infections, and the observed percent phagocytosis during coinfection. *P*-values of <0.05 were considered significant.

III. RESULTS

Size alone can protect against phagocytosis

Cryptococcus is typically inhaled into the lungs and lodges in alveoli. At early stages of infection, the primary innate immune cells present in the lungs are resident alveolar macrophages (Heitman and American Society for Microbiology. 2011). Thus, early interactions between *Cryptococcus* and alveolar macrophages are critical for the survival of fungal cells and establishment of infection. We showed previously that titan cells are not phagocytosed in the lungs (Okagaki, Strain et al. 2010). While titan cells can be 50-100 µm in diameter (Okagaki, Strain et al. 2010; Zaragoza, Garcia-Rodas et al. 2010), alveolar macrophages are generally only 10-20 µm in diameter (Cannon and Swanson 1992). These data suggest that titan cells could be protected from phagocytosis due to their large size.

To determine if titan cells could be protected from phagocytosis based on their size alone, large and small inert polystyrene beads were introduced into the lungs of mice using the intranasal infection model typically used for titan cell experiments. 30 µm beads were used to simulate the large titan cells while 10 µm beads were used to simulate normal size cryptococcal cells. The beads were opsonized with BSA followed by anti-BSA IgG to simulate recognition of the titan or normal size cryptococcal cells, stimulate interaction with phagocytes, and subsequent phagocytosis. At three days post inoculation, beads were recovered by bronchoalveolar lavage (BAL). Samples were fixed immediately and examined for phagocytosis by microscopy. Approximately 90% of the 10 µm beads were phagocytosed showing that normal size cryptococcal cells are small

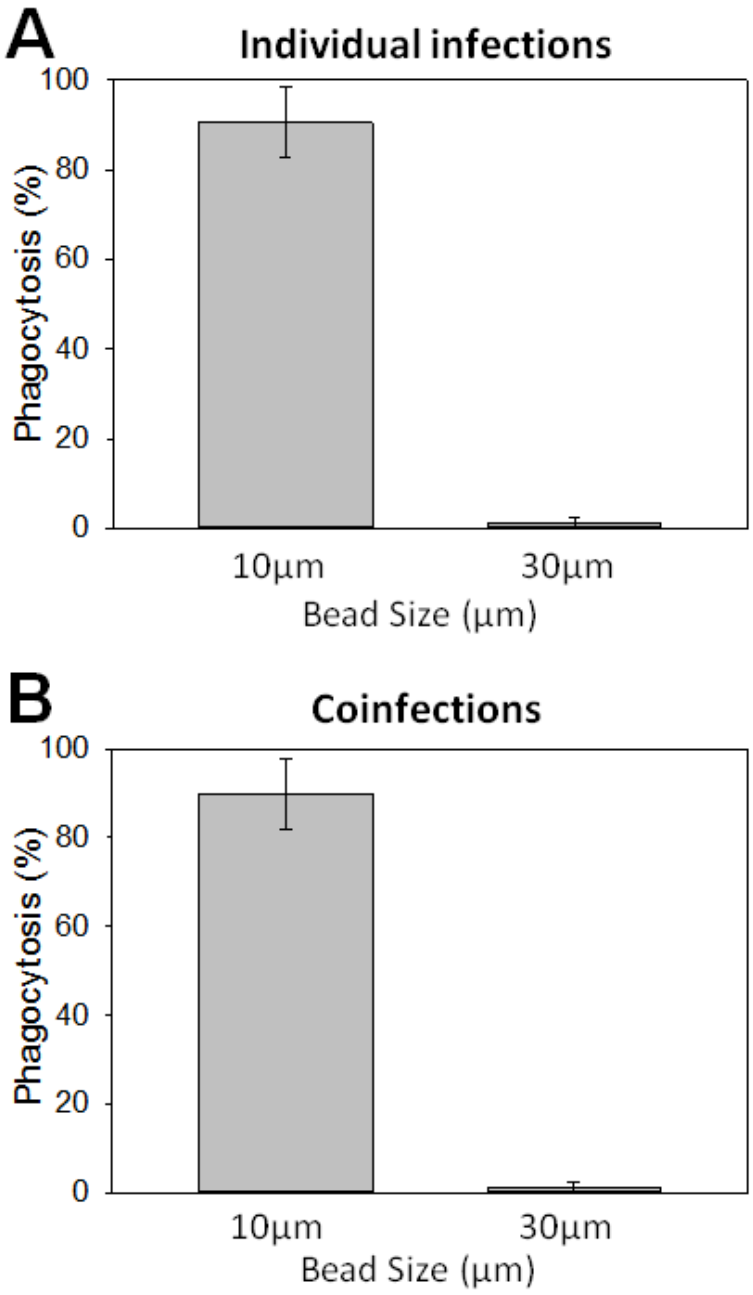

Figure 4.1. Large size cannot provide cross-protection from phagocytosis. Mice were intranasally infected with $3.5x10^6$ large 30 µm or small 10 µm inert beads. At three days post inoculation, lungs were lavaged, samples were fixed, and examined by microscopy to determine phagocytosis of the beads. A) Individual infections with either 30 µm inert beads or 10 µm inert beads. B) Coinfections with a 1:1 ratio of 30 µm and 10 µm beads. Greater than 100 beads were counted per sample. Error bars represent standard deviation for 3 mice per treatment.

enough to be phagocytosed by resident alveolar macrophages (**Figure 4.1A**). In contrast, no 30 μm beads were phagocytosed suggesting that the large size of titan cells could provide protection from phagocytosis (**Figure 4.1A**). These data show that size alone can block phagocytosis and suggest that titan cells could be protected from phagocytosis by their large size.

Association between phagocytosis and titan cell production is non-linear

While titan cells themselves are not phagocytosed (Okagaki, Strain et al. 2010; Zaragoza, Garcia-Rodas et al. 2010), the nature of the relationship between titan cell production and cryptococcal cell phagocytosis in the lungs remained unclear. There are at least two possible hypotheses for how titan cell production can reduce phagocytosis (**Figure 4.2A**). First, the titan cells themselves could be protected by size alone, resulting in a direct correlation between titan cell production and phagocytosis – a linear relationship (**Figure 4.2A** – dotted line). Alternatively, titan cell production could result in a global decrease in phagocytosis where small changes in titan cell production would reduce overall levels of phagocytosis – a non-linear relationship (**Figure 4.2A** – solid line).

Four strains with differences in titan cell production were utilized to determine the relationship between titan cell formation and phagocytosis: (i) the wild-type strain KN99α that exhibited approximately 20% titan cell formation ((Nielsen, Cox et al. 2003); (ii) a *gpr5Δ* mutant strain that produced 2-3% titan cells (Okagaki, Wang et al. 2011); (iii) a *gpr4Δgpr5Δ* double mutant strain that had minimal titan cell production (Xue, Bahn et al. 2006; Okagaki, Wang et al. 2011); and (iv) an *otc1*Δ (overproducer of titan

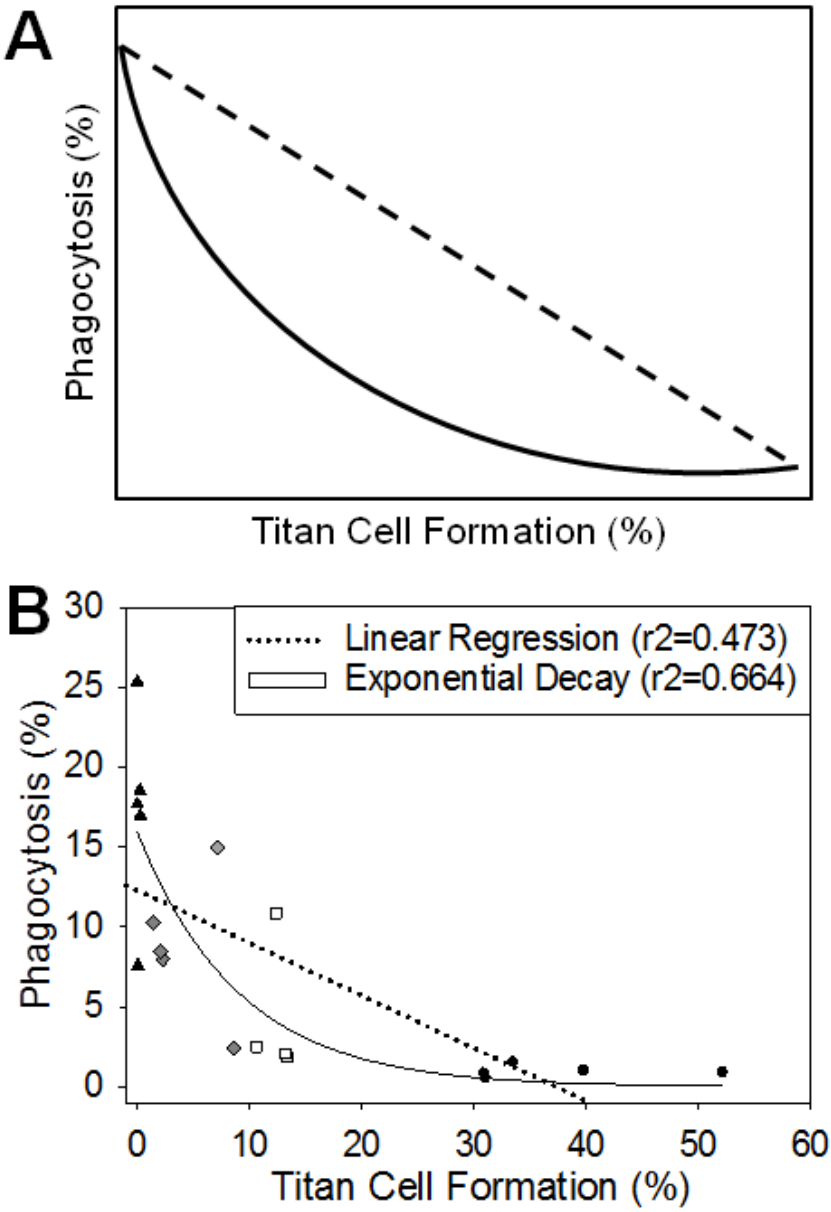

Figure 4.2. The relationship between titan cell production and phagocytosis is non-linear. A) Two hypothesized relationships between titan cell production and phagocytosis include a linear relationship where titan cells are protected from phagocytosis by size alone (dotted line), and a non-linear relationship where small amounts of titan cell production result in a global decrease in phagocytosis (solid line). B) Mice were intranasally inoculated with $5x10^6$ wild-type or mutant cryptococcal strains that exhibit altered titan cell formation. At three days post-infection, lungs were lavaged, resulting BAL samples fixed, and examined by microscopy for titan cell production and phagocytosis. Black triangles, gray diamonds, white squares, and black circles indicate infections with the *gpr4Δgpr5Δ*, *gpr5Δ*, wild-type and *otc1Δ* strains, respectively. R^2 values were calculated based on linear regression and exponential decay curves. Four to five mice were inoculated per treatment and >2000 cells were examined per mouse.

cells) mutant strain that produced >50% titan cells by 3 days post-infection. The *otc1Δ* strain contains a mutation in a single gene with unknown function that enhances titan cell production *in vivo* (Okagaki and Nielsen, unpublished). All four of these strains produce wild-type levels of other known virulence factors including growth at 37°C, melanin production, capsule formation, and urease production. Additionally, all four of these strains produce normal size cells when grown *in vitro*.

Titan cell production and phagocytosis were determined in mice intranasally inoculated with 5x10^{6} cryptococcal cells. Cells were collected at 3 days post-infection by bronchoalveolar lavage (BAL), fixed immediately and examined by microscopy for cryptococcal cell size and phagocytosis. The relationship between titan cell production and phagocytosis for all strains was determined (**Figure 4.2B**). The *gpr4Δgpr5Δ* strain, with no titan cell production, exhibited the highest rate of phagocytosis at approximately 17-19% (**Figure 4.2B**, black triangles). The *gpr5Δ* strain, with low levels of titan cell production had slightly less phagocytosis (**Figure 4.2B**, grey diamonds). In contrast, the wild-type (**Figure 4.2B**, white squares) and *otc1Δ* (**Figure 4.2B**, black circles) strains exhibited the lowest levels of phagocytosis, ranging from 0.5-2.5% phagocytosis. Linear regression and decay curves were calculated and r^2 values determined for the data set. The r^2 for the decay curve (r^2= 0.664) was higher than the linear regression line (r^2= 0.473), thus the relationship between titan cell formation and phagocytosis fits the decay curve model better than the linear model. These data show that small changes in titan cell production dramatically reduce phagocytosis and suggest that titan cell production has a global effect on phagocytosis.

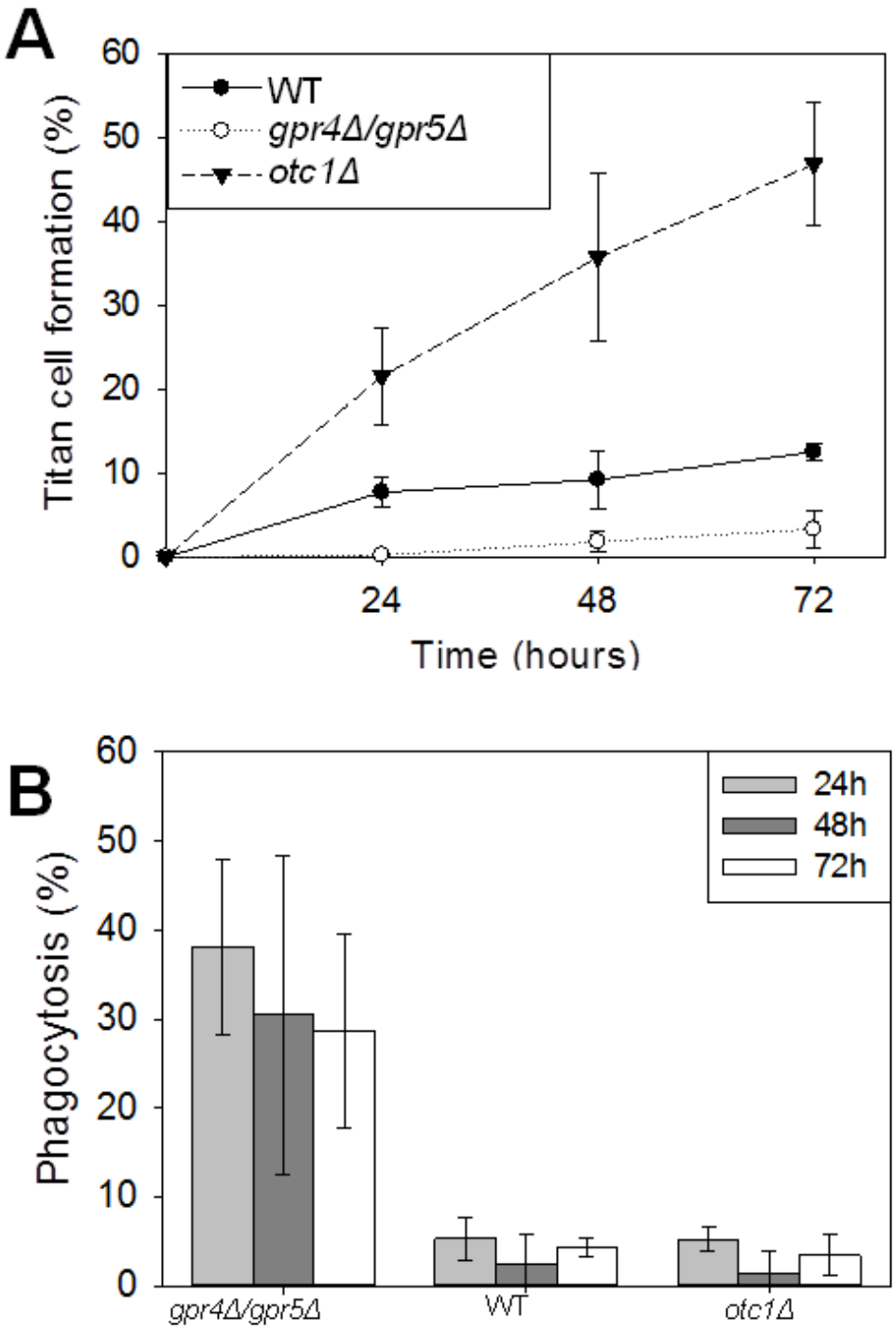

Figure 4.3. Titan cell production reduces phagocytosis by 24 hours post-infection. Mice were intranasally inoculated with $5x10^6$ wild-type, *gpr4Δgpr5Δ*, or *otc1Δ* strains. At 24, 48, or 72 hours post-infection, lungs were lavaged and the resulting samples were fixed immediately. Samples were examined for titan cell production (A) and phagocytosis (B). Error bars represent standard deviation from three to five mice per strain. Greater than 300 cells per mouse were examined.

To determine the timeframe in which titan cell production reduced phagocytosis, titan cell production and phagocytosis were monitored at 24, 48, and 72 hours post-infection with the *gpr4Δgpr5Δ*, wild-type, and *otc1Δ* strains (**Figure 4.3**). As observed previously, the *gpr4Δgpr5Δ* strain had minimal titan cell production over the course of the experiment (Figure 3A). In contrast, the wild-type strain showed moderate increases in titan cell formation while the *otc1Δ* mutant strain exhibited significant increases in titan cell production over the course of the experiment (**Figure 4.3A**). Even though the *otc1Δ* strain exhibited differences in titan cell production over time, no difference in phagocytosis between the time points was observed **(Figure 4.3B**; p=0.27). In fact, no difference in phagocytosis in any of the strains was observed over the course of the experiment (p=0.054 for *gpr4Δgpr5Δ*, p=0.081 for wild-type) suggesting that titan cell production within the first 24 hours of the infection was able to block phagocytosis (**Figure 4.3B**). Consistent with the non-linear relationship between titan cell production and phagocytosis observed above, the *gpr4Δgpr5Δ* strain that lacks titan cell formation had significantly more phagocytosis than the strains that generated titan cells (p-values <0.0001 for comparisons of individual time points in *gpr4Δgpr5Δ* and wild-type or *otc1Δ*) while no difference in phagocytosis was observed between the wild-type strain that has moderate titan cell formation compared to the *otc1Δ* strain with high titan cell production (p-values >0.400 for comparisons of individual time points in wild-type and *otc1Δ*).

These data show that as little as 10% titan cell production almost completely abolished phagocytosis of all cryptococcal cells during the early pulmonary infection. Thus, titan cell production resulted in a global decrease in phagocytosis that did not

directly correlate with the number of titan cells present in the sample. Not only were titan cells themselves protected from phagocytosis, but the presence of titan cells reduced overall levels of phagocytosis.

Nascent cells exhibit reduced titan cell formation and phagocytosis

The time course data presented above show that titan cell production during the first 24 hours of the infection dramatically decreased phagocytosis but additional titan cell formation at later times did not provide any further benefit. Previous studies examining transcriptional changes in response to phagocytosis by macrophages *in vitro* suggest that cryptococcal cells inhaled into the lungs need time to adjust to the host environment (Fan, Kraus et al. 2005). Thus, the initial infecting inoculums may exhibit higher rates of phagocytosis and benefit more from titan cell production whereas cells that have already adapted to the host environment may not benefit from titan cell production.

To test this hypothesis, mice were infected with cryptococcal cells stained with AF488 or AF594. These stains bind to components in the cryptococcal cell wall that are not transferred to the daughter cell upon cell division. Thus, only the initial inoculum was fluorescently-labeled while nascent daughter cells produced *in vivo* were unlabeled. Mice were infected with the fluorescently-labeled wild-type, *otc1Δ*, or *gpr4Δgpr5Δ* strains. At 72 hours post-infection, cells were recovered from the lungs by BAL, fixed, and phagocytosis, titan cell production, and fluorescence were determined by microscopy.

Titan cell production by cells in the original inoculum was higher than that observed for the *in vivo* produced nascent cells for both the wild-type and *otc1Δ* strains (**Figure 4.4A**). In the wild-type strain, cells in the original inoculum produced approximately 20%

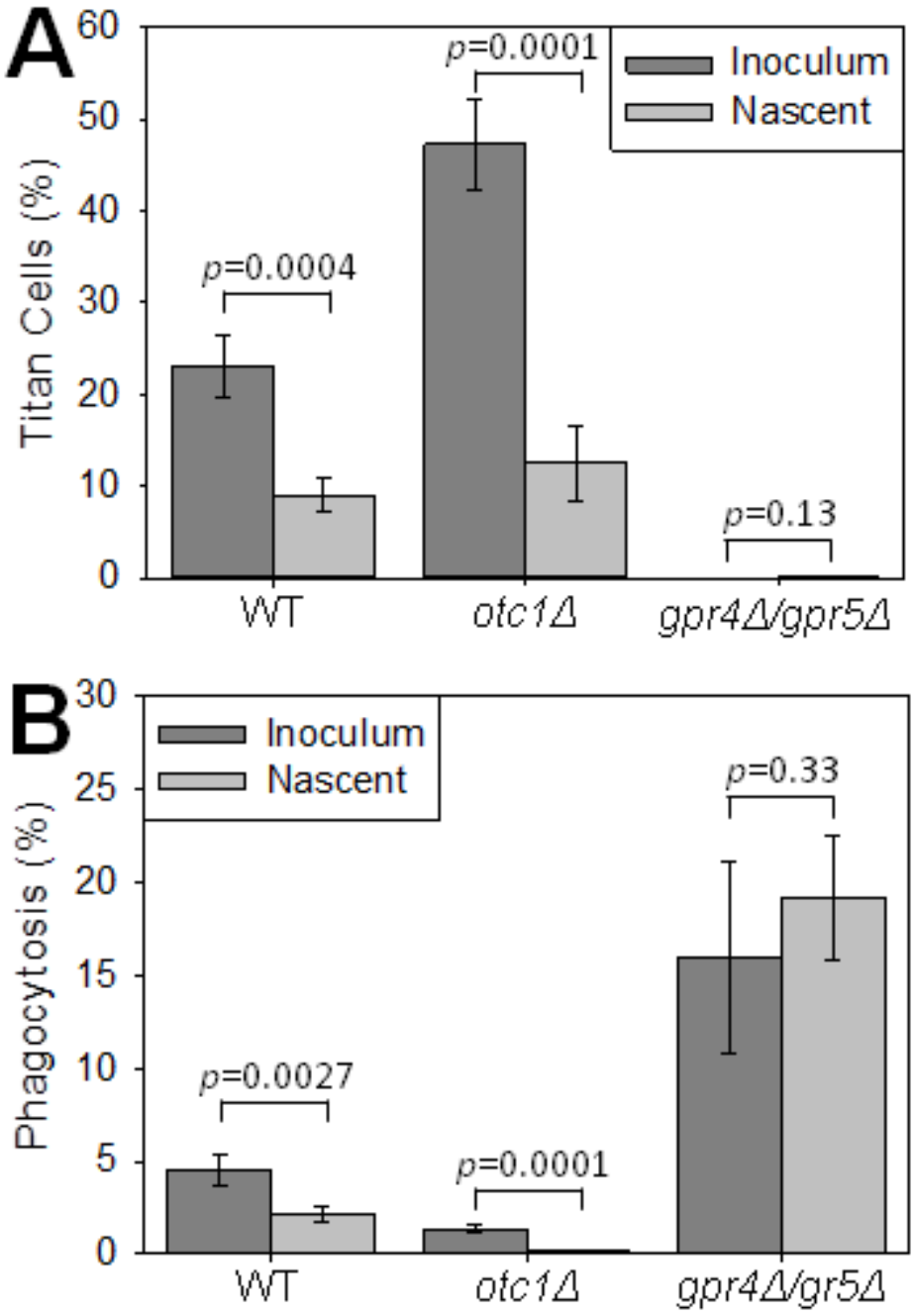

Figure 4.4. Nascent cells exhibit reduced phagocytosis. Mice were intranasally infected with $5x10^6$ cells of AlexaFluor 488 wild-type cells, AlexaFluor 488 *otc1Δ* cells, or AlexaFluor 594 *gpr5Δ* cells. At three days post-infection, lungs were lavaged and the samples were fixed and examined by microscopy. Titan cell formation (A) and phagocytosis (B) were quantified in unstained and stained populations of cells in each lavage sample. Error bars indicate standard deviation from three to five mice per strain and >2000 cells per mouse.

titan cells while the nascent cells exhibited only 10% titan cell production (**Figure 4.4A**, *p*=0.0004). A similar trend was observed in the *otc1Δ* mutant where titan cell production in the nascent cells was one fifth that observed in the original inoculum (**Figure 4.4A**, *p*=0.0001). Interestingly, infections with the wild-type strain exhibited phagocytosis rates of approximately 5% in the original inoculum and phagocytosis was significantly reduced in the nascent cells produced *in vivo* to 2.5% **(Figure 4.4B**, *p*=0.0027). Similar results were observed with the titan cell over-producing strain *otc1Δ* where phagocytosis of the nascent cells was almost completely abolished (**Figure 4.4B**, *p*=0.0001). Neither titan cell production nor phagocytosis was altered in the *gpr4Δgpr5Δ* nascent cells compared to cells in the original inoculum (**Figure 4.4**, *p*=0.13 and *p*=0.33, respectively) suggesting that early production of titan cells was required to alter phagocytosis of the nascent cells produced *in vivo* and any subsequent titan cell formation by the newly-formed cryptococcal cells. These data suggest that titan cells produced in the first 24 hours of the infection influence both protection from phagocytosis and titan cell formation in the subsequent nascent cell populations.

Titan cell production protects normal size cryptococcal cells from phagocytosis

Titan cells produced in the first 24 hours of the infection reduced phagocytosis of nascent cells produced *in vivo*. In addition, titan cell production resulted in a global decrease in phagocytosis in a non-linear manner. These data suggested titan cell production may protect normal size cryptococcal cells from phagocytosis.

To test this hypothesis directly, we coinfected the *gpr5Δ* strain that has limited titan cell production with the wild-type strain that has approximately 20% titan cell production

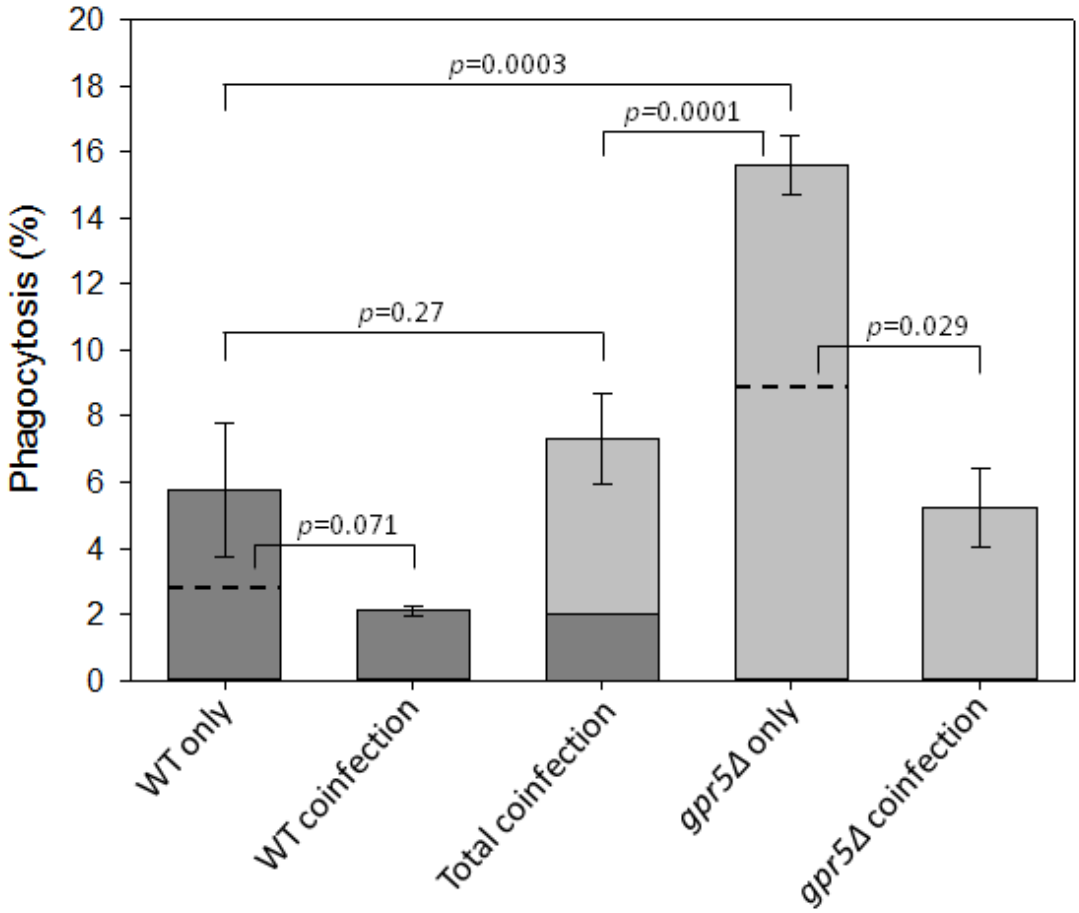

Figure 4.5. Titan cell production provides cross-protection from phagocytosis to normal size cryptococcal cells. Mice were intranasally inoculated with $5x10^6$ cells of AlexaFluor 488 stained wild-type cells, AlexaFluor 594 stained *gpr5Δ* cells, or an approximate 1:1 ratio of wild-type and *gpr5Δ* cells. At three days post-infection, lungs were lavaged, the BAL samples were fixed, and examined by microscopy for titan cell production, phagocytosis, and fluorescence. Dotted line indicates half of the phagocytosis observed in the individual infections. The total coinfection bar indicates the total amount of phagocytosis observed during the coinfection with wild-type cells indicated in dark gray and gpr5Δ cells indicated in light gray. Error bars represent standard deviation from three to five mice per treatment and >500 cells examined per mouse.

(**Figure 4.5**). The goal of this experiment was to see if the titan cells generated by the wild-type strain could protect the *gpr5Δ* cells from phagocytosis. Mice were intranasally inoculated with $5x10^6$ AF488-labeled wild-type cells, AF594-labeled *gpr5Δ* cells, or a 1:1 ratio of fluorescently-labeled wild-type and *gpr5Δ* cells. At 3 days post-infection, cells were recovered from the lungs by BAL, fixed, and examined for phagocytosis. In the coinfection, wild-type cells were identified by their green fluorescence (AF488) while *gpr5Δ* cells were identified by their red fluorescence (AF594). The total number of cells in the inoculums ($5x10^6$ cells) was the same for the individual and coinfections. Because the coinfections contained equal ratios of the two strains, half the number of cells of each strain was present in the coinfections compared to the individual infections.

If titan cell production did not confer protection from phagocytosis to normal size cryptococcal cells, then the coinfections would exhibit half the amount of phagocytosis for each strain compared to that observed during individual infections (indicated by dotted lines in **Figure 4.5**) because only half the number of cells was present in the coinfection. If the titan cells produced by the wild-type strain protected the *gpr5Δ* cells from phagocytosis, then the amount of phagocytosis in the *gpr5Δ* strain should decrease in the coinfection.

Similar to experiments described above, phagocytosis of the *gpr5Δ* cells was significantly higher than phagocytosis of the wild-type cells in the individual infections (**Figure 4.5**, p=0.0003). Upon coinfection, phagocytosis of the wild-type strain did not differ significantly from the hypothesized phagocytosis level based on the wild-type control infection (p=0.071). In contrast, the *gpr5Δ* strain exhibited significantly less phagocytosis than hypothesized based on the control *gpr5Δ* infection (p=0.029).

Additionally, the total amount of phagocytosis in the coinfection was equivalent to the wild-type control infection and significantly less than the *gpr5Δ* control (p=0.27 and p=0.0001, respectively). Taken together, these data show that the presence of titan cells produced by the wild-type strain was able to confer cross-protection to *gpr5Δ* cells during coinfection. These data support the hypothesis that titan cell production protects normal size cryptococcal cells from phagocytosis.

Size alone does not confer cross-protection from phagocytosis

Macrophages can experience frustrated phagocytosis when a particle, such as a large asbestos particle, is too large to be engulfed (Cannon and Swanson 1992). To determine whether the cross-protection of normal size cells from phagocytosis could be due to the large size of the titan cells, mice were coinfected with inert beads to mimic the differences in size observed during the cryptococcal infections. Large 30 beads were used to simulate the titan cell size while small 10 µm beads were used to simulate normal size cryptococcal cells. Beads were opsonized as described previously to stimulate phagocytosis and an approximate 1:1 ratio of large and small beads was used to simulate maximal titan cell production during cryptococcal infections. In contrast to the cryptococcal infections, the presence of large beads did not provide protection from phagocytosis to the small beads (**Figure 4.1B**). These data show that the presence of 30 µm particles does not provide protection from phagocytosis to smaller particles and suggests that titan cells are providing cross-protection to normal size cryptococcal cells through mechanisms other than cell size.

IV. DISCUSSION

Cryptococcal titan cells exhibit characteristics that may protect the cells from the host immune response. Titan cells are resistant to oxygen and nitrogen free radicals released by host immune cells to kill pathogens (Okagaki, Strain et al. 2010; Zaragoza, Garcia-Rodas et al. 2010). In addition, the highly cross-linked capsule and thickened cell wall of titan cells may act as defensive barriers making it very difficult for host immune cells to gain access to the titan cell (Zaragoza, Garcia-Rodas et al. 2010). Perhaps most intriguing is the observation that titan cells are not phagocytosed by cells of the host immune system and have altered antibody and complement binding (Okagaki, Strain et al. 2010; Zaragoza, Garcia-Rodas et al. 2010). We further explored the interaction between host phagocytes and cryptococcal cells during the pulmonary infection.

Titan cell production affects phagocytosis during cryptococcal infections in a non-linear manner. As few as 5-10% titan cells in the entire cryptococcal cell population almost completely abolished phagocytosis of the cryptococcal cells. Less than 5% titan cell production resulted in significantly higher rates of phagocytosis while titan cell production above 10% did not provide additional protection. While higher levels of titan cell production do not have deleterious effects on cryptococcal survival in the lungs, over-production of titan cells in the lungs can inhibit cryptococcal dissemination to the central nervous system (Okagaki, Strain et al. 2010). This may explain why only a small proportion of the total population converts to titan cells during the infectious process.

Protection from phagocytosis was most apparent within the first 24 hours post-infection. Typical human exposure to *C. neoformans* from the environment is likely to be a low number of desiccated yeast cells or spores. Titan cell production and subsequent

protection from phagocytosis within the first 24 hours may increase the population of the initial inoculum that can survive the early phagocytic immune response to establish the pulmonary infection.

Titan cells are typically 30 µm or more in diameter with some titan cells as large as 50-100 µm in diameter (Okagaki, Strain et al. 2010; Zaragoza, Garcia-Rodas et al. 2010). Thus titan cells are much larger than resident alveolar macrophages that are typically only 10-20 µm in diameter (Cannon and Swanson 1992). Using simulations with inert beads, we showed that the large size of titan cells can be protective against phagocytosis. Yet titan cells also provide cross-protection to normal-sized cells during early pulmonary infection. Previous studies have shown that large particles, such as asbestos particles, cannot by phagocytosed and induce a phenomenon referred to as "frustrated" phagocytosis (Takemura, Stenberg et al. 1986; Cannon and Swanson 1992). Frustrated phagocytosis leads to reductions in overall phagocytosis and can lead to the production of IL-1β that induces a strong inflammatory response (Oghiso and Kubota 1986; Oghiso and Kubota 1987; Netea, Simon et al. 2010). We cannot rule out the possibility that titan cell formation may induce changes in the immune response that overlap with frustrated phagocytosis. However, inoculating mice with large inert beads of equivalent size to titan cells did not confer protection from phagocytosis to small beads equivalent in size to normal size cryptococcal cells - even though host cells could not phagocytose the larger beads. These data suggest that other mechanisms beyond frustrated phagocytosis alone may be contributing to the protection of non-titan cells from phagocytosis. Instead, titan cell production may alter the host immune response by modulating immune activity through other mechanisms.

Titan cells could directly alter the activity of host phagocytes through cell-cell contact or close proximity. The capsule of *Haemophilus influenzae* has been shown to inhibit recognition and prevent uptake of cells that come in direct contact with macrophages (Noel, Hoiseth et al. 1992). The M protein produced by *Streptococcus pyogenes* can inhibit engulfment by blocking complement binding to the bacterial cell surface and subsequent recognition by host macrophages (Thern, Wastfelt et al. 1998; Courtney, Hasty et al. 2006). Thus, the altered capsule produced by titan cells may be able to modulate the phagocytic activity of host cells through direct cell-cell contact.

It is also possible that titan cells could stimulate killing of phagocytes, either by toxin production or by morphological switch. Exotoxin A produced by *Pseudomonas aeruginosa* is one of several bacterial toxins that have been shown to be cytotoxic to macrophages, inhibiting phagocytic activity and causing cell death (Pollack and Anderson 1978). *C. neoformans* has been shown to produce extracellular vesicles that contain immune modulating compounds (Rodrigues, Nakayasu et al. 2008; Oliveira, Freire-de-Lima et al. 2010). Titan cells have large vacuoles with abundant multivesicular bodies (Zaragoza, Garcia-Rodas et al. 2010; Choi, Vogl et al. 2012), suggesting extracellular vesicle formation may be enhanced in titan cells. Titan cells could also produce modified vesicles containing compounds that could modulate the immune response or kill host cells.

Engulfment of a normal size cryptococcal cell by resident alveolar macrophages could stimulate titan cell production. The rapid cell enlargement associated with titan cell formation could lyse the macrophage. The commensal fungus *Candida albicans* is stimulated to switch from the easily phagocytosed yeast form to the hyphal form upon

phagocytosis. The hyphae eventually grow too large to be contained by the host cells and will ultimately lyse the macrophage and escape killing (Lorenz, Bender et al. 2004; Ghosh, Navarathna et al. 2009).

Alternatively, titan cell production may alter the host immune response systemically rather than locally. Altered host-pathogen interactions, as exhibited in the presence of titan cells, may result in altered recruitment of host cells to the lungs. Reduced recruitment of phagocytes, such as monocytes, to the lungs could result in a lower phagocyte to cryptococcal cell ratio. The increase in phagocytosis observed in titan cell mutants such as *gpr5Δ* and *gpr4Δgpr5Δ* may be the result of increased recruitment of host cells to the lungs compared to the wild-type infection. Microscopic examination of the titan cell deficient infections did reveal large aggregates of host cells that are lacking in the wild-type infection (Okagaki and Nielsen, unpublished) indicating that either recruitment or adhesion are altered in the presence of titan cells. *Streptococcus* species produce the small molecule streptolysin S, which inhibits chemotaxis and recruitment of neutrophils, reducing the inflammatory response at the site of infection (Lin, Loughman et al. 2009). *Clostridium perfringens* produces a toxin similar in structure to streptolysin S, called Θ toxin that also prevents chemotaxis of phagocytes (Stevens, Mitten et al. 1987). Thus, titan cells may be inhibiting phagocytosis by modulating the influx of leukocytes via the production of a small molecule chemotaxis inhibitor.

The data presented here are the first evidence that titan cell production in *C. neoformans* protects normal size cells from phagocytosis in the host pulmonary environment. Therefore, titan cell production by *C. neoformans* may be instrumental in the initial establishment of infection, promoting increased fungal burden in the lungs.

While the mechanism of this protection from phagocytosis remains unknown, studies from other organisms suggest that titan cell production likely results in a dramatic remodeling of the host pulmonary immune response. This remodeling could be either through direct interactions or production of small molecules, resulting in a reduction in global phagocytosis rates and subsequent promotion of cryptococcal survival within the host.

Chapter 5

Conclusions and Final Remarks

I. Titan Cells in Pulmonary Infection

Many of the human fungal pathogens undergo morphological changes that are critical during infection. For the dimorphic fungi, the yeast form is necessary for pulmonary pathogenesis and intracellular parasitism. In *C. albicans*, both the yeast form and the hyphal form are required for virulence. Phenotypic switching, such as capsule formation and white-opaque switching, in *Cryptococcus neoformans* and *C. albicans*, respectively, may make the yeast cells more suitable to the varying conditions found in the host body. Cell enlargement has been shown to protect fungal cells from phagocytosis and provides a mechanism for replication. *C. neoformans* undergoes a unique morphological transition to titan cells upon exposure to the host pulmonary environment. The production of titan cells affects host-pathogen interactions (Chapters 2 and 4), and is regulated by pathways that also regulate other cryptococcal virulence factors (Chapter 3). Alterations in ploidy (Chapter 2), capsule structure (Zaragoza, Garcia-Rodas et al. 2010), cell wall (Zaragoza, Garcia-Rodas et al. 2010), and resistance to stress (Chapter 2) suggest that titan cell production has specific roles in infection.

Titan Cells Are Important in Establishment of the Pulmonary Infection

The first stage of infection for *C. neoformans*, like many other human fungal pathogens, is the establishment of infection in the host pulmonary environment. The dimorphic fungi undergo a transition from either the filamentous or spore form to the yeast form to survive the host pulmonary environment and to establish infection. The data presented here suggest that the primary role of cryptococcal titan cells is in the establishment of early pulmonary infection. Titan cells are visible by microscopy by 24

hours post-infection indicating that they form early in infection (Chapter 2, **Figure 5.1A**). Time course studies showed that titan cells are produced primarily in the lungs, and production reaches its peak between 5 and 7 days post-infection. Levels of titan cells in the lungs remain constant beyond 7 days post-infection. In addition, while cryptococcal cells can be recovered from the spleen and the brain between 7 and 14 days post-infection, few titan cells are observed in the spleen or brain, even at 21 days post-infection (Chapter 2). These data suggest that titan cell production is promoted by the pulmonary environment and that these very large cells are not produced in or disseminating to other body sites.

Titan cells are protected from phagocytosis and provide cross-protection from phagocytosis to normal-sized cells during early pulmonary infection (Chapter 4, **Figure 5.1A**). Protection from phagocytosis promotes the survival of the initial inoculum within the first 24 to 72 hours post-infection and also may promote the increase in lung fungal burden at later stages of infection. Studies examining the fungal burden in the lungs, spleen, and brain detected a lower fungal burden in the lungs of mice infected with a strain that is unable to produce titan cells than in mice infected with the wild type strain even though the titan deficient strain has a similar doubling time *in vivo* compared to the wild type (Okagaki, Crabtree, and Nielsen, unpublished). These data suggest that titan cell production promotes a higher fungal burden in the lungs.

In a typical human cryptococcal infection the initial inoculum is likely a low number of cells or spores. Density-dependent experiments show that fewer cells in initial inocula produced a higher proportion of titan cells (Appendix). In an infection with a low inoculum, there are fewer cells that can establish the initial infection. Increased titan

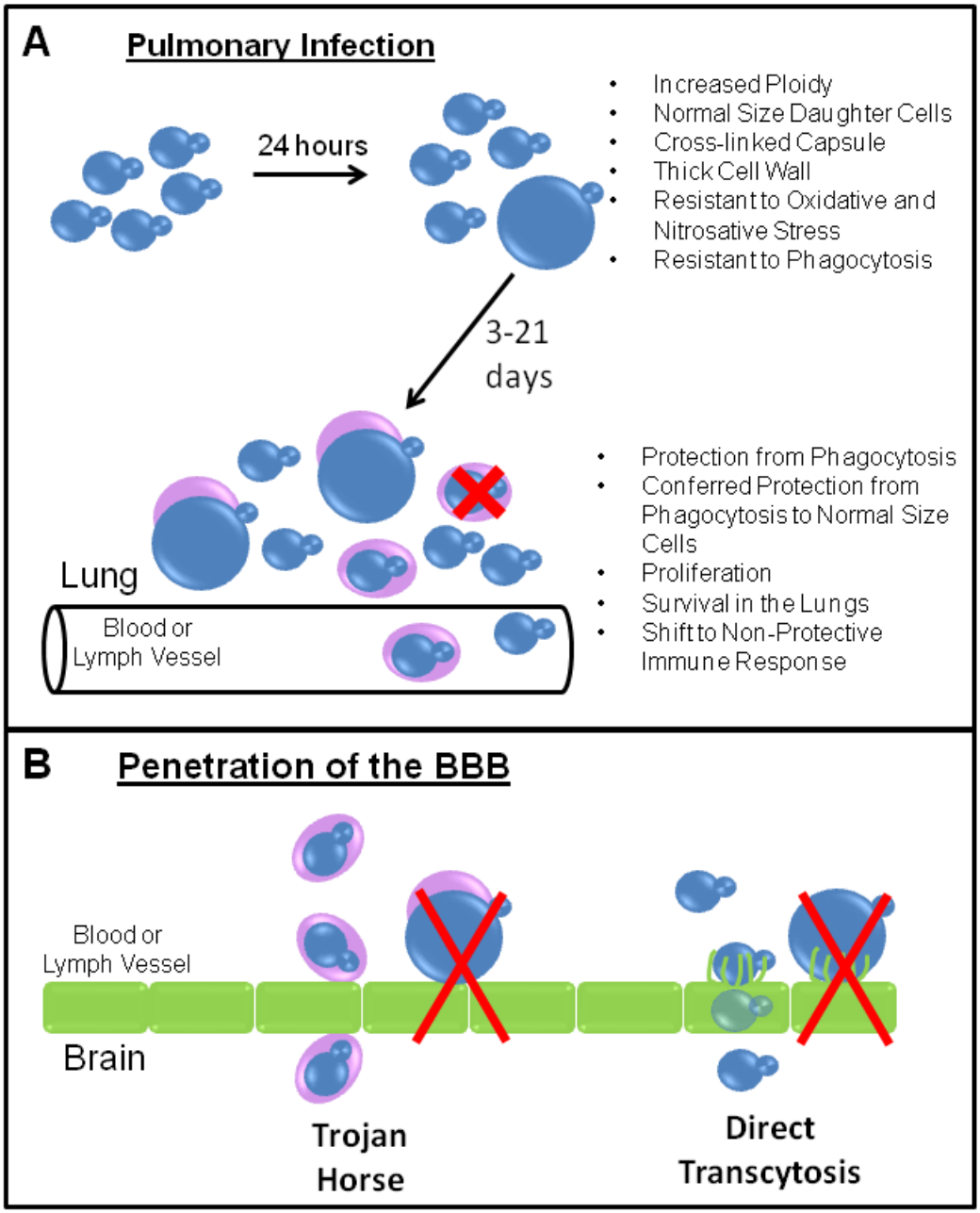

Figure 5.1. Titan Cell Production and Pathogenesis. Titan cells are produced in the lungs as early as 24 hours post-infection (**A**), and exhibit a number of traits that protect them in the pulmonary environment, including alterations the host immune response. Titan cells are protected from phagocytosis by host cells (denoted by purple ovals), and can protect normal-sized cells from phagocytosis. Finally, titan cell production alters the penetration of the blood brain barrier (**B**). Titan cells are too large to be phagocytosed and carried into the brain by either host phagocytes or the endothelial cells at the blood brain barrier.

cell production and protection from phagocytosis may increase the proportion of the initial inoculum that can survive in the host environment.

Finally, titan cells are actively replicating and producing normal-sized daughter cells by budding (**Figure 5.1A**) (Okagaki, Strain et al. 2010). Cell enlargement in *Pneumocystis* and *Coccidioides* is a mechanism that results in the production and maturation of progeny cells (Lubarsky and Plunkett 1955; Drutz, Huppert et al. 1981; Johannesson, Kasuga et al. 2006; Hung, Xue et al. 2007). Titan cell production may act in a similar manner, where titan cells are protected from phagocytosis during bud formation (Chapters 2 and 4), and can confer protection from phagocytosis to daughter cells from phagocytosis (**Figure 5.1A** and Chapter 4). Electron microscopy revealed that titan cells appear to transfer some of their highly cross-linked capsule to their daughter cells during replication (**Figure 1.3**, **Figure 5.1A**, and (Zaragoza, Garcia-Rodas et al. 2010)), and it is possible that transfer of the titan cell capsule to can promote survival of the daughter cells in the lungs. In addition, production of large numbers of progeny cells rapidly may overwhelm local phagocytes and limit the proportion of cryptococcal cells that can be phagocytosed.

It is important to understand the nature of the protection conferred to small cells by the presence of titan cells, and should be the focus of additional studies. There are several ways that titan cells may promote the survival of cells in the lungs, such as altered activation of macrophages, modulation of the immune response to a non-protective response, or killing of host cells in the pulmonary environment. Additional characterization of titan cells, including exploring the interaction between titan cells and macrophages, may provide insight into the host-pathogen interactions during early

infection that can alter the outcome of infection. In addition, understanding the titan cell cycle and how titan cells produce large numbers of daughter cells may identify novel targets to either prevent the establishment of pulmonary infection or limit the severity of infection at later stages cryptococcosis.

Titan Cell Production May Promote Dormancy

While the primary role of titan cell production is most likely during the establishment of pulmonary infection, titan cells may also contribute to dormant infections. *C. neoformans* infections can be the result of recent exposure to fungal cells, or may be a reactivation of a dormant infection. An acute infection can be acquired from the environment when a patient is already immune-compromised. Studies performed by the Nielsen lab suggest that cases of cryptococcosis are associated with the dry season, and about a month later patients present with cryptococcal meningitis (Strain, Goettge, and Nielsen, unpublished). In contrast, a patient can acquire a cryptococcal infection prior to becoming immune-compromised, with the fungal infection being contained by immune cell functions. Upon immune suppression, the dormant infection is no longer contained and can produce an active infection. Studies examining *C. neoformans* isolates from African immigrant patients in France found that several patients had strains similar to those found in Africa even in the absence of recent travel (Dromer, Varma et al. 1994), suggesting that the patients had activated a dormant infection. Importantly, the mechanism by which *C. neoformans* establishes a dormant infection is unknown. Titan cell characteristics, including increased resistance to oxidative and nitrosative stress and decreased phagocytosis, suggest that titan cells may survive in the pulmonary

environment longer than normal-sized cells and thus may contribute to a dormant infection in healthy hosts.

During cryptococcal infection in the lungs, CD4+ T-cells surround the fungal cells in an attempt to contain the infection (Hill 1992). The CD4+ T-cells also induce macrophage fusion, producing multinucleate mammalian giant cells to further contain the cryptococcal infection (Hill 1992). The collection of CD4+ T-cells and giant cells to the site of infection produces a granuloma. Within the granuloma, host cells produce antimicrobial reactive oxygen and nitrogen species; importantly, titan calls are more resistant to the nitrosative and oxidative stresses (Chapter 2), suggesting that they may have increased survival within granulomas or when in close contact with cells with antimicrobial activity. The inability of host cells to phagocytose titan cells may result in the recruitment of host cells to the titan cell and eventual granuloma formation around the titan cells.

Microscopic examination of titan cells revealed that they contain a large vacuole that can account for as much as 90% of the volume of the cell ((Zaragoza, Garcia-Rodas et al. 2010) and Chapter 2). Based on these observations, I hypothesize that there are several possible functions of the vacuole in titan cells: turgor pressure, filling cell volume, and nutrient storage. First, the enlarged vacuole may simply provide the turgor pressure needed to enlarge the cell rapidly. Second, the vacuole may be important in taking up cell volume so that the cell doesn’t need to produce large amounts of cytosolic proteins needed to fill such a large volume. Third, because the vacuole appears to push the cell contents towards the cell wall, it may shorten the distance necessary for nutrient and metabolite diffusion. Finally, a less likely hypothesis is that the vacuole could

contain nutrients needed for the production of daughter cells or for long term survival in a nutrient limited environment. *Coccidioides* spherules also contain a large vacuole and it has been suggested that the vacuole contains nutrients necessary for the production of large numbers of progeny cells. Like the vacuoles found in *Coccidioides*, the titan cell vacuole may be harboring nutrients necessary for the rapid cell division observed in titan cells (Zaragoza, Garcia-Rodas et al. 2010).

To further explore the hypothesis that titan cells promote dormancy, some basic observations must be made. Are titan cells involved in granuloma formation at early stages of lung infection? To test this, wild type, titan deficient, and titan over-producing strains should be examined for granuloma formation and for the localization of each immune cell type within any formed granulomas. It is possible that titan cells are able to recruit a different subset of host cells to the site of granuloma formation compared to normal-sized cells. The proportion of titan cells and small cells in granulomas can also be quantified. Can titan cell-deficient strains produce a dormant infection? Currently, a dormancy model is being developed by the Nielsen lab to understand how a latent infection can become reactivated upon immune suppression. Once this model is established, strains with altered titan cell production can be tested for their ability to produce a dormant infection that can be reactivated in the absence of CD4+ T cells, mimicking the effects of HIV.

Titan Cells and Penetration of the Blood Brain Barrier

Morphogenesis in human pathogenic fungi is accompanied by traits that can make some morphologies better-suited than others for survival in specific host. In *C. albicans*,

the yeast form is ideal for dissemination in the blood stream, while the hyphal form adheres to tissues and produces enzymes necessary for tissue invasion. The morphologies found in *C. neoformans* may also have niche-specific roles during infection, similar to the yeast-hyphal switch in *C. albicans*. The titan cell morphology is likely to be more suited for survival in the lungs and the establishment of the initial pulmonary infection than it is in other tissues or other stages of infection. For example, titan cell production appears to inhibit dissemination from the lungs or reduce penetration of the blood brain barrier. The data presented here shows that titan cell over production can alter host-pathogen interactions that may be altering the outcome of disease (**Figure 5.1B**). During coinfection with both cryptococcal mating types simultaneously, titan cell production is increased in mating type **a** cells. At later stages of infection, fewer mating type **a** cells are recovered from the brain, suggesting that increased titan cell production may be reducing the ability of mating type **a** cells to penetrate the blood-brain barrier.

There are two hypotheses for the mechanism by which *C. neoformans* penetrates the blood brain barrier (**Figure 5.1B**): direct transcytosis and the Trojan horse model. In direct transcytosis, cryptococcal cells must be trafficked to the brain via the blood stream, where they are able to interact with the vascular endothelial cells at the blood brain barrier. The endothelial cells take up the fungal cells and release them into the brain on the other side of the endothelium. The Trojan horse model of cryptococcal penetration of the blood brain barrier suggests that cryptococcal cells are carried into the brain inside of host phagocytes (denoted by the purple circles in **Figure 5.1**).

Titan cell production could affect the efficiency of direct transcytosis at several stages. Cryptococcal meningitis is caused by cells escaping the lungs, disseminating

through the blood stream and reaching the endothelial cells of the blood brain barrier. In infections with titan over-producing strains of *C. neoformans*, dissemination from the lungs is impaired, and CFUs are not recovered from the spleen or brain at late stages of infection with *otc1Δ*. These data suggest that titan cell over production limits the infection to the pulmonary environment (Crabtree and Nielsen, unpublished) and thereby reduces opportunities for interactions between cryptococcal cells and the endothelial cells at the blood brain barrier. However, *otc1Δ* is locked into the titan cell form and by three days post-infection few cells are producing daughter cells, suggesting that *otc1Δ* may be experiencing cell cycle arrest (Okagaki and Nielsen, unpublished). Thus, reduced dissemination could be due to secondary effects (e.g., the absence of yeast daughter cells that are able to disseminate and traverse the BBB). Further investigation with strains that produce only a partial increase in titan cells will be necessary to fully understand whether this is due to the inability of titan cells to disseminate or a possible role of titan cells in preventing the dissemination of other, smaller *C. neoformans* cells.

Previous studies showed that during **a**/α coinfection, which stimulates overproduction of titan cell formation in mating type **a** cells, equivalent numbers of mating type **a** and mating type α cells are recovered from the spleen and lungs, while penetration of the blood brain barrier is reduced in mating type **a** cells, suggesting that escape from the lungs is unaffected by increased titan cell formation. Based on these observations, it is more likely that titan cell production may be inhibiting penetration of the blood brain barrier rather than inhibiting escape from the lungs. Fungal cells must be able to traffic to the brain vascular bed in order to interact with the endothelial cells. Titan cells may be too large to pass through capillary beds of the brain. This hypothesis

can be tested by isolating titan cells and small cells from the lungs of infected mice, intravenously injecting the titan cells or small cells into uninfected mice, and monitoring the ability of the cryptococcal cells to reach the kidneys, liver and brain tissues until the animals succumb to infection. Over-production of titan cells may result in the inability to reach the brain vascular bed, preventing cryptococcal interactions with the vascular endothelial cells.

Even if titan cells are able to leave the lungs and traffic to the brain vascular bed, they simply may be too large to be taken up by the endothelial cells (**Figure 5.1B**). We cannot, however, discount that there may be altered interactions between the titan cells and the vascular endothelial cells, possibly due to capsule alterations. In *C. albicans*, yeast cells are more suited for dissemination, while the larger hyphal form is more suited for adhesion and invasion of tissues. Titan cell production, and subsequent capsule alterations, may also be more suited for the pulmonary environment rather than penetration of the blood brain barrier.

An alternative hypothesis is that titan cell capsule alterations may be preventing titan cells from interacting with the brain microvascular endothelial cells (BMECs). CD44 on the surface of BMECs interacts with hyaluronic acid in the capsule of *C. neoformans*. Disruption of either CD44 in the host or the hyaluronic acid in the capsule reduced penetration of the blood brain barrier both *in vitro* and *in vivo* (Jong, Wu et al. 2008; Jong, Wu et al. 2012). Further experiments looking at the amount and availability of hyaluronic acid in the capsule of titan cells will be necessary to ask if altered capsule is contributing to the lowered penetration of the blood brain barrier by titan cells. In addition, titan cells can be recovered from the lungs of infected mice and added to

monolayers of BMECs *in vitro* and tested for adhesion, or added to BMECs in a transwell assay to monitor crossing of the blood brain barrier.

There are several lines of evidence suggesting that interactions with monocytes and macrophages are necessary for the penetration of the blood brain barrier, providing evidence for the Trojan horse model(Luberto, Martinez-Marino et al. 2003; Del Poeta 2004; Charlier, Nielsen et al. 2009). Pre-incubation of cryptococcal cells with monocytes, followed by tail vein injection showed that cryptococcal cells that had been phagocytosed are more efficient at penetrating the blood brain barrier (Charlier, Nielsen et al. 2009). Therefore, if titan cell production is increased, fewer fungal cells should be available to be phagocytosed, possibly reducing the number of intracellular cryptococcal cells. Lower numbers of intracellular cryptococcal cells may reduce the probability that those cells are able to traffic to the brain and cross the blood brain barrier inside of the phagocyte (**Figure 5.1B**).

Histoplasma is another pulmonary fungal pathogen that survives inside of host macrophages. Yet *Histoplasma* is rarely found in the brain (Bonifaz, Vazquez-Gonzalez et al. 2011), even though intracranial injections of *Histoplasma* into the brains of mice showed that the fungal cells are able to survive and grow in the brain (Haynes, Connolly et al. 2002). If *Histoplasma* like cryptococcal cells interacts with, and survives inside of, the same subset of host cells, the alveolar macrophages, then why can *C. neoformans* penetrate the blood brain barrier while *Histoplasma* cannot?

In addition to the transcytosis and Trojan horse models, are two alternative hypotheses to explain how *C. neoformans* might penetrate the blood brain barrier. The first hypothesis is that *C. neoformans* may induce changes in the monocytes or

macrophages that increase host immune cell crossing of the blood brain barrier. The second hypothesis is that rather than macrophages or monocytes carrying the cryptococcal cells across the vascular endothelium, phagocytosis may alter capsule or gene expression in *C. neoformans* cells that facilitate uptake by endothelial cells. In either hypothesis, phagocytosis is required for efficient penetration of the blood brain barrier. Importantly, titan cell evasion of phagocytosis would prevent interactions with host phagocytes necessary for crossing into the brain and thus could explain why. Taken together, our data suggests that titan cells are not well suited to penetration of the blood brain barrier, but are better suited for the host pulmonary environment and promotion of lung infection.

Titan Cells May Modulate the Host Immune Response

Morphological switching in the human fungal pathogens is often associated with the up-regulation of proteins that assist in immune evasion and in modulation of the host immune response. The dimorphic fungi produce secreted proteins, such as BAD1, CBP, and gp70, which are able to bind to host cells and alter macrophage activation or alter cytokine secretion to reduce the inflammatory response (Klein, Sondel et al. 1992; Newman, Chaturvedi et al. 1995; Klein and Newman 1996; Batanghari, Deepe et al. 1998; Patel, Batanghari et al. 1998; Sebghati, Engle et al. 2000; Finkel-Jimenez, Wuthrich et al. 2001; Rooney, Sullivan et al. 2001; Finkel-Jimenez, Wuthrich et al. 2002; de Mattos Grosso, de Almeida et al. 2003; Beck, Dekoster et al. 2009) . I propose that *C. neoformans* titan cells may modulate the immune response in a similar manner, reducing

the inflammatory response or altering the activation of macrophages to prevent killing activity (**Figure 5.1A**).

An effective response to cryptococcal infection is primarily mediated by Th1 polarized T-cells (Heitman and American Society for Microbiology. 2011). However, both Th2 and Th17 responses have been observed in experimental models (Jain, Zhang et al. 2009; Zhang, Wang et al. 2009). The Th1 response is required to activate macrophages and to induce killing of internalized cryptococcal cells and to control pulmonary infection (Clemons, Brummer et al. 1994; Joly, Saint-Julien et al. 1994; Kawakami, Kohno et al. 1994; Kawakami, Qifeng et al. 1996; Kawakami, Tohyama et al. 1996; Kawakami, Tohyama et al. 1996; Kawakami, Qureshi et al. 1997; Qureshi, Zhang et al. 1999; Clemons, Lutz et al. 2001). I propose that titan cells may modulate the immune system, recruiting fewer phagocytes to the pulmonary environment, resulting in a reduction in phagocytosis.

Recruitment is likely suppressed by alterations in the capsule of titan cells. In a titan only infection, little normal capsule is present and is less likely to be shed into the pulmonary environment. Thus, fewer host cells are being stimulated by the titan cell capsule, resulting in the host immune response recognizing *C. neoformans* as an extracellular pathogen. Recognition of titan cell capsule by alternate receptors may activate alternative subsets of immune cells compared to the capsule of normal-sized cells. Analysis of cell recruitment at 5 days post-infection with wild type or a titan over producing strain revealed that there is an increase in the number of dendritic cells, mast cells, and basophils in the lungs during titan cell infection, and fewer macrophages and monocytes (Crabtree and Nielsen, Unpublished). Thus, titan cells may be altering the

recruitment of host cells to the lungs, from a subset of cells that can protect the host, such as macrophages, to a non-protective subset of cells.

Macrophages can experience frustrated phagocytosis when a particle, such as a large asbestos particle, is too large to be engulfed (Takemura, Stenberg et al. 1986; Cannon and Swanson 1992). Frustrated phagocytosis leads to the production of IL-1β, which induces a strong inflammatory response ((Oghiso and Kubota 1986; Oghiso and Kubota 1987) and reviewed in (Netea, Simon et al. 2010)). I hypothesized that titan cells are inducing frustrated phagocytosis,however, my studies showed that inoculating mice with large inert beads did not confer protection from phagocytosis to small cells even though host cells could not phagocytose the large particles (Chapter 4, **Figure 4.1**). Therefore, these data suggest that other mechanisms beyond frustrated phagocytosis alone may be contributing to the protection of non-titan cells from phagocytosis.

The *C. neoformans* capsule found on normal-sized cells plays a critical role in pathogenesis, including binding of opsonins, masking surface antigens, and inducing apoptosis in host cells responding to cryptococcal infection (Zaragoza, Taborda et al. 2003; Gates and Kozel 2006; Pericolini, Cenci et al. 2006; Zaragoza and Casadevall 2006; Villena, Pinheiro et al. 2008). The capsule produced by titan cells is highly cross-linked and has altered complement and antibody binding compared to the capsule of normal-sized cells (Zaragoza, Garcia-Rodas et al. 2010).

Titan cells may not be recognized by the same mechanism that is used by macrophages to recognize normal-sized cells. Binding to different receptors on macrophage surfaces may alter the activation status of the macrophages. Production of HSP60 alters macrophage interactions with *Histoplasma* by binding to β_2 integrin on the

macrophage surfaces and inducing a non-killing mechanism of phagocytosis (Gomez, Allendoerfer et al. 1995; Long, Gomez et al. 2003; Guimaraes, Frases et al. 2009). Titan cell production and subsequent alterations in the capsule may act in a similar manner, by interacting with other cell surface receptors and suppressing phagocytosis, by preventing the activating macrophages, or by suppressing the killing activity of macrophages, compared with normal-sized cells.

Alternatively, titan cell production may act more systemically, making the immune response non-protective. Preliminary data suggest that titan cells alter the immune system systemically rather than only locally. In lavage samples of mice infected with titan-deficient strains of *C. neoformans*, increased numbers of host cells were recovered when observed by microscopy (Okagaki and Nielsen, unpublished). Titan cell production may suppress the recruitment of host cells to the lungs; therefore, when titan cells are no longer present, normal-sized cells induce the influx of host cells.

Future work to explore cytokine production in cell cultures inoculated with normal-sized cells or titan cells could clarify how titan cells may be modulating the host immune response. Titan cells and normal-sized cells can be isolated from the lungs of infected mice and added to *in vitro* cultures of host cells, such as macrophages or neutrophils. Measurements of secreted cytokines may show alterations in the titan cell-host cell co-cultures.

II. Titan Cell Signaling and Regulation

Multiple Signals are Required for Titan Cell Stimulation

We identified PKA as a major regulator of titan cell production in *C. neoformans*. PKA signaling regulates morphological changes in the dimorphic fungi as well as in *C. albicans*. Titan cell production is regulated by the PKA pathway, and our data suggests that multiple signals are required for the induction of titan cell production. This conclusion is based upon several observations. First, use of a Gpa1 constitutively active strain produced only 40% titan cells, rather than converting all of the cells in the infection to titan cells. Second, a *gpa1Δpkr1Δ* double mutant strain, which has constitutively active PKA signaling, had wild type levels of titan cell production, and not an over-production of titan cells, which would be expected if PKA directly regulates titan cell production (Okagaki and Nielsen, unpublished). PKA signaling may regulate the expression of components of other signaling pathways that induce titan cell production and thus that disruption of PKA signaling may affect multiple signaling pathways. Accordingly, PKA signaling would be necessary for the second pathway to function.

During our studies, we identified two receptors, Ste3**a** and Gpr5 that regulates titan cell production. Our studies, however, were limited in their scope, only testing 7 GPCRs of the 42 predicted GPCRs. In other words, it is quite possible that one of the other putative GPCRs regulates titan cell formation as well. Future experiments measuring at titan cell production in the strains carrying mutation in other GPCRs, or in sensing and signaling pathways that are not dependent on G-protein signaling, has the potential to identify additional regulators of titan cell production.

Titan cell production is stimulated by a signal that is found in the pulmonary environment during early stages of cryptococcal infection. The host factors required for titan cell formation remains elusive. *In vitro* systems for stimulating titan cell formation have yielded some clues, but because titan cells can be induced to a higher degree at 30°C compared with 37°C in spent media from specific cell lines suggests that more than one signal may be necessary to induce morphogenesis. It is possible that *C. neoformans* is sensing either the absence or presence of a nutrient or compound. The signal may be part of the pulmonary system, such as nutrient limitation, surfactant, epithelial cells, or oxygen and CO_2 concentrations. Cytokine production, contact with host immune cells, or immune cell metabolites are other possible sources for the signal that stimulates titan cell production.

Because the PKA pathway is associated with stress sensing, we tested a variety conditions that mimic the stress found in the host pulmonary environment: oxidative and nitrosative stress, temperature, CO_2 levels, iron chelation, and hypoxia to name a few (**Table 5.1**). Gpr4 senses methionine and Gpr5 has a high sequence homology to Gpr4, therefore we tested a variety of amino acids for their ability to induce titan cell production, using both drop in and drop out media. Neither the presence of, nor the absence of, any of the amino acids tested had an effect on titan cell production. More recent studies showed that the presence of phospholipids and hypoxic conditions may induce titan cell production (Chrisman, Albuquerque et al. 2011), however, the results of those studies were not reproducible in our lab. In addition, the *Galleria* model, where larva are injected with *C. neoformans* and incubated at 37°C has been used to stimulate

Table 5.1 Stimulation of titan cells *in vitro*

Condition	Titan Cells (%)	Notes
Coculture		
MHS cells	None	Macrophage like cell line
J774	None	Macrophage like cell line
Raw	None	Macrophage cell line
Activation Status (classical or alternative)	None	Stimulated with LPS orIL13 and IL4
Spent Media		
MHS	~1-4%	DMEM at 30C yielded more titan cells than at 37C
J774	~1%	RPMI
A594	~1%	Mouse lung epithelial cells
HUVEC	~1%	Epithelial Growth Media
Growth Conditions		
20% CO_2	None	
Hypoxia	None	
pH	None	
Temperature	None	25, 30 and 37C
Serum level	None	1, 5, 10, 20%
Serum activation	None	Heat inactivated or untreated
Still cultures	None	
Organ culture	None	Lung and brain cultures
Lung agar	None	Lung homogenized in PBS and 2% agar
Brain agar	None	Brain homogenized in PBS and 2% agar
Iron limitation	None	BPS iron chelation
Nutrient limitation	None	Minimal media, SD media and MM from REF
Amino acids	None	Drop in and drop out
Carbon source- activated charcoal	None	
Carbon source- raffinose	None	
Carbon source- glycerol	None	
Carbon source- maltose	None	
Carbon source-galactose	None	
Carbon source- succinate	None	
Carbon source- no sugar	None	
Chemicals		
H2O2	None	3mM
NaNO3	None	10mM
Fluconazole	None	2, 4, 8, 16, 32, 64, and 128 μg/mL
Phospholipids	None	Reported in (Chrisman, Albuquerque et al. 2011)
Other		
Mouse Background	None	C57BL/6 and AJ, Lung only of BALBc
Galleria mellonella model	None	Reported in (Garcia-Rodas, Casadevall et al. 2011)
Caenorhabditis elegans model	None	
Macrophage density in co-culture	None	Confluent, 1:3, 1:6, 1:12, 1:24

titan cell production (Garcia-Rodas, Casadevall et al. 2011). However, these results also were not reproducible in our lab. Spent media used to grow a murine macrophage-like cells line, MH-S cells, stimulated a low level (about 1-4%) of titan production. Spent media from other cell lines also induced titan cell production, but only about 1% of the cells differentiate into titan cells. Interestingly, co-culture with MH-S cells or other macrophage cell lines does not stimulate titan cell production, likely due to high levels of phagocytosis of the normal-sizes cells used to inoculate the mice before they could develop into titan cells. In addition, co-culture with other cell lines, including pulmonary epithelial cells (A549), did not induce titan cell production. These data suggest that the signal required for titan cell production may be produced by macrophages, however, additional experiments are required to eliminate other possibilities. In summary, signaling studies, *in vivo* models, and *in vitro* conditions all suggest that titan cell production requires more than one signal, and that the signal may be specific to macrophages.

Induction of Titan Cell Production Results in an Altered Cell Cycle.

In many organisms, including flowering plants and fruit flies, increased ploidy results in increased cell size (Inze and De Veylder 2006; Eguren, Manchado et al. 2011). Increased ploidy in *Saccharomyces cerevisiae* can also result in enlarged cell size (Sloat, Adams et al. 1981; Galitski, Saldanha et al. 1999). It has been suggested that increased ploidy is required for the timely production of proteins and phospholipids required to support a large cell size (Sloat, Adams et al. 1981; Galitski, Saldanha et al. 1999). Additional copies of the genome provide additional sites for transcription and increasing mRNA levels for translation. In some organisms, such as some plants, a mechanism

called endoreduplication, in which DNA is replicated but mitosis does not ensue, results in increased ploidy (Inze and De Veylder 2006; Eguren, Manchado et al. 2011). Similarly, titan cells may be produced through endoreduplication, which would increase both cell ploidy and cell size.

Cryptococcal titan cells isolated from the lungs in infected animals are tetraploid or octoploid, suggesting that they may be undergoing DNA replication without cell division (Chapter 2). However, titan cells are found in all stages of the cell cycle in lavage samples, thus they are actively replicating and dividing (Chapter 2). These observations, increased DNA and active mitosis, suggest that titan cells are undergoing a delayed or altered cell cycle. When titan cells are isolated from the lungs and cultured in rich media *in vitro*, the first generation of daughter cells is 2N. After several rounds of replication, the 2N cells eventually yield haploid daughter cells (Okagaki and Nielsen, unpublished). When observed by microscopy, enlarged cells remain visible in the cultures, suggesting that titan cells do not revert to a normal cell size after cell division.

Unlike *Pneumocystis* cysts or *Coccidioides* spherules, titan cells are not multinucleate. Instead they reproduce by budding and produce one daughter cell per division. In addition, recent studies examining increased ploidy during mixed infections with **a** and α cells showed no evidence of cell-cell fusion. Thus, these observations bring up a number of questions about titan cell production. How do titan cells become diploid or even higher ploidies? If the mechanism is endoreduplication, is titan cell endoreduplication similar to that observed in other organisms? What signals *C. neoformans* to switch from active replication to endoreduplication and then back to active mitosis in a nutrient poor environment, such as the lungs?

To understand the cell cycle regulation in titan cells, future work must characterize the normal *C. neoformans* cell cycle. Putative cyclins have been identified (Fu and Nielsen, unpublished), and their expression is being characterized using real-time PCR. Our studies on titan cell signaling and regulation have provided several tools for the examination of the titan cell cycle. First, we identified at mutant, *otc1Δ*, which contains an independently segregating mutation that locks cells into the titan cell morphology when used to inoculate mice. Cyclin expression in a titan-only strain can then be compared with wild-type and non-titan producing strains, to identify possible alterations in the cell cycle. Transcriptional analysis using RNA-seq has identified five transcripts that are not expressed in *otc1Δ* titan cells (Moskalenko and Nielsen, unpublished, **Table 5.2**). All five of the genes identified are of unknown function, and only one, CNAG_00400, has altered expression in *pkaΔ* and *rim101Δ* mutant strains (**Table 5.2**), and is differentially regulated in DMEM compared to growth in YPD (Ballou, Okagaki, Nielsen, and Alspaugh unpublished). BLAST analysis did not reveal any domains with a known function nor did it detect any similar proteins with known function. No CNAG_00400 mutant is available in the current cryptococcal mutant library (Liu, Chun et al. 2008), thus a targeted knock out must be constructed and then tested for titan cell production. We cannot rule out the hypothesis that the *otc1Δ* mutant is a loss of function mutant in a transcription factor, resulting in reduced or absent transcription of the five transcripts that are not expressed in the *otc1Δ* mutant strain. In addition, *otc1Δ* may be a gain of function mutant, resulting in the over production of titan cells. Genome sequencing the entire genome of the *otc1Δ* mutant would permit detection of all deletions

Table 5.2 *otc1Δ* Potential Genes

Locus	Gene Name	*pkaΔ*	*rim101Δ*	DMEM
CNAG_01534	Predicted Protein	N	N	N
CNAG_03650	Conserved Hypothetical Protein	N	N	N
CNAG_02834	UDP-glucose:sterol glucosyltransferase	N	N	N
CNAG_00400	Conserved Hypothetical Protein	-2.8	-2.4	+3
CNAG_00849	Predicted Protein	N	N	N

Fold Changes are compared to growth in YPD at 30°C.

or point mutations that might further identify the *otc1Δ* mutation.

In *C. neoformans*, several signaling pathway components have paralogs with unknown function. I hypothesize that the paralogs for some of the signaling pathways, including Ras signaling, make up a parallel pathway that regulates titan cell formation. Cdc42 has a paralog, Cdc420, with an approximately 84% sequence homology (Ballou, Nichols et al. 2010), but deletion of Cdc420 only results in altered titan cell production and no other virulence phenotype. Screening of a selection of strains from the cryptococcal mutant library revealed that the Rho1 GTPase protein paralog *rho104Δ* is also a titan over-producing strain. *rho104Δ* exhibits a similar phenotype as *otc1Δ*, however, no additional analysis has been performed on this strain. There are also two Ras genes in *C. neoformans*, Ras1 and Ras2. Ras1 regulates hyphal formation during mating and high temperature growth, but the function of Ras2 is poorly understood. However, Ras2 does appear to affect titan cell production when observed by microscopy. Ras2 mutants grown *in vitro* have increased cell size, resulting in cells between 10 and 15 μm in diameter (Okagaki and Nielsen, unpublished). When recovered from infected lungs, Ras2 mutant strains do not contain an enlarged vacuole nor are changes in the cell wall visible under DIC microscopy. Thus, the deletion of Ras2 may result in a titan cell deficiency; however, this must be confirmed by other experimental techniques.

To further explore the hypothesis that the signaling paralogs are responsible for titan cell production, additional experiments are necessary. Once the transcription profiles of titan cells and normal cells are identified, titan specific transcripts can be identified and used as a diagnostic tool for the identification of titan cell production in the absence

of visible cell alterations. GFP reporters can then be used to determine if the Ras2 mutant strain is truly unable to produce titan cells.

III. The Importance of Titan Cells in Global Health

Titan Cell Production is a Virulence Factor

Our data suggests that titan cell production is a virulence factor in *C. neoformans*. Host-pathogen interactions are altered (Chapters 2 and 4) and have effects on later stages of infection, including penetration of the blood brain barrier (Chapter 2, Crabtree and Nielsen, unpublished).

The signaling pathways that regulate titan cell production are conserved in many of the human pathogenic fungi that require a morphological switch in order to maintain virulence. In *Paracoccidioides* and *Sporothrix*, the PKA pathway and cAMP signaling induces morphological transitions (Rodriguez-Del Valle, Debs-Elias et al. 1984; Chen, Janganan et al. 2007). The PKA pathway of *C. albicans* regulates a number of virulence factors including morphogenesis and hyphal specific genes that are critical for tissue damage and invasion (Bockmuhl and Ernst 2001; Leng, Lee et al. 2001; Sohn, Urban et al. 2003). Similarly, titan cell production is regulated by cAMP signaling via the PKA pathway. Interestingly, the PKA pathway is responsible for the production of the other virulence factors in *C. neoformans*, including capsule production, melanin production, and mating. These observations suggest that titan cell production, which is also regulated by the PKA pathway, may also be a virulence factor. Survival studies using titan cell mutants showed that the absence of titan cell production resulted in attenuated virulence

(Crabtree and Nielsen, unpublished). Additional studies will likely further elucidate the role of titan cells in virulence and clarify the mechanism by which titan cells affect the host immune response in the lungs.

Implications of Titan Cell Production on Human Cryptococcosis

Understanding how cryptococcal titan cell production promotes *C. neoformans* survival during the initial immune response in the pulmonary environment and establish infection may provide opportunities for prophylactic treatment options. Increased ploidy in *C. neoformans* and in *C. albicans* contributes to fluconazole drug resistance (Selmecki, Forche et al. 2006; Sionov, Lee et al. 2010). Because titan cells are tetraploid or octoploid, they may be more resistant to treatment with fluconazole. Thus, further examination of titan cells and their sensitivity to various drugs is necessary to determine if titan cell production is contributing to poor response to current antifungal drug treatment strategies.

In *Pneumocystis*, because of differences in the cell wall during cyst formation, some drugs are effective against cysts while others are effective against the trophic form (Cushion, Linke et al. 2010). By analogy, *C. neoformans* titan cells may respond to different drugs than those that have been shown to be effective in *in vitro* antifungal efficacy tests with normal-sized cells. Cell wall changes, altered gene expression, or altered ploidy all may contribute to titan cell responses to different classes of antifungal drugs. Additional experiments must be performed to determine the composition of the titan cell wall and to ask if titan cells are more resistant than normal-sized cells to different classes antifungal drugs.

Even if titan cells are not more resistant to antifungal drug treatment than normal-sized cryptococcal cells, the altered morphology and host-pathogen interactions observed in titan cells may be exploited in other ways to prevent or treat cryptococcosis. Because titan cell production affects penetration of the blood brain barrier, over-stimulation of titan cell production in the lungs has the potential to contain the infection and prevent the development of fatal meningitis.

IV. Final Remarks

Cryptococcus neoformans has become an important pathogen, causing a million cases of disease per year and a fatality rate of about 60%. Taken together, our data suggests that titan cells play a critical role in cryptococcal infection. Titan cells promote the survival of cryptococcal cells in the lungs during early infection, which implies that titan cell production is critical for the establishment of pulmonary infection. This thesis work has demonstrated that titan cells are more resistant to phagocytosis, oxidative stress, and nitrosative stress, implying that titan cells are more fit to survive in the lung environment during the early host immune response. In addition, titan cell production involves increased ploidy, which has the potential to alter antifungal drug response. Finally, titan cell production is co-regulated with the other cryptococcal virulence factors, suggesting that titan cell production is also a virulence factor. These studies provide a sturdy foundation concerning the role of cell morphology in *C. neoformans* infections and pathogenesis.

REFERENCES

Alby, K. and R. J. Bennett (2009). "Stress-induced phenotypic switching in *Candida albicans*." Mol Biol Cell **20**(14): 3178-3191.

Aliouat-Denis, C. M., A. Martinez, et al. (2009). "The *Pneumocystis* life cycle." Mem Inst Oswaldo Cruz **104**(3): 419-426.

Alspaugh, J. A., J. R. Perfect, et al. (1997). "*Cryptococcus neoformans* mating and virulence are regulated by the G-protein α subunit GPA1 and cAMP." Genes Dev **11**(23): 3206-3217.

Alspaugh, J. A., R. Pukkila-Worley, et al. (2002). "Adenylyl cyclase functions downstream of the Gα protein Gpa1 and controls mating and pathogenicity of *Cryptococcus neoformans*." Eukaryot Cell **1**(1): 75-84.

Alvarez, M. and A. Casadevall (2006). "Phagosome extrusion and host-cell survival after *Cryptococcus neoformans* phagocytosis by macrophages." Curr Biol **16**(21): 2161-2165.

Alvarez, M. and A. Casadevall (2007). "Cell-to-cell spread and massive vacuole formation after *Cryptococcus neoformans* infection of murine macrophages." BMC Immunol **8**: 16.

Andalis, A. A., Z. Storchova, et al. (2004). "Defects arising from whole-genome duplications in *Saccharomyces cerevisiae*." Genetics **167**(3): 1109-1121.

Anderson, J. M. and D. R. Soll (1987). "Unique phenotype of opaque cells in the white-opaque transition of *Candida albicans*." J Bacteriol **169**(12): 5579-5588.

Andrianopoulos, A. (2002). "Control of morphogenesis in the human fungal pathogen *Penicillium marneffei*." Int J Med Microbiol **292**(5-6): 331-347.

Antunes, L. C., R. B. Ferreira, et al. (2010). "Quorum sensing in bacterial virulence." Microbiology **156**(Pt 8): 2271-2282.

Arechiga-Carvajal, E. T. and J. Ruiz-Herrera (2005). "The RIM101/pacC homologue from the basidiomycete *Ustilago maydis* is functional in multiple pH-sensitive phenomena." Eukaryot Cell **4**(6): 999-1008.

Baek, Y. U., S. J. Martin, et al. (2006). "Evidence for novel pH-dependent regulation of *Candida albicans* Rim101, a direct transcriptional repressor of the cell wall β-glycosidase Phr2." Eukaryot Cell **5**(9): 1550-1559.

Bahn, Y. S., J. K. Hicks, et al. (2004). "Adenylyl cyclase-associated protein Aca1 regulates virulence and differentiation of *Cryptococcus neoformans* via the cyclic AMP-protein kinase A cascade." Eukaryot Cell **3**(6): 1476-1491.

Ballou, E. R., C. B. Nichols, et al. (2009). "Two CDC42 paralogues modulate *Cryptococcus neoformans* thermotolerance and morphogenesis under host physiological conditions." Mol Microbiol.

Ballou, E. R., C. B. Nichols, et al. (2010). "Two CDC42 paralogues modulate *Cryptococcus neoformans* thermotolerance and morphogenesis under host physiological conditions." Mol Microbiol **75**(3): 763-780.

Barwell, K. J., J. H. Boysen, et al. (2005). "Relationship of DFG16 to the Rim101p pH response pathway in *Saccharomyces cerevisiae* and *Candida albicans*." Eukaryot Cell **4**(5): 890-899.

Batanghari, J. W., G. S. Deepe, Jr., et al. (1998). "*Histoplasma* acquisition of calcium and expression of CBP1 during intracellular parasitism." Mol Microbiol **27**(3): 531-539.

Beck, J. M. and M. T. Cushion (2009). "*Pneumocystis* Workshop: 10th Anniversary Summary." Eukaryot Cell.

Beck, M. R., G. T. Dekoster, et al. (2009). "NMR structure of a fungal virulence factor reveals structural homology with mammalian saposin B." Mol Microbiol **72**(2): 344-353.

Bensen, E. S., S. J. Martin, et al. (2004). "Transcriptional profiling in *Candida albicans* reveals new adaptive responses to extracellular pH and functions for Rim101p." Mol Microbiol **54**(5): 1335-1351.

Blader, I. J. and J. P. Saeij (2009). "Communication between *Toxoplasma gondii* and its host: impact on parasite growth, development, immune evasion, and virulence." APMIS **117**(5-6): 458-476.

Bloom, J. and F. R. Cross (2007). "Multiple levels of cyclin specificity in cell-cycle control." Nat Rev Mol Cell Biol **8**(2): 149-160.

Bockmuhl, D. P. and J. F. Ernst (2001). "A potential phosphorylation site for an A-type kinase in the Efg1 regulator protein contributes to hyphal morphogenesis of *Candida albicans*." Genetics **157**(4): 1523-1530.

Bonifaz, A., D. Vazquez-Gonzalez, et al. (2011). "Endemic systemic mycoses: coccidioidomycosis, histoplasmosis, paracoccidioidomycosis and blastomycosis." J Dtsch Dermatol Ges **9**(9): 705-714; quiz 715.

Botts, M. R., K. K. Ersland, et al. (2011). "*Cryptococcus neoformans* spores from avirulent yeast strains cause disseminated disease in mice." 8th International Conference on *Cryptococcus* and Cryptococcosis.

Botts, M. R., S. S. Giles, et al. (2009). "Isolation and characterization of *Cryptococcus neoformans* spores reveal a critical role for capsule biosynthesis genes in spore biogenesis." Eukaryot Cell **8**(4): 595-605.

Breslau, A. M. and M. Y. Kubota (1964). "Continuous *in vitro* Cultivation of Spherules of *Coccidioides Immitis*." J Bacteriol **87**: 468-472.

Brown, G. D. and S. Gordon (2001). "Immune recognition. A new receptor for β-glucans." Nature **413**(6851): 36-37.

Bulmer, G. S., M. D. Sans, et al. (1967). "*Cryptococcus neoformans*. I. Nonencapsulated mutants." J Bacteriol **94**(5): 1475-1479.

Cannon, G. J. and J. A. Swanson (1992). "The macrophage capacity for phagocytosis." J Cell Sci **101 (Pt 4)**: 907-913.

Casadevall, A. and J. R. Perfect (1998). *Cryptococcus neoformans*. Washington, D.C., ASM Press.

Chandran, K. and M. L. Nibert (2003). "Animal cell invasion by a large nonenveloped virus: reovirus delivers the goods." Trends Microbiol **11**(8): 374-382.

Chang, Y. C., R. Cherniak, et al. (1997). "Structure and biological activities of acapsular *Cryptococcus neoformans* 602 complemented with the *CAP64* gene." Infect Immun **65**(5): 1584-1592.

Chang, Y. C. and K. J. Kwon-Chung (1994). "Complementation of a capsule-deficient mutation of *Cryptococcus neoformans* restores its virulence." Mol Cell Biol **14**(7): 4912-4919.

Chang, Y. C. and K. J. Kwon-Chung (1998). "Isolation of the third capsule-associated gene, *CAP60*, required for virulence in *Cryptococcus neoformans*." Infect Immun **66**(5): 2230-2236.

Chang, Y. C., G. F. Miller, et al. (2003). "Importance of a developmentally regulated pheromone receptor of *Cryptococcus neoformans* for virulence." Infect Immun **71**(9): 4953-4960.

Chang, Y. C., L. A. Penoyer, et al. (1996). "The second capsule gene of *Cryptococcus neoformans*, *CAP64*, is essential for virulence." Infect Immun **64**(6): 1977-1983.

Chang, Y. C., M. F. Stins, et al. (2004). "Cryptococcal yeast cells invade the central nervous system via transcellular penetration of the blood-brain barrier." Infect Immun **72**(9): 4985-4995.

Charlier, C., F. Chretien, et al. (2005). "Capsule structure changes associated with *Cryptococcus neoformans* crossing of the blood-brain barrier." Am J Pathol **166**(2): 421-432.

Charlier, C., K. Nielsen, et al. (2009). "Evidence of a role for monocytes in dissemination and brain invasion by *Cryptococcus neoformans*." Infect Immun **77**(1): 120-127.

Chen, D., T. K. Janganan, et al. (2007). "The cAMP pathway is important for controlling the morphological switch to the pathogenic yeast form of *Paracoccidioides brasiliensis*." Mol Microbiol **65**(3): 761-779.

Chen, S. H., M. F. Stins, et al. (2003). "*Cryptococcus neoformans* induces alterations in the cytoskeleton of human brain microvascular endothelial cells." J Med Microbiol **52**(Pt 11): 961-970.

Cherniak, R. (1988). "Soluble polysaccharides of *Cryptococcus neoformans*." Curr Top Med Mycol **2**: 40-54.

Cherniak, R., L. C. Morris, et al. (1995). "Variation in the structure of glucuronoxylomannan in isolates from patients with recurrent cryptococcal meningitis." Infect Immun **63**(5): 1899-1905.

Cherniak, R., H. Valafar, et al. (1998). "*Cryptococcus neoformans* chemotyping by quantitative analysis of 1H nuclear magnetic resonance spectra of glucuronoxylomannans with a computer-simulated artificial neural network." Clin Diagn Lab Immunol **5**(2): 146-159.

Choi, J., A. W. Vogl, et al. (2012). "Regulated expression of cyclic AMP-dependent protein kinase A reveals an influence on cell size and the secretion of virulence factors in *Cryptococcus neoformans*." Mol Microbiol **Submitted**.

Chretien, F., O. Lortholary, et al. (2002). "Pathogenesis of cerebral *Cryptococcus neoformans* infection after fungemia." J Infect Dis **186**(4): 522-530.

Chrisman, C. J., P. Albuquerque, et al. (2011). "Phospholipids Trigger *Cryptococcus neoformans* Capsular Enlargement during Interactions with Amoebae and Macrophages." PLoS Pathog **7**(5): e1002047.

Chrisman, C. J., P. Albuquerque, et al. (2011). "Phospholipids trigger *Cryptococcus neoformans* capsular enlargement during interactions with amoebae and macrophages." PLoS Pathog **7**(5): e1002047.

Chung, S., M. Karos, et al. (2002). "Molecular analysis of *CPRα*, a MATα-specific pheromone receptor gene of *Cryptococcus neoformans*." Eukaryot Cell **1**(3): 432-439.

Clemons, K. V., E. Brummer, et al. (1994). "Cytokine treatment of central nervous system infection: efficacy of interleukin-12 alone and synergy with conventional antifungal therapy in experimental cryptococcosis." Antimicrob Agents Chemother **38**(3): 460-464.

Clemons, K. V., J. E. Lutz, et al. (2001). "Efficacy of recombinant γ-interferon for treatment of systemic cryptococcosis in SCID mice." Antimicrob Agents Chemother **45**(3): 686-689.

Cloutier, M., R. Castilla, et al. (2003). "The two isoforms of the cAMP-dependent protein kinase catalytic subunit are involved in the control of dimorphism in the human fungal pathogen *Candida albicans*." Fungal Genet Biol **38**(1): 133-141.

Cole, G. T. and T. N. Kirkland (1993). "Identification of antigens of *Coccidioides immitis* which stimulated immune T lymphocytes." Arch Med Res **24**(3): 281-291.

Cole, G. T., T. N. Kirkland, et al. (1988). "Immunoreactivity of a surface wall fraction produced by spherules of *Coccidioides immitis*." Infect Immun **56**(10): 2695-2701.

Cole, G. T., J. Xue, et al. (2006). Virulence Mechanisms of *Coccidioides*. Molecular Prinicples of Fungal Pathogenesis. J. Heitman, S. G. Filler, J. E. Edwards Jr and A. Mitchell. Washington, D.C., ASM Press**:** 363-391.

Comai, L. (2005). "The advantages and disadvantages of being polyploid." Nat Rev Genet **6**(11): 836-846.

Courtney, H. S., D. L. Hasty, et al. (2006). "Anti-phagocytic mechanisms of *Streptococcus pyogenes*: binding of fibrinogen to M-related protein." Mol Microbiol **59**(3): 936-947.

Cramer, K. L., Q. D. Gerrald, et al. (2006). "Transcription factor Nrg1 mediates capsule formation, stress response, and pathogenesis in *Cryptococcus neoformans*." Eukaryot Cell **5**(7): 1147-1156.

Cruickshank, J. G., R. Cavill, et al. (1973). "*Cryptococcus neoformans* of unusual morphology." Appl Microbiol **25**(2): 309-312.

Currie, B. P. and A. Casadevall (1994). "Estimation of the prevalence of cryptococcal infection among patients infected with the human immunodeficiency virus in New York City." Clin Infect Dis **19**(6): 1029-1033.

Cushion, M. T. (2004). "*Pneumocystis*: unraveling the cloak of obscurity." Trends Microbiol **12**(5): 243-249.

Cushion, M. T., M. J. Linke, et al. (2010). "Echinocandin treatment of pneumocystis pneumonia in rodent models depletes cysts leaving trophic burdens that cannot transmit the infection." PLoS One **5**(1): e8524.

D'Souza, C. A., J. A. Alspaugh, et al. (2001). "Cyclic AMP-dependent protein kinase controls virulence of the fungal pathogen *Cryptococcus neoformans*." Mol Cell Biol **21**(9): 3179-3191.

Daniels, K. J., T. Srikantha, et al. (2006). "Opaque cells signal white cells to form biofilms in *Candida albicans*." EMBO J **25**(10): 2240-2252.

Davidson, R. C., J. R. Blankenship, et al. (2002). "A PCR-based strategy to generate integrative targeting alleles with large regions of homology." Microbiology **148**(Pt 8): 2607-2615.

Davidson, R. C., M. C. Cruz, et al. (2000). "Gene disruption by biolistic transformation in serotype D strains of *Cryptococcus neoformans*." Fungal Genet Biol **29**(1): 38-48.

Davidson, R. C., T. D. Moore, et al. (2000). "Characterization of the MFα pheromone of the human fungal pathogen *Cryptococcus neoformans*." Mol Microbiol **38**(5): 1017-1026.

Davidson, R. C., C. B. Nichols, et al. (2003). "A MAP kinase cascade composed of cell type specific and non-specific elements controls mating and differentiation of the fungal pathogen *Cryptococcus neoformans*." Mol Microbiol **49**(2): 469-485.

Davis-Hanna, A., A. E. Piispanen, et al. (2008). "Farnesol and dodecanol effects on the *Candida albicans* Ras1-cAMP signalling pathway and the regulation of morphogenesis." Mol Microbiol **67**(1): 47-62.

Davis, D., J. E. Edwards, Jr., et al. (2000). "*Candida albicans* RIM101 pH response pathway is required for host-pathogen interactions." Infect Immun **68**(10): 5953-5959.

Davis, D., R. B. Wilson, et al. (2000). "RIM101-dependent and-independent pathways govern pH responses in *Candida albicans*." Mol Cell Biol **20**(3): 971-978.

Davis, D. A. (2009). "How human pathogenic fungi sense and adapt to pH: the link to virulence." Curr Opin Microbiol **12**(4): 365-370.

de Mattos Grosso, D., S. R. de Almeida, et al. (2003). "Characterization of gp70 and anti-gp70 monoclonal antibodies in *Paracoccidioides brasiliensis* pathogenesis." Infect Immun **71**(11): 6534-6542.

Del Poeta, M. (2004). "Role of phagocytosis in the virulence of *Cryptococcus neoformans*." Eukaryot Cell **3**(5): 1067-1075.

Dromer, F., P. Aucouturier, et al. (1988). "*Cryptococcus neoformans* antibody levels in patients with AIDS." Scand J Infect Dis **20**(3): 283-285.

Dromer, F., A. Varma, et al. (1994). "Molecular typing of *Cryptococcus neoformans* serotype D clinical isolates." J Clin Microbiol **32**(10): 2364-2371.

Drutz, D. J. and M. Huppert (1983). "Coccidioidomycosis: factors affecting the host-parasite interaction." J Infect Dis **147**(3): 372-390.

Drutz, D. J., M. Huppert, et al. (1981). "Human sex hormones stimulate the growth and maturation of *Coccidioides immitis*." Infect Immun **32**(2): 897-907.

Dubey, J. P. (2004). "Toxoplasmosis - a waterborne zoonosis." Vet Parasitol **126**(1-2): 57-72.

Eguren, M., E. Manchado, et al. (2011). "Non-mitotic functions of the Anaphase-Promoting Complex." Semin Cell Dev Biol **22**(6): 572-578.

Eissenberg, L. G. and W. E. Goldman (1988). "Fusion of lysosomes with phagosomes containing *Histoplasma capsulatum*: use of fluoresceinated dextran." Adv Exp Med Biol **239**: 53-61.

Fan, W., P. R. Kraus, et al. (2005). "*Cryptococcus neoformans* gene expression during murine macrophage infection." Eukaryot Cell **4**(8): 1420-1433.

Feldmesser, M., Y. Kress, et al. (2001). "Dynamic changes in the morphology of *Cryptococcus neoformans* during murine pulmonary infection." Microbiology **147**(Pt 8): 2355-2365.

Feldmesser, M., Y. Kress, et al. (2000). "*Cryptococcus neoformans* is a facultative intracellular pathogen in murine pulmonary infection." Infect Immun **68**(7): 4225-4237.

Feldmesser, M., A. Mednick, et al. (2002). "Antibody-mediated protection in murine *Cryptococcus neoformans* infection is associated with pleotrophic effects on cytokine and leukocyte responses." Infect Immun **70**(3): 1571-1580.

Feldmesser, M., S. Tucker, et al. (2001). "Intracellular parasitism of macrophages by *Cryptococcus neoformans*." Trends Microbiol **9**(6): 273-278.

Finkel-Jimenez, B., M. Wuthrich, et al. (2001). "The WI-1 adhesin blocks phagocyte TNF-α production, imparting pathogenicity on *Blastomyces dermatitidis*." J Immunol **166**(4): 2665-2673.

Finkel-Jimenez, B., M. Wuthrich, et al. (2002). "BAD1, an essential virulence factor of *Blastomyces dermatitidis*, suppresses host TNFα production through TGFβ-dependent and -independent mechanisms." J Immunol **168**(11): 5746-5755.

Fraser, J. A., R. L. Subaran, et al. (2003). "Recapitulation of the sexual cycle of the primary fungal pathogen *Cryptococcus neoformans* var. *gattii*: implications for an outbreak on Vancouver Island, Canada." Eukaryot Cell **2**(5): 1036-1045.

Fromtling, R. A., H. J. Shadomy, et al. (1982). "Decreased virulence in stable, acapsular mutants of *Cryptococcus neoformans*." Mycopathologia **79**(1): 23-29.

Fu, Y., A. S. Ibrahim, et al. (2002). "*Candida albicans* Als1p: an adhesin that is a downstream effector of the EFG1 filamentation pathway." Mol Microbiol **44**(1): 61-72.

Futai, E., T. Maeda, et al. (1999). "The protease activity of a calpain-like cysteine protease in *Saccharomyces cerevisiae* is required for alkaline adaptation and sporulation." Mol Gen Genet **260**(6): 559-568.

Galgiani, J. N. (1986). "Inhibition of different phases of *Coccidioides immitis* by human neutrophils or hydrogen peroxide." J Infect Dis **153**(2): 217-222.

Galitski, T., A. J. Saldanha, et al. (1999). "Ploidy regulation of gene expression." Science **285**(5425): 251-254.

Garcia-Hermoso, D., F. Dromer, et al. (2004). "*Cryptococcus neoformans* capsule structure evolution *in vitro* and during murine infection." Infect Immun **72**(6): 3359-3365.

Garcia-Hermoso, D., G. Janbon, et al. (1999). "Epidemiological evidence for dormant *Cryptococcus neoformans* infection." J Clin Microbiol **37**(10): 3204-3209.

Garcia-Rodas, R., A. Casadevall, et al. (2011). "*Cryptococcus neoformans* capsular enlargement and cellular gigantism during *Galleria mellonella* infection." PLoS One **6**(9): e24485.

Gates, M. A. and T. R. Kozel (2006). "Differential localization of complement component 3 within the capsular matrix of *Cryptococcus neoformans*." Infect Immun **74**(6): 3096-3106.

Geiger, J., D. Wessels, et al. (2004). "Release of a potent polymorphonuclear leukocyte chemoattractant is regulated by white-opaque switching in *Candida albicans*." Infect Immun **72**(2): 667-677.

Ghosh, S., D. H. Navarathna, et al. (2009). "Arginine-induced germ tube formation in *Candida albicans* is essential for escape from murine macrophage line RAW 264.7." Infect Immun **77**(4): 1596-1605.

Giles, S. S., T. R. Dagenais, et al. (2009). "Elucidating the pathogenesis of spores from the human fungal pathogen *Cryptococcus neoformans*." Infect Immun **77**(8): 3491-3500.

Golden, J. W., J. Linke, et al. (2002). "Addition of exogenous protease facilitates reovirus infection in many restrictive cells." J Virol **76**(15): 7430-7443.

Goldman, D., Y. Cho, et al. (1996). "Expression of inducible nitric oxide synthase in rat pulmonary *Cryptococcus neoformans* granulomas." Am J Pathol **148**(4): 1275-1282.

Goldman, D., S. C. Lee, et al. (1994). "Pathogenesis of pulmonary *Cryptococcus neoformans* infection in the rat." Infect Immun **62**(11): 4755-4761.

Goldman, D. L., J. Davis, et al. (2006). "Enhanced allergic inflammation and airway responsiveness in rats with chronic *Cryptococcus neoformans* infection: potential role for fungal pulmonary infection in the pathogenesis of asthma." J Infect Dis **193**(8): 1178-1186.

Goldman, D. L., S. C. Lee, et al. (2000). "Persistent *Cryptococcus neoformans* pulmonary infection in the rat is associated with intracellular parasitism, decreased inducible nitric oxide synthase expression, and altered antibody responsiveness to cryptococcal polysaccharide." Infect Immun **68**(2): 832-838.

Gomez-Raja, J. and D. A. Davis (2012). "The β-arrestin-like protein Rim8 is hyperphosphorylated and complexes with Rim21 and Rim101 to promote adaptation to neutral-alkaline." Eukaryot Cell.

Gomez, F. J., R. Allendoerfer, et al. (1995). "Vaccination with recombinant heat shock protein 60 from *Histoplasma capsulatum* protects mice against pulmonary histoplasmosis." Infect Immun **63**(7): 2587-2595.

Granger, D. L., J. R. Perfect, et al. (1985). "Virulence of *Cryptococcus neoformans*. Regulation of capsule synthesis by carbon dioxide." J Clin Invest **76**(2): 508-516.

Guimaraes, A. J., S. Frases, et al. (2009). "Monoclonal antibodies to heat shock protein 60 alter the pathogenesis of *Histoplasma capsulatum*." Infect Immun **77**(4): 1357-1367.

Han, T. L., R. D. Cannon, et al. (2011). "The metabolic basis of *Candida albicans* morphogenesis and quorum sensing." Fungal Genet Biol **48**(8): 747-763.

Harashima, T., S. Anderson, et al. (2006). "The kelch proteins Gpb1 and Gpb2 inhibit Ras activity via association with the yeast RasGAP neurofibromin homologs Ira1 and Ira2." Mol Cell **22**(6): 819-830.

Harold, F. M. (1990). "To shape a cell: an inquiry into the causes of morphogenesis of microorganisms." Microbiol Rev **54**(4): 381-431.

Hawser, S. P. and L. J. Douglas (1995). "Resistance of *Candida albicans* biofilms to antifungal agents *in vitro*." Antimicrob Agents Chemother **39**(9): 2128-2131.

Haynes, R. R., P. A. Connolly, et al. (2002). "Antifungal therapy for central nervous system histoplasmosis, using a newly developed intracranial model of infection." J Infect Dis **185**(12): 1830-1832.

He, W., A. Casadevall, et al. (2003). "Phagocytic activity and monocyte chemotactic protein expression by pulmonary macrophages in persistent pulmonary cryptococcosis." Infect Immun **71**(2): 930-936.

Heitman, J. and American Society for Microbiology. (2011). *Cryptococcus* : from human pathogen to model yeast. Washington, DC, ASM Press.

Heitman, J. and American Society for Microbiology. (2011). *Cryptococcus* : from human pathogen to model yeast. Washington, DC, ASM Press.

Hicks, J. K., Y. S. Bahn, et al. (2005). "Pde1 phosphodiesterase modulates cyclic AMP levels through a protein kinase A-mediated negative feedback loop in *Cryptococcus neoformans*." Eukaryot Cell **4**(12): 1971-1981.

Hill, J. O. (1992). "CD4+ T cells cause multinucleated giant cells to form around *Cryptococcus neoformans* and confine the yeast within the primary site of infection in the respiratory tract." J Exp Med **175**(6): 1685-1695.

Hogan, L. H. and B. S. Klein (1994). "Altered expression of surface α-1,3-glucan in genetically related strains of *Blastomyces dermatitidis* that differ in virulence." Infect Immun **62**(8): 3543-3546.

Howard, D. H. (1959). "Observations on tissue cultures of mouse peritoneal exudates inoculated with *Histoplasma capsulatum*." J Bacteriol **78**(1): 69-78.

Hoyer, L. L., T. L. Payne, et al. (1998). "*Candida albicans* ALS3 and insights into the nature of the ALS gene family." Curr Genet **33**(6): 451-459.

Hsueh, Y. P., J. A. Fraser, et al. (2008). "Transitions in sexuality: recapitulation of an ancestral tri- and tetrapolar mating system in *Cryptococcus neoformans*." Eukaryot Cell **7**(10): 1847-1855.

Hsueh, Y. P., A. Idnurm, et al. (2006). "Recombination hotspots flank the *Cryptococcus* mating-type locus: implications for the evolution of a fungal sex chromosome." PLoS Genet **2**(11): e184.

Hsueh, Y. P., C. Xue, et al. (2007). "G protein signaling governing cell fate decisions involves opposing Gα subunits in *Cryptococcus neoformans*." Mol Biol Cell **18**(9): 3237-3249.

Hsueh, Y. P., C. Xue, et al. (2009). "A constitutively active GPCR governs morphogenic transitions in *Cryptococcus neoformans*." EMBO J **28**(9): 1220-1233.

Huang, G., T. Srikantha, et al. (2009). "CO_2 regulates white-to-opaque switching in *Candida albicans*." Curr Biol **19**(4): 330-334.

Huang, G., H. Wang, et al. (2006). "Bistable expression of WOR1, a master regulator of white-opaque switching in *Candida albicans*." Proc Natl Acad Sci U S A **103**(34): 12813-12818.

Hull, C. M., M. J. Boily, et al. (2005). "Sex-specific homeodomain proteins Sxi1α and Sxi2**a** coordinately regulate sexual development in *Cryptococcus neoformans*." Eukaryot Cell **4**(3): 526-535.

Hull, C. M., R. C. Davidson, et al. (2002). "Cell identity and sexual development in *Cryptococcus neoformans* are controlled by the mating-type-specific homeodomain protein Sxi1α." Genes Dev **16**(23): 3046-3060.

Hung, C. Y., N. M. Ampel, et al. (2000). "A major cell surface antigen of *Coccidioides immitis* which elicits both humoral and cellular immune responses." Infect Immun **68**(2): 584-593.

Hung, C. Y., J. Xue, et al. (2007). "Virulence mechanisms of *Coccidioides*." Ann N Y Acad Sci **1111**: 225-235.

Hung, C. Y., J. J. Yu, et al. (2002). "A parasitic phase-specific adhesin of *Coccidioides immitis* contributes to the virulence of this respiratory Fungal pathogen." Infect Immun **70**(7): 3443-3456.

Huppert, M., S. H. Sun, et al. (1982). "Morphogenesis throughout saprobic and parasitic cycles of *Coccidioides immitis*." Mycopathologia **78**(2): 107-122.

Idnurm, A., Y. S. Bahn, et al. (2005). "Deciphering the model pathogenic fungus *Cryptococcus neoformans*." Nat Rev Microbiol **3**(10): 753-764.

Inze, D. and L. De Veylder (2006). "Cell cycle regulation in plant development." Annu Rev Genet **40**: 77-105.

Izacc, S. M., F. J. Gomez, et al. (2001). "Molecular cloning, characterization and expression of the heat shock protein 60 gene from the human pathogenic fungus *Paracoccidioides brasiliensis*." Med Mycol **39**(5): 445-455.

Jacobson, E. S. and G. M. Compton (1996). "Discordant regulation of phenoloxidase and capsular polysaccharide in *Cryptococcus neoformans*." J Med Vet Mycol **34**(4): 289-291.

Jain, A. V., Y. Zhang, et al. (2009). "Th2 but not Th1 immune bias results in altered lung functions in a murine model of pulmonary *Cryptococcus neoformans* infection." Infect Immun **77**(12): 5389-5399.

Janeway, C., K. P. Murphy, et al. (2008). Janeway's immunobiology. New York, NY, Garland Science.

Jayatilake, J. A., Y. H. Samaranayake, et al. (2005). "An ultrastructural and a cytochemical study of candidal invasion of reconstituted human oral epithelium." J Oral Pathol Med **34**(4): 240-246.

Johannesson, H., T. Kasuga, et al. (2006). "Phase-specific gene expression underlying morphological adaptations of the dimorphic human pathogenic fungus, *Coccidioides posadasii*." Fungal Genet Biol **43**(8): 545-559.

Joly, V., L. Saint-Julien, et al. (1994). "In vivo activity of interferonγ in combination with amphotericin B in the treatment of experimental cryptococcosis." J Infect Dis **170**(5): 1331-1334.

Jong, A., C. H. Wu, et al. (2012). "Hyaluronic acid receptor CD44 deficiency is associated with decreased *Cryptococcus neoformans* brain infection." J Biol Chem.

Jong, A., C. H. Wu, et al. (2008). "Involvement of human CD44 during *Cryptococcus neoformans* infection of brain microvascular endothelial cells." Cell Microbiol **10**(6): 1313-1326.

Jung, K. W., S. Y. Kim, et al. "Ste50 adaptor protein governs sexual differentiation of *Cryptococcus neoformans* via the pheromone-response MAPK signaling pathway." Fungal Genet Biol **48**(2): 154-165.

Justice, S. S., D. A. Hunstad, et al. (2008). "Morphological plasticity as a bacterial survival strategy." Nat Rev Microbiol **6**(2): 162-168.

Kanetsuna, F. and L. M. Carbonell (1971). "Cell wall composition of the yeastlike and mycelial forms of *Blastomyces dermatitidis*." J Bacteriol **106**(3): 946-948.

Karos, M., Y. C. Chang, et al. (2000). "Mapping of the *Cryptococcus neoformans* MATα locus: presence of mating type-specific mitogen-activated protein kinase cascade homologs." J Bacteriol **182**(21): 6222-6227.

Kawakami, K., S. Kohno, et al. (1994). "Activation of macrophages and expansion of specific T lymphocytes in the lungs of mice intratracheally inoculated with *Cryptococcus neoformans*." Clin Exp Immunol **96**(2): 230-237.

Kawakami, K., X. Qifeng, et al. (1996). "Contribution of tumour necrosis factor-α (TNF-α) in host defence mechanism against *Cryptococcus neoformans*." Clin Exp Immunol **106**(3): 468-474.

Kawakami, K., M. H. Qureshi, et al. (1997). "IL-18 protects mice against pulmonary and disseminated infection with Cryptococcus neoformans by inducing IFNγ production." J Immunol **159**(11): 5528-5534.

Kawakami, K., M. Tohyama, et al. (1996). "Contribution of interferonγ in protecting mice during pulmonary and disseminated infection with *Cryptococcus neoformans*." FEMS Immunol Med Microbiol **13**(2): 123-130.

Kawakami, K., M. Tohyama, et al. (1996). "IL-12 protects mice against pulmonary and disseminated infection caused by *Cryptococcus neoformans*." Clin Exp Immunol **104**(2): 208-214.

Kawakami, K., T. Zhang, et al. (1997). "*Cryptococcus neoformans* inhibits nitric oxide production by murine peritoneal macrophages stimulated with interferon-γ and lipopolysaccharide." Cell Immunol **180**(1): 47-54.

Kent, C. R., P. Ortiz-Bermudez, et al. (2008). "Formulation of a defined V8 medium for induction of sexual development of *Cryptococcus neoformans*." Appl Environ Microbiol **74**(20): 6248-6253.

Kim, S., M. J. Wolyniak, et al. (2007). "A 368-base-pair cis-acting HWP1 promoter region, HCR, of *Candida albicans* confers hypha-specific gene regulation and binds architectural transcription factors Nhp6 and Gcf1p." Eukaryot Cell **6**(4): 693-709.

Klein, B. S. and S. L. Newman (1996). "Role of cell-surface molecules of *Blastomyces dermatitidis* in host-pathogen interactions." Trends Microbiol **4**(6): 246-251.

Klein, B. S., P. M. Sondel, et al. (1992). "WI-1, a novel 120-kilodalton surface protein on *Blastomyces dermatitidis* yeast cells, is a target antigen of cell-mediated immunity in human blastomycosis." Infect Immun **60**(10): 4291-4300.

Klein, B. S. and B. Tebbets (2007). "Dimorphism and virulence in fungi." Curr Opin Microbiol **10**(4): 314-319.

Klengel, T., W. J. Liang, et al. (2005). "Fungal adenylyl cyclase integrates CO_2 sensing with cAMP signaling and virulence." Curr Biol **15**(22): 2021-2026.

Klotz, S. A., D. J. Drutz, et al. (1984). "The critical role of CO_2 in the morphogenesis of *Coccidioides immitis* in cell-free subcutaneous chambers." J Infect Dis **150**(1): 127-134.

Kolotila, M. P. and R. D. Diamond (1990). "Effects of neutrophils and *in vitro* oxidants on survival and phenotypic switching of *Candida albicans* WO-1." Infect Immun **58**(5): 1174-1179.

Kondorosi, E., F. Roudier, et al. (2000). "Plant cell-size control: growing by ploidy?" Curr Opin Plant Biol **3**(6): 488-492.

Kozel, T. R. and J. Cazin (1971). "Nonencapsulated Variant of *Cryptococcus neoformans* I. Virulence Studies and Characterization of Soluble Polysaccharide." Infect Immun **3**(2): 287-294.

Kozel, T. R. and E. C. Gotschlich (1982). "The capsule of *Cryptococcus neoformans* passively inhibits phagocytosis of the yeast by macrophages." J Immunol **129**(4): 1675-1680.

Kozel, T. R., M. A. Wilson, et al. (1991). "Early events in initiation of alternative complement pathway activation by the capsule of *Cryptococcus neoformans*." Infect Immun **59**(9): 3101-3110.

Kraus, P. R., M. J. Boily, et al. (2004). "Identification of *Cryptococcus neoformans* temperature-regulated genes with a genomic-DNA microarray." Eukaryot Cell **3**(5): 1249-1260.

Krombach, F., S. Munzing, et al. (1997). "Cell size of alveolar macrophages: an interspecies comparison." Environ Health Perspect **105 Suppl 5**: 1261-1263.

Kvaal, C., S. A. Lachke, et al. (1999). "Misexpression of the opaque-phase-specific gene PEP1 (SAP1) in the white phase of *Candida albicans* confers increased virulence in a mouse model of cutaneous infection." Infect Immun **67**(12): 6652-6662.

Kvaal, C. A., T. Srikantha, et al. (1997). "Misexpression of the white-phase-specific gene WH11 in the opaque phase of *Candida albicans* affects switching and virulence." Infect Immun **65**(11): 4468-4475.

Kwon-Chung, K. J. (1976). "Morphogenesis of *Filobasidiella neoformans*, the sexual state of *Cryptococcus neoformans*." Mycologia **68**(4): 821-833.

Kwon-Chung, K. J., J. C. Edman, et al. (1992). "Genetic association of mating types and virulence in *Cryptococcus neoformans*." Infect Immun **60**(2): 602-605.

Langmead, B., C. Trapnell, et al. (2009). "Ultrafast and memory-efficient alignment of short DNA sequences to the human genome." Genome Biol **10**(3): R25.

Laxalt, K. A. and T. R. Kozel (1979). "Chemotaxigenesis and activation of the alternative complement pathway by encapsulated and non-encapsulated *Cryptococcus neoformans*." Infect Immun **26**(2): 435-440.

Leng, P., P. R. Lee, et al. (2001). "Efg1, a morphogenetic regulator in *Candida albicans*, is a sequence-specific DNA binding protein." J Bacteriol **183**(13): 4090-4093.

Levitz, S. M. (1991). "Activation of human peripheral blood mononuclear cells by interleukin-2 and granulocyte-macrophage colony-stimulating factor to inhibit *Cryptococcus neoformans*." Infect Immun **59**(10): 3393-3397.

Levitz, S. M., S. H. Nong, et al. (1999). "*Cryptococcus neoformans* resides in an acidic phagolysosome of human macrophages." Infect Immun **67**(2): 885-890.

Li, L., M. Schmelz, et al. (2007). "Nuclear labeling of *Coccidioides posadasii* with green fluorescent protein." Ann N Y Acad Sci **1111**: 198-207.

Li, L., G. Shen, et al. (2007). "Canonical heterotrimeric G proteins regulating mating and virulence of *Cryptococcus neoformans*." Mol Biol Cell **18**(11): 4201-4209.

Li, M., S. J. Martin, et al. (2004). "*Candida albicans* Rim13p, a protease required for Rim101p processing at acidic and alkaline pHs." Eukaryot Cell **3**(3): 741-751.

Lian, T., M. I. Simmer, et al. (2005). "Iron-regulated transcription and capsule formation in the fungal pathogen *Cryptococcus neoformans*." Mol Microbiol **55**(5): 1452-1472.

Lin, A., J. A. Loughman, et al. (2009). "Streptolysin S inhibits neutrophil recruitment during the early stages of *Streptococcus pyogenes* infection." Infect Immun **77**(11): 5190-5201.

Lin, X., J. C. Jackson, et al. (2010). "Transcription factors Mat2 and Znf2 operate cellular circuits orchestrating opposite- and same-sex mating in *Cryptococcus neoformans*." PLoS Genet **6**(5): e1000953.

Liu, O. W., C. D. Chun, et al. (2008). "Systematic genetic analysis of virulence in the human fungal pathogen *Cryptococcus neoformans*." Cell **135**(1): 174-188.

Liu, Z. H., M. Li, et al. (2010). "Higher concentration of CO_2 and 37 degrees C stabilize the less virulent opaque cell of *Candida albicans*." Chin Med J (Engl) **123**(17): 2446-2450.

Lohse, M. B. and A. D. Johnson (2008). "Differential phagocytosis of white versus opaque *Candida albicans* by Drosophila and mouse phagocytes." PLoS One **3**(1): e1473.

Long, K. H., F. J. Gomez, et al. (2003). "Identification of heat shock protein 60 as the ligand on *Histoplasma capsulatum* that mediates binding to CD18 receptors on human macrophages." J Immunol **170**(1): 487-494.

Lorenz, M. C., J. A. Bender, et al. (2004). "Transcriptional response of *Candida albicans* upon internalization by macrophages." Eukaryot Cell **3**(5): 1076-1087.

Love, G. L., G. D. Boyd, et al. (1985). "Large *Cryptococcus neoformans* isolated from brain abscess." J Clin Microbiol **22**(6): 1068-1070.

Lubarsky, R. and O. A. Plunkett (1955). "*In vitro* production of the spherule phase of *Coccidioides immitis*." J Bacteriol **70**(2): 182-186.

Luberto, C., B. Martinez-Marino, et al. (2003). "Identification of App1 as a regulator of phagocytosis and virulence of *Cryptococcus neoformans*." J Clin Invest **112**(7): 1080-1094.

Ma, H., J. E. Croudace, et al. (2006). "Expulsion of live pathogenic yeast by macrophages." Curr Biol **16**(21): 2156-2160.

Macher, A. M., J. E. Bennett, et al. (1978). "Complement depletion in cryptococcal sepsis." J Immunol **120**(5): 1686-1690.

Maidan, M. M., L. De Rop, et al. (2005). "The G protein-coupled receptor Gpr1 and the Gα protein Gpa2 act through the cAMP-protein kinase A pathway to induce morphogenesis in *Candida albicans*." Mol Biol Cell **16**(4): 1971-1986.

Major, A. S., S. Joyce, et al. (2006). "Lipid metabolism, atherogenesis and CD1-restricted antigen presentation." Trends Mol Med **12**(6): 270-278.

Maresca, B., L. Carratu, et al. (1994). "Morphological transition in the human fungal pathogen *Histoplasma capsulatum*." Trends Microbiol **2**(4): 110-114.

Maresca, B. and G. S. Kobayashi (1989). "Dimorphism in *Histoplasma capsulatum*: a model for the study of cell differentiation in pathogenic fungi." Microbiol Rev **53**(2): 186-209.

Matsumoto, Y. and Y. Yoshida (1984). "Sporogony in *Pneumocystis carinii*: synaptonemal complexes and meiotic nuclear divisions observed in precysts." J Protozool **31**(3): 420-428.

Mavor, A. L., S. Thewes, et al. (2005). "Systemic fungal infections caused by Candida species: epidemiology, infection process and virulence attributes." Curr Drug Targets **6**(8): 863-874.

McClelland, C. M., Y. C. Chang, et al. (2004). "Uniqueness of the mating system in *Cryptococcus neoformans*." Trends Microbiol **12**(5): 208-212.

McCormack, F. X., R. Gibbons, et al. (2003). "Macrophage-independent fungicidal action of the pulmonary collectins." J Biol Chem **278**(38): 36250-36256.

McFadden, D. C., B. C. Fries, et al. (2007). "Capsule structural heterogeneity and antigenic variation in *Cryptococcus neoformans*." Eukaryot Cell **6**(8): 1464-1473.

Medoff, J., E. Jacobson, et al. (1981). "Regulation of dimorphism in *Histoplasma capsulatum* by cyclic adenosine 3',5'-monophosphate." J Bacteriol **145**(3): 1452-1455.

Miller, M. G. and A. D. Johnson (2002). "White-opaque switching in *Candida albicans* is controlled by mating-type locus homeodomain proteins and allows efficient mating." Cell **110**(3): 293-302.

Mitchell, T. G. and J. R. Perfect (1995). "Cryptococcosis in the era of AIDS--100 years after the discovery of *Cryptococcus neoformans*." Clin Microbiol Rev **8**(4): 515-548.

Moffat, J. and B. Andrews (2004). "Late-G1 cyclin-CDK activity is essential for control of cell morphogenesis in budding yeast." Nat Cell Biol **6**(1): 59-66.

Morrow, B., J. Anderson, et al. (1989). "Bidirectional stimulation of the white-opaque transition of *Candida albicans* by ultraviolet irradiation." J Gen Microbiol **135**(5): 1201-1208.

Morrow, C. A. and J. A. Fraser (2009). "Sexual reproduction and dimorphism in the pathogenic basidiomycetes." FEMS Yeast Res **9**(2): 161-177.

Murphy, K. P., P. Travers, et al. (2008). Janeway's immunobiology. New York, Garland Science.

Nazarko, V. Y., J. M. Thevelein, et al. (2008). "G-protein-coupled receptor Gpr1 and G-protein Gpa2 of cAMP-dependent signaling pathway are involved in glucose-induced pexophagy in the yeast *Saccharomyces cerevisiae*." Cell Biol Int **32**(5): 502-504.

Nemecek, J. C., M. Wuthrich, et al. (2006). "Global control of dimorphism and virulence in fungi." Science **312**(5773): 583-588.

Netea, M. G., A. Simon, et al. (2010). "IL-1β processing in host defense: beyond the inflammasomes." PLoS Pathog **6**(2): e1000661.

Nett, J. E., K. M. Guite, et al. (2008). "Reduced biocide susceptibility in *Candida albicans* biofilms." Antimicrob Agents Chemother **52**(9): 3411-3413.

Newman, S. L., S. Chaturvedi, et al. (1995). "The WI-1 antigen of *Blastomyces dermatitidis* yeasts mediates binding to human macrophage CD11b/CD18 (CR3) and CD14." J Immunol **154**(2): 753-761.

Newman, S. L., L. Gootee, et al. (1997). "Activation of human macrophage fungistatic activity against *Histoplasma capsulatum* upon adherence to type 1 collagen matrices." J Immunol **158**(4): 1779-1786.

Nguyen, V. Q. and A. Sil (2008). "Temperature-induced switch to the pathogenic yeast form of *Histoplasma capsulatum* requires Ryp1, a conserved transcriptional regulator." Proc Natl Acad Sci U S A **105**(12): 4880-4885.

Nibert, M. L., D. B. Furlong, et al. (1991). "Mechanisms of viral pathogenesis. Distinct forms of reoviruses and their roles during replication in cells and host." J Clin Invest **88**(3): 727-734.

Nichols, C. B., Z. H. Perfect, et al. (2007). "A Ras1-Cdc24 signal transduction pathway mediates thermotolerance in the fungal pathogen *Cryptococcus neoformans*." Mol Microbiol **63**(4): 1118-1130.

Nielsen, K., G. M. Cox, et al. (2005). "*Cryptococcus neoformans* α strains preferentially disseminate to the central nervous system during coinfection." Infect Immun **73**(8): 4922-4933.

Nielsen, K., G. M. Cox, et al. (2003). "Sexual cycle of *Cryptococcus neoformans* var. *grubii* and virulence of congenic **a** and α isolates." Infect Immun **71**(9): 4831-4841.

Nielsen, K., G. M. Cox, et al. (2003). "Sexual cycle of *Cryptococcus neoformans* var. *grubii* and virulence of congenic **a** and α isolates." Infect Immun **71**(9): 4831-4841.

Nielsen, K., A. L. De Obaldia, et al. (2007). "*Cryptococcus neoformans* mates on pigeon guano: implications for the realized ecological niche and globalization." Eukaryot Cell **6**(6): 949-959.

Nielsen, K. and J. Heitman (2007). "Sex and virulence of human pathogenic fungi." Adv Genet **57**: 143-173.

Nobile, C. J., J. E. Nett, et al. (2006). "Function of *Candida albicans* adhesin Hwp1 in biofilm formation." Eukaryot Cell **5**(10): 1604-1610.

Noel, G. J., S. K. Hoiseth, et al. (1992). "Type b capsule inhibits ingestion of *Haemophilus influenzae* by murine macrophages: studies with isogenic encapsulated and unencapsulated strains." J Infect Dis **166**(1): 178-182.

O'Meara, T. R., D. Norton, et al. (2010). "Interaction of *Cryptococcus neoformans* Rim101 and protein kinase A regulates capsule." PLoS Pathog **6**(2): e1000776.

Odds, F. C. (1985). "Morphogenesis in *Candida albicans*." Crit Rev Microbiol **12**(1): 45-93.

Oghiso, Y. and Y. Kubota (1986). "Enhanced interleukin 1 production by alveolar macrophages and increase in Ia-positive lung cells in silica-exposed rats." Microbiol Immunol **30**(11): 1189-1198.

Oghiso, Y. and Y. Kubota (1987). "Interleukin 1 production and accessory cell function of rat alveolar macrophages exposed to mineral dust particles." Microbiol Immunol **31**(3): 275-287.

Okagaki, L. H., A. K. Strain, et al. (2010). "Cryptococcal cell morphology affects host cell interactions and pathogenicity." PLoS Pathog **6**(6): e1000953.

Okagaki, L. H., Y. Wang, et al. (2011). "Cryptococcal titan cell formation is regulated by G-protein signaling in response to multiple stimuli." Eukaryot Cell **10**(10): 1306-1316.

Oliveira, D. L., C. G. Freire-de-Lima, et al. (2010). "Extracellular vesicles from *Cryptococcus neoformans* modulate macrophage functions." Infect Immun **78**(4): 1601-1609.

Olszewski, M. A., M. C. Noverr, et al. (2004). "Urease expression by *Cryptococcus neoformans* promotes microvascular sequestration, thereby enhancing central nervous system invasion." Am J Pathol **164**(5): 1761-1771.

Osman, A. (2004). "Yeast two-hybrid assay for studying protein-protein interactions." Methods Mol Biol **270**: 403-422.

Otto, S. P. (2007). "The evolutionary consequences of polyploidy." Cell **131**(3): 452-462.

Park, B. J., K. A. Wannemuehler, et al. (2009). "Estimation of the current global burden of cryptococcal meningitis among persons living with HIV/AIDS." AIDS **23**(4): 525-530.

Parnanen, P., J. H. Meurman, et al. (2010). "Human oral keratinocyte E-cadherin degradation by *Candida albicans* and *Candida glabrata*." J Oral Pathol Med **39**(3): 275-278.

Patel, J. B., J. W. Batanghari, et al. (1998). "Probing the yeast phase-specific expression of the CBP1 gene in *Histoplasma capsulatum*." J Bacteriol **180**(7): 1786-1792.

Perfect, J. R. and A. Casadevall (2002). "Cryptococcosis." Infect Dis Clin North Am **16**(4): 837-874, v-vi.

Pericolini, E., E. Cenci, et al. (2006). "*Cryptococcus neoformans* capsular polysaccharide component galactoxylomannan induces apoptosis of human T-cells through activation of caspase-8." Cell Microbiol **8**(2): 267-275.

Phan, Q. T., C. L. Myers, et al. (2007). "Als3 is a *Candida albicans* invasin that binds to cadherins and induces endocytosis by host cells." PLoS Biol **5**(3): e64.

Pollack, M. and S. E. Anderson, Jr. (1978). "Toxicity of *Pseudomonas aeruginosa* exotoxin A for human macrophages." Infect Immun **19**(3): 1092-1096.

Pukkila-Worley, R., Q. D. Gerrald, et al. (2005). "Transcriptional network of multiple capsule and melanin genes governed by the *Cryptococcus neoformans* cyclic AMP cascade." Eukaryot Cell **4**(1): 190-201.

Qureshi, M. H., T. Zhang, et al. (1999). "Combined effects of IL-12 and IL-18 on the clinical course and local cytokine production in murine pulmonary infection with *Cryptococcus neoformans*." Eur J Immunol **29**(2): 643-649.

Ramirez-Zavala, B., O. Reuss, et al. (2008). "Environmental induction of white-opaque switching in *Candida albicans*." PLoS Pathog **4**(6): e1000089.

Rinaldi, J., J. Wu, et al. (2010). "Structure of yeast regulatory subunit: a glimpse into the evolution of PKA signaling." Structure **18**(11): 1471-1482.

Rincon, S., P. M. Coll, et al. (2007). "Spatial regulation of Cdc42 during cytokinesis." Cell Cycle **6**(14): 1687-1691.

Rodrigues, M. L., E. S. Nakayasu, et al. (2008). "Extracellular vesicles produced by *Cryptococcus neoformans* contain protein components associated with virulence." Eukaryot Cell **7**(1): 58-67.

Rodriguez-Del Valle, N., N. Debs-Elias, et al. (1984). "Effects of caffeine, cyclic 3', 5' adenosine monophosphate and cyclic 3', 5' guanosine monophosphate in the development of the mycelial form of *Sporothrix schenckii*." Mycopathologia **86**(1): 29-33.

Rooney, P. J., T. D. Sullivan, et al. (2001). "Selective expression of the virulence factor BAD1 upon morphogenesis to the pathogenic yeast form of *Blastomyces dermatitidis*: evidence for transcriptional regulation by a conserved mechanism." Mol Microbiol **39**(4): 875-889.

Saijo, S., N. Fujikado, et al. (2007). "Dectin-1 is required for host defense against *Pneumocystis carinii* but not against *Candida albicans*." Nat Immunol **8**(1): 39-46.

San-Blas, G., L. R. Travassos, et al. (2000). "Fungal morphogenesis and virulence." Med Mycol **38 Suppl 1**: 79-86.

Santangelo, R., H. Zoellner, et al. (2004). "Role of extracellular phospholipases and mononuclear phagocytes in dissemination of cryptococcosis in a murine model." Infect Immun **72**(4): 2229-2239.

Schaffner, A., C. E. Davis, et al. (1986). "*In vitro* susceptibility of fungi to killing by neutrophil granulocytes discriminates between primary pathogenicity and opportunism." J Clin Invest **78**(2): 511-524.

Sebghati, T. S., J. T. Engle, et al. (2000). "Intracellular parasitism by Histoplasma capsulatum: fungal virulence and calcium dependence." Science **290**(5495): 1368-1372.

Selmecki, A., A. Forche, et al. (2006). "Aneuploidy and isochromosome formation in drug-resistant *Candida albicans*." Science **313**(5785): 367-370.

Shao, X., A. Mednick, et al. (2005). "An innate immune system cell is a major determinant of species-related susceptibility differences to fungal pneumonia." J Immunol **175**(5): 3244-3251.

Shao, X., J. Rivera, et al. (2005). "A dual role for TGFβ1 in the control and persistence of fungal pneumonia." J Immunol **175**(10): 6757-6763.

Shapiro, R. S., P. Uppuluri, et al. (2009). "Hsp90 Orchestrates Temperature-Dependent *Candida albicans* Morphogenesis via Ras1-PKA Signaling." Curr Biol.

Shea, J. M., T. B. Kechichian, et al. (2006). "The cryptococcal enzyme inositol phosphosphingolipid-phospholipase C confers resistance to the antifungal effects of macrophages and promotes fungal dissemination to the central nervous system." Infect Immun **74**(10): 5977-5988.

Shen, G., Y. L. Wang, et al. (2008). "The RGS protein Crg2 regulates pheromone and cyclic AMP signaling in *Cryptococcus neoformans*." Eukaryot Cell **7**(9): 1540-1548.

Shen, W. C., R. C. Davidson, et al. (2002). "Pheromones stimulate mating and differentiation via paracrine and autocrine signaling in *Cryptococcus neoformans*." Eukaryot Cell **1**(3): 366-377.

Sia, R. A., K. B. Lengeler, et al. (2000). "Diploid strains of the pathogenic basidiomycete *Cryptococcus neoformans* are thermally dimorphic." Fungal Genet Biol **29**(3): 153-163.

Sionov, E., H. Lee, et al. (2010). "*Cryptococcus neoformans* overcomes stress of azole drugs by formation of disomy in specific multiple chromosomes." PLoS Pathog **6**(4): e1000848.

Sloat, B. F., A. Adams, et al. (1981). "Roles of the CDC24 gene product in cellular morphogenesis during the *Saccharomyces cerevisiae* cell cycle." J Cell Biol **89**(3): 395-405.

Slutsky, B., J. Buffo, et al. (1985). "High-frequency switching of colony morphology in *Candida albicans*." Science **230**(4726): 666-669.

Slutsky, B., M. Staebell, et al. (1987). ""White-opaque transition": a second high-frequency switching system in *Candida albicans*." J Bacteriol **169**(1): 189-197.

Smulian, A. G., T. Sesterhenn, et al. (2001). "The *STE3* pheromone receptor gene of *Pneumocystis carinii* is surrounded by a cluster of signal transduction genes." Genetics **157**(3): 991-1002.

Sohn, K., I. Senyurek, et al. (2006). "An *in vitro* assay to study the transcriptional response during adherence of *Candida albicans* to different human epithelia." FEMS Yeast Res **6**(7): 1085-1093.

Sohn, K., C. Urban, et al. (2003). "EFG1 is a major regulator of cell wall dynamics in *Candida albicans* as revealed by DNA microarrays." Mol Microbiol **47**(1): 89-102.

Soll, D. R., C. J. Langtimm, et al. (1987). "High-frequency switching in Candida strains isolated from vaginitis patients." J Clin Microbiol **25**(9): 1611-1622.

Staab, J. F., S. D. Bradway, et al. (1999). "Adhesive and mammalian transglutaminase substrate properties of *Candida albicans* Hwp1." Science **283**(5407): 1535-1538.

Staab, J. F. and P. Sundstrom (1998). "Genetic organization and sequence analysis of the hypha-specific cell wall protein gene HWP1 of *Candida albicans*." Yeast **14**(7): 681-686.

Steenbergen, J. N. and A. Casadevall (2003). "The origin and maintenance of virulence for the human pathogenic fungus *Cryptococcus neoformans*." Microbes Infect **5**(7): 667-675.

Stevens, D. L., J. Mitten, et al. (1987). "Effects of α and θ toxins from *Clostridium perfringens* on human polymorphonuclear leukocytes." J Infect Dis **156**(2): 324-333.

Storchova, Z., A. Breneman, et al. (2006). "Genome-wide genetic analysis of polyploidy in yeast." Nature **443**(7111): 541-547.

Strasser, J. E., S. L. Newman, et al. (1999). "Regulation of the macrophage vacuolar ATPase and phagosome-lysosome fusion by *Histoplasma capsulatum*." J Immunol **162**(10): 6148-6154.

Sugar, A. M. and M. Picard (1991). "Macrophage- and oxidant-mediated inhibition of the ability of live *Blastomyces dermatitidis* conidia to transform to the pathogenic yeast phase: implications for the pathogenesis of dimorphic fungal infections." J Infect Dis **163**(2): 371-375.

Takemura, R., P. E. Stenberg, et al. (1986). "Rapid redistribution of clathrin onto macrophage plasma membranes in response to Fc receptor-ligand interaction during frustrated phagocytosis." J Cell Biol **102**(1): 55-69.

Tamaki, H. (2007). "Glucose-stimulated cAMP-protein kinase A pathway in yeast *Saccharomyces cerevisiae*." J Biosci Bioeng **104**(4): 245-250.

Tamaki, H., C. W. Yun, et al. (2005). "Glucose-dependent cell size is regulated by a G protein-coupled receptor system in yeast *Saccharomyces cerevisiae*." Genes Cells **10**(3): 193-206.

Taylor, M. L., M. E. Espinosa-Schoelly, et al. (1989). "Evaluation of phagolysosome fusion in acridine orange stained macrophages infected with *Histoplasma capsulatum*." Clin Exp Immunol **75**(3): 466-470.

Thern, A., M. Wastfelt, et al. (1998). "Expression of two different antiphagocytic M proteins by *Streptococcus pyogenes* of the OF+ lineage." J Immunol **160**(2): 860-869.

Thomas, C. F., Jr. and A. H. Limper (2004). "Pneumocystis pneumonia." N Engl J Med **350**(24): 2487-2498.

Thomas, C. F., J. G. Park, et al. (2001). "Analysis of a pheromone receptor and MAP kinase suggest a sexual replicative cycle in *Pneumocystis carinii*." J Eukaryot Microbiol **Suppl**: 141S.

Thomas, P. W., E. E. Wyckoff, et al. (1997). "The hsp60 gene of the human pathogenic fungus *Coccidioides immitis* encodes a T-cell reactive protein." Gene **199**(1-2): 83-91.

Trapnell, C., L. Pachter, et al. (2009). "TopHat: discovering splice junctions with RNA-Seq." Bioinformatics **25**(9): 1105-1111.

Trapnell, C., B. A. Williams, et al. (2010). "Transcript assembly and quantification by RNA-Seq reveals unannotated transcripts and isoform switching during cell differentiation." Nat Biotechnol **28**(5): 511-515.

Tsuchimori, N., L. L. Sharkey, et al. (2000). "Reduced virulence of HWP1-deficient mutants of *Candida albicans* and their interactions with host cells." Infect Immun **68**(4): 1997-2002.

Tucker, S. C. and A. Casadevall (2002). "Replication of *Cryptococcus neoformans* in macrophages is accompanied by phagosomal permeabilization and accumulation of vesicles containing polysaccharide in the cytoplasm." Proc Natl Acad Sci U S A **99**(5): 3165-3170.

Turner, S. H., R. Cherniak, et al. (1992). "Structural variability in the glucuronoxylomannan of *Cryptococcus neoformans* serotype A isolates determined by 13C NMR spectroscopy." Carbohydr Res **233**: 205-218.

Villena, S. N., R. O. Pinheiro, et al. (2008). "Capsular polysaccharides galactoxylomannan and glucuronoxylomannan from *Cryptococcus neoformans* induce macrophage apoptosis mediated by Fas ligand." Cell Microbiol **10**(6): 1274-1285.

Vuk-Pavlovic, Z., E. K. Mo, et al. (2006). "Surfactant protein D enhances *Pneumocystis* infection in immune-suppressed mice." Am J Physiol Lung Cell Mol Physiol **290**(3): L442-449.

Waugh, M. S., C. B. Nichols, et al. (2002). "Ras1 and Ras2 contribute shared and unique roles in physiology and virulence of *Cryptococcus neoformans*." Microbiology **148**(Pt 1): 191-201.

Webster, R. H. and A. Sil (2008). "Conserved factors Ryp2 and Ryp3 control cell morphology and infectious spore formation in the fungal pathogen *Histoplasma capsulatum*." Proc Natl Acad Sci U S A **105**(38): 14573-14578.

Wilder, J. A., G. K. Olson, et al. (2002). "Complementation of a capsule deficient *Cryptococcus neoformans* with CAP64 restores virulence in a murine lung infection." Am J Respir Cell Mol Biol **26**(3): 306-314.

Wolf, J. M. and D. A. Davis (2010). "Mutational analysis of *Candida albicans* SNF7 reveals genetically separable Rim101 and ESCRT functions and demonstrates divergence in bro1-domain protein interactions." Genetics **184**(3): 673-694.

Wolf, J. M., D. J. Johnson, et al. (2010). "The *Candida albicans* ESCRT pathway makes Rim101-dependent and -independent contributions to pathogenesis." Eukaryot Cell **9**(8): 1203-1215.

Woods, J. P. (2002). "*Histoplasma capsulatum* molecular genetics, pathogenesis, and responsiveness to its environment." Fungal Genet Biol **35**(2): 81-97.

Xue, C., Y. S. Bahn, et al. (2006). "G protein-coupled receptor Gpr4 senses amino acids and activates the cAMP-PKA pathway in *Cryptococcus neoformans*." Mol Biol Cell **17**(2): 667-679.

Xue, C., T. Liu, et al. (2010). "Role of an expanded inositol transporter repertoire in *Cryptococcus neoformans* sexual reproduction and virulence." MBio **1**(1).

Xue, C., Y. Tada, et al. (2007). "The human fungal pathogen *Cryptococcus* can complete its sexual cycle during a pathogenic association with plants." Cell Host Microbe **1**(4): 263-273.

Yong, S. J., Z. Vuk-Pavlovic, et al. (2003). "Surfactant protein D-mediated aggregation of *Pneumocystis carinii* impairs phagocytosis by alveolar macrophages." Infect Immun **71**(4): 1662-1671.

Yuan, X., B. M. Mitchell, et al. (2010). "The RIM101 signal transduction pathway regulates *Candida albicans* virulence during experimental keratomycosis." Invest Ophthalmol Vis Sci **51**(9): 4668-4676.

Zaragoza, O. and A. Casadevall (2006). "Monoclonal antibodies can affect complement deposition on the capsule of the pathogenic fungus *Cryptococcus neoformans* by both classical pathway activation and steric hindrance." Cell Microbiol **8**(12): 1862-1876.

Zaragoza, O., B. C. Fries, et al. (2003). "Induction of capsule growth in *Cryptococcus neoformans* by mammalian serum and CO_2." Infect Immun **71**(11): 6155-6164.

Zaragoza, O., R. Garcia-Rodas, et al. (2010). "Fungal cell gigantism during mammalian infection." PLoS Pathog **6**(6): e1000945.

Zaragoza, O., C. P. Taborda, et al. (2003). "The efficacy of complement-mediated phagocytosis of *Cryptococcus neoformans* is dependent on the location of C3 in the polysaccharide capsule and involves both direct and indirect C3-mediated interactions." Eur J Immunol **33**(7): 1957-1967.

Zaragoza, O., A. Telzak, et al. (2006). "The polysaccharide capsule of the pathogenic fungus *Cryptococcus neoformans* enlarges by distal growth and is rearranged during budding." Mol Microbiol **59**(1): 67-83.

Zhang, Y., F. Wang, et al. (2009). "Robust Th1 and Th17 immunity supports pulmonary clearance but cannot prevent systemic dissemination of highly virulent *Cryptococcus neoformans* H99." Am J Pathol **175**(6): 2489-2500.

Zhao, X., S. H. Oh, et al. (2004). "ALS3 and ALS8 represent a single locus that encodes a *Candida albicans* adhesin; functional comparisons between Als3p and Als1p." Microbiology **150**(Pt 7): 2415-2428.

Zordan, R. E., D. J. Galgoczy, et al. (2006). "Epigenetic properties of white-opaque switching in *Candida albicans* are based on a self-sustaining transcriptional feedback loop." Proc Natl Acad Sci U S A **103**(34): 12807-12812.

Zou, J., H. Friesen, et al. (2009). "Regulation of cell polarity through phosphorylation of Bni4 by Pho85 G1 cyclin-dependent kinases in *Saccharomyces cerevisiae*." Mol Biol Cell **20**(14): 3239-3250.

Zuber, S., M. J. Hynes, et al. (2002). "G-protein signaling mediates asexual development at 25 degrees C but has no effect on yeast-like growth at 37 degrees C in the dimorphic fungus *Penicillium mameffei*." Eukaryot Cell **1**(3): 440-447.

Zuber, S., M. J. Hynes, et al. (2003). "The G-protein alpha-subunit GasC plays a major role in germination in the dimorphic fungus *Penicillium marneffei*." Genetics **164**(2): 487-499.

Appendix

Quorum Sensing Influences Titan Cell Production

I. INTRODUCTION

Unicellular organisms including many pathogenic bacteria and fungi have mechanisms for sensing similar organisms. When microbial populations reach a threshold, small molecule production is stimulated and the microbes produce quorum sensing molecules (reviewed in (Antunes, Ferreira et al. 2010; Han, Cannon et al. 2011)). Quorum sensing can induce many different complex biosynthetic pathways including the production of antibiotics, induction of plasmid transfer, and secretion of metabolites or enzymes (Antunes, Ferreira et al. 2010; Han, Cannon et al. 2011).

Cryptococcus neoformans is an opportunistic fungal pathogen that commonly causes pulmonary infections, skin lesions, and meningitis (Heitman and American Society for Microbiology. 2011). Upon exposure to the host pulmonary environment, a subset of *C. neoformans* cells become enlarged "titan" cells. Approximately 20% of the population of a wild type infection become titan cells, which are approximately 5-10 fold larger than cells grown *in vitro* (Okagaki, Strain et al. 2010). The exact signal that induces titan cell production is unknown, however, *in vitro* studies suggest that a soluble host factor can induce cryptococcal morphogenesis (Okagaki, Strain et al. 2010). Titan cell production is regulated by signaling via the Gα protein, Gpa1, and the PKA pathway, which regulates the major virulence factors in *C. neoformans*.

Early studies suggested that titan cell production in *Cryptococcus neoformans* was increased in mice that received a poor inoculum during infection (Zaragoza, Garcia-Rodas et al. 2010), suggesting that titan cell production may be density dependent. Therefore, we sought to confirm the role of density in titan cell production in wild type cells and in strains that exhibit reduced titan cell production.

II. MATERIALS AND METHODS

Ethics Statement. All animals were handled in strict accordance with good animal practice as defined by the relevant national and/or local animal welfare bodies, and all animal work was approved by the Institutional Animal Care and Use Committee (IACUC) under protocol number 1010A91133.

Strains and Media. The *C. neoformans* var. *grubii* strains KN99α (wild type) (Nielsen, Cox et al. 2003), CDX18 (*gpr4Δ/gpr5Δ*) (Xue, Bahn et al. 2006; Okagaki, Wang et al. 2011), CDX6 (*gpr4Δ*) (Xue, Bahn et al. 2006) and CDX11 (*gpr5Δ*) (Okagaki, Wang et al. 2011) were used in this study. Strains were stored as glycerol stocks at -80°C and grown at 30°C in yeast extract-peptone-dextrose (YPD) agar or broth medium (BD, Hercules, CA).

***In vivo* titan cell and phagocytosis assay.** *C. neoformans* cells were cultured overnight in YPD broth. The resulting yeast cells were pelleted and resuspended in sterile phosphate-buffered saline (PBS) at a concentration of $1x10^6$ or $1x10^8$ cells/ml based on hemocytometer count. Groups of 6- to 8-week-old female C57BL/6 mice (Jackson Labs, Bar Harbor, ME) were anesthetized by intraperitoneal pentobarbital injection. Three to five mice per treatment were infected intranasally with $5x10^4$ or $5x10^6$ cells in 50 μl phospho-buffered saline (PBS, Lonza, Rockland, ME). At 3 days post-infection mice were sacrificed by CO_2 inhalation. Lungs were lavaged with 1.5 mL sterile PBS three times using an 18.5 gauge needle placed in the trachea. Cells in the lavage fluid were

pelleted at 16,000*g*, resuspended in 3.7% formaldehyde, and incubated at room temperature for 30 minutes. Cells were then washed once with PBS and >100 cells per animal for the moderate inoculum and >500 cells per animal for the high inoculum were analyzed for size and phagocytosis by microscopy (AxioImager, Carl Zeiss, Inc). Cell body size was measured and cells were classified as small cells (<10 µm in diameter), or titan cells (>10 µm in diameter).

Statistical Analysis. All analyses were performed using Analyse-It (Analyse-it Ltd., Leeds, England). One-way ANOVA was used to analyze differences in titan cell production and phagocytosis and *P*-values <0.05 were considered significant.

III. RESULTS AND DISCUSSION

Quorum sensing has been identified in bacteria and pathogenic fungi as a mechanism for cell-cell communication and sensing of population size. Previous observations suggested that mice with poor *C. neoformans* infectionsappeared to have increased proportions of titan cells. To further explore density dependence in *C. neoformans*, mice were inoculated with moderate ($5x10^4$), or high ($5x10^6$) concentrations of cells. Four strains were examined for titan cell production: wild type, *gpr4Δ*, *gpr5Δ*, and *gpr4Δ/gpr5Δ*. At three days post-infection, fungal cells were recovered by bronchoalveloar lavage. Samples were fixed immediately in 3.7% formaldehyde and examined for cell size by microscopy. In all strains, the ratio of titan cells was less when recovered from mice infected with a high inoculum than were recovered from mice

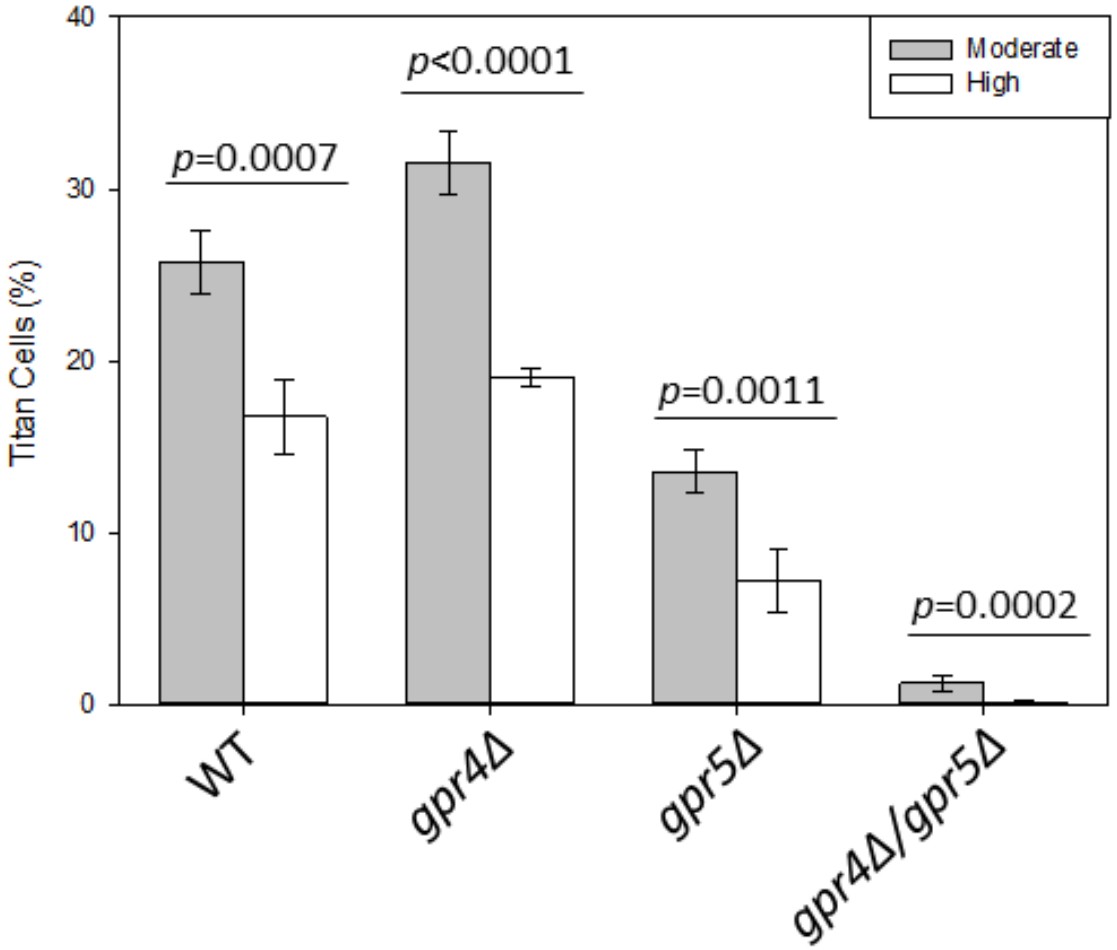

Figure A1. Titan cell production is density dependent. Mice were intranasally inoculated with $5x10^4$ (grey bars) or $5x10^6$ (white bars) cells of wild type, *gpr4Δ*, *gpr5Δ*, or *gpr4Δ/gpr5Δ*. At three days post-infection, lungs were lavaged and the samples were fixed immediately. Samples were examined for titan cell production. Three to five mice were inoculated per treatment and >100 cells per sample for moderate inoculum and >500 cells per sample for high inoculum were examined for titan cell production. Error bars represent standard deviation (SD).

infected with a moderate inoculum (**Figure A1**). Even in strains with very low levels of titan cell production like the *gpr4Δ/gpr5Δ*, significantly fewer titan cells were recovered in the high inoculum compared to the moderate inoculum. Thus, infecting mice with a high inoculum results in a lower production of titan cells compared to mice infected with a moderate inoculum.

These data suggest that titan cell production is density dependent, where high density reduces titan cell production. There are several possible mechanisms for density dependence in *C. neoformans* titan cell production: quorum sensing, nutrient limitation, or stimulant limitation.

Quorum sensing is cell-cell signaling in microbes via the production of small molecules that can be sensed by nearby cells. Quorum sensing has been shown extensively in bacteria, and more specifically, bacterial biofilm production. More recently, quorum sensing in *Candida albicans* has been observed during biofilm formation and environmental sensing (reviewed in (Han, Cannon et al. 2011)). In *C. neoformans*, quorum sensing may be due to the production and release of metabolites or other small molecules that are stimulated by exposure to the host pulmonary environment.

Density dependent titan cell production may also be the result of nutrient or stimulant limitation. Titan cell production can be induced by culturing *C. neoformans* in filter sterilized spent media from a macrophage cell line (Chapter 2 and Conclusions), suggesting that the factor or nutrient that stimulates titan cell production is soluble. It is possible that there is a limited pool of the soluble factor or nutrient available in the lungs of infected mice. Thus, nutrient or stimulant limitation may result in fewer cryptococcal

cells receiving adequate signal stimulation. In addition, deletion of Gpr4 or Gpr5 did not eliminate changes in titan cell production due to density. Thus, other sensing mechanisms are likely responsible for quorum or nutrient sensing that leads to titan cell production. Additional experiments determining the signals that stimulate titan cell production are necessary to further understand density dependent titan cell production.